

Asymmetric Brønsted Acid Catalysis:

ACETALS

&

CONFINED CATALYSTS

Inaugural-Dissertation

zur

Erlangung des Doktorgrades

der Mathematisch-Naturwissenschaftlichen Fakultät

der Universität zu Köln

vorgelegt von

Ilija Čorić

aus Zagreb (Kroatien)

Köln 2012

Berichtersteller: Prof. Dr. Benjamin List

Prof. Dr. Hans-Günther Schmalz

Prof. Dr. Axel Klein

Tag der mündlichen Prüfung: 25 Juni 2012

TABLE OF CONTENTS

ABSTRACT	IV
KURZZUSAMMENFASSUNG	V
LIST OF SIMBOLS AND ABBREVIATIONS.....	VI
ACKNOWLEDGEMENTS	VIII
1. INTRODUCTION	1
1.1. Acetals	1
1.2. Brønsted acid catalysis with small and unbiased substrates.....	3
2. BACKGROUND.....	5
2.1. Asymmetric catalysis.....	5
2.2. Asymmetric organocatalysis.....	8
2.3. Asymmetric Brønsted acid catalysis	11
2.4. Chiral phosphoric acids and derivatives	16
2.4.1. Chiral environment.....	16
2.4.2. Phosphoric acid derivatives.....	18
2.5. Asymmetric synthesis of acetals.....	21
2.5.1. Chiral starting materials	21
2.5.2. Catalytic asymmetric methods.....	22
2.5.3. Catalytic asymmetric syntheses of <i>N,X</i> -acetals (<i>X</i> = N, O, S, Se).....	26
3. OBJECTIVES OF THIS PH.D. WORK.....	29
3.1. Catalytic Asymmetric Acetalizations.....	29
3.2. Confined Brønsted acids.....	31
4. RESULTS AND DISCUSSION	32
4.1. Catalytic asymmetric transacetalization	32
4.1.1. Reaction design and optimization.....	32
4.1.2. Substrate scope	34
4.1.3. Discussion	37
4.2. Kinetic resolution of homoaldols via catalytic asymmetric transacetalization	41
4.2.1. Reaction design and optimization.....	41
4.2.2. Substrate scope	43
4.2.3. Utility of the products	48

4.2.4. Discussion	49
4.3. Catalytic asymmetric spiroacetalization	51
4.3.1. Reaction design and optimization	51
4.3.2. Substrate scope	57
4.3.3. Nonthermodynamic and thermodynamic spiroacetals	60
4.3.4. Discussion	62
4.4. Confined Brønsted acids.....	66
4.4.1. Design	66
4.4.2. Synthesis.....	71
4.4.3. X-Ray structures	73
4.4.4. Discussion	77
5. SUMMARY	80
5.1. Catalytic asymmetric transacetalization	80
5.2. Kinetic resolution of homoaldols via catalytic asymmetric transacetalization	81
5.3. Catalytic asymmetric spiroacetalization	82
5.4. Confined Brønsted acids.....	83
6. OUTLOOK.....	85
6.1. Kinetic resolutions of homoaldols	85
6.2. Catalytic asymmetric transesterification.....	86
6.3. Imidodiphosphoric acids as the second generation of stronger Brønsted acids	87
7. EXPERIMENTAL SECTION	90
7.1. General Experimental Conditions	90
7.2. Catalytic asymmetric transacetalization	93
7.2.1. Starting materials	93
7.2.2. Products.....	105
7.2.3. X-Ray data for compound 3d	114
7.3. Kinetic resolution of homoaldols via catalytic asymmetric transacetalization	119
7.3.1. Optimization of the reaction conditions	119
7.3.2. Substrates.....	121
7.3.3. Products.....	131
7.3.4. Transformations of 5c , determination of absolute configurations, and natural product syntheses	147

7.4. Catalytic asymmetric spiroacetalization	152
7.4.1. Substrates.....	152
7.4.2. Products.....	161
7.5. Confined Brønsted acids.....	172
7.5.1. Synthesis.....	172
7.5.2. X-Ray data for compounds 13a-c	200
8. BIBLIOGRAPHY	226
9. APPENDIX	233
9.1. Erklärung.....	233
9.2. Lebenslauf.....	234

ABSTRACT

The developments of Brønsted acid catalyzed asymmetric syntheses of acetals and a novel class of confined Brønsted acid catalysts are described. The first highly enantioselective intramolecular transacetalization reaction catalyzed by the chiral BINOL-derived phosphoric acid TRIP was developed to access chiral acetals with the acetal carbon as the only stereogenic center.

The practical utility of the catalytic asymmetric transacetalization reaction was demonstrated in a kinetic resolution of homoaldol acetals. Both secondary and tertiary homoaldols were resolved with high enantioselectivity using phosphoric acid STRIP based on a 1,1'-spirobiindane backbone.

The first catalytic asymmetric spiroacetalization reaction was developed, enabling access to small unfunctionalized spiroacetal compounds, including the natural product olean, which possesses a spiroacetal center as the only source of chirality. In addition, the catalyst controlled access to thermodynamic and nonthermodynamic spiroacetals was achieved offering a solution to this long standing issue in synthesis of spiroacetal natural products.

Most significantly, to enable the spiroacetalization reaction a novel class of chiral Brønsted acids, termed confined Brønsted acids was designed and developed. Confined Brønsted acids based on a C_2 -symmetric imidodiphosphate anion feature an extremely sterically demanding chiral microenvironment with a single catalytically relevant and geometrically constrained bifunctional active site. This catalyst design is expected to find wide utility in various asymmetric reactions involving small and functionally unbiased substrates.

KURZZUSAMMENFASSUNG

Die Entwicklung der Brønsted-Säure katalysierten asymmetrischen Synthese von Acetalen und eine neue Klasse von beengten Brønsted-Säure Katalysatoren wird beschrieben. Die erste hoehenantioselektive intramolekulare Transacetalisierung katalysiert durch die chirale, von BINOL abgeleitete Phosphorsäure TRIP wurde entwickelt und macht chirale Acetale zugänglich in denen der Acetalkohlenstoff das einzige stereogene Zentrum ist.

Der praktische Nutzen der katalytisch asymmetrischen Transacetalisierung wurde durch die kinetische Resolution von Homoaldolacetalen demonstriert. Sowohl sekundäre als auch tertiäre Homoaldole reagierten mit hoher Enantioselektivität, wenn die Phosphorsäure STRIP auf Basis des 1,1'-Spirobiindangerüstes verwendet wurde.

Die erste katalytisch asymmetrische Spiroacetalisierung wurde entwickelt. Hierdurch wurden kleine, unfunktionalisierte Spiroacetale zugänglich, darunter der Naturstoff Olean, in welchem das Spiroacetal das einzige chirale Zentrum darstellt. Zusätzlich hierzu konnten unter Katalysatorkontrolle thermodynamische und nicht-thermodynamische Spiroacetale dargestellt werden. Dies stellt einen Lösungsansatz zu diesem lange bestehenden Selektivitätsproblem in der Synthese von Spiroacetalnaturstoffen dar.

Am wichtigsten jedoch ist, dass, um die Spiroacetalisierung zu ermöglichen, eine neue Klasse von chiralen Brønsted Säuren, genannt beengte Brønsted Säuren, entworfen und entwickelt wurde. Beengte Brønsted Säuren auf Basis des C_2 -symmetrischen Imidodiphosphatanions zeichnen sich durch eine sterisch extrem anspruchsvolle Mikroumgebung mit einem einzigen katalytisch relevanten und geometrisch eingeschränkten bifunktionellen aktiven Zentrum aus. Dieses Katalysatormotiv wird vermutlich breite Anwendung in der Katalyse von asymmetrischen Reaktionen mit kleinen und nicht vorfunktionalisierten Substraten finden.

LIST OF SIMBOLS AND ABBREVIATIONS

*	designating chiral moiety
Ac	acetyl
Ar	aryl, aromatic
aq.	aqueous
Boc	<i>tert</i> -butyloxycarbonyl
calcd	calculated
BINOL	1,1'-bi-2-naphthol
Bn	benzyl
cat.	catalyst/catalytic
conv.	conversion
d	doublet
DCE	1,2-dichloroethane
DCM	dichloromethane
DMF	dimethylformamide
DMSO	dimethylsulfoxide
dr	diastereomeric ratio
EI	electron impact
<i>ent</i>	enantiomer(ic)
equiv	equivalent(s)
er	enantiomeric ratio
Et	ethyl
ESI	electrospray ionization
GC (GC-MS)	gas chromatography (gas chromatography coupled with mass detection)
H8-BINOL	5,5'.6,6',7,7',8,8'-octahydro-1,1'-2-naphtol
HMDS	hexamethyldisilazane
HMPA	hexamethylphosphoramide
HOMO	highest occupied molecular orbital
HPLC	high performance liquid chromatography
HRMS	high resolution mass spectrometry
HX*	designating chiral Brønsted acids, e.g. chiral phosphoric acid diesters
L	ligand (abbreviation used in schemes)
LDA	lithium diisopropylamide
LiHMDS	lithium hexamethyldisilazide
LUMO	lowest unoccupied molecular orbital
<i>m</i>	<i>meta</i>
m	multiplet
M	metal (abbreviation used in schemes)
M	molar (concentration)
Me	methyl
MS	mass spectrometry, molecular sieves
Ms	methylsulfonyl
MTBE	methyl <i>tert</i> -butyl ether
MW	molecular weight
<i>m/z</i>	atomic mass units per charge
N	normal (concentration)

LIST OF ABBREVIATIONS

NMR	nuclear magnetic resonance spectroscopy
NOE(SY)	nuclear Overhauser effect (spectroscopy)
NuH/Nu	nucleophile
<i>o</i>	<i>ortho</i>
<i>p</i>	<i>para</i>
Ph	phenyl
PG	protecting group
Pr	propyl
Py	pyridine
quint	quintet
<i>rac.</i>	racemic
r.t.	room temperature
sept	septet
sext	sextet
SPINOL	1,1'-spirobiindane-7,7'-diol
<i>t</i>	<i>tert, tertiary</i>
t	triplet
TBS	<i>tert</i> -butyl-dimethylsilyl
TFA	trifluoroacetic acid
THF	tetrahydrofuran
TLC	thin layer chromatography
TMS	trimethylsilyl
TRIP	3,3'-bis(2,4,6-triisopropylphenyl)-1,1'-binaphthyl-2,2'-diyl hydrogen phosphate

ACKNOWLEDGEMENTS

I am grateful to Prof. Dr. Benjamin List for giving me the opportunity to work in the beautiful research environment of the Max-Planck Institut für Kohlenforschung. Working with Ben was highly inspiring. Even during less successful research periods talking to him was always encouraging and without pressure for immediate results. He always advised me to approach research by tackling the more challenging (and rewarding) problems rather than more obvious ones. Such a collegial and inspiring scientific atmosphere has encouraged me to always give my best and has lead to the research results described in this thesis.

I am indebted to Katica Antol and Jasna Blaženčić, my chemistry professors during elementary school and high school education. Their dedication in teaching and scientific enthusiasm had a profound influence on my choice of chemistry as a career. I also owe my sincere gratitude to many professors at the Chemistry Department of the Faculty of Science, University of Zagreb, Croatia and especially to Prof. Vitomir Šunjić, my diploma thesis supervisor.

The results presented in this thesis wouldn't have been possible without fruitful collaborations with Dr. Steffen Müller, who made the famous STRIP catalyst and worked with me on the kinetic resolution project, and with Dr. Sreekumar Vellalath, who designed many inspiring catalyst structures and collaborated with me on the acetalization reactions. Help from Natascha Wippich was indispensable for the completion of the spiroacetalization project. I would also like to thank Ji Hye Kim, Saihu Liao and Tjøstil Vlaar for collaborating on the transesterification, sulfoxidation, and acetalization projects described in the Outlook of this thesis.

I am grateful to Adrienne Hermes, Marianne Hannappel, Simone Marcus, Hendrik van Thienen, Pascal Wallkamp, and Arno Döring for managing the laboratory and making it a pleasant and safe place to work, and assistant professors Dr. Nuno Maulide and Dr. Martin Klußman for leading Ph.D. seminars. Assistance and expertise of the GC, HPLC, and mass departments at the Max-Planck Institut für Kohlenforschung is gratefully acknowledged. Finally, I am grateful to many of my colleagues from the List, Klußman and Maulide groups for sharing their chemicals and ideas, as well as for their friendship inside and outside of the lab.

1. INTRODUCTION

1.1. Acetals

Acetals are among the most common stereocenters in nature. They form glycosidic bonds that link together essential molecules of life, carbohydrates, including starch and cellulose, the most abundant organic material on Earth (Scheme 1.1).^[1] Stereogenic acetals are ubiquitous in other natural products, ranging from simple insect pheromones to complex spiroketal polyketides.^[2-4] Controlling their relative and absolute configuration can be extremely important. For example, starch and cellulose only vary in the configuration at their anomeric acetal stereocenter. The importance of chiral acetals is further illustrated with their occurrence in several chiral pharmaceuticals^[5-6] and their potential as diastereocontrolling elements in organic synthesis.^[7-10] Nevertheless, methods for the enantioselective synthesis of stereogenic acetals are very limited and usually based on chiral starting materials or reagents.^[11-16]



Cellulose:

- basic structural component of plant cell walls
- about 33 percent of all vegetable matter (90 percent of cotton and 50 percent of wood)
- nondigestible to humans
- **the most abundant organic material on Earth**

Starch:

- manufactured in the green leaves of plants from excess glucose
- serves the plant as a reserve food supply
- food for humans and animals

Scheme 1.1. Acetal group in cellulose and starch.

Spiroacetals

A structurally particularly distinctive subgroup of acetals are spiroacetals, compounds in which two oxygen containing rings are joined at a single carbon. These fascinating small spirocycles are a core motif of a variety of natural products.^[2-4] To mention a few, protein phosphatase inhibitor okadaic acid is a toxin associated with diarrhetic shellfish poisoning;^[17] spongistatins are structurally complex tubulin polymerization-inhibiting macrolides that display extraordinary antitumor activities;^[2] integrumycin is an HIV-1 protease inhibitor,^[18] and the

ionophore monensin A is an antibiotic widely used in animal feeds.^[19] The spiroacetal subunit was demonstrated to be a privileged pharmacophore, essential for the biological activity of natural products.^[20-23]

Controlling the relative and absolute configuration of spiroacetals can be extremely important. A number of syntheses of natural products were met with formidable challenges in cases when the configuration of the spiroacetal stereocenter differed from the thermodynamically preferred one.^[2] Furthermore, natural products that contain a spiroacetal as the only source of chirality are well known.^[24] Even the parent 6,6-spiroacetal is a natural product, olean, the major female-produced sex pheromone of the olive fruit fly (*Bactrocera oleae*) (Scheme 1.2).^[25] Although it has been isolated as a racemate from natural sources, its two mirror images, enantiomers, display the remarkable property that one mirror image (*R*) is active on males, and the other (*S*) on females of the specie.^[26]

Several asymmetric syntheses have been published, however these invariably rely on chiral starting materials or reagents.^[27-28] It was shown that enzymes are capable of stereospecific spiroacetal formation,^[29] and organic chemists have developed several powerful synthetic methods for stereoselective formation of suitably substituted spiroacetals.^[30-33] However, in spite of attempts,^[34] access to spiroacetal motifs in a catalytic highly enantioselective manner has not been previously described.



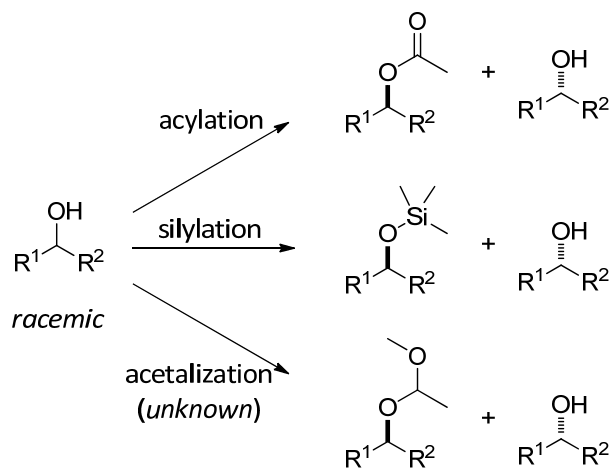
Scheme 1.2. Two enantiomers of olean from olive fruit fly.

Kinetic resolution of alcohols via acetal formation

In organic synthesis, acetals are common functional groups used for the protection of aldehydes, ketones and alcohols. Due to an easy access to racemic chiral alcohols, and the possibility of inverting the alcohol stereocenter, the kinetic resolution of alcohols is an attractive route for accessing enantioenriched chiral alcohols and their derivatives. Most attractive methods of resolution are asymmetric placements of common protective groups, which can be easily removed or utilized further in the synthesis. In this regard asymmetric

1. INTRODUCTION

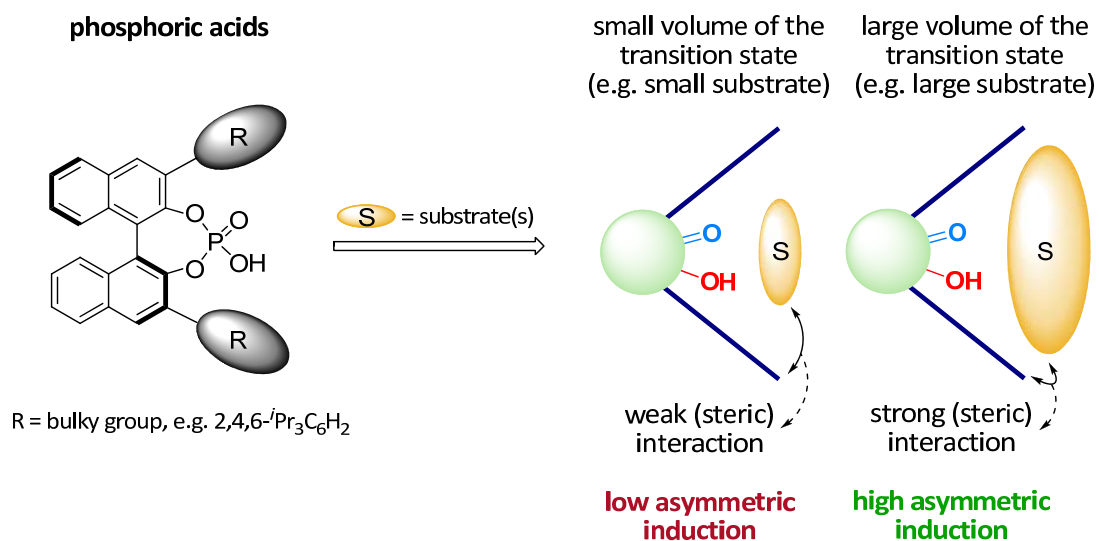
resolutions that place acyl groups and silyl groups obtaining esters and silyl ethers are well known (Scheme 1.3). The acetal moiety is stable under basic or mildly acidic conditions, and in the presence of fluoride anion making it a complementary protecting group to ester or silyl ether groups. However, kinetic resolutions of alcohols that form an acetal, a very common alcohol protecting group, have not been described prior to our study (Scheme 1.3).



Scheme 1.3. Kinetic resolution of alcohols.

1.2. Brønsted acid catalysis with small and unbiased substrates

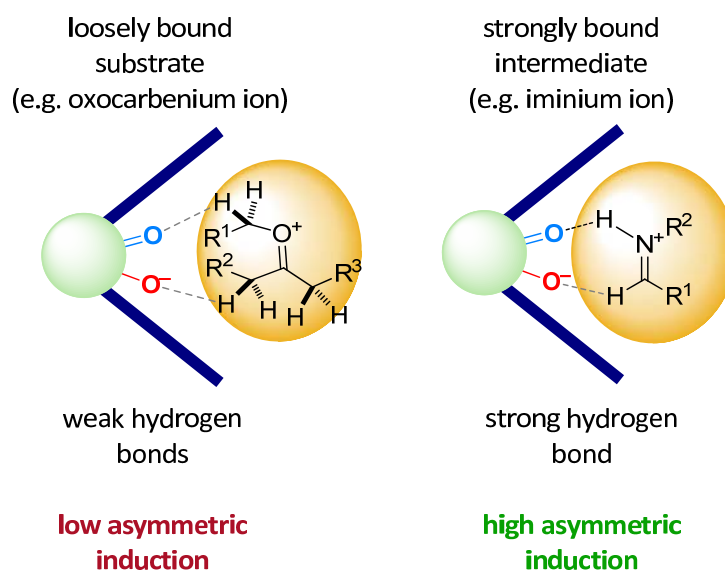
Asymmetric Brønsted acid catalysis, in particular with stronger Brønsted acids such as chiral phosphoric acid type catalysts, is one of the most successful subfields of organocatalysis.^[35-36] However, asymmetric versions of numerous reactions are still elusive, and in the laboratory smallest substrates frequently give poor selectivity (Scheme 1.4).



Scheme 1.4. Limitations of phosphoric acid type catalysts with small molecules.

1. INTRODUCTION

Additionally, successful asymmetric reactions with transition states that are not well organized with covalent or hydrogen bonding interactions between the catalyst and the substrates are very rare. Such a situation is encountered with the oxocarbenium ion, commonly invoked intermediate in the synthesis of acetals (Scheme 1.5). As opposed to the reactions involving related iminium ion featuring a strong hydrogen bond there are only scarce examples of the addition of nucleophiles to oxocarbenium ions.^[37-39]



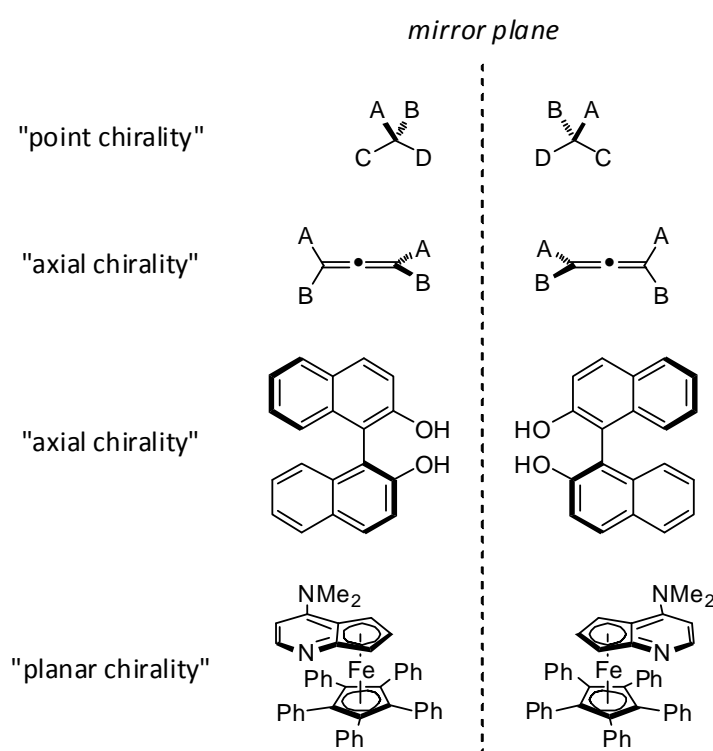
Scheme 1.5. Limitations of phosphoric acid type catalysts with loosely bound intermediates.

Brønsted acids that provide extremely sterically demanding and readily tunable active sites can solve mentioned problems and their development is probably the most important result of this thesis.

2. BACKGROUND

2.1. Asymmetric catalysis

Chirality is a property of an object making it nonsuperimposable with its mirror image.^[1] In chemistry, particularly in molecules there are several elements which can cause this property. The most common one is a tetrasubstituted carbon atom with all four substituents different, although there are many other molecular substructures that cause molecules to be chiral (Scheme 2.1).



Scheme 2.1. Some examples of chiral elements.

Like other molecular properties that make molecules different, chirality is as well a distinct structural feature. Molecules which are mirror images of one another, or enantiomers, are different compounds, although they cannot be differentiated in an achiral environment. However all living beings are composed of molecules that are chiral, and often only one enantiomer is found in nature. Therefore, when making single compounds, rather than mixtures, chirality as well as any other structural property of the molecule must be controlled.

The importance of accessing pure enantiomers of chiral molecules is a current tremendous effort in organic synthesis. Most importantly, the requirement of the

2. BACKGROUND

pharmaceutical industry has increased in recent decades due to serious issues related to the use of usually more easily available equal, or racemic, mixtures of enantiomers. As our bodies, e.g. proteins, sugars, DNA, are composed of single enantiomers of chiral compounds, we present a chiral environment for any external chiral molecule, and the enantiomers of that molecule are expected to have different interaction with our organism. Sometimes these effects are minor, for example, with enantiomers of the drug having different levels of activity. However the effects can also be profoundly different with serious consequences.^[1]

There are several ways to access single enantiomers of chiral compounds. Diastereoselective synthesis makes use of preexisting chiral building blocks, most frequently originating from nature, which will become parts of the final molecules, or are used to make chiral auxiliaries or reagents. The resolution approach uses racemic mixtures, which are separated by interaction with enantiopure chiral material, for example using a chiral base or acid for making a salt of one of the enantiomers, or by chromatography on a chiral column. The main drawback of the resolution method is that the second unwanted enantiomer, which represents half of the total synthesized material, is usually a waste. Therefore, the most attractive way to make enantioenriched molecules is asymmetric catalysis.

Catalysts are materials, molecules or molecular assemblies capable of accelerating a chemical reaction. They operate by enabling an alternative reaction pathway, proceeding through different “catalyst stabilized” transition states and “catalyst stabilized” intermediates, which are all lower in relative energy than the energetically highest transition state of an uncatalyzed reaction. By doing so the catalyst can even direct the reaction to alternative products, which are unfavored or cannot even be obtained in an uncatalyzed reaction.

In asymmetric catalysis the role of the catalyst is dual, it accelerates the reaction, but it also forms thermodynamically unfavored composition of the products, favoring one of the enantiomers. The origin of this enantioselectivity is the different ability of a single enantiomer of the catalyst to form two different, diastereomeric transition states that lead to two enantiomers of the product. The appeal of asymmetric catalysis is in the fact that a small amount of a pure enantiomer of the catalyst can produce a large amount of enantioenriched product molecules.

Today, there are three main fields in asymmetric catalysis: metal catalysis, organocatalysis, and enzymatic catalysis, with recent research efforts being largely focused on metal catalysis and organocatalysis. Importance of asymmetric metal catalysis has been

2. BACKGROUND

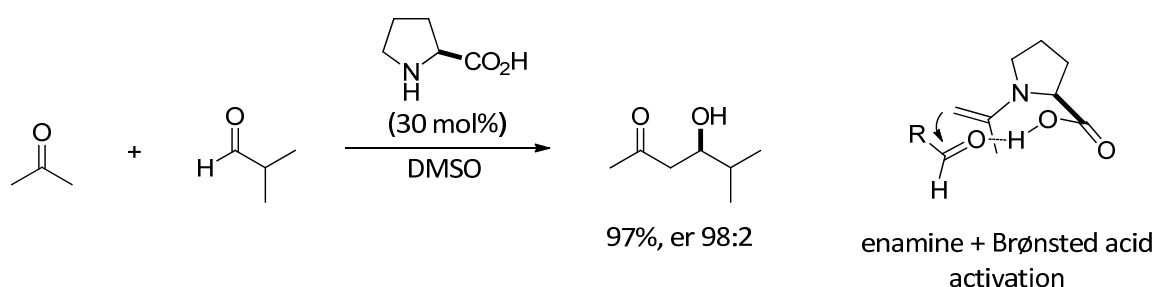
recently recognized with Nobel Prize to K. Barry Sharpless for enantioselective oxidations and to William Knowles and Ryoji Noyori for enantioselective reduction reactions.

Next to metal catalysts and enzymes, recently simple organic molecules have emerged as powerful catalysts. Although some reactions performed with organocatalysts seem to be alternatives to known metal-catalyzed processes, especially those where the metal plays a role of the Lewis acid, these two fields are largely complementary.

2.2. Asymmetric organocatalysis

The year 2000 marked an emergence of organocatalysis as a new field in asymmetric catalysis,^[40-41] one which in the subsequent decade has placed itself shoulder to shoulder with metal catalysis and biocatalysis.^[42-43] In organocatalysis, simple organic molecules are used as catalysts instead of metals or enzymes. Distinct advantages offered are the activation of various common functional groups, mild reaction conditions, exclusion of expensive metals and related toxic impurities, and usually easy access to both enantiomers of the catalyst and possibility of their versatile structural modification.

Initial independent reports by List^[40] and MacMillan^[41], described the use of small secondary amines as catalysts for the activation of aldehydes and ketones in asymmetric reactions. List demonstrated that the amino acid L-proline can activate acetone via the formation of an enamine intermediate in a direct aldol reaction (Scheme 2.2). Enamines, compared to the corresponding enols have a higher HOMO (highest occupied molecular orbital) and are better nucleophiles. In the same report a transition state was proposed, which was later refined, that involved the Brønsted acidic carboxylic acid moiety of proline in simultaneous activation of aldehyde electrophile. All of these concepts, enamine catalysis, bifunctional activation of nucleophile and electrophile, and chiral Brønsted acid catalysis, have proven to be very general in the field of organocatalysis.

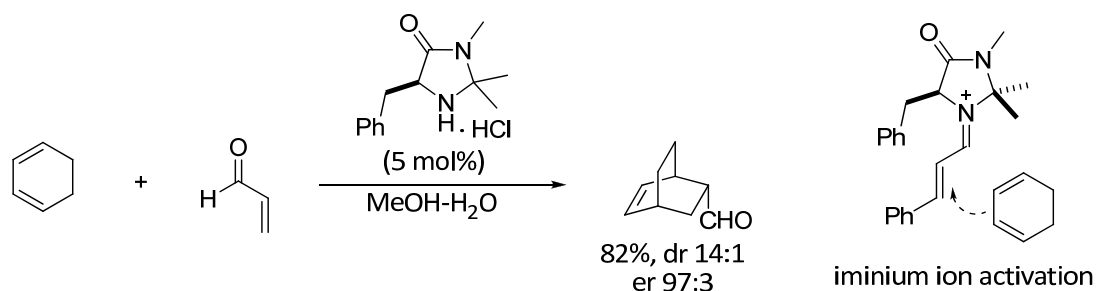


Scheme 2.2. Proline catalyzed aldol reaction.

Only slightly later, MacMillan reported that enals can be activated with a chiral imidazolidinone catalyst via the intermediate iminium ion towards a Diels-Alder reaction with dienes (Scheme 2.3). Iminium ions, compared to the corresponding aldehydes have a lower LUMO (lowest unoccupied molecular orbital) and are better electrophiles. The stereochemistry of the products was explained with the shielding effect of one of the faces of the iminium intermediate by the benzyl group of the catalyst. Iminium catalysis and the use of catalysts

2. BACKGROUND

with bulky shielding groups have also proven to be very general concepts in the field of asymmetric organocatalysis.



Scheme 2.3. Imidazolidinone catalyzed Diels-Alder reaction.

Mechanistic insight provided by List's and Macmillan's papers, invoking familiar enamine and iminium intermediates, as well as importance of aldol and Diels-Alder reactions, was undoubtedly responsible for the immediate wide acceptance of this type of catalysis by other groups. Numerous reactions and catalysts have been developed since, and new modes of organocatalysis have been discovered.

Catalytic asymmetric reactions employing small organic molecules are not novel, and prior to reports by List and MacMillan a number of reactions was performed.^[44] In 1912 Bredig and Fiske reported cinchona alkaloid promoted addition of hydrogen cyanide to benzaldehyde with low enantioselectivity,^[45-46] and in 1960 Pracejus found a cinchona alkaloid catalyzed asymmetric addition of methanol to ketenes.^[47] The proline catalyzed aldol reaction has been reported already in 1971 independently by Hajos and Parish^[48-49] and by Eder, Sauer and Wiechert^[50-51]. However poor mechanistic interpretations and lack of conceptual formulations were responsible for the lack of general interest from the synthetic community. After accomplishments by List and MacMillan many of these older organocatalytic reactions were reexamined and the activation modes of the small organic catalysts that were employed are now well appreciated.

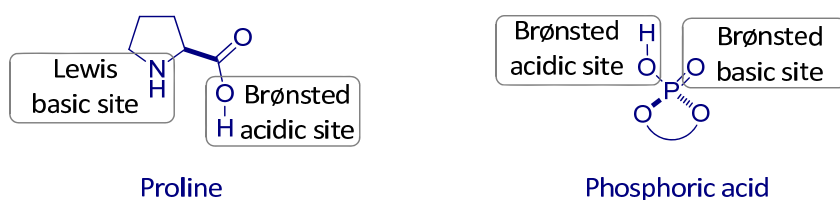
Classification of modern organocatalysis and the role of bifunctionality

Organocatalysts can operate by activating substrates either covalently by forming σ and π bonds with the substrate or noncovalently utilizing hydrogen bonding, protonating, or deprotonating the substrate.

In 2004 Seayad and List suggested a classification system for organocatalysts^[52] based on Lewis and Brønsted acid-base theories. Based on the nature of their interaction with

2. BACKGROUND

substrates many organocatalysts can be classified as electron donors (Lewis bases), electron acceptors (Lewis acids), proton acceptors (Brønsted bases) and proton donors (Brønsted acids). However, organocatalysts can, and usually do, utilize these modes simultaneously. The success of many organocatalysts has been attributed to the cooperative “bifunctional” activation of the substrates. For example, proline amino group acts as a Lewis base employing its electrons to form a covalent enamine adduct with aldehydes while the Brønsted acidic carboxylic acid moiety activates electrophiles by hydrogen bonding and protonation (Scheme 2.4). The remarkable success of chiral phosphoric acids in asymmetric catalysis is also attributed to bifunctional activation, in which Brønsted acidic site ($-OH$) and Brønsted basic site ($=O$) simultaneously activate the electrophile and the nucleophile, respectively (Scheme 2.4).

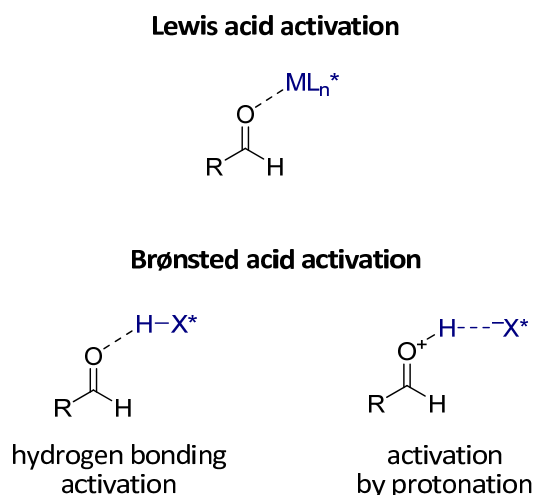


Scheme 2.4. Bifunctional organocatalysts.

2.3. Asymmetric Brønsted acid catalysis

Metal Lewis acid catalysis

A Lewis acid is a chemical species that is an electron-pair acceptor and therefore able to react with a Lewis base, a chemical species able to provide a pair of electrons, to form a Lewis adduct, by sharing the electron pair furnished by the Lewis base.^[53] In a more general sense the acid-base concept can be extended to include a single electron acceptors and donors. For several decades metal based Lewis acids with chiral ligands have been employed in numerous asymmetric reactions. Their activation mode is based on the formation of a Lewis pair with a substrate resulting in lowering of the electron density of the substrate making it more susceptible to nucleophilic attack and other transformations (Scheme 2.5).



Scheme 2.5. Activation of aldehydes by Lewis and Brønsted acids.

Brønsted acid catalysis

The proton is included in the definition of a Lewis acid, although the term Lewis acid usually refers to heavier elements. Instead, the term Brønsted acid is used to describe a chemical species capable of donating a proton to a Brønsted base, a chemical species capable of accepting the proton. It is well known that a proton can activate substrates similar to Lewis acids. However, as the proton does not possess substituents, which could be rendered chiral, asymmetric catalysis with Brønsted acids has remained undeveloped until 2004, while the field of Lewis acid catalysis flourished. Only recently with the advent of organocatalysis, it was recognized that a protonated substrate can be closely associated with its anion, which can

2. BACKGROUND

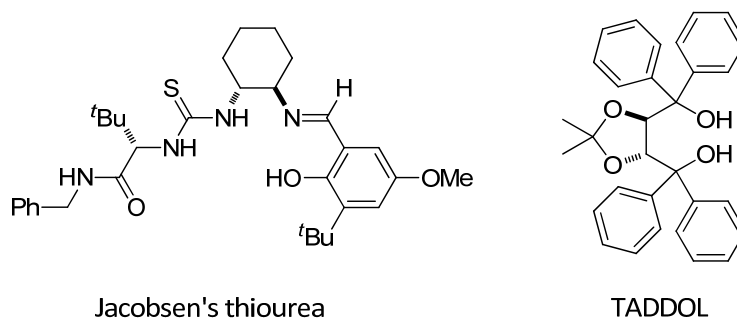
impart enantioselectivity to the reaction. The mode of activation of substrates by chiral Brønsted acids is conceptually similar to the activation by Lewis acids (Scheme 2.5).

Asymmetric Brønsted acid catalysis has emerged as one of the most prominent subfields of organocatalysis, and these organocatalysts are capable of activating the widest range of functional groups. Compared to Lewis acids, Brønsted acids are generally easier to handle and are usually stable to oxygen and water. Their metal-free nature makes them also an attractive alternative to metal catalysts in the pharmaceutical industry, where traces of toxic metal impurities are sometimes hard to remove from the final products. Chiral Brønsted acids are generally divided into two categories, hydrogen bonding catalysts and stronger (or strong) Brønsted acids.

Hydrogen bonding catalysts can be classified as *general acid catalysts* which are incapable of protonating the substrate. Instead, the proton transfer occurs to the transition state in the rate determining step. Strong Brønsted acids can act as *specific acid catalysts* fully protonating the substrate prior to the subsequent transformation. However this mechanistic classification should be considered more as a guideline than a rule, as the exact mechanism involved in the specific case is substrate and reaction dependant.

Hydrogen-bonding catalysts

Hydrogen-bonding catalysts are weak Brønsted acids which act by hydrogen bonding to the substrate, rather than fully transferring the proton to it. The most notable examples of this type of catalysts are chiral thioureas and diols (Scheme 2.6). Chiral thioureas as catalysts were serendipitously discovered by Sigman and Jacobsen in 1998 for the Strecker reaction.^[54] However, the recognition of the general hydrogen-bonding activation mode of these catalysts has waited for several years and was inspired by the emergence of organocatalysis.



Scheme 2.6. Chiral hydrogen bonding catalysts.

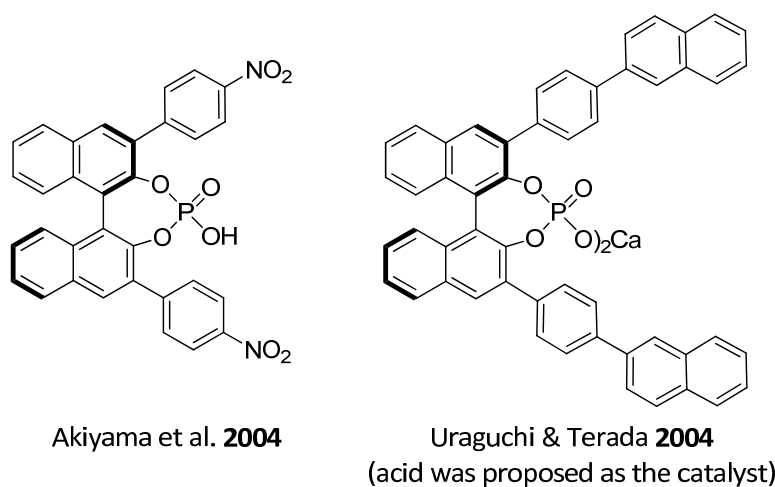
2. BACKGROUND

Based on the known fact that polar protic solvents accelerate certain Diels-Alder reactions the group of Rawal developed an asymmetric version of this reaction using a chiral diol TADDOL as the catalyst (Scheme 2.6).^[55]

Within the field of organocatalysis, hydrogen-bonding catalysis acquired a prominent role, and numerous reactions and catalysts have been reported utilizing hydrogen-bonding moiety for activation of electrophiles.^[56-57]

Moderately strong and strong Brønsted acids

In 2004 independent reports by Akiyama^[58] and coworkers, and Uraguchi and Terada^[59] opened a new avenue in organocatalysis, by describing that relatively strong BINOL-derived phosphoric acids are efficient catalysts for carbon-carbon bond forming reactions (Scheme 2.7). However it was later shown that In Terada's case the phosphoric acid was not the true catalyst, but rather the calcium salt.^[60] Unfortunately, when purified by column chromatography on silica gel, the acidic proton of the phosphoric acid is exchanged with metal ions present in the silica gel, resulting in the isolation of the phosphate salt or its mixture with phosphoric acid. It is known that in several reports following the initial discoveries, metal salts were the true catalysts, although Brønsted acid catalysis mechanisms were conceived.^[60-61] In some cases the phosphate salt only acts as the inactive impurity, effectively requiring higher catalyst loadings.^[61] However in many cases sodium^[61] and calcium phosphates show activity and importantly different and even reversed enantioselectivity.^[60]

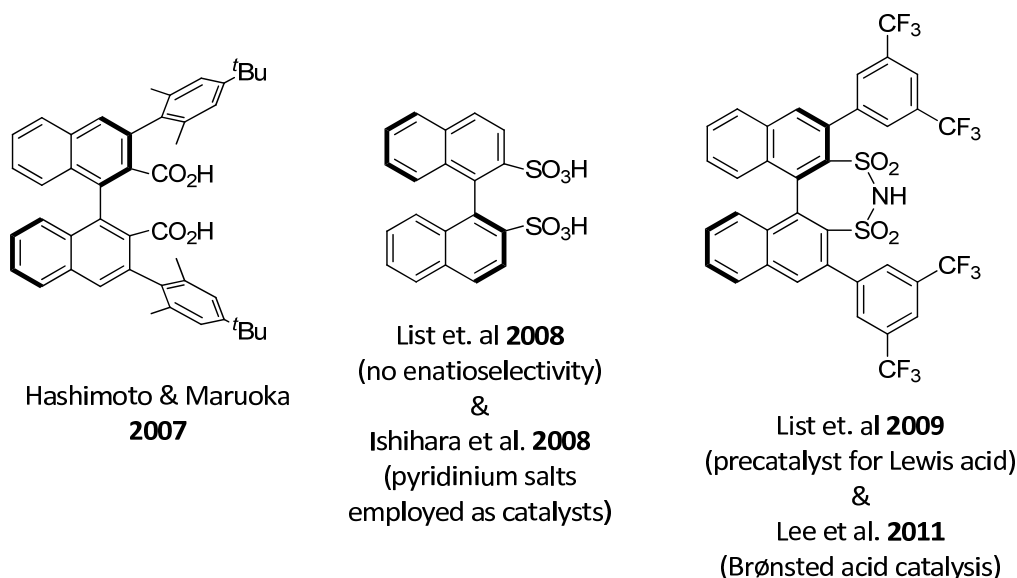


Scheme 2.7. Phosphoric acid catalysts from initial reports.

2. BACKGROUND

Although causing much confusion in the field of Brønsted acid catalysis, lately chiral phosphate salts of alkali and alkaline earth metals were recognized as a powerful class of Lewis acid catalysts. More detailed description of the developments of phosphoric acids and their derivatives is provided in the following section.

The success of chiral phosphoric acid catalysts prompted a number of attempts to prepare chiral catalysts possessing other functional groups. BINOL-derived dicarboxylic acid were introduced by Hashimoto and Maruoka as highly enantioselective catalysts for Mannich reaction of arylaldehyde *N*-Boc imines and diazo compounds (Scheme 2.8).^[62] In 2008 List et al. used previously known BINOL-derived disulfonic acid as a chiral catalyst in a three-component Hosomi–Sakurai reaction without achieving enantioselectivity.^[63] However Ishihara et al. found that pyridinium BINOL-disulfonates were effective catalyst in an enantioselective Mannich-type reaction.^[64] Highly acidic disulfonic acids alone were not reported as successful catalysts for asymmetric reactions so far. Disulfonimides were initially reported by List et al. as precatalysts for silicon Lewis acids in Mukaiyama aldol reactions of silyl ketene acetals with aldehydes.^[65] Lately disulfonimides were also used as true Brønsted acid catalysts for already well-established asymmetric Friedel-Crafts alkylation of indoles with imines.^[66]

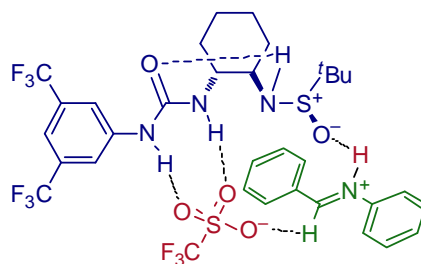


Scheme 2.8. Other chiral stronger Brønsted acid motives.

Chiral disulfonic acids and disulfonimides in Scheme 2.8 are stronger acids than phosphoric acids and can catalyze reactions inaccessible with chiral phosphoric acid catalysis, however their application in asymmetric Brønsted acid catalysis has proven challenging.

2. BACKGROUND

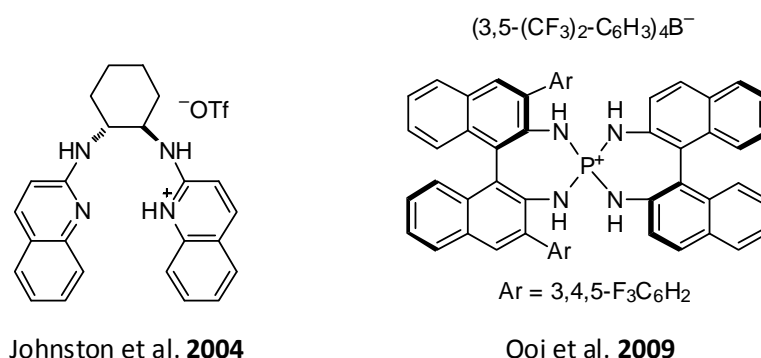
Recently Jacobsen introduced the interesting concept of asymmetric cooperative catalysis with achiral strong Brønsted acids and chiral ureas involving a network of attractive noncovalent interactions between the urea bound anion and the electrophile (Scheme 2.9).^[67] Although it is a beautiful demonstration of catalyst design, the generality of this concept remains to be fully explored.^[68]



Jacobsen et. al **2010**
(urea + $\text{CF}_3\text{SO}_3\text{H}$ + imine)

Scheme 2.9. Chiral urea and achiral strong acid cooperative catalysis.

In contrast to neutral Brønsted acids mentioned above, a number of cationic Brønsted acids has been also reported. Johnston and co-workers developed an ammonium salt for the aza-Henry reaction (Scheme 2.10).^[69] However, these types of catalysts are significantly less acidic than phosphoric acids. Ooi et al. introduced a chiral arylaminophosphonium barfate as charged Brønsted acid for highly enantioselective conjugate addition of arylamines to nitroolefins (Scheme 2.10).^[70]



Johnston et al. **2004**

Ooi et al. **2009**

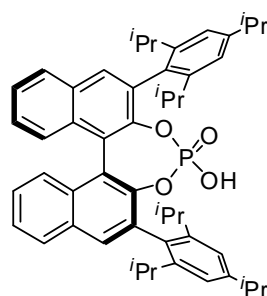
Scheme 2.10. Chiral cationic Brønsted acids.

In spite of the development of various catalyst classes phosphoric acids and *N*-triflyl phosphoramides (discussed in the following section) are currently by far the most successful strong Brønsted catalysts.

2.4. Chiral phosphoric acids and derivatives

2.4.1. Chiral environment

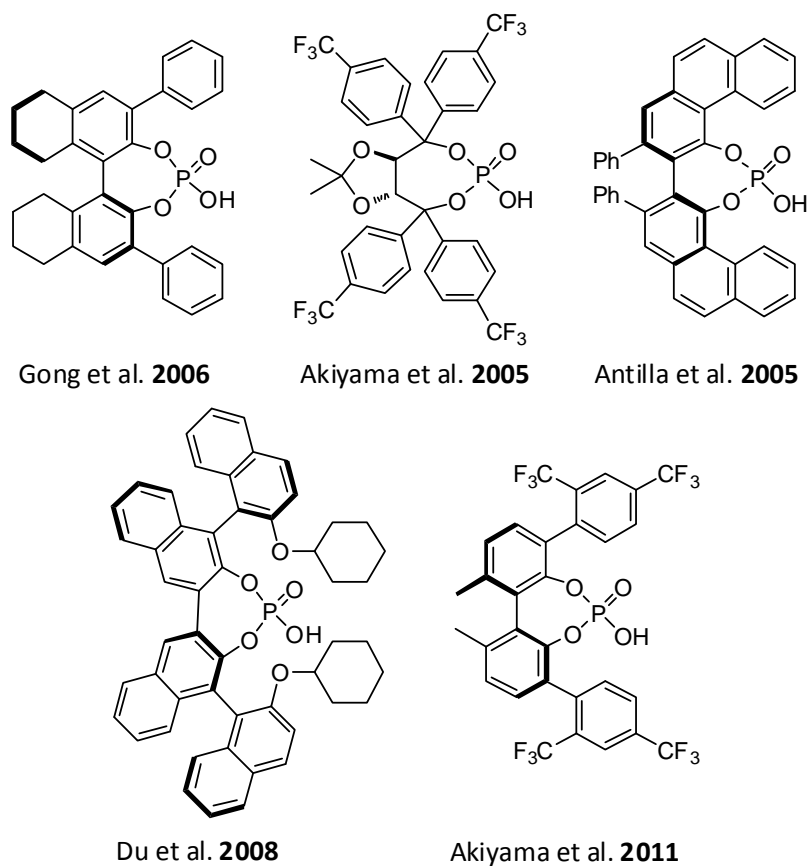
Since the initial reports describing chiral phosphoric acids as catalysts, they have become popular catalysts in asymmetric catalysis, and numerous reactions have been reported.^[35-36] Much of their success has been accredited to the readily modified 3,3'-substituents which provided an opportunity to place bulky groups near the active site. The placement of a bulky 2,4,6-*i*-Pr₃C₆H₂-group resulted in one of the most successful phosphoric acid catalysts, TRIP which was initially reported by List et al. for asymmetric transfer hydrogenation of imines (Scheme 2.11).^[71-72] The TRIP anion was also the counteranion of choice in pioneering studies in asymmetric-counteranion directed catalysis (ACDC) reported by Mayer and List in 2006^[73], a principle later also applied in metal catalysis by Toste et al.,^[74] and Mukherjee and List^[75].



TRIP
List et al. 2005

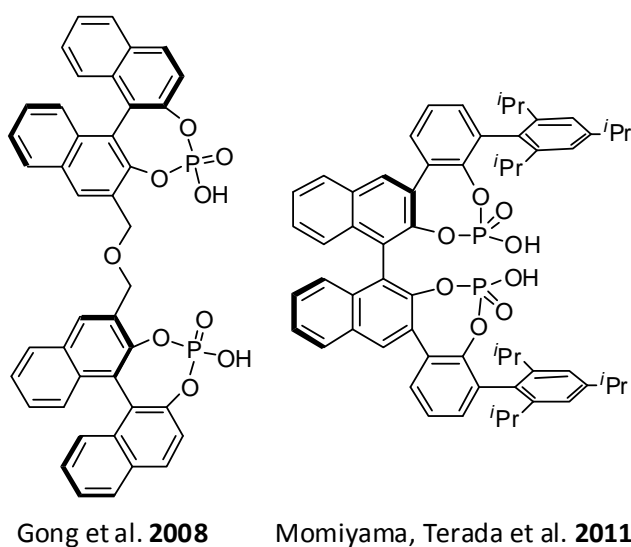
Scheme 2.11. One of the most successful phosphoric acid catalysts.

The success of BINOL-derived catalysts also prompted the development of catalysts with alternative backbones, with the aim of modifying geometrical parameters of the active site. The closely related H8-BINOL backbone proved more successful than BINOL backbone in certain cases (Scheme 2.12).^[76] Akiyama et al. introduced TADDOL-derived Brønsted acids, however these catalysts failed to promote highly enantioselective transformations.^[77] VAPOL-derived phosphoric acid introduced by Antilla et al. for synthesis of aminals proved superior to BINOL-derived catalysts in several cases (Scheme 2.12).^[78] A bis-BINOL derived phosphoric acid was introduced by Du et al. as the catalyst for the transfer hydrogenation of quinolines (Scheme 2.12).^[79] Biphenol-derived phosphoric acids were demonstrated as efficient catalysts for asymmetric C–H functionalization via an internal redox process (Scheme 2.12).^[80]



Scheme 2.12. Alternatives backbones for chiral phosphoric acids.

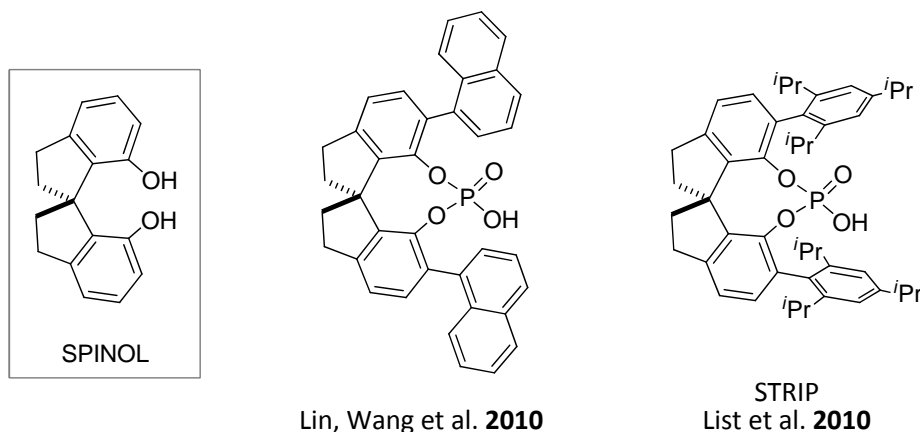
A bis-phosphoric acid developed by Gong et al. has been demonstrated as excellent catalyst for a three component 1,3-dipolar cycloaddition reaction (Scheme 2.13).^[81] Terada and coworkers reported in 2011 that a new bisphosphoric acid is capable of performing a highly enantioselective Diels–Alder reaction of α,β -unsaturated aldehydes with amidodienes (Scheme 2.13).^[82]



Scheme 2.13. Bisphosphoric acids.

2. BACKGROUND

Recently two independent reports presented the development of phosphoric acids based on SPINOL backbone.^[83-84] Ling, Wang and coworkers showed that naphthyl-substituted phosphoric acid is competent catalyst for the venerable asymmetric Friedel-Crafts reaction of indoles with imines (Scheme 2.14),^[83] giving comparable results to BINOL-derived phosphoric acid. Simultaneously our group has demonstrated that the SPINOL-derived phosphoric acid STRIP is a superior catalyst to the corresponding BINOL derived phosphoric acid TRIP in a kinetic resolution of alcohols via intramolecular transacetalization which is discussed in this thesis (Scheme 2.14).^[84] Since these two reports, several groups have utilized SPINOL-based phosphoric acids as Brønsted acid catalysts, in some cases demonstrating distinct advantages over BINOL counterparts.

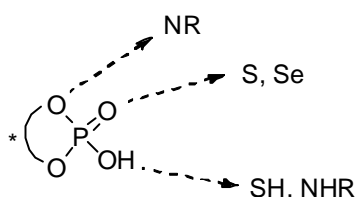


Scheme 2.14. SPINOL-derived phosphoric acids.

SPINOL-based catalysts seem to be comparably successful to the BINOL-derived phosphoric acids, however their application might be hampered by current long and demanding synthesis which includes more than 10 steps involving a resolution step.^[83-84]

2.4.2. Phosphoric acid derivatives

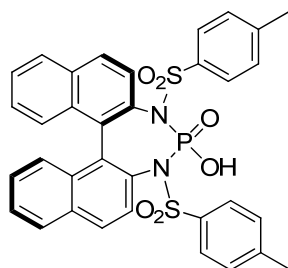
Replacing oxygen atoms of the phosphoric acid diester moiety with other atoms or groups leads to various derivatives, several of which were shown to be highly efficient stronger chiral Brønsted acids (Scheme 2.15).



Scheme 2.15. Derivatization of the phosphoric acid moiety.

2. BACKGROUND

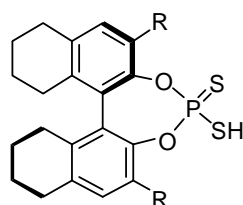
Terada's group developed a phosphordiamidic acid, which was employed in the direct Mannich reaction of *N*-acyl imines with 1,3-dicarbonyl compounds (Scheme 2.16).^[85] However, only low enantioselectivity was achieved.



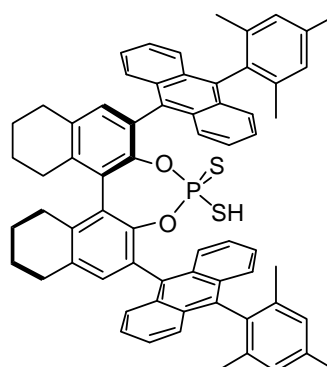
Terada et al. 2006

Scheme 2.16. Phosphordiamidic acid.

Dithiophosphoric acids were initially reported by Blanchet et al. and were demonstrated as highly active catalysts, although only low enantioselectivity was achieved (Scheme 2.17).^[86] Recently Toste et al. demonstrated a novel mode of Brønsted acid catalysis with chiral dithiophosphoric acids involving covalent activation of dienes and allenes (Scheme 2.17).^[87]



Blanchet et al. 2009



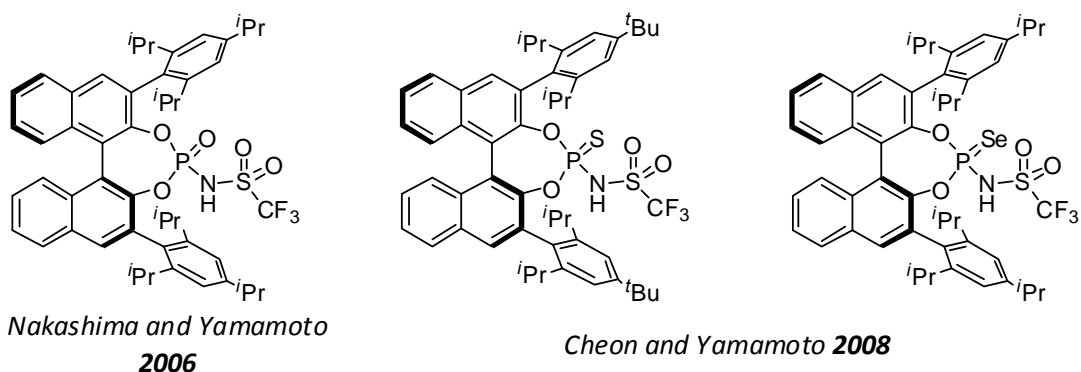
Toste et al. 2011

Scheme 2.17. Dithiophosphoric acids.

A major breakthrough in Brønsted acid catalysis was the discovery of chiral *N*-triflyl phosphoramides as strong chiral Brønsted acids by Nakashima and Yamamoto (Scheme 2.18).^[88] They demonstrated its application in the asymmetric Diels-Alder reaction for which the corresponding phosphoric acids are inactive catalysts due to their insufficient acidity. A number of other reactions could be catalyzed with chiral *N*-triflyl phosphoramides with high enantioselectivity and these catalysts are often referred to as Yamamoto's catalysts.^[89-90] Often the higher acidity of the chiral *N*-triflyl phosphoramides was crucial for the success of the

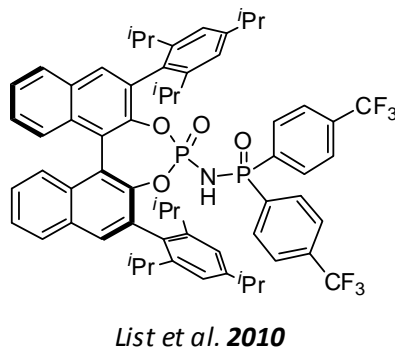
2. BACKGROUND

reaction. Later Cheon and Yamamoto also introduced thio- and seleno-derivatives for the protonation of enol silanes.^[91]



Scheme 2.18. *N*-triflyl phosphoramides and derivatives.

List et al. introduced a novel class of stronger Brønsted acids by replacing the triflyl group of Yamamoto's catalyst with a different electron-withdrawing moiety. The use of a phosphinyl moiety resulted in chiral *N*-phosphinyl phosphoramides which could be additionally structurally optimized by modifying the structure of the achiral phosphinyl moiety.^[92] These novel catalysts enabled a highly enantioselective direct asymmetric *N,O*-acetalization of aldehydes.



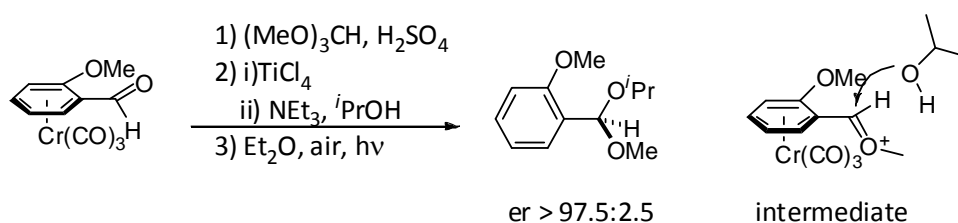
Scheme 2.19. *N*-phosphinyl phosphoramides.

Phosphoric acid catalysts based on BINOL or other backbones, although followed by several different acidic motives, are by far the most successful catalysts. With exception of Yamamoto's catalyst, all other moderately strong and strong Brønsted acid motives are very reaction specific. It is reasonable to say that the second generation of stronger chiral Brønsted acid catalysts has not been discovered yet.

2.5. Asymmetric synthesis of acetals

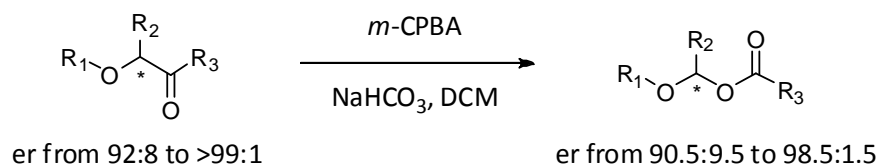
2.5.1. Chiral starting materials

Methods for the enantioselective synthesis of an acetal stereocenter are very limited. They are usually based on chiral starting materials or reagents. In 1996 Davies and Correia reported a stereoselective reaction of enantiopure *o*-substituted benzaldehyde chromium complex to give *o*-anisaldehyde methyl isopropyl acetal (Scheme 2.20).^[12] The enantioenriched aldehyde chromium complex was obtained by chromatographic separation of diastereomeric valinol imine derivatives.



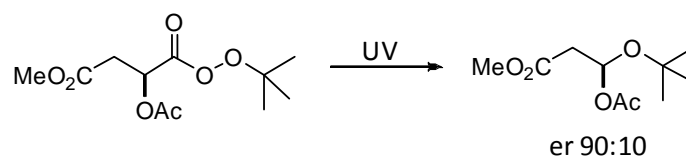
Scheme 2.20. From enantioenriched metal complexes.

Enantioenriched acyl alkyl acetals can be obtained from enantioenriched α -alkoxy ketones via Bayer-Villiger oxidation (Scheme 2.21).^[11]



Scheme 2.21. From enantioenriched α -alkoxy ketones.

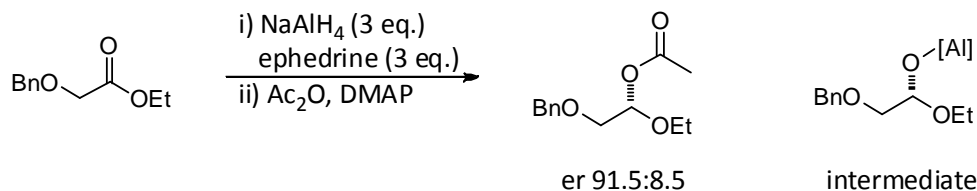
A recently reported photolytic decarboxylation of enantiopure α -acyloxy peresters also provides a route to enantioenriched acyl alkyl acetals (Scheme 2.22).^[13]



Scheme 2.22. From enantioenriched α -acyloxy peresters.

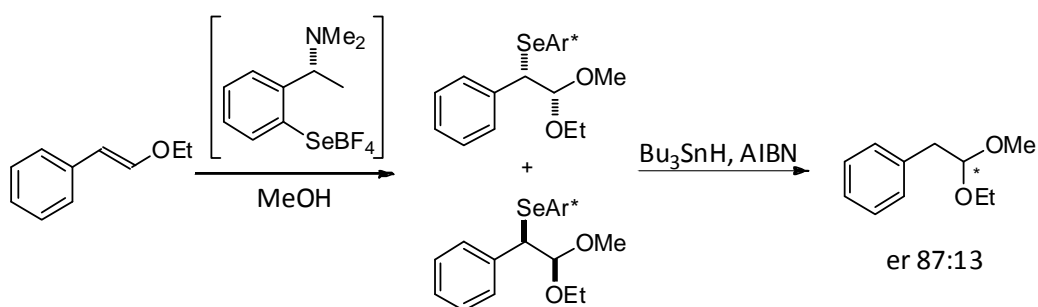
2. BACKGROUND

Another approach to acyl alkyl acetals has been described from achiral esters using a chiral reducing reagent with in situ acetylation of the enantioenriched alkoxy-aluminum intermediate (Scheme 2.23).^[15]



Scheme 2.23. Using enantioenriched reducing reagent.

Uchiyama et al. developed methoxyselenenylation of alkyl vinyl ethers with enantioenriched selenium reagent affording acetals with moderate to good enantioselectivity after removal of the selenium group (Scheme 2.24).^[14, 16]



Scheme 2.24. Using enantioenriched selenium reagents.

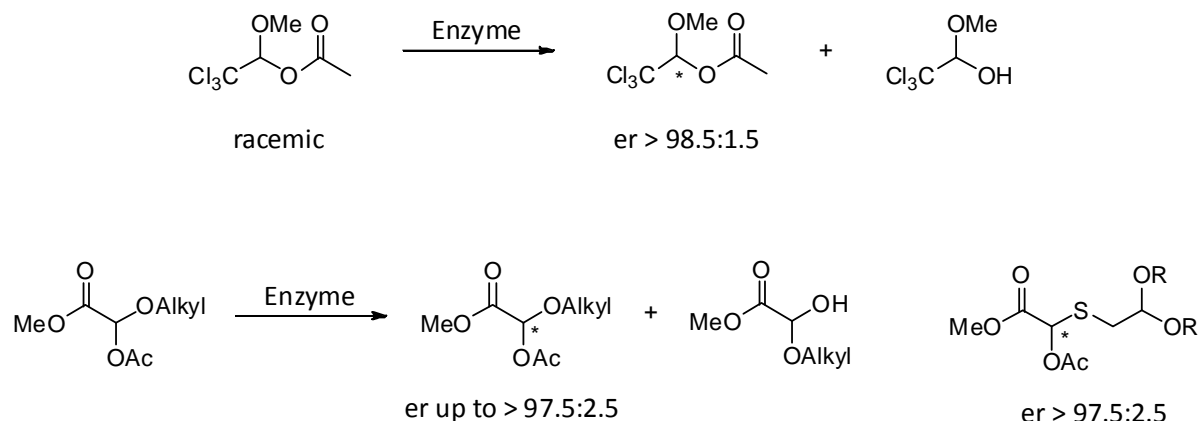
The aforementioned methods are either very substrate specific and/or not highly enantioselective and there are still no general approaches to chiral acetals with acetals carbon as the only stereogenic center from chiral enantioenriched starting materials or reagents.

2.5.2. Catalytic asymmetric methods

The most straightforward method to enantioenriched compounds is their catalytic asymmetric synthesis. The few catalytic asymmetric approaches to acetals with the acetal center as the only stereogenic element can be divided into reactions that do not involve the acetal carbon as the reaction center, and those which include the formation of the acetal moiety. For the later case only a single report existed prior to the work described in this thesis.

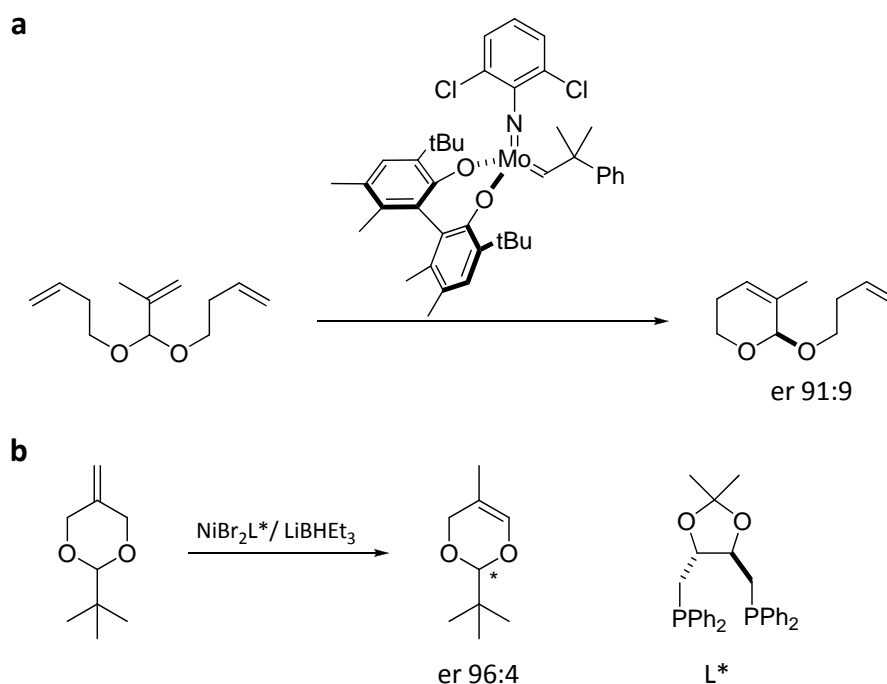
Transformations not involving acetal carbon

Enantioenriched acyl alkyl acetals can be accessed with enzymatic kinetic resolutions, which involve hydrolysis of an ester moiety as the enantioselective step (Scheme 2.25).^[93-95]



Scheme 2.25. Enantioenriched acetals via enzymatic kinetic resolution.

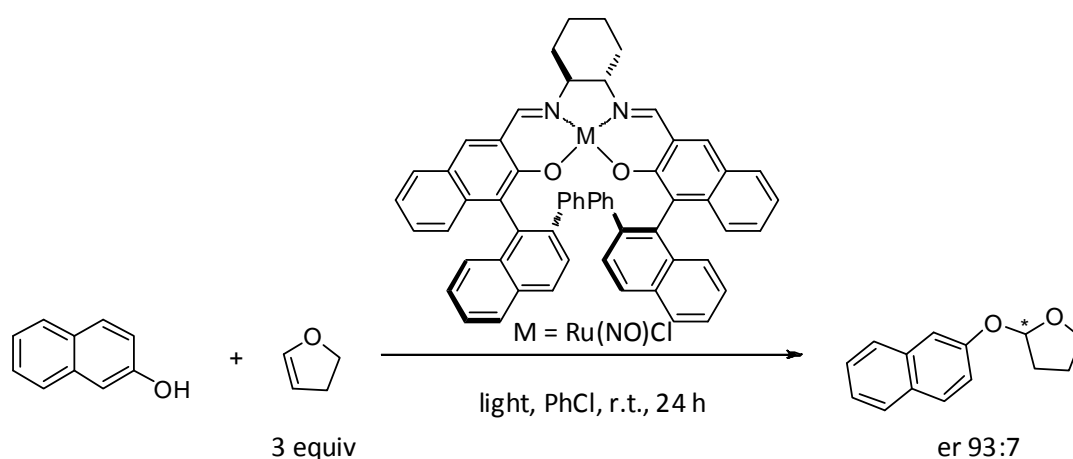
Catalytic asymmetric approaches to alkyl alkyl acetals with artificial catalysts have been described using metal catalyzed desymmetrizations. Ring closing metathesis of achiral triene acetals with a chiral molybdenum catalyst leads to enantioenriched cyclic acetals with good enantioselectivity (Scheme 2.26a).^[96-97] With a chiral nickel catalyst, an alkene isomerization of exocyclic double bonds to more stable endocyclic position can be achieved with high enantioselectivity giving highly enantioenriched acetals (Scheme 2.26b).^[98-99]



Scheme 2.26. Enantioenriched acetals via metal catalyzed desymmetrizations.

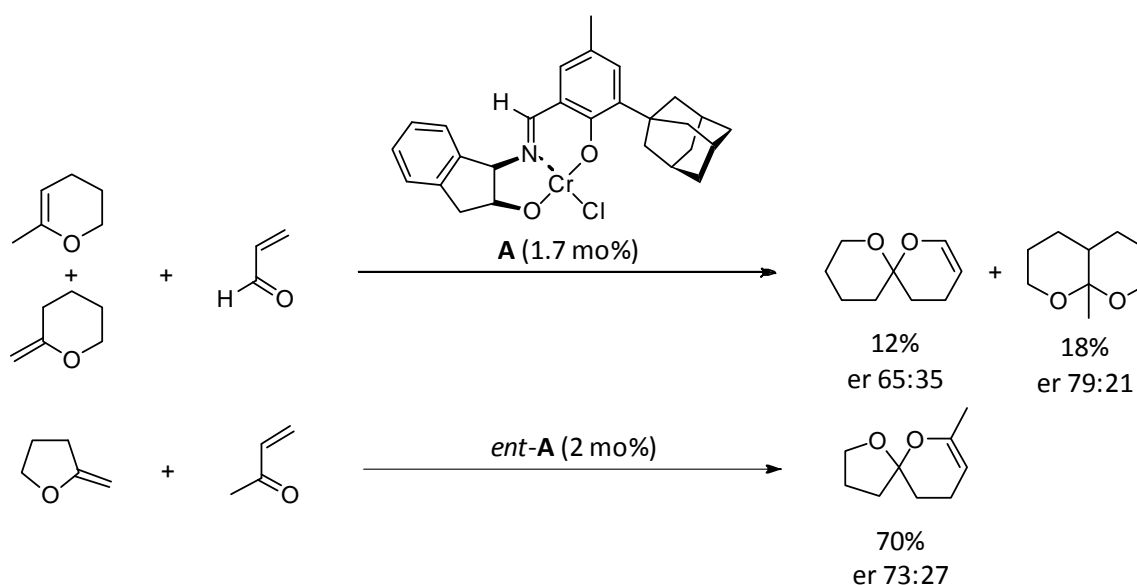
Transformations involving acetal carbon

Prior to our work a single catalytic asymmetric formation of acetals was achieved by Nagano and Katsuki via a metal-catalyzed hydroetherification of enol ethers (Scheme 2.27).^[100] Enantiomeric ratios up to 93:7 could be achieved with ruthenium catalyst although the exact mechanism of this transformation is unknown. This reaction is to the best of our knowledge the first catalytic asymmetric acetalization reaction, and only precedent prior to the work described in this thesis.



Scheme 2.27. First catalytic asymmetric acetal formation reaction.

A few attempts towards an asymmetric synthesis of spiroacetals have been described in the Ph.D. thesis of M. Fritzsche, from the research group of Prof. W. Francke (Scheme 2.28).^[34]

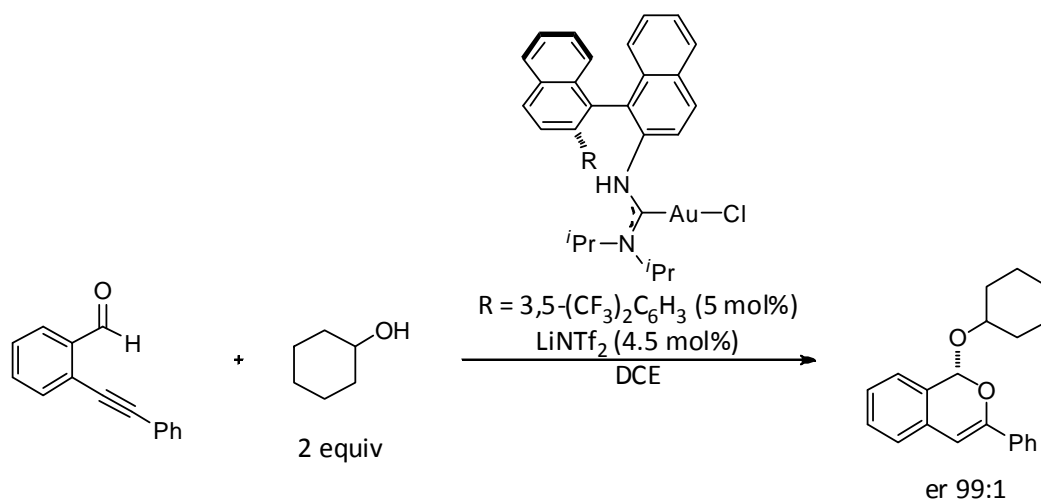


Scheme 2.28. Asymmetric synthesis of acetals and spiroacetals via Diels-Alder reaction.

2. BACKGROUND

They described a chiral chromium complex catalyzed Diels-Alder reaction^[30] between enol ethers and acrolein or methyl vinyl ketone yielding spiroacetals and fused bicyclic acetal with low to moderate enantioselectivity (Scheme 2.28).

Very recently, after our studies described in this thesis were published, Handa and Slaughter reported enantioselective alkynylbenzaldehyde cyclizations catalyzed by chiral gold(I) diaminocarbene complexes giving acetals with very high enantioselectivity (Scheme 2.29).^[101]

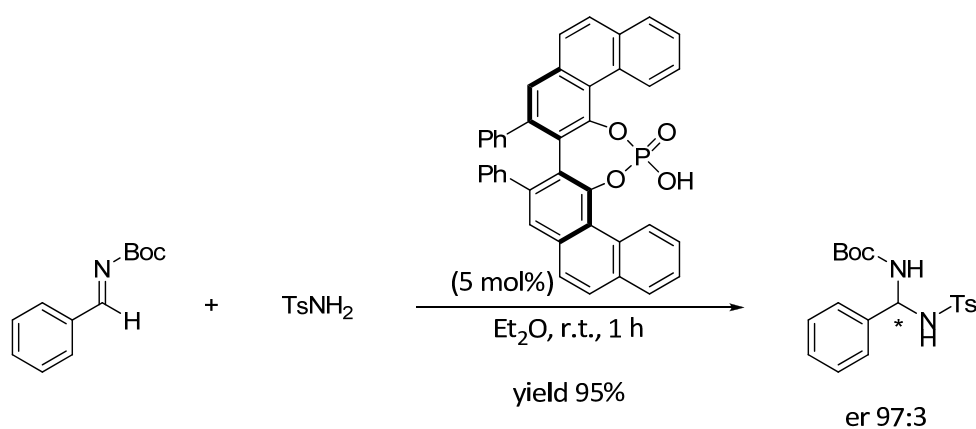


Scheme 2.29. Gold catalyzed asymmetric acetal formation.

2.5.3. Catalytic asymmetric syntheses of *N,X*-acetals (*X* = N, O, S, Se)

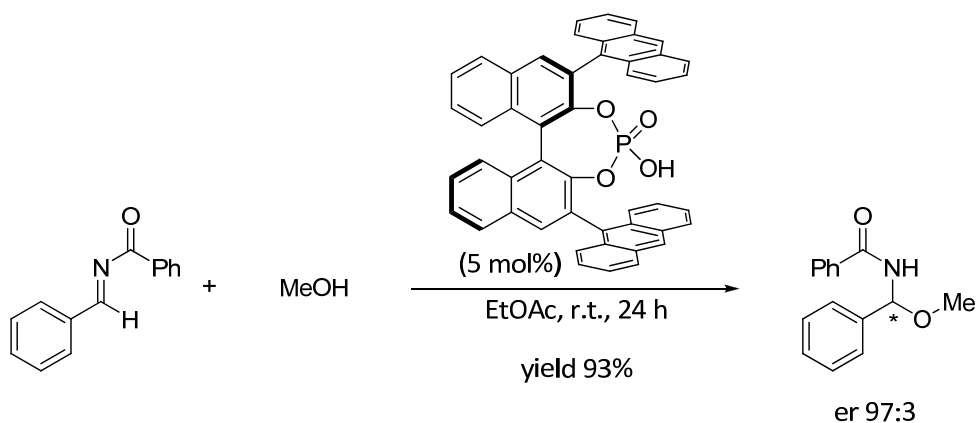
Although *N,N*-, *N,O*-, and *N,S*- acetals, compared to *O,O*-acetals, are far less common motives in natural products and organic synthesis their catalytic asymmetric syntheses have been developed recently. All of the reported reactions are based on the well known ability of phosphoric acids and their derivatives to catalyze asymmetric additions of nucleophiles to imines.

Asymmetric syntheses of *N,N*-acetals catalyzed by a chiral Brønsted acid were initially reported by Antilla et al. in 2005 (Scheme 2.30).^[78, 102]



Scheme 2.30. Catalytic asymmetric synthesis of *N,N*-acetals.

Later the Antilla group also developed a catalytic asymmetric addition of alcohols to imines giving chiral *N,O*-acetals with high enantioselectivity (Scheme 2.31).^[103]

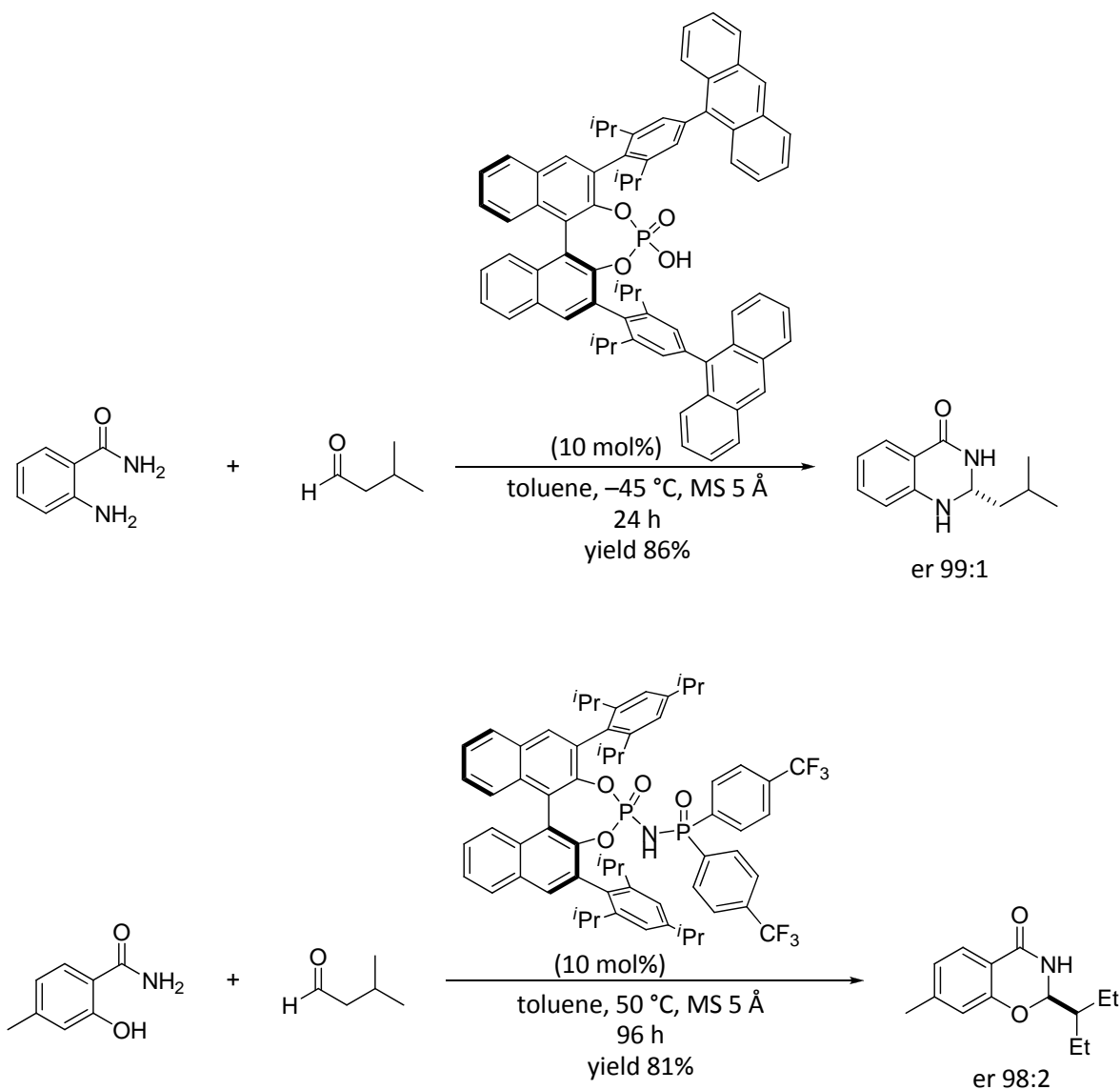


Scheme 2.31. Catalytic asymmetric synthesis of *N,O*-acetals.

Subsequently List et al. developed direct asymmetric *N,N*- and *N,O*-acetalizations of aldehydes to access cyclic *N,N*- and *N,O*-acetals, which are found in several pharmaceuticals (Scheme

2. BACKGROUND

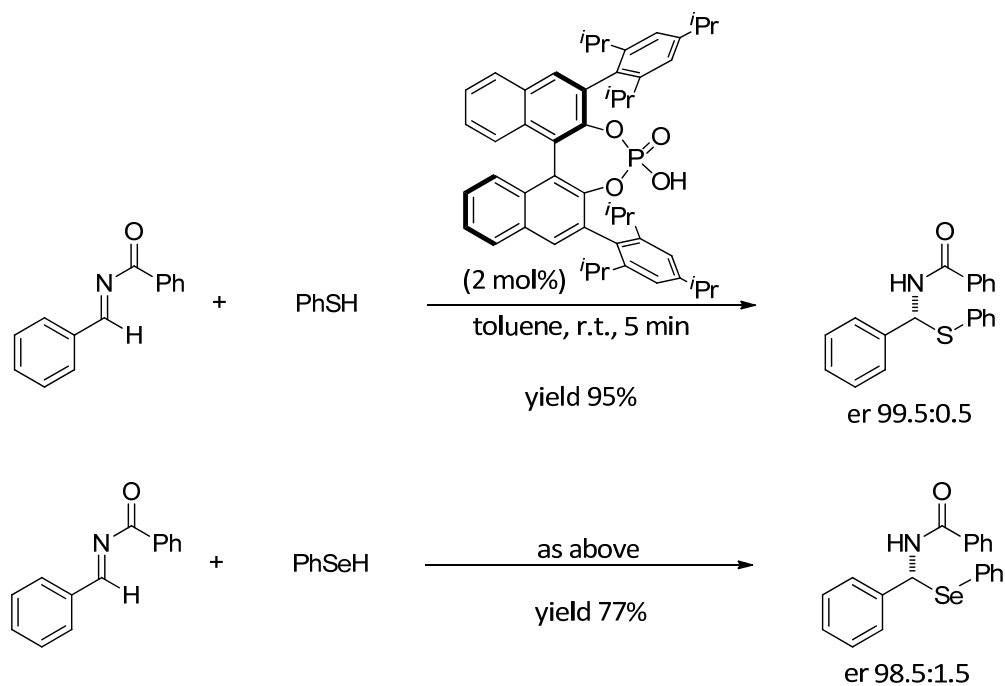
2.32).^[92, 104] The crucial step of these reactions is the intramolecular asymmetric addition to an imine intermediate. Later a variant of the direct asymmetric *N,N*-acetalization of aldehydes employing aromatic aldehydes was published by Rueping et al.^[105]



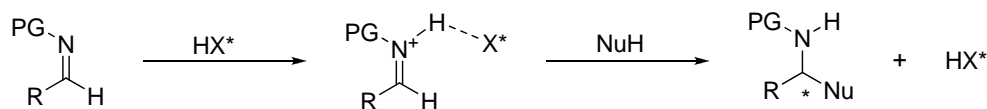
Scheme 2.32. Direct catalytic asymmetric *N,N*- and *N,O*- acetalizations of aldehydes.

More recently Antilla et al. also reported syntheses of enantioenriched *N,S*- and *N,Se*-acetals starting from imines (Scheme 2.33).^[106]

All of the above mentioned *N,X*-acetalizations ($X = N, O, S, Se$) are based on the enantioselective addition to an iminium ion intermediate. Imines are readily activated by Brønsted acids due to their basicity and the intermediate iminium salts possess strong hydrogen bonding to the chiral anion of the Brønsted acid (Scheme 2.34). This makes the ion pair reasonably well organized enabling an efficient enantiocontrol.



Scheme 2.33. Catalytic asymmetric synthesis of *N,S*- and *N,Se*-acetals.



Scheme 2.34. Mechanism of Brønsted acid catalyzed asymmetric *N,X*-acetalizations.

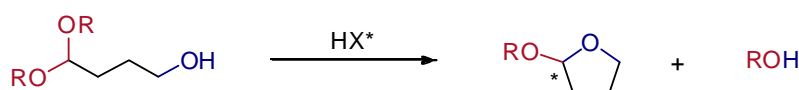
O,O-Acetals present an additional challenge as enantioselective additions to oxocarbenium ion intermediates that could potentially lead to chiral *O,O*-acetals, are much less explored compared to additions of nucleophiles to imines.^[37-39]

3. OBJECTIVES OF THIS PH.D. WORK

3.1. Catalytic Asymmetric Acetalizations

The objectives of this Ph.D. work were identification and optimization of reactions which would enable the formation of an acetal stereocenter in an enantioselective fashion, with a focus on Brønsted acid catalyzed reactions.

One of the reactions targeted was a transacetalization reaction, in which one alkoxy-group of an acetal is exchanged with another one. Although transacetalization reactions usually require relatively strong Brønsted acid catalysts, it was reasoned that an intramolecular variant might be amenable to mild asymmetric Brønsted acid catalysis (Scheme 3.1). An additional challenge present within this transformation was the asymmetric substitution of simple *O,O*-acetals using chiral Brønsted acid catalysts, which has not been described previously.

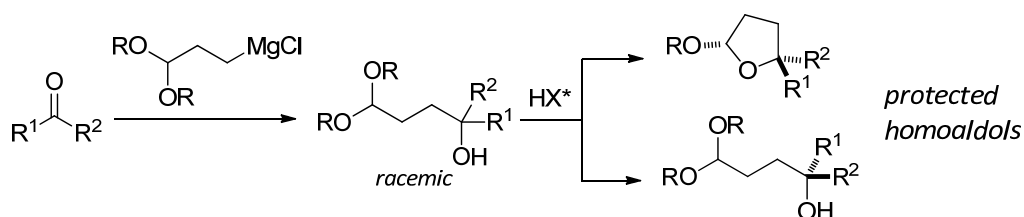


Challenges:

- catalytic highly enantioselective acetal formation
- catalytic asymmetric substitution of acetals using chiral Brønsted acids
- potential product racemization

Scheme 3.1. Intramolecular transacetalization.

Both starting materials and products of the intramolecular transacetalization reaction are protected γ -hydroxycarbonyl compounds, or homoaldols. Homoaldols are versatile motifs in organic synthesis that can be easily transformed into a vast array of important chiral compounds such as γ -lactones, tetrahydrofurans, pyrrolidines, and others. Based on the transacetalization reaction, the development of a practical kinetic resolution to obtain these useful compounds was next sought after (Scheme 3.2).



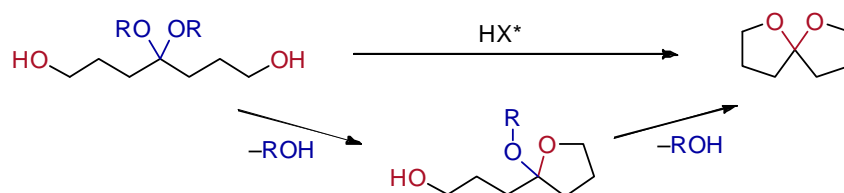
Scheme 3.2. Kinetic resolution of aldehyde homoaldols.

3. OBJECTIVES OF THIS PH.D. WORK

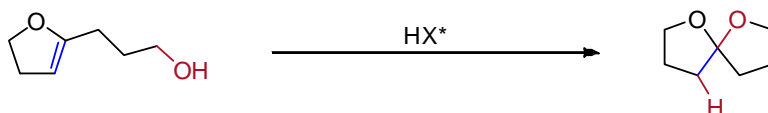
The reaction would present the first example of a kinetic resolution of alcohols via acetal formation, and of a Brønsted acid catalyzed kinetic resolution of alcohols.

Spiroacetals

The next objective of this work was the development of a Brønsted acid catalyzed asymmetric spiroacetalization reaction. Two approaches were targeted: double catalytic asymmetric transacetalization (Scheme 3.3) and spiroacetalization of hydroxyenoethers (Scheme 3.4).



Scheme 3.3. Spiroacetals via double transacetalization.

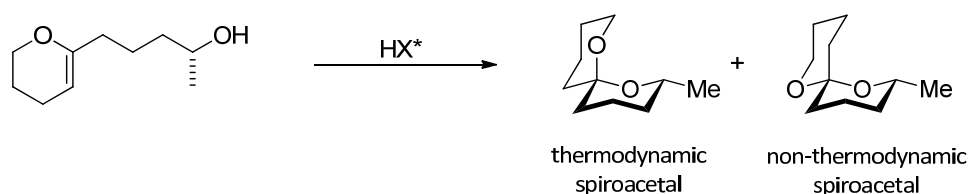


Challenges:

- *asymmetric reaction with a small molecule*
- *asymmetric addition of heteroatom nucleophiles to oxocarbenium intermediates*

Scheme 3.4. Spiroacetals from hydroxyenoethers.

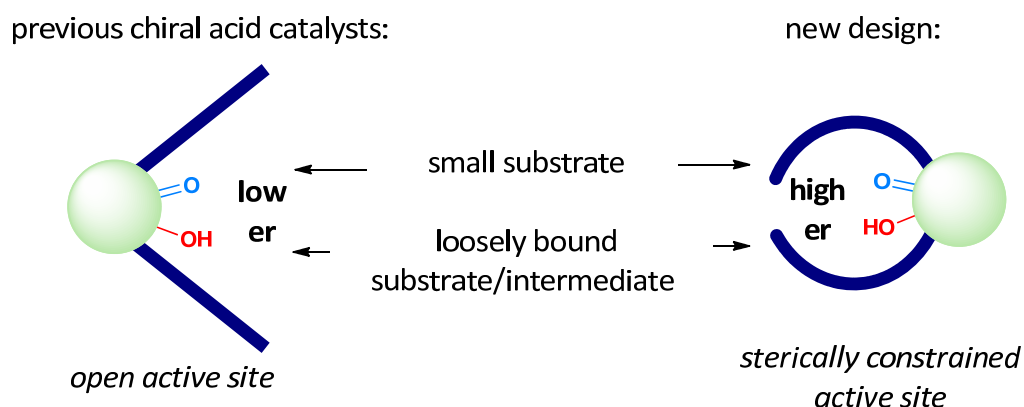
When other stereocenters are present in the target molecule, accessing the spiroacetal stereocenter in the most stable thermodynamic configuration is usually trivial. However, the formation of fragile nonthermodynamic spiroacetals, having the less stable configuration of the spiroacetal stereocenter, presents a formidable challenge for organic synthesis.^[2, 31-33] An ideal solution would be provided by a catalyst that could override the inherent thermodynamic preference and control the spiroacetal configuration. If a catalytic asymmetric spiroacetalization would be achieved, this goal could be also targeted (Scheme 3.5).



Scheme 3.5. Catalyst directed synthesis of nonthermodynamic or thermodynamic spiroacetal.

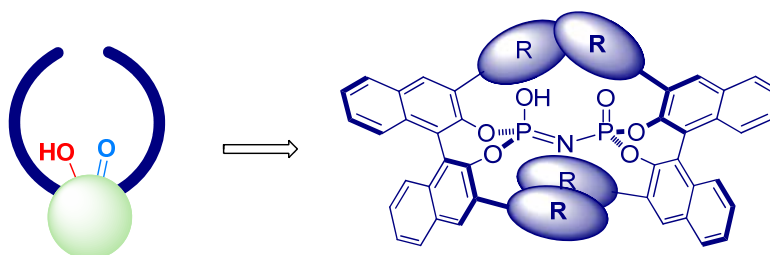
3.2. Confined Brønsted acids

The field of Brønsted acid catalysis has acquired wide popularity and importance in recent years. However, reactions of small aliphatic substrates that do not possess sterically demanding protecting groups, large aromatic/planar surfaces, or bulky substituents are still extremely rare.^[35-36, 58-59, 88, 92] This might be due to the inability of current synthetic Brønsted acid catalysts to provide a truly compact chiral microenvironment. Presumably, such an environment could effectively restrict molecular motion, leading to efficient enantiodiscrimination even of substrates or intermediates, which lack spatially defined interactions such as hydrogen bonding with the catalyst. The design of new Brønsted acid catalysts that display a sterically highly demanding and rigid chiral microenvironment was targeted in this work to enable asymmetric acetalizations and other reaction types that are beyond the ability of the currently known catalysts (Scheme 3.6).



Scheme 3.6. New catalyst design.

After detailed analysis of existing stronger Brønsted acid catalysts, C_2 -symmetric imidodiphosphoric acids were targeted as the motifs that could be suitable for achieving this goal (Scheme 3.7).



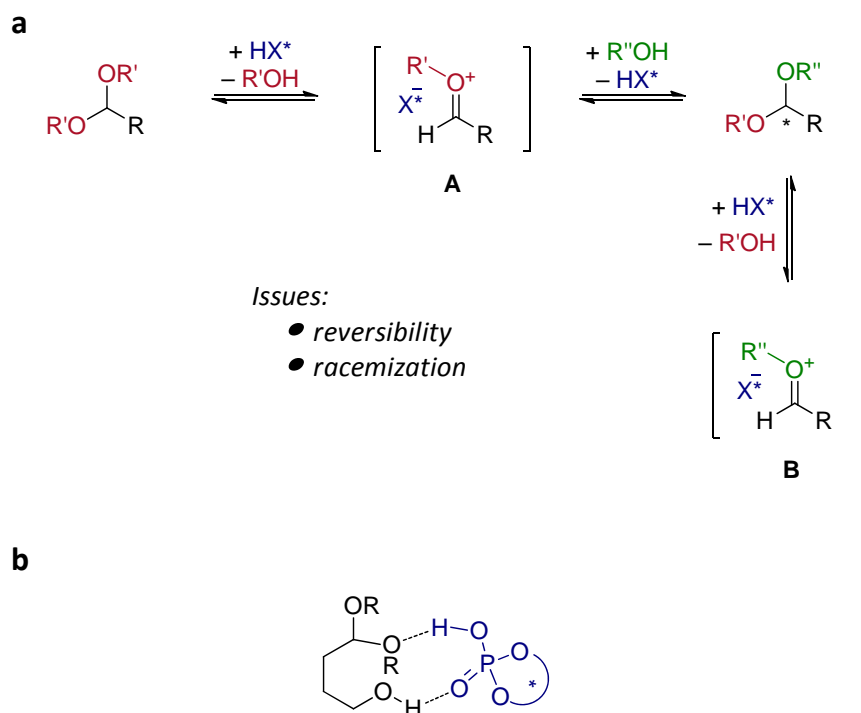
Scheme 3.7. Confined C_2 -symmetric imidodiphosphoric acids.

4. RESULTS AND DISCUSSION

4.1. Catalytic asymmetric transacetalization

4.1.1. Reaction design and optimization

Transacetalization reactions usually require relatively strong Brønsted acid catalysts and proceed via oxocarbenium ion intermediates (Scheme 4.1a). An obvious issue related to the transacetalization reaction lies in the functional similarity of the starting material and the product. Both are acetals, and the product could be activated by the catalysts as well, reversibly forming oxocarbenium ions **A** and **B** (Scheme 4.1a), leading to racemization of the product.



Scheme 4.1. a) Intermolecular transacetalization reaction; b) proposed bifunctional activation of the substrate in the intramolecular version.

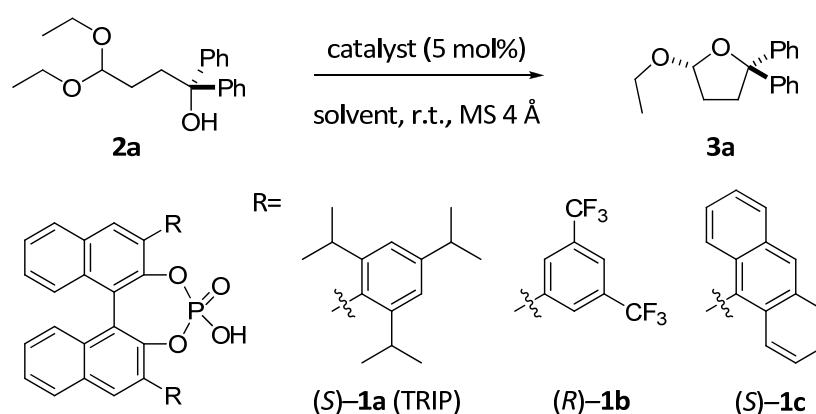
However, we reasoned that an intramolecular variant of the transacetalization reaction might be amenable to mild asymmetric Brønsted acid catalysis.^[107] A hydrogen bonded complex of the substrate and a chiral acid might be formed, selectively activating the hydroxyl acetal over the product, which does not possess OH moiety (Scheme 4.1b). The hydroxyl moiety in the substrate might serve as a catalyst directing group and also increase the acidity of the

4. RESULTS AND DISCUSSION

phosphoric acid through hydrogen bonding. We envisioned that this design could potentially address problems resulting from the reversibility of the reaction and product racemization. We expected that by using chiral Brønsted acid catalyst, a chiral counteranion for the oxocarbenium ion would provide an asymmetric environment for the subsequent alcohol attack.^[37-39, 73]

We began our investigation by studying the reaction of alcohol **2a** to give acetal **3a** using phosphoric acid catalyst **1a** ((*S*)-TRIP), with bulky 2,4,6-*i*-Pr₃C₆H₂ substituents in 3,3'-positions (Table 4.1).^[71-72] With 5 mol% of (*S*)-TRIP in CHCl₃, the intramolecular transacetalization of substrate **2a** proceeded with a promising er of 76:24 (Table 4.1, Entry 1).

Table 4.1. Optimization of reaction conditions.^a



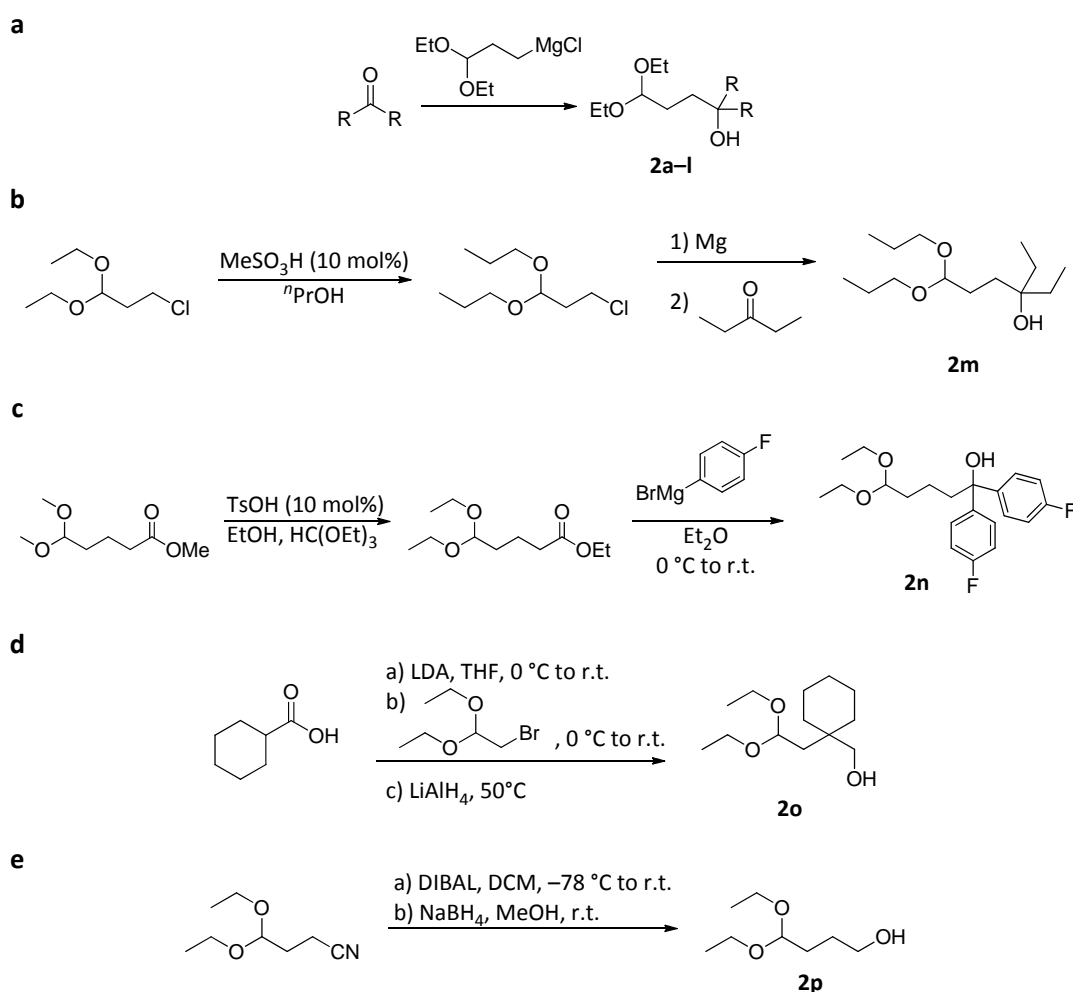
entry	catalyst	solvent	time	er
1 ^b	1a	CHCl ₃	6 h	76:24
2	1a	CHCl ₃	4 h	91:9
3	1a	toluene	2 h	87:13
4	1a	hexane	1 h	71:29
5	1a	benzene	2 h	90:10
6	1a	CHCl ₃ /benzene 1:1	3 h	91.5:8.5
7	1b	CHCl ₃ /benzene 1:1	< 1 h	22:78
8	1c	CHCl ₃ /benzene 1:1	< 1 h	82:18
9 ^c	1a (1 mol%)	benzene	2 days	94.5:5.5

a) Unless otherwise specified reactions were performed on 0.025 mmol scale (0.1 M solution), 4 Å MS (10 mg) at room temperature. *b)* Without MS. *c)* 0.025 M solution, 20 °C.

Gratifyingly, prolonged reaction time did not lead to any observable decrease in optical purity, suggesting that under the reaction conditions, the rates of the reverse reaction and product epimerization via oxocarbenium ion were negligible. With molecular sieves a significant increase in enantioselectivity was observed (entry 2). This suggested that ethanol, which is formed during the reaction has a detrimental effect on the enantioselectivity. Additional solvent and catalyst screening (including acids **1b** and **1c**) left TRIP as the optimal catalyst (entries 3-8). Gratifyingly, reduction in both the catalyst loading and the concentration had beneficial effects on the enantioselectivity and an er of 94.5:5.5 was achieved with only 1 mol% of TRIP (entry 9).^[107]

4.1.2. Substrate scope

With optimized conditions in hand, we set out to explore the substrate scope.^[107] The starting materials **2** were available in one or two steps from commercial materials (Scheme 4.2).



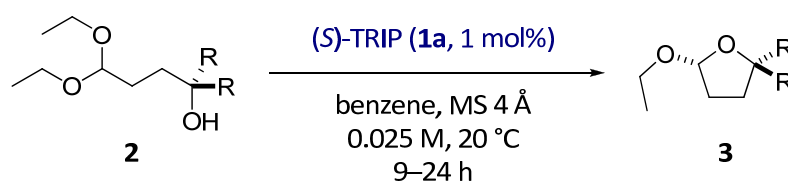
Scheme 4.2. Preparation of substrates.

4. RESULTS AND DISCUSSION

Notably, standard substrates, 4,4-disubstituted γ -hydroxyacetals, are easily accessible from the corresponding ketones via the Grignard reaction (Scheme 4.2a).

It was observed in some cases that neat substrates **2** undergo a slow intramolecular transacetalization spontaneously. However this can be avoided by storing the substrates as solutions in basic solvents such as diethyl ether or ethyl acetate, and removing the solvent shortly before the asymmetric reaction. It was found that various tertiary alcohols form five-membered cyclic acetals **3** in excellent yields and with high enantiomeric ratios (Table 4.2). Both aliphatic and aromatic substituents on the alcohol are well tolerated. Electron rich or poor aromatic substituents resulted in equally successful reactions (entries 2-3). Increasing the steric demand of aliphatic substituents led to higher enantioselectivity, with isopropyl substituted alcohol **3h** giving the highest enantiomeric ratio of 98:2 (entry 8). A more bulky alcohol **3i** with *tert*-butyl substituents gave the same result (entry 9).

Table 4.2. Substrate scope of the transacetalization reaction.^a



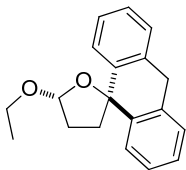
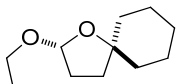
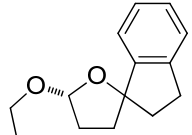
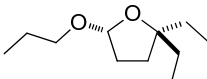
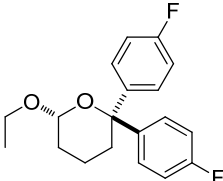
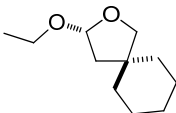
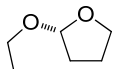
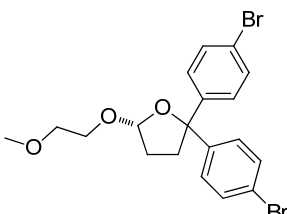
entry	product	yield/%	er	
1	R = C ₆ H ₅	3a	95	94.5:5.5
2	R = 4-(MeO)C ₆ H ₄	3b	96	95.5:4.5
3	R = 4-FC ₆ H ₄	3c	98	97:3
4 ^b	R = 4-BrC ₆ H ₄	3d	99	97:3
5 ^c		3e	86	95.5:4.5
6	R = Me	3f	84	94.5:5.5
7	R = Et	3g	92	97:3
8	R = ⁱ Pr	3h	93	98:2
9	R = ^t Bu	3i	90	98:2
10	R = CH ₂ Ph	3j	98	97:3

Table 4.2. continued

11		3k	94	97:3
12	 dr (<i>cis/trans</i>) = 1.1:1	3l	96	91:9 (<i>cis</i>) 96:4 (<i>trans</i>)
13		3m	95	95:5
14 ^c		3n	96	82:18
15 ^c		3o	94	82.5:17.5
16		3p	76	79:21
17 ^d		3q	94	79:21

a) Unless otherwise specified reactions were performed on 0.3 mmol scale with molecular sieves (50 mg/0.1 mmol). All yields refer to isolated yields. Enantiomeric ratios were determined by HPLC or GC analysis on a chiral stationary phase. b) Reaction performed on 0.9 mmol scale. c) Reaction time: **3e**, 7 days; **3n**, 4 days; **3o**, 30 min. d) With 10 mol% of TRIP, reaction time: 3 days.

We have also applied our intramolecular transacetalization reaction to the parallel kinetic resolution of chiral tertiary alcohol **2l**. Acetal **3l**, which contains a quaternary carbon stereogenic center was obtained in excellent yield and high enantioselectivity for both diastereomers (er 91:9 and er 96:4, entry 12). The effect of the pre-existing tertiary alcohol stereogenic center on the stereochemical outcome of the reaction appears to be small. An acetal containing longer *O*-alkyl substituents at the acetal moiety is also well tolerated (entry

13), however a slight decrease in the enantioselectivity was observed compared to ethyl acetal (entry 7). An attempt to extend the intramolecular transacetalization to a six-membered acetal was met with limited success, giving moderate enantioselectivity (entry 14). Likewise primary alcohols do not seem to be very successful substrates. Due to the Thorpe-Ingold effect the reaction of hydroxyacetal **2o** proceeded very fast giving full conversion in less than 30 minutes (entry 15). Simple acetal **3p** could also be obtained however only with moderate enantiomeric ratio (entry 16). The synthesis of methoxyethyl acetal **3q** required increased catalyst loading, and only moderate enantioselectivity was achieved (entry 17).

The absolute configuration of bromo-substituted acetal **3d** was determined to be (*R*) by single-crystal X-ray analysis (Figure 4.1), and configurations of other products were assigned by analogy. Product **3d** was obtained on a 0.9 mmol scale with a 99% isolated yield and enantiomeric ratio of 97:3 using 1 mol% of (*S*)-TRIP catalyst.^[107]

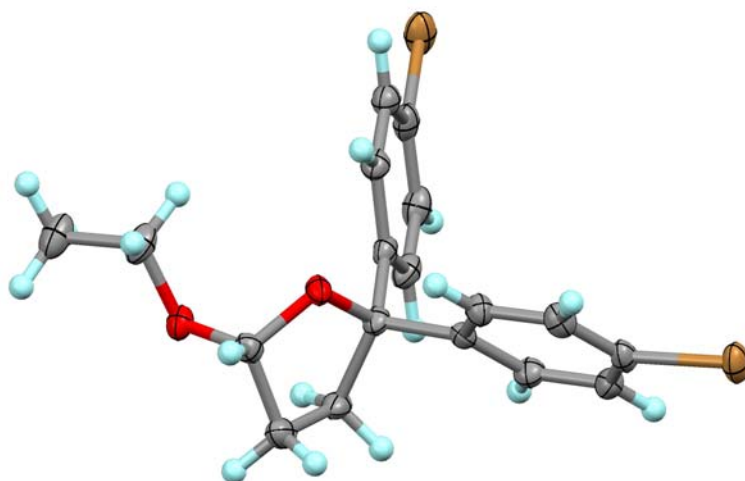
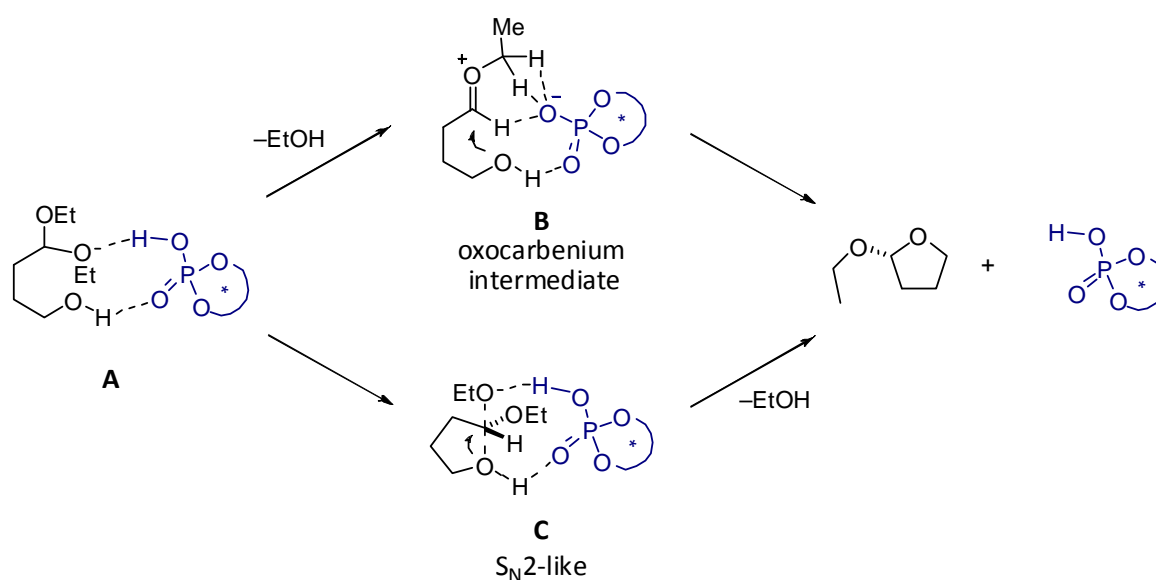


Figure 4.1. X-ray structure of acetal **3d**.^[107]

4.1.3. Discussion

The catalytic asymmetric transacetalization reaction was successfully established giving access to chiral acetals with the acetal carbon as the only stereogenic center.^[107] For the first time a catalytic asymmetric formation of an acetal stereocenters could be achieved with high enantioselectivity. In addition the reaction presents, to the best of our knowledge, a first example of phosphoric acid catalyzed enantioselective addition of nucleophiles to simple *O,O*-acetals.

Regarding the mechanism of the reaction, we believe that the bifunctional character of the phosphoric acid is essential for the observed selective reactivity and enantioselectivity. A hydrogen bonded complex such as **A** might account for the selective activation of the hydroxyl acetal over the product, which does not possess an OH-moiety (Scheme 4.3). The hydroxyl moiety in the substrate might serve as a catalyst directing group and also increase the acidity of the phosphoric acid through hydrogen bonding. Subsequent cyclization might proceed through an oxocarbenium intermediate, in which the phosphate anion provides a chiral environment through hydrogen bonding interactions with the oxocarbenium ion moiety and the hydroxyl group (**B**, Scheme 4.3). Another possibility is an S_N2 -like pathway in which the catalyst bridges the pentacoordinate transition state activating simultaneously the leaving group by protonation and the alcohol nucleophile with the Brønsted basic oxygen of the phosphate (**C**, Scheme 4.3).^[107]



Scheme 4.3. Possible mechanisms.

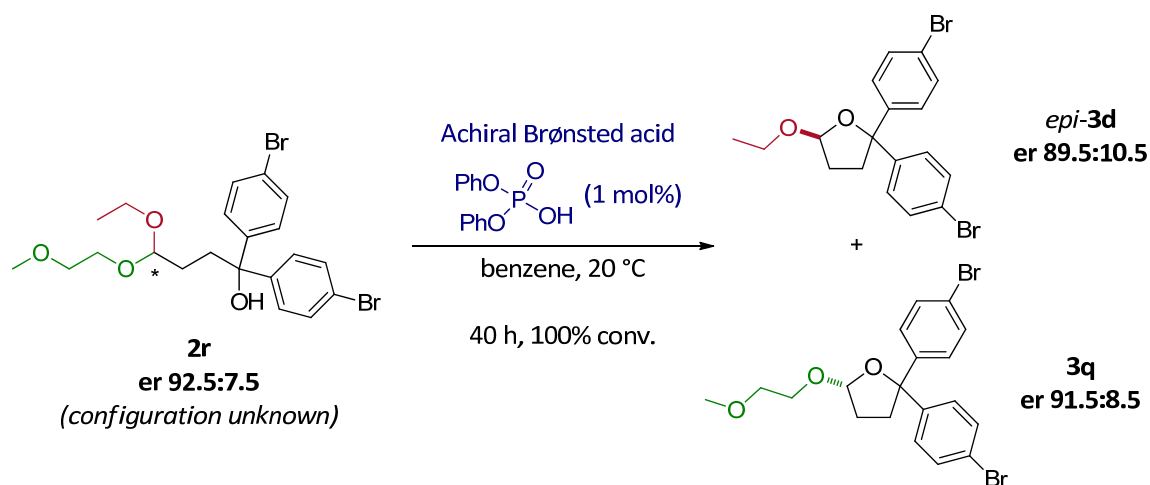
Mechanistic studies

To differentiate these two mechanistic scenarios we have designed an experiment with enantioenriched mixed acetal **2r** as a stereochemical probe (Scheme 4.4). Enantioenriched **2r** was obtained after HPLC separation of enantiomers on a chiral stationary phase. If an S_N2 -type mechanism is involved then the transacetalization reaction has to proceed with inversion at the acetal carbon. Reacting **2r** with achiral phosphoric acid catalyst resulted in the formation of acetals *epi-3d* and **3q** with almost complete preservation of the stereochemical information (Scheme 4.4). Somewhat lower er of the products is probably a result of slow racemization.

4. RESULTS AND DISCUSSION

Increased reaction time was required for the complete conversion due to lower reactivity of **2r** compared to standard diethyl hydroxyacetal substrates.

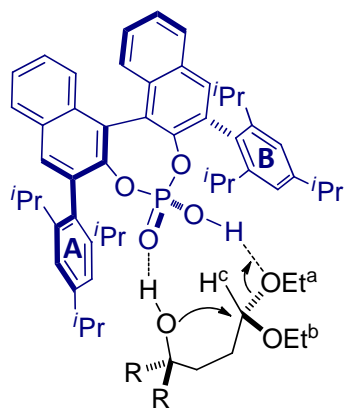
Although preservation of the stereochemical information suggests an S_N2 -type mechanism, determination of the absolute configuration of the starting material is necessary to confirm the inversion at the acetal carbon. However, attempts to obtain crystals of **2r** for X-ray analysis were not successful so far. Without the absolute configuration of the acetal **2r** some kind of an S_N1 -type mechanism, which would include a memory of chirality effect cannot be excluded at this point.



Scheme 4.4. Mechanistic investigations: stereospecific substitution.

Stereochemical model

If an S_N2 -type mechanism is operational than the stereochemical model in Scheme 4.5 might account for the observed enantioselectivity. In the model the catalyst simultaneously activates the leaving group OEt^a and the alcohol nucleophile. The hydrogen atom H^c is probably oriented towards the phosphate due to sterical reasons, and might engage in hydrogen bonding interactions with the phosphate in the transition state. The OEt^b group which remains in the product is positioned away from the bulky substituent **B** on the catalyst (Scheme 4.5). This arrangement of OEt groups in the transition state is consistent with the observed (*R*)-stereochemistry of the products. The initial DFT studies performed in collaboration with M. Patil (group of Prof. W. Thiel) also supports the stereochemical model in Scheme 4.5 and an S_N2 -type mechanism.



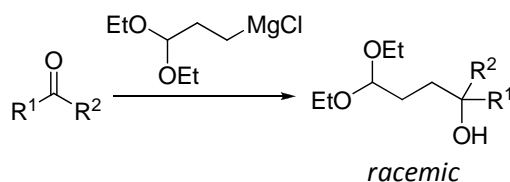
Scheme 4.5. Proposed stereochemical model for the S_N2-type transacetalization mechanism.

4.2. Kinetic resolution of homoaldols via catalytic asymmetric transacetalization

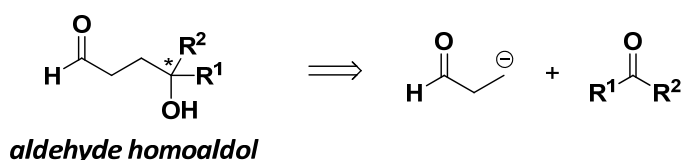
(with S. Müller)^[108]

4.2.1. Reaction design and optimization

The γ -hydroxyacetals used for the transacetalization reaction are easily accessible in one step from the corresponding carbonyl compounds (Scheme 4.6). These compounds are acetal protected homoaldols, highly valuable compounds with 1,4-dioxygenation pattern. For aldols, which possess 1,3-dioxygenation pattern, numerous asymmetric aldol-type reactions are available. However, corresponding 1,4-dioxygenated pattern presents a problematic disconnection in asymmetric catalysis (Scheme 4.7).

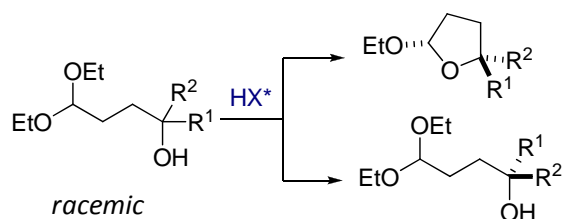


Scheme 4.6. Preparation of acetal protected homoaldols.



Scheme 4.7. Problematic homoaldol retrosynthetic disconnection.

We hypothesized that for racemic chiral homoaldols ($R^1 \neq R^2$, Scheme 4.6) our transacetalization reaction might proceed with kinetic resolution, giving enantioenriched homoaldols in the form of cyclic acetal products and acyclic starting homoaldols (Scheme 4.8).^[84]



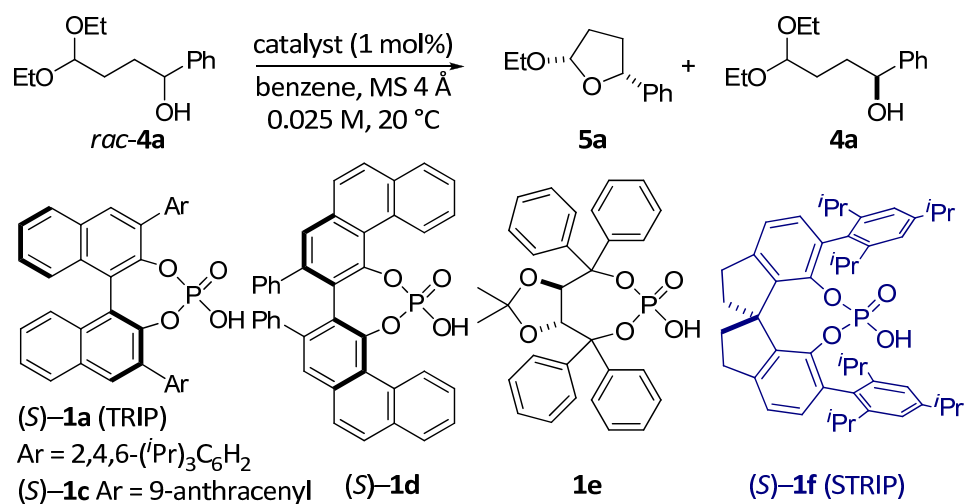
Scheme 4.8. Kinetic resolution of acetal protected homoaldols via transacetalization.

The studies on the kinetic resolution of homoaldols were initiated with secondary homoaldol *rac-4a*, by employing TRIP catalyst (**1a**),^[71-72] which was identified as the best catalyst in the

4. RESULTS AND DISCUSSION

transacetalization studies (Table 4.1).^[107] However, under identical conditions only moderate enantioselectivity (er 25:75) for cyclic acetal **5a** was obtained at 41% conversion (Table 4.3, entry 1). Other previously described phosphoric acid catalysts **1c-e** based on different backbones gave only inferior results.

Table 4.3. Optimization of reaction conditions.



entry	cat.	conv.	er 5a	er <i>5-epi-5a</i>	dr	er 4a
1	1a	41%	25:75	6.5:93.5	14:1	36:64
2	1c	47%	39:61	16.5:83.5	17:1	42:58
3	1d	41%	62.5:37.5	61:39	7:1	57:43
4	1e	26%	45:55	33.5:66.5	7:1	49:51
5	1f	51%	95:5	>99.5:0.5	21:1	92:8
6 ^a	1f	55%	96.5:3.5	>99.5:0.5	12:1	99:1

a) CH₂Cl₂ was used as solvent.

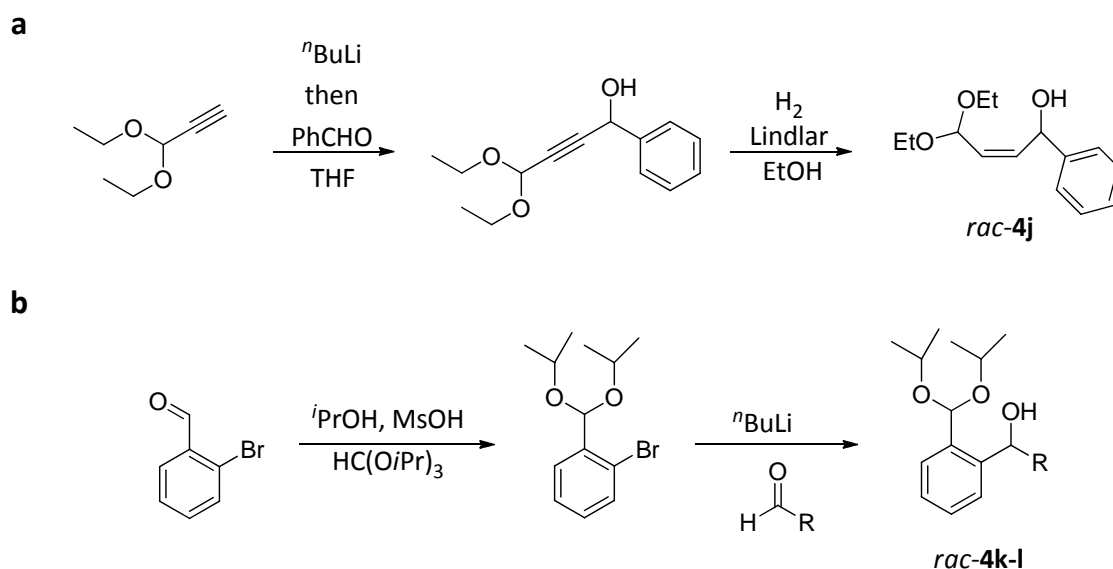
Since the reports of Akiyama and Terada,^[35-36, 58-59] BINOL-derived phosphoric acids became one of the most successful organocatalysts. However, the design of new chiral phosphoric acids has been mainly limited to variations of the 3,3'-substituents of the BINOL-derived catalysts, with the exception of VAPOL-hydrogenphosphate **1d**, and less successful TADDOL-derived phosphoric acids, such as **1e**.^[77-78] Although the 1,1'-spirobiindane backbone is well explored in metal catalysis,^[109-111] the corresponding phosphoric acids were not used as catalysts.^[112] Recently, phosphoric acids based on 1,1'-spirobiindane backbone have been

developed in our group by S. Müller.^[108] We expected that these phosphoric acids might provide a different and more rigid chiral environment than the corresponding BINOL-derived acids enabling access to complementary space for asymmetric transformations.

Remarkably, the spirocyclic phosphoric acid STRIP (**1f**) provided superior result. The STRIP-catalyzed kinetic resolution of homoaldol *rac*-**4a** delivered cyclic acetal **5a** with enantiomeric ratio of 95:5 and left enantioenriched **4a** with an er of 92:8 at 51% conversion (Table 4.3, entry 5). Using dichloromethane instead of benzene as the solvent resulted in higher reactivity and increased enantioselectivity. At 55% conversion both **5a** and **4a** were obtained in excellent enantiomeric ratios of 96.5:3.5 and 99:1, respectively (entry 6). Cyclic acetal **5a** was obtained as the *cis*-diastereomer with a dr of 12:1. The minor *trans*-diastereomer 5-*epi*-**5a** was obtained as a single enantiomer with the opposite configuration at the alcohol derived stereocenter.^[84]

4.2.2. Substrate scope

After optimal conditions have been found, we started to explore the generality of the reaction.^[84] Importantly, racemic homoaldols *rac*-**4a-i** and *rac*-**4m-o** are readily available in good to high yields from commercial materials in a single step via the addition of an acetal protected Grignard reagent to aldehydes and ketones (Scheme 4.6). Acetal protected homoaldols possessing *cis*-double bond (*rac*-**4j**, Scheme 4.9a) or aromatic tether (*rac*-**4k-l**, Scheme 4.9b) were also easily available in two steps.



Scheme 4.9. Preparation of acetal protected homoaldols.

4. RESULTS AND DISCUSSION

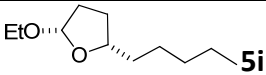
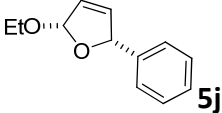
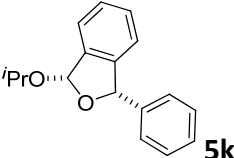
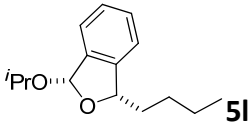
Exploration of the substrate scope revealed that various secondary homoaldols undergo a very efficient kinetic resolution in the presence of only 1 mol% of STRIP (Table 4.4).^[84] In almost all cases, both, cyclic acetal **5** and acetal homoaldol **4** were obtained with excellent enantioselectivity, with er values over 95:5. Various aromatic substrates *rac*-**4a-e** and heteroaromatic substrate *rac*-**4f** underwent superb kinetic resolutions (Table 4.4, entries 1-6). The nature of the aromatic substituent does not seem to have a significant effect on the reaction, electron rich or poor substrates provided equally excellent results. Homoaldols with vinyl or bulky aliphatic substituent behaved equally well (entries 7 and 8).^[84]

Table 4.4. Kinetic resolution of secondary homoaldols^a

rac-**4** $\xrightarrow[\text{0.025 M, 20 }^\circ\text{C}]{\text{(S)-STRIP (1f) (1 mol\%)}, \text{CH}_2\text{Cl}_2, \text{MS 4 \AA}}$ **5** + **4**

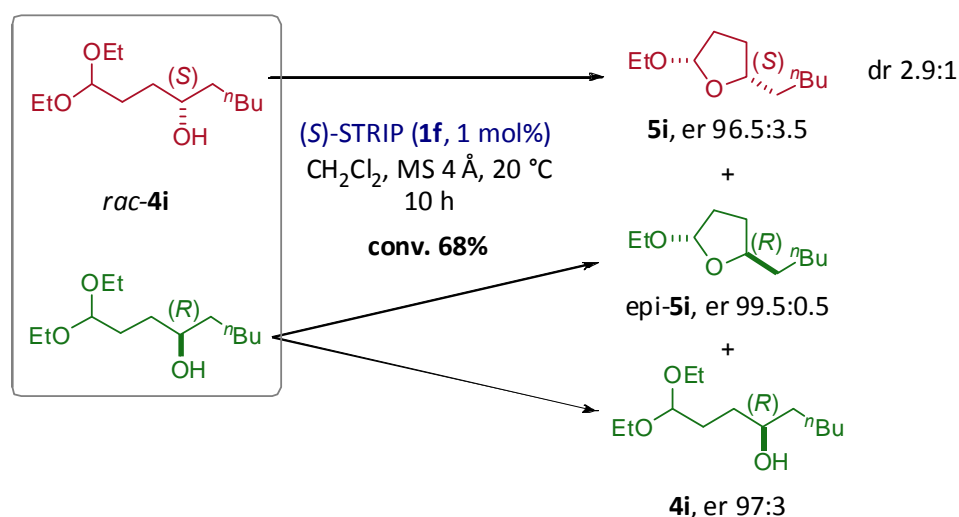
entry	conv. (time)	5	er 5	dr 5 ^b	er 4
1	55% (18 h)		97:3	13:1	98.5:1.5
2	55% (16 h)		97:3	12:1	98:2
3	54% (14 h)		96.5:3.5	13:1	97.5:2.5
4	54% (16 h)		96.5:3.5	14:1	96.5:3.5
5	52% (16 h)		97:3	20:1	96:4
6	53% (14 h)		97.5:2.5	19:1	98.5:1.5
7	56% (14 h)		98:2	8:1	98:2
8	55% (4 h)		93.5:6.5	19:1	98:2

Table 4.4. continued

9	68% (10 h)		96.5:3.5	2.9:1	97:3
10	54% (1 h)		89:11	>50:1	95:5
11	55% (12 h)		89.5:10.5	44:1	96.5:3.5
12	64% (6 h)		85:15	8:1	97.5:2.5

a) Reactions were performed on 0.1 mmol scale with molecular sieves (50 mg). b) Separable by column chromatography, except for **5j-l**. Only one enantiomer of minor *trans*-diastereomer could be detected, except for: 5-*epi-5h*, er 97:3; 5-*epi-5i*, er 99.5:0.5; 5-*epi-5k*, er 71:29; 5-*epi-5l*, er 83.5:16.5.

The reaction of linear aliphatic substituted homoaldol *rac-4i* illustrates a remarkable aspect of our reaction. As an additional acetal stereocenter is created in the transacetalization, the high catalyst control of its formation results in a divergent reaction on a racemic mixture.^[113-115] Thus, even in cases where the enantiodifferentiation of the starting material is not very pronounced, the less reactive enantiomer is converted into the minor *trans*-diastereomer (Scheme 4.10).



This effect enabled us to obtain the major diastereomer of cyclic acetal **5i** with an er of 96.5:3.5 and a perfect theoretical yield (50%) at 68% conversion (Table 4.4, entry 9). For

4. RESULTS AND DISCUSSION

comparison, a simple kinetic resolution would require a selectivity factor of 94 to achieve this result.

The STRIP-catalyzed kinetic resolution of homoaldols is also readily applicable to other substrate classes: for example homoaldols with a *cis*-double bond (*rac*-**4j**) or aromatic tether (*rac*-**4k** and *rac*-**4l**) are also viable substrates (Table 4.4, entries 10-12). However, the kinetic resolution was not as successful as with substrates **4a-h**.^[84]

Tertiary homoaldols

The excellent results obtained with STRIP for secondary homoaldols encouraged us to also explore the kinetic resolution of tertiary homoaldols.^[84] Although chemical kinetic resolutions of secondary alcohols are well developed,^[115] these methods are usually not readily applicable to kinetic resolutions of tertiary alcohols and biocatalytic processes are also rare and of limited scope.^[116-117] The few nonenzymatic methods include chiral reagents,^[118-119] and catalytic methods with peptide based catalysts^[120-122] and metal catalysts.^[123-125]

Gratifyingly, tertiary alcohols perform exceptionally well in our asymmetric transacetalization reaction and the resolution of tertiary homoaldols *rac*-**4m-r** proceeded as efficiently as with secondary homoaldols (Table 4.5).^[84] Both, cyclic acetals **5m-r** and acyclic acetal homoaldols **4m-r**, featuring valuable quaternary stereocenters were obtained with excellent enantioselectivity.

Table 4.5. Kinetic resolution of tertiary homoaldols.^a

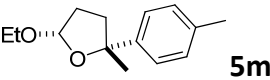
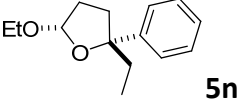
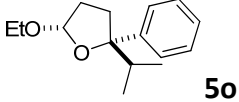
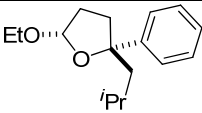
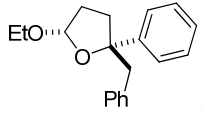
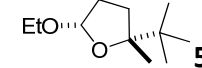
entry	conv.(time)	5	er 5	dr 5 ^b	er 4
1	55% (10 h)		98.5:1.5	9:1	96:4
2	55% (12 h)		98.5:1.5	9:1	98.5:1.5
3	55% (28 h)		97.5:2.5	7:1	92:8

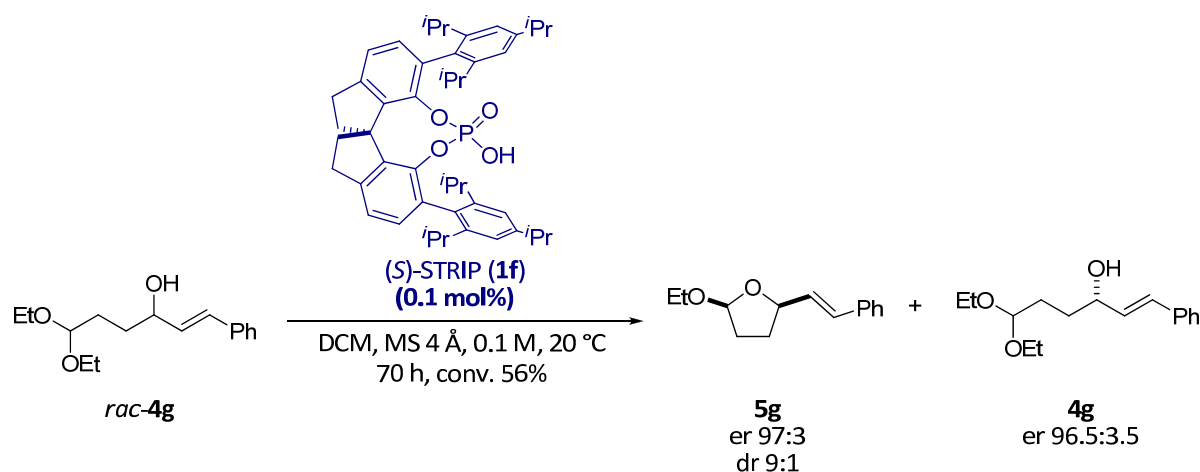
Table 4.5. continued

4	57% (24 h)		99:1	5:1	95:5
5	54% (40 h)		99:1	11:1	97.5:2.5
6	51% (3 h)		99:1	18:1	96.5:3.5

a) Reactions were performed on 0.1 mmol scale with molecular sieves (50 mg). b) Separable by column chromatography, except **5p-q**. Only one enantiomer of minor *trans*-diastereomer could be detected, except for: 5-*epi*-**5m**, er 99.5:0.5; 5-*epi*-**5p**, er 99.5:0.5; 5-*epi*-**5r**, er 96.5:3.5.

The results of kinetic resolutions with substrates possessing sterically similar substituents are remarkable. Highly efficient enantiodifferentiation is observed between aryl and bulky aliphatic groups (Table 4.5, entries 3-4) and even between aryl and benzyl groups (entry 5). Excellent results were also obtained with substrate *rac*-**4r** having only aliphatic substituents (entry 6). For comparison, a classic kinetic resolution would have to operate at a selectivity factor of >300 to deliver **5r** in 48% yield with 99:1 er.

The transacetalization reaction can be performed with only 0.1 mol% catalyst loading employing a more concentrated reaction mixture. For example, the kinetic resolution of *rac*-**4g** proved to be equally effective under these conditions resulting in almost identical enantiomeric ratios compared to the reaction with 1 mol% of the catalyst (Scheme 4.11, compare with Table 4.4, entry 7).^[84]

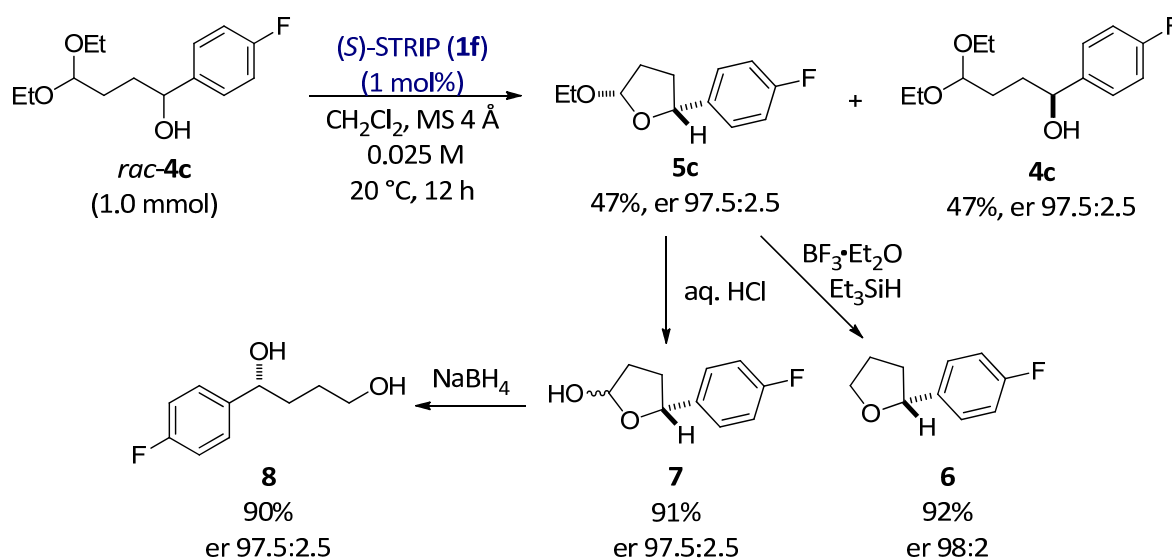


Scheme 4.11. Kinetic resolution of homoaldols using 0.1 mol% of the catalyst.

Relative configurations of cyclic acetals **5a**, **5k-l**, **5m** were determined by NOESY experiments. The absolute configuration of tetrahydrofuran **5a** was determined by comparison of the optical rotation of the γ -butyrolactone derivative, obtained after Jones oxidation, with a literature value. The configurations of other secondary homoaldol products were assigned by analogy.

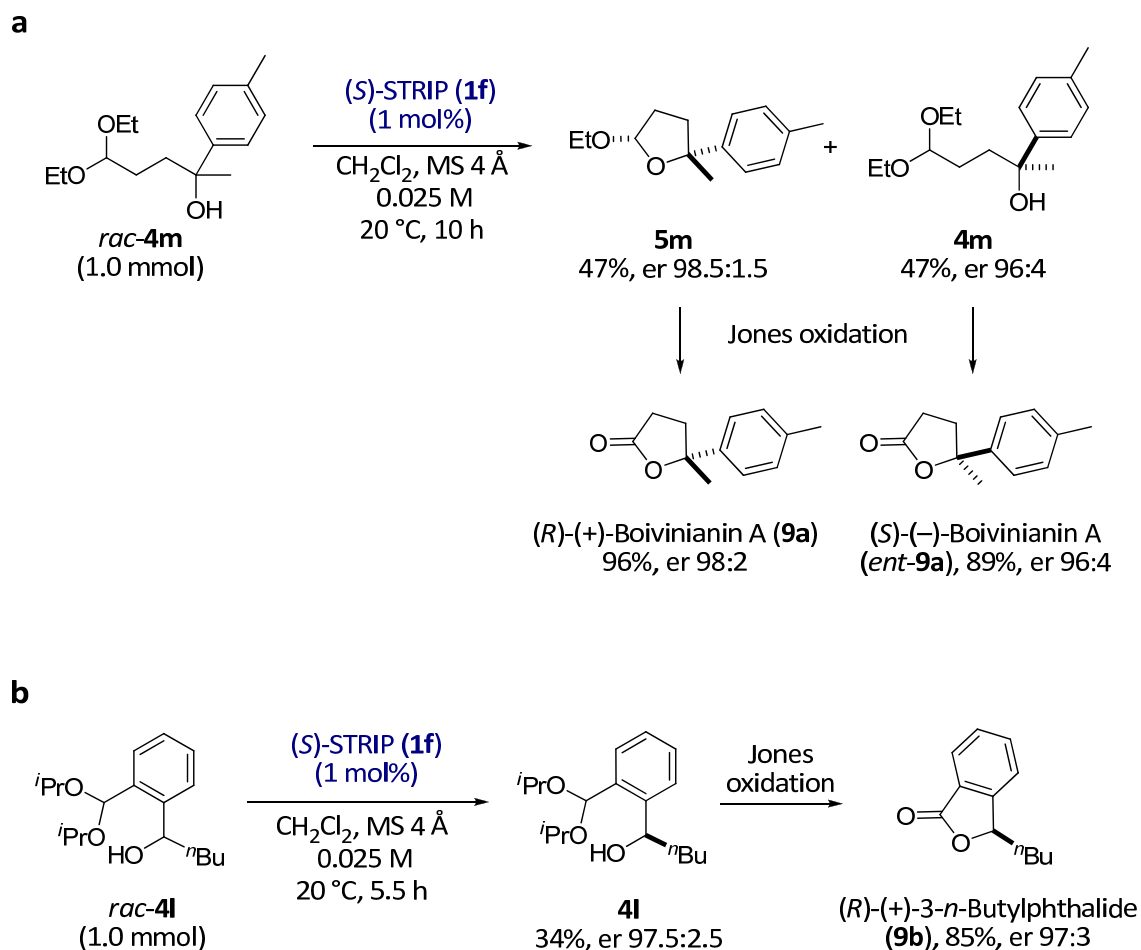
4.2.3. Utility of the products

The acetal group in cyclic acetals, like our products **5**, can be regarded as a useful functional group, enabling an access to a wide variety of products.^[126-134] As a demonstration we performed the kinetic resolution of homoaldol *rac*-**4c** on a preparative scale (1.0 mmol) to obtain enantiomerically enriched **4c** and **5c** in high yields and enantiomeric ratios (Scheme 4.12). Direct reduction of **5c** led to tetrahydrofuran **6**, whereas hydrolysis of **5c** gives the aldehyde homoaldol **7**, which is readily reduced to diol **8**.^[84]



Scheme 4.12. Utility of cyclic acetals **5**.

To verify the absolute configurations of tertiary homoaldols and further exemplify the application of our method we submitted products **5m** and **4m** to Jones oxidation conditions.^[84] Both products of kinetic resolution reaction could be utilized directly to obtain both enantiomers of the natural product Boivinianin A (**9a**) in excellent yields and enantiomeric ratios (Scheme 4.13a).^[135] Similarly, straightforward oxidation of benzene fused acetal **4l** provided access to phthalides, an important and diverse class of natural products and bioactive compounds.^[136] 3-*n*-Butylphthalide (**9b**) is found in a variety of plants, such as celery, and possesses a wide range of pharmacological activities (Scheme 4.13b).^[137]



Scheme 4.13. Application in natural product synthesis.

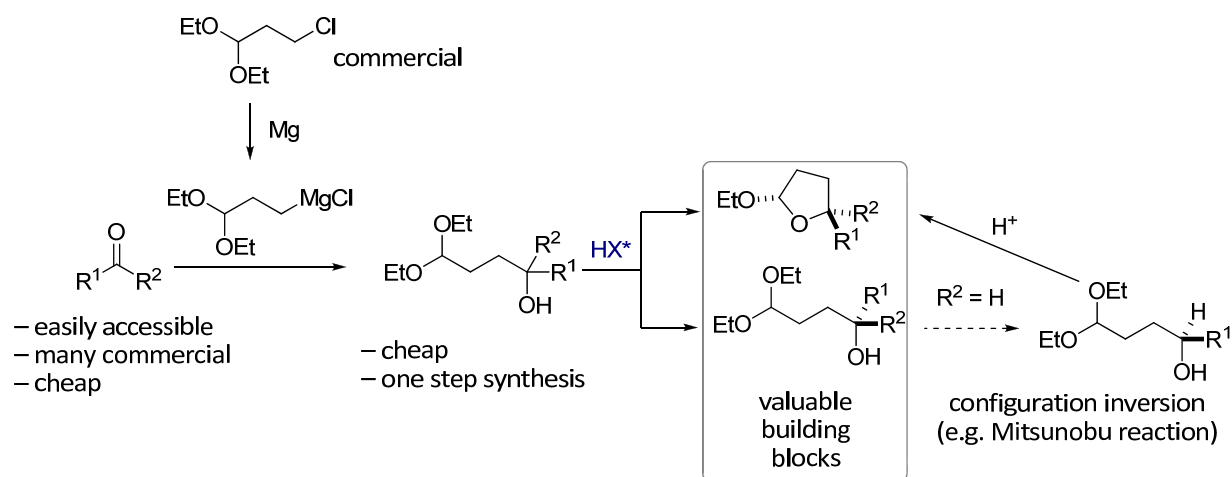
4.2.4. Discussion

We have developed a highly enantioselective kinetic resolution of alcohols tethered to an acetal moiety via a catalytic asymmetric transacetalization reaction.^[84, 108] Key to this highly enantioselective transformation is the spirocyclic phosphoric acid STRIP.^[108] It is noteworthy that our kinetic resolution represents a very atom economic method that, unlike common alternative resolution methods, does not require any stoichiometric reagents, and forms ethanol as the only byproduct. The acetal group in cyclic acetals **5** can be easily modified, e.g. oxidized, reduced or substituted giving access to enantioenriched tetrahydrofurans and γ -butyrolactones. Our method is applicable to the resolution of a wide range of secondary and tertiary homoaldols, providing straightforward access to valuable building blocks for asymmetric synthesis.

Kinetic resolutions are in principle wasteful methods as theoretical yield of 50% cannot be exceeded. However, if the racemic starting material is cheap and easily accessible, and

4. RESULTS AND DISCUSSION

methods for accessing enantioenriched compound are limited, than kinetic resolution presents an attractive option, as is the case with our reaction (Scheme 4.14). With secondary alcohols the possibility of inverting the alcohol stereocenter of the recovered starting material via substitution reaction could remove the 50% maximum yield limitation (Scheme 4.14).



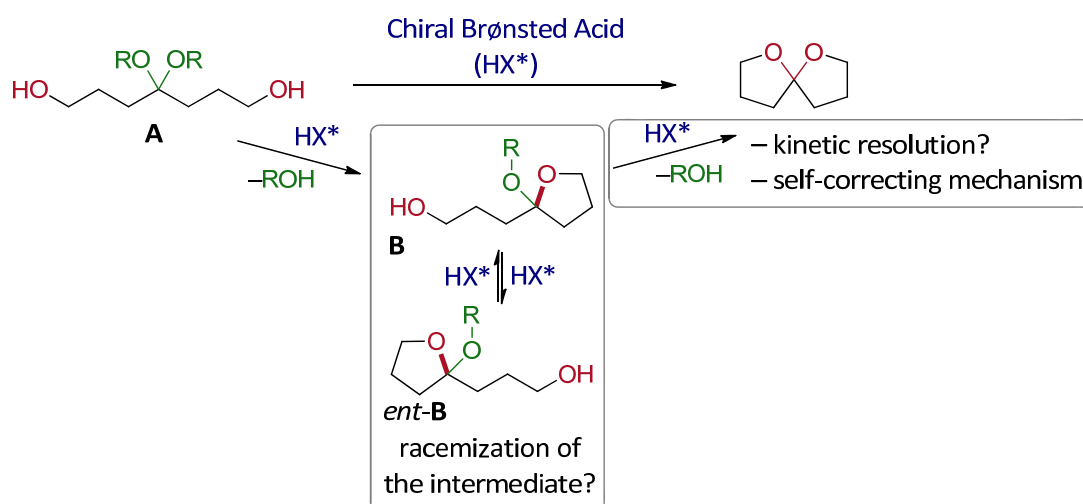
Scheme 4.14. Practical considerations of the kinetic resolution of homoaldols.

4.3. Catalytic asymmetric spiroacetalization

4.3.1. Reaction design and optimization

Double transacetalization

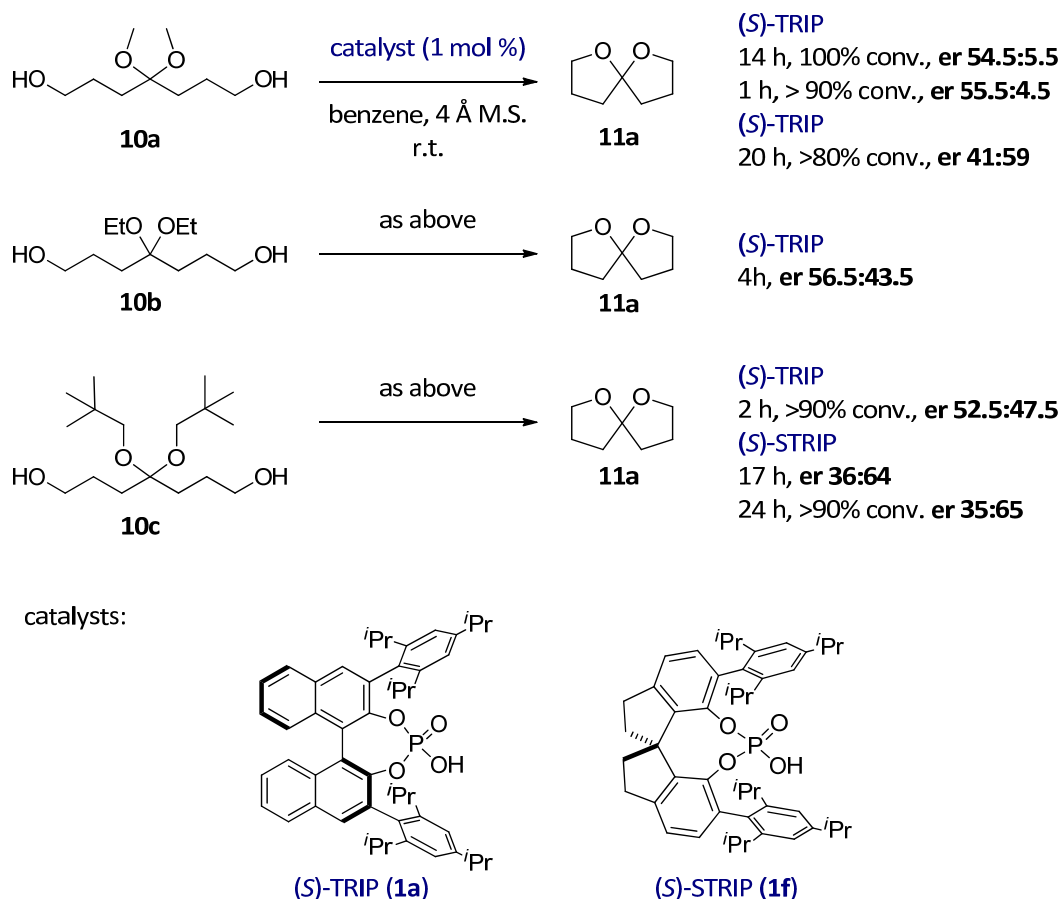
Encouraged by our studies on catalytic asymmetric acetalizations, we envisioned an access to spiroacetals via a double spiroacetalization of acetal protected hydroxyketones **A** (Scheme 4.15). The reaction would proceed through monocyclic intermediate **B** which could possibly be racemized under acidic conditions. As we have found in our transacetalization reaction that the configuration of the starting acetal determines the configuration of the product this racemization might provide a self-correcting pathway if the first transacetalization is not highly enantioselective. In this way the reaction might have the second opportunity for increasing the enantioselectivity by a kinetic resolution effect in the second transacetalization (Scheme 4.15).



Scheme 4.15. Spiroacetals via double transacetalization.

We prepared starting materials **10a-c** with different acetal groups and treated them with Brønsted acid catalysts TRIP (**1a**) and STRIP (**1f**) that were optimal for the transacetalization studies.^[84, 107] The reactions proceeded well at room temperature in benzene, however TRIP gave low enantioselectivity independent of starting material used (Scheme 4.16). However, it was encouraging that no racemization occurred during prolonged reaction time. With substrate **10a** and TRIP as the catalyst, enantiomeric ratios after 1h and 14 h at room temperature were almost the same (Scheme 4.16). Results with STRIP were more promising and starting material **10c** with a bulky neopentyl acetal gave better results than dimethyl acetal **10a**. In this effect we saw an opportunity to optimize the reaction enantioselectivity by

designing an appropriate substrate with a more bulky acetal group. However synthetic attempts towards the diisopropyl acetal substrate were met with failures probably due to sterical reasons. Consequently we focused on designing a novel reaction for the asymmetric synthesis of spiroacetals.



Scheme 4.16. Attempted double transacetalization.

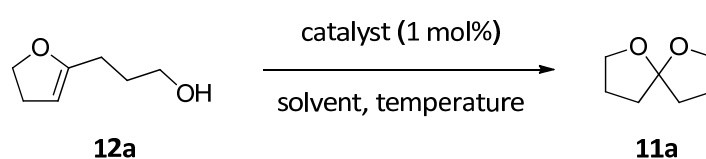
Asymmetric spiroacetalization of hydroxyenoethers

We next targeted the chiral Brønsted acid catalyzed spiroacetalization of readily available hydroxyenoether **12a** (Table 4.6).^[138] While the envisioned asymmetric hydroetherification of enol ethers has been unknown with chiral Brønsted acid catalysts,^[100] achiral acids are routinely used to perform the non-asymmetric reaction. Substrate **12a** was treated with the TRIP catalyst under standard conditions developed for the transacetalization reaction. A very fast reaction was observed, with complete conversion in less than 15 minutes. Gratifyingly, a very promising enantiomeric ratio of 30:70 was obtained (Table 4.6, entry 1). We found that molecular sieves did not have a significant effect on the enantioselectivity (entry 2). Next, we

4. RESULTS AND DISCUSSION

replaced the solvent with toluene to enable low temperature studies. Although the reaction at room temperature gave the same result as with benzene (entry 3), the reaction at $-78\text{ }^{\circ}\text{C}$ surprisingly gave a very low enantiomeric ratio of 47.5:52.5 (entry 4). Testing various other solvents at room temperature and $-78\text{ }^{\circ}\text{C}$ gave no improvement (entries 5–14), with enantiomeric ratio of 29.5:70.5 obtained in toluene at room temperature remaining the best result. Changing the catalyst to STRIP which proved superior to TRIP in the kinetic resolution of homoaldols did not result in an improvement of the enantioselectivity (entries 15–18).^[138]

Table 4.6. Initial reaction development.



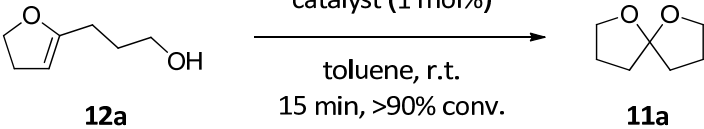
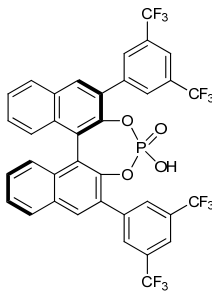
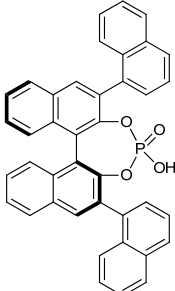
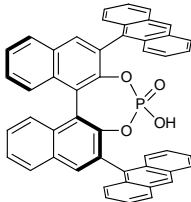
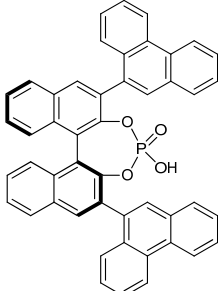
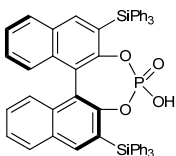
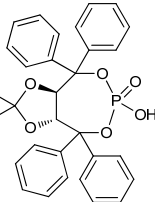
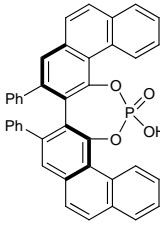
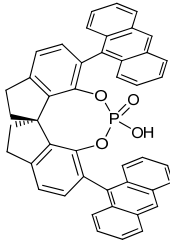
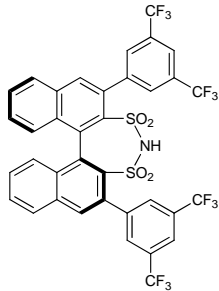
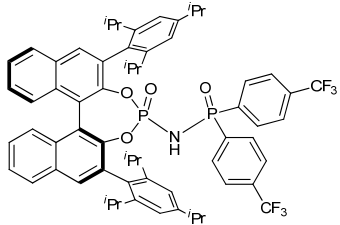
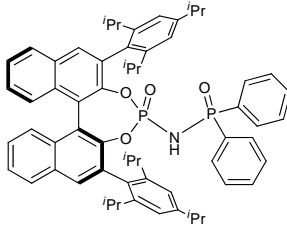
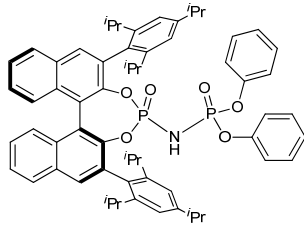
Catalyst	Entry	Solvent	Temperature	Time	Conversion	er
(S)-TRIP (1a)	1 ^a	benzene	r.t.	15 min	>90%	30:70
	2	benzene	r.t.	15 min	>90%	29.5:70.5
	3	toluene	r.t.	15 min	>90%	29.5:70.5
	4	toluene	$-78\text{ }^{\circ}\text{C}$	16 h	>90%	47.5:52.5
	5	CH_2Cl_2	r.t.	15 min	>90%	35.5:64.5
	6	CH_2Cl_2	$-78\text{ }^{\circ}\text{C}$	16 h	>90%	30:70
	7	Et_2O	r.t.	15 min	>90%	36:64
	8	Et_2O	$-78\text{ }^{\circ}\text{C}$	16 h	low	30:70
	9	EtOAc	r.t.	15 min	>90%	39.5:60.5
	10	EtOAc	$-78\text{ }^{\circ}\text{C}$	16 h	low	30:70
	11	pentane	r.t.	15 min	>90%	44:56
	12	pentane	$-78\text{ }^{\circ}\text{C}$	16 h	low	53:47
	13	MeOH	r.t.	15 min	>50%	50:50
	14	MeOH	$-78\text{ }^{\circ}\text{C}$	16 h	low	55.5:44.5
(S)-STRIP (1f)	15	toluene	r.t.	15 min	>90%	64:36
	16	toluene	$-78\text{ }^{\circ}\text{C}$	16 h	>90%	60:40
	17	CH_2Cl_2	r.t.	15 min	>90%	55:45
	18	CH_2Cl_2	$-78\text{ }^{\circ}\text{C}$	16 h	>90%	47:53

a) With 12.5 mg of 4 Å molecular sieves.

4. RESULTS AND DISCUSSION

We next performed an extensive screening of a wide range of known chiral Brønsted acids (Table 4.7).^[138] However only disappointing results were obtained in the generation of the spiroacetal product with er of 29.5:70.5 obtained with TRIP remaining as the best result.

Table 4.7. Catalyst screening.

		catalyst (1 mol%) toluene, r.t. 15 min, >90% conv.			
					
	12a				11a
Catalyst ^[58-59]					
er	52:48	50:50	50.5:49.5	45:55	
Catalyst ^[65, 77-78, 139-140]					
er	48:52	48.5:51.5	46:54	32:68	50:50
Catalyst ^[92]					
er	47:53	42:58	41:59		

Similarly as with the double transacetalization reaction (Scheme 4.16) we again faced a failure to perform a highly enantioselective spiroacetalization reaction. At this point we considered finding a more suitable class of hydroxyenoether substrates for the spiroacetalization reaction.

Placing aromatic tethers or suitable bulky substituents could have lead to the desired catalytic asymmetric spiroacetalization with known catalysts. Instead we decided to focus on designing a novel catalyst to perform the spiroacetalization reaction with substrate **12a**. We found this approach much more challenging and potentially more rewarding because a solution could potentially also tackle an important issue of broader significance in current Brønsted acid catalysis. In the field of Brønsted acid catalysis, reactions including small aliphatic substrates without sterically demanding protecting groups, large aromatic/planar surfaces, or bulky substituents are still extremely rare. A catalyst that would solve the asymmetric spiroacetalization reaction with substrate **12a** could provide a solution to these challenges in Brønsted acid catalysis. At this point we undertook a rational catalyst design which is described in chapter 4.4. (“Confined Brønsted acids”) of this thesis.^[138]

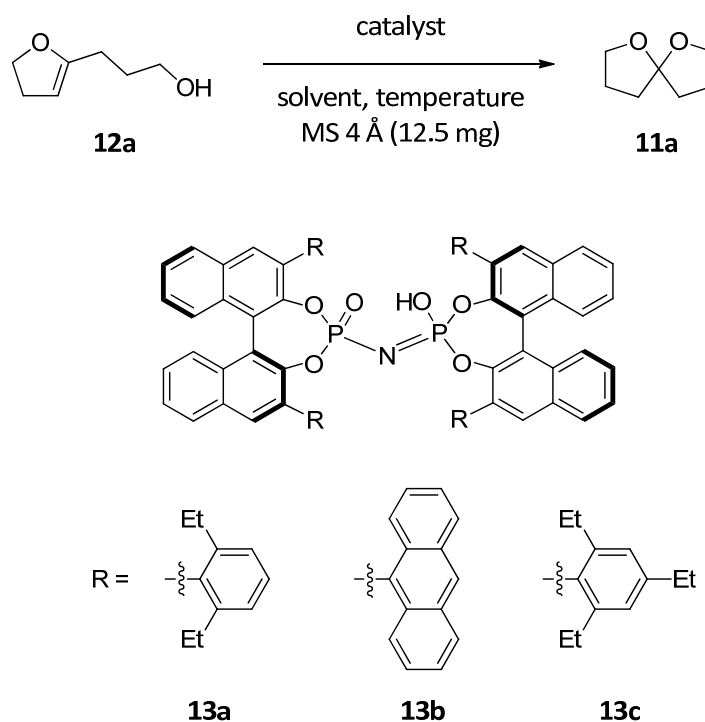
As the result of our catalyst development we have synthesized several novel catalysts termed confined Brønsted acids.^[138] Having in our hands Brønsted acids featuring an extremely sterically demanding chiral cavity we again examined the spiroacetalization reaction with hydroxyenoether **12a**. Gratifyingly, the novel catalyst **13a** gave an improvement in the spiroacetalization reaction and an er of 80.5:19.5 in toluene at room temperature (Table 4.8, entry 1). The reaction in dichloromethane proceeded with even higher enantiomeric ratio of 84:16 in less than 10 minutes at room temperature (Table 4.8, entry 2). Lowering the temperature had a positive effect on enantioselectivity and an er of 90.5:9.5 could be achieved (entry 4). Anthracenyl-substituted catalyst **13b** did not improve the enantioselectivity (entry 5), however with catalyst **13c** an er of 93:7 could be obtained at –25 °C (entry 6). Lowering the reaction temperature to –55 °C allowed for further increase in the enantioselectivity to give the excellent enantiomeric ratio of 96.5:3.5 (Table 4.8, entry 7). Remarkably, catalyst loading could be decreased to 0.1 mol% without deleterious effect on the enantioselectivity (entry 8). With 3 Å molecular sieves an enantiomeric ratio of 97:3 could be achieved (entry 9).^[138]

We simultaneously approached the synthesis of 6,6-spiroacetal **11b**, which is the natural product oleon. Although, both enol ether ring size and the size of the ring being formed are changed compared to substrate **12a** the spiroacetalization reaction with confined acid catalyst **13c** proceeded with equal level of enantioselectivity in dichloromethane at –25 °C (Table 4.9, entry 2). However, as spiroacetalization substrate **12b** was less reactive than **12a**, we opted for a solvent screening at –25 °C rather than lowering the temperature. Gratifyingly, the spiroacetalization reaction proceeded with high enantioselectivity in 1,2-dichloroethane

4. RESULTS AND DISCUSSION

(DCE) (entry 3), Et₂O (entry 4) and *tert*-butylmethyl ether (MTBE) (Table 4.9, entry 6), although lower reactivity was observed with ether solvents.^[138]

Table 4.8. Spiroacetalization with confined Brønsted acids.



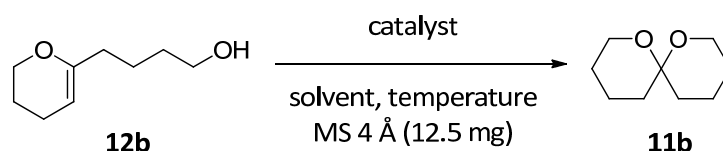
Entry	Catalyst	Solvent	Temperature	Time	Conversion	er
1	13a (1 mol%)	toluene	r.t.	10 min	>90%	80.5:19.5
2	13a (1 mol%)	CH ₂ Cl ₂	r.t.	10 min	>90%	84:16
3	13a (1 mol%)	toluene	-25 °C	12 h	>50%	89.5:10.5
4	13a (1 mol%)	CH ₂ Cl ₂	-25 °C	12 h	>90%	90.5:9.5
5	13b (1 mol%)	CH ₂ Cl ₂	-25 °C	14 h	>90%	90.5:9.5
6	13c (1 mol%)	CH ₂ Cl ₂	-25 °C	12 h	>90%	93:7
7 ^{a,b}	13c (1 mol%)	CH ₂ Cl ₂	-55 °C	12 h	>90%	96.5:3.5
8 ^{a,b}	13c (0.1 mol%)	CH ₂ Cl ₂	-55 °C	12 h	>90%	96.5:3.5
9 ^{a,c}	13c (0.1 mol%)	CH ₂ Cl ₂	-55 °C	12 h	>90%	97:3

a) 0.25 mmol scale; b) MS 4 Å (50 mg); c) MS 3 Å (125 mg).

High conversion could be achieved in Et₂O by increasing the temperature to 0 °C with an enantiomeric ratio of 96.5:3.5 (entry 5). Alternatively, increasing the catalyst loading from 1 mol% to 5 mol% with MTBE as the solvent resulted in high conversion after 12 h at -25 °C and

enantiomeric ratio of 98:2 (entry 7). These results with 5,5- and 6,6-spiroacetals represented the first catalytic highly enantioselective spiroacetalization reactions.^[138]

Table 4.9. Olean via asymmetric spiroacetalization.



Entry	Catalyst	Solvent	Temperature	Time	Conversion	er
1	13a (1 mol%)	CH ₂ Cl ₂	-25 °C	12 h	>90%	90.5:9.5
2	13c (1 mol%)	CH ₂ Cl ₂	-25 °C	12 h	>90%	93:7
3	13c (1 mol%)	DCE	-25 °C	12 h	>90%	96.5:3.5
4	13c (1 mol%)	Et ₂ O	-25 °C	12 h	low	97.5:2.5
5	13c (1 mol%)	Et ₂ O	0 °C	12 h	>90%	96.5:3.5
6	13c (1 mol%)	MTBE	-25 °C	12 h	low	98:2
7 ^a	13c (5 mol%)	MTBE	-25 °C	12 h	>90%	98:2

a) 5 mg of molecular sieves.

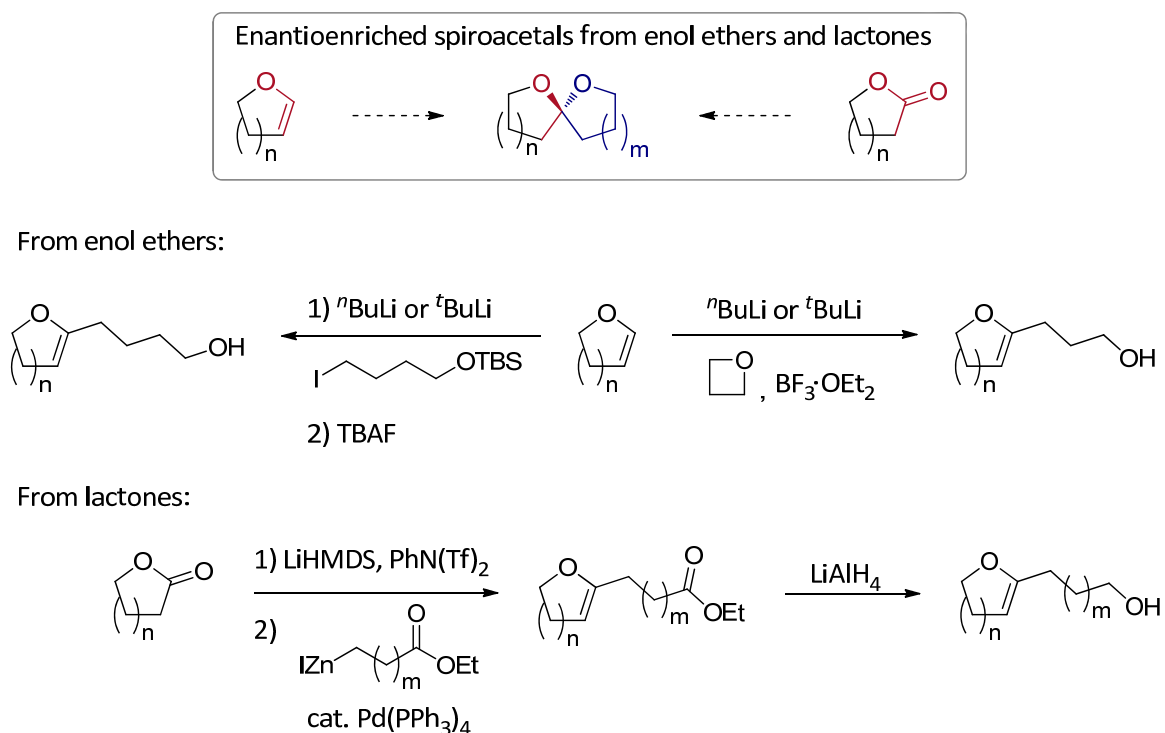
During the optimization studies it became obvious that catalyst **13c** is able to perform highly enantioselective spiroacetalizations in different solvents, therefore during the exploration of the substrate scope, usually DCE and MTBE solvents were tested, together with either 3 Å or 4 Å molecular sieves.

4.3.2. Substrate scope

With the novel sterically extremely demanding catalyst **13c** and optimized reaction conditions in hand we performed a substrate scope targeting the synthesis of small spiroacetals.^[138] Importantly, starting materials were easily accessible from enol ethers and lactones (Scheme 4.17).^[141-144] Five or six membered cyclic enol ethers were deprotonated in the 2-position by alkyl lithium bases, and alkylated with primary alkyl iodides (Scheme 4.17). After the deprotection of the alcohol group the spiroacetalization substrates were obtained. Lithiated enol ethers can also be directly alkylated with oxetane in the presence of BF₃·Et₂O (Scheme 4.17). Hydroxyenoether based spiroacetalization substrates can alternatively be accessed from common lactones (Scheme 4.17). Sensitive hydroxyenoethers **12** were used for the

4. RESULTS AND DISCUSSION

spiroacetalization reaction immediately after the purification by column chromatography on alumina.^[138]



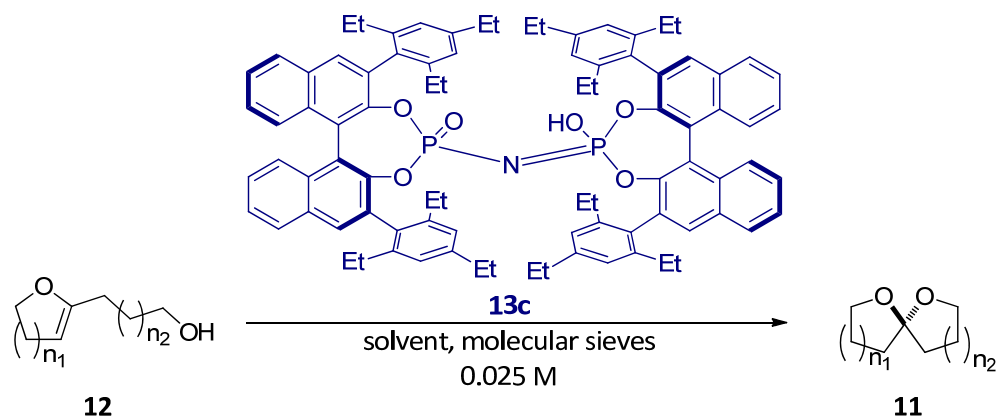
Scheme 4.17. Synthetic strategies for spiroacetalization substrates.

The spiroacetalization of **12a** proceeded with only 0.1 mol% of catalyst **13c** to construct the small 5,5-spiroacetal (Table 4.10, entry 1). The catalyst enabled the first catalytic asymmetric synthesis of the natural product olean (**11b**) (entry 2). A highly enantioselective catalytic spiroacetalization reaction of alcohol **12a** in MTBE with 5 mol% of the catalyst resulted in an excellent enantiomeric ratio of 98:2. The (*R*)-enantiomer of olean was easily obtained by using the other enantiomer of the catalyst (entry 3). Imidodiphosphoric acid catalyst **13c** proved quite general and various other spiroacetals were obtained with high enantioselectivity. The 5,6-spiroacetal motif could be accessed equally successful by cyclization of either five or six-membered rings (entries 4 and 5). Both of these spiroacetalization reactions required only 1 mol% of the catalyst at $-35\text{ }^{\circ}\text{C}$. Comparison with the reaction of substrate **12b** demonstrated that the 5-membered enol ether is more reactive than the 6-membered one and that the spiroacetalization to form a 5-membered ring is significantly faster than that to form a 6-membered ring. Different enol ether ring sizes are similarly tolerated as demonstrated by highly enantioselective reactions to form the corresponding 7,6- and 7,5-spiroacetals (entries 6 and 7). Spiroacetal **11f** was obtained with excellent enantiomeric ratio of 98.5:1.5. 7-

4. RESULTS AND DISCUSSION

Membered enol ether substrates showed higher reactivity than 6-membered substrate **12b**, and only 1 mol% of the catalyst was necessary. Notably, all these small spiroacetals in Table 4.10 are core structures of many natural products.^[2-4, 138]

Table 4.10. Catalytic asymmetric spiroacetalization.^a



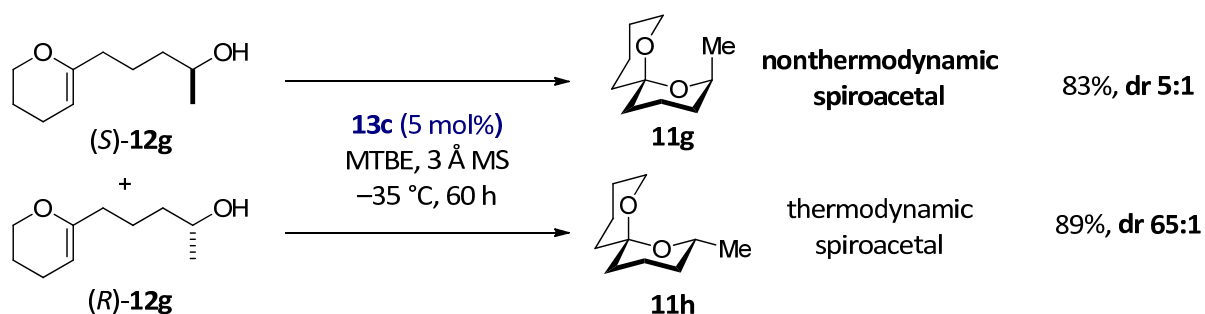
Entry	Substrate	Reaction details	Product	Yield	er
1	12a	13c (0.1 mol%) -55 °C, CH ₂ Cl ₂	11a	62%	96:4
2	12b	13c (5 mol%) -25 °C, MTBE	(S)-11b	77%	98:2
3	12b	<i>ent</i> - 13c (5 mol%) -25 °C, MTBE	(R)-11b	70%	97.5:2.5
4	12c	13c (1 mol%) -35 °C, DCE	11c	81%	95.5:4.5
5	12d	13c (1 mol%) -35 °C, MTBE	11c	69%	96:4
6	12e	13c (1 mol%) -25 °C, MTBE	11e	78%	96:4
7	12f	13c (1 mol%) -35 °C, MTBE	11f	88%	98.5:1.5

^a Reactions were run in the presence of molecular sieves (see Experimental section).

4.3.3. Nonthermodynamic and thermodynamic spiroacetals

The formation of nonthermodynamic spiroacetals, featuring the less stable configuration of the spiroacetal stereocenter, presents a substantial challenge for organic synthesis.^[2] An ideal solution for the formation of nonthermodynamic spiroacetals would be a catalyst controlled reaction that could override thermodynamic preference and control the spiroacetal configuration. Gratifyingly, with our confined Brønsted acid catalyst **13c** this goal could be achieved.^[138]

A racemic mixture of (*S*)-**12g** and (*R*)-**12g** was treated with the confined catalyst in MTBE at $-35\text{ }^{\circ}\text{C}$ (Scheme 4.18).^[138] Independent of the stereochemistry of the starting material, the formation of the spiroacetal stereocenter was controlled by the catalyst to give preferably the (*S*)-configuration. With (*S*)-**12g** a nonthermodynamic spiroacetal was obtained with 5:1 dr, although under thermodynamic conditions (aq. 3 N HCl), the thermodynamic diastereomer is preferred with a dr of 1:124 (Scheme 4.18). Under kinetic conditions with achiral diphenylphosphoric acid an equal 1:1 mixture of thermodynamic and nonthermodynamic spiroacetal is obtained. Although the thermodynamic spiroacetal can be easily obtained in strongly acidic conditions that epimerize the acetal stereocenter, our catalyst is capable of providing the thermodynamic spiroacetal under kinetic conditions furnishing a dr of 65:1 (Scheme 4.18).^[138] Such mild conditions for the spiroacetalization reaction might be essential in syntheses when other acid sensitive groups are present in the molecule, e.g. other acetals and spiroacetals.

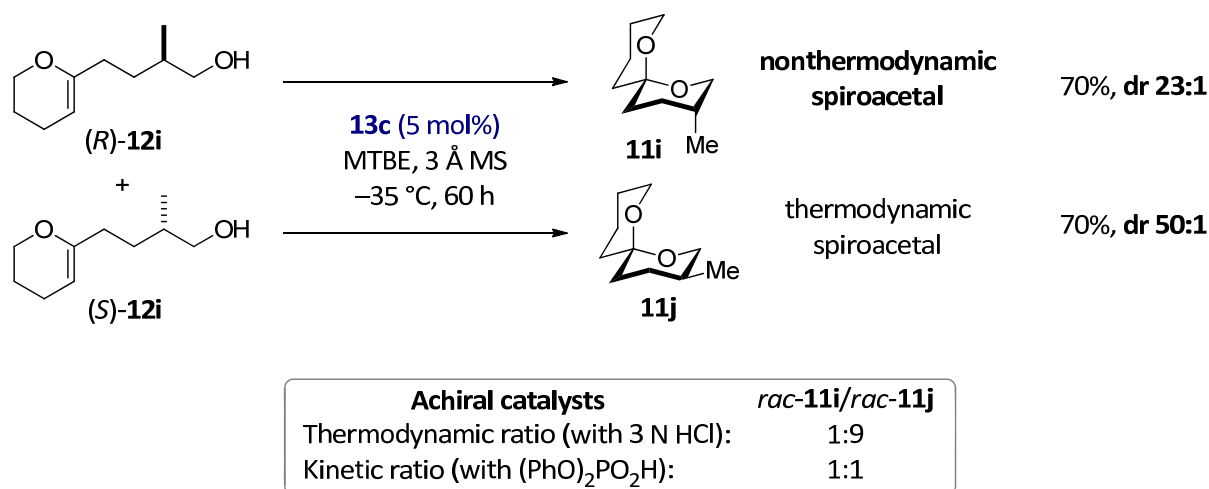


Achiral catalysts	<i>rac</i> - 11g / <i>rac</i> - 11h
Thermodynamic ratio (with 3 N HCl):	1:124
Kinetic ratio (with $(\text{PhO})_2\text{PO}_2\text{H}$):	1:1

Scheme 4.18. Nonthermodynamic and thermodynamic spiroacetals.

4. RESULTS AND DISCUSSION

We next examined substrates with different substitution patterns. Hydroxyenoethers (*R*)-**12i** and (*S*)-**12i** with the methyl group placed one carbon further away from the alcohol group were reacted with catalyst **13c** under the same conditions as for substrates **12g**. The formation of the spiroacetal stereocenter was excellently controlled by the catalyst to give either nonthermodynamic or thermodynamic spiroacetals with dr values >20:1 in both cases. With (*R*)-**12i**, a nonthermodynamic spiroacetal **11i** was obtained with a dr of 23:1, although under thermodynamic conditions, the other, thermodynamic diastereomer is preferred with a dr of 1:9 (Scheme 4.19). Under kinetic conditions with the achiral diphenylphosphoric acid an equal 1:1 mixture of thermodynamic and nonthermodynamic spiroacetal was obtained. The thermodynamic spiroacetal **11j** could be obtained under mild kinetic conditions with a dr of 50:1, which even exceeds the thermodynamic ratio of 9:1 obtained under strongly acidic conditions (Scheme 4.19).^[138]

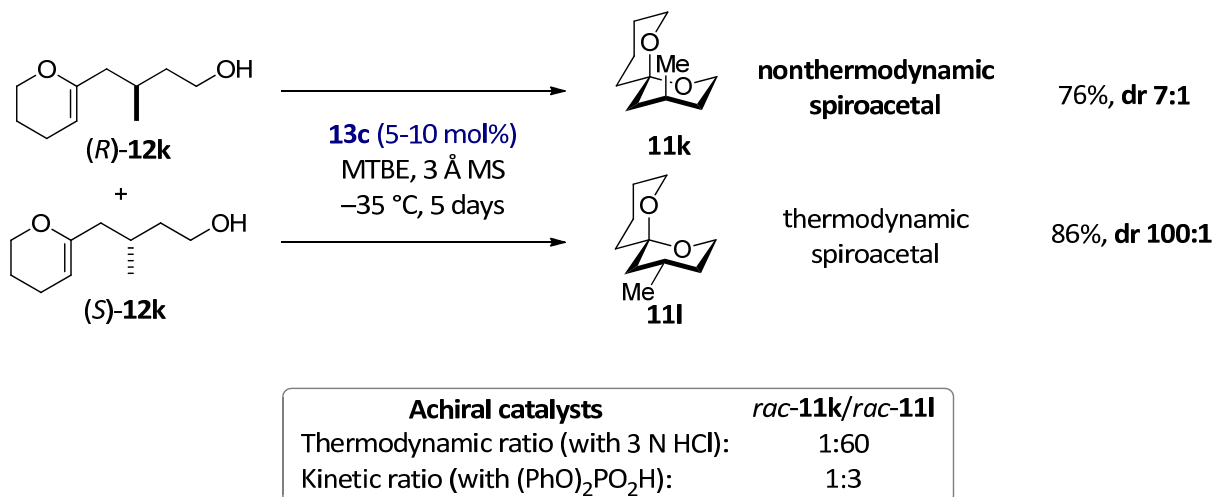


Scheme 4.19. Nonthermodynamic and thermodynamic spiroacetals.

Substrates (*R*)-**12k** and (*S*)-**12k** required higher catalyst loading and longer reaction time for completion (Scheme 4.20). However, as in the other cases, catalyst **13c** gave excellent results. With substrate (*R*)-**12k** a nonthermodynamic spiroacetal **11k** was obtained with dr 7:1, against the thermodynamic preference with a dr of 1:60 for the other diastereomer (Scheme 4.20). Under kinetic conditions with achiral diphenylphosphoric acid, the thermodynamic spiroacetal was preferred with a dr of 1:3. With confined catalyst **13c** the thermodynamic spiroacetal **11l** could be obtained under mild kinetic conditions with a dr of 100:1, which exceeded the thermodynamic ratio of 60:1 obtained with aq. HCl (Scheme 4.20).^[138]

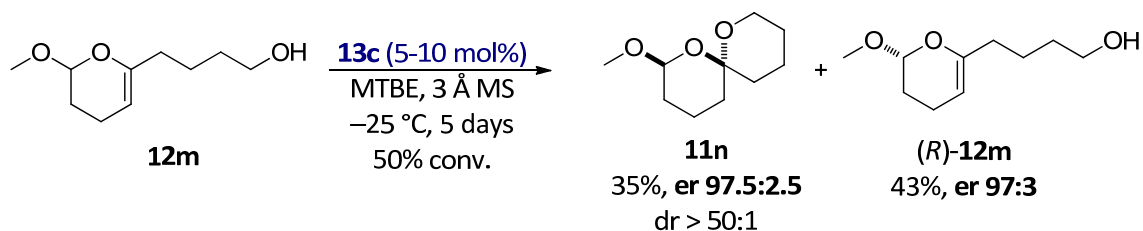
4. RESULTS AND DISCUSSION

The results presented in Scheme 4.18, Scheme 4.19, and Scheme 4.20 represent to the best of our knowledge, the first examples of chiral catalyst controlled diastereoselectivity in the formation of thermodynamic and nonthermodynamic spiroacetals.^[138]



Scheme 4.20. Nonthermodynamic and thermodynamic spiroacetals.

Spiroacetalization of substituted enol ether **12m** revealed another powerful capability of the confined Brønsted acid **13c** (Scheme 4.21).^[138] An efficient kinetic resolution occurred, delivering both bisacetal **11n** and enolacetal **(R)-12m** with excellent enantioselectivity. Asymmetric synthesis of these sensitive motifs by any other method would present a considerable challenge.



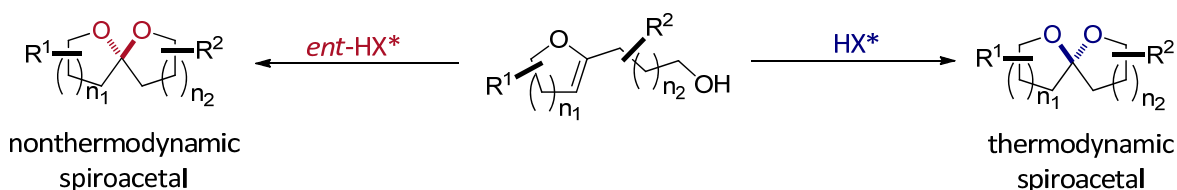
Scheme 4.21. Kinetic resolution via asymmetric spiroacetalization.

4.3.4. Discussion

We have discovered the first catalytic asymmetric spiroacetalization reaction and synthesized small spiroacetals which are cores of many natural products.^[138] For the first time, a catalyst controlled spiroacetalization provides access to nonthermodynamic spiroacetals against a strong thermodynamic preference for the other, thermodynamic diastereomer.^[138] Moreover,

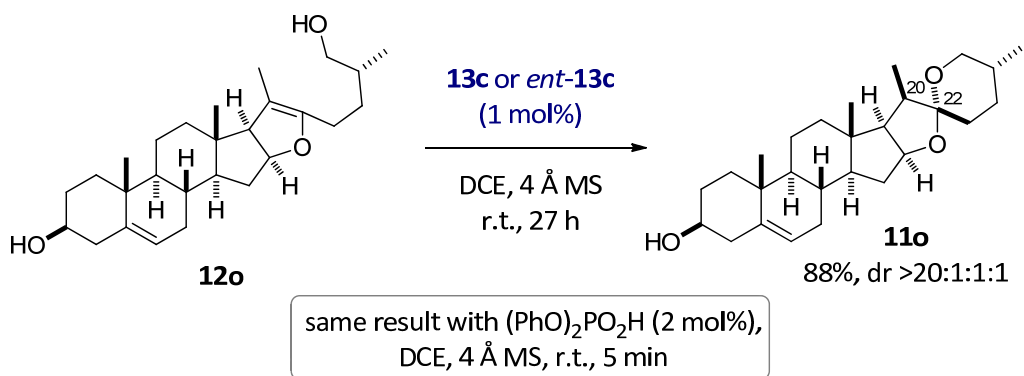
4. RESULTS AND DISCUSSION

when the catalyst control matches the inherent thermodynamic substrate preference, thermodynamic spiroacetals can be obtained with excellent diastereoselectivities that can even exceed thermodynamic ratios. In this way thermodynamic spiroacetals can be obtained under very mild, kinetic conditions, as compared to the relatively strongly acidic conditions typically required for thermodynamic equilibration. Our spiroacetalization reaction is expected to find applications in the synthesis of diverse natural products and biologically active molecules for which the desired spiroacetal stereocenter configuration cannot be accessed under thermodynamic conditions (Scheme 4.22). This method could also be applicable to obtaining either spiroacetal epimers in reactions that give similar mixtures of spiroacetal isomers under thermodynamic conditions (Scheme 4.22).



Scheme 4.22. Catalytic control of spiroacetal configuration in functionalized chiral molecules.

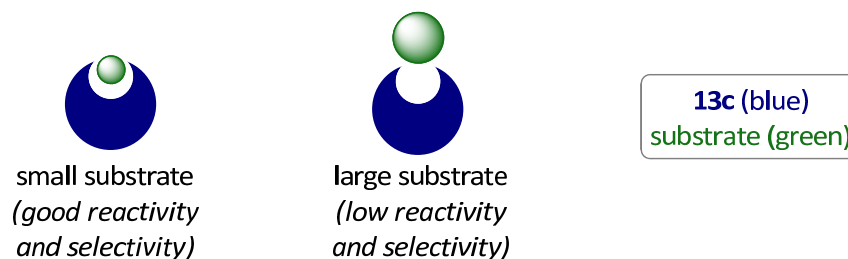
The spiroacetalization of hydroxyenolethers should be applicable even in the synthesis of large, natural product like spiroacetals by using a less bulky Brønsted acid catalysts that are capable of accommodating such substrates. As our confined Brønsted acid **13c** is designed to feature an extremely sterically demanding active site, we expected that large substrates will not be accepted by this particular catalyst. To explore this behavior of our catalyst, we examined large substrate **12o**, an open form of the steroidal sapogenin diosgenin (Scheme 4.23).^[145-146] As expected, the reactivity was rather low using either catalyst enantiomer, although only a single diastereomer (the known nonthermodynamic isomer 20-epi-diosgenin) was obtained.



Scheme 4.23. Low reactivity of confined acid **13c** with large substrate.

4. RESULTS AND DISCUSSION

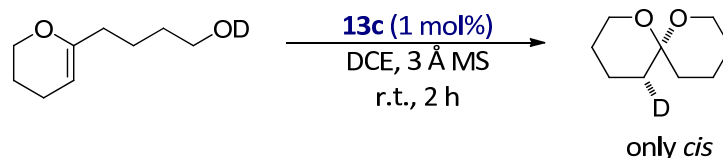
The lack of activity and selectivity for large substrate **12o** with catalyst **13c** presumably originates from the inability of the substrate to fit into the active site of the catalyst (Scheme 4.24). However, our spiroacetalization reaction could also be applied to large substrates using less sterically demanding catalysts. Even known phosphoric acids could be efficient and selective catalysts in these cases.



Scheme 4.24. Schematic representation of the confined acid catalyst behavior with small and large substrates.

Mechanistic studies

In a hope to clarify the mechanism of the reaction we have performed a spiroacetalization reaction with a deuterium labeled substrate (Scheme 4.25). Due to the lower reactivity of the deuterated substrate the reaction was performed at room temperature in DCE. Interestingly only product resulting from the *syn* addition of the deuterium and the oxygen nucleophile was observed (Scheme 4.25). Such a result could be rationalized with a concerted mechanism in which the D and O atoms are simultaneously added over the C=C bond. Alternatively, after the initial H⁺/D⁺ transfer and the oxocarbenium ion formation, a fast cyclization occurs before the ion pair reorganization.



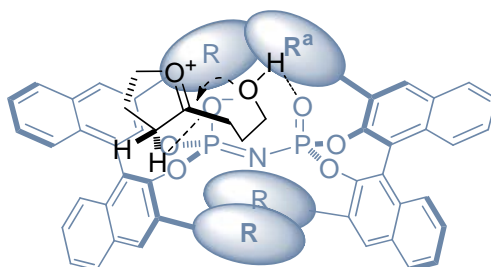
Scheme 4.25. Mechanistic investigations: deuterium labeling.

Stereochemical model

Based on the deuterium labeling experiment we propose the stereochemical model in Scheme 4.26. The hydroxyl group of the substrate is initially hydrogen bonded to the imidodiphosphoric acid moiety of the catalyst, followed by the approach of the enol ether moiety from the *re* face avoiding the steric interaction of the aliphatic cycle with the R^a

4. RESULTS AND DISCUSSION

substituent on the catalyst (Scheme 4.26). After proton transfer the oxocarbenium ion remains bound to the anion which directs the alcohol attack from the same (*re*) face (Scheme 4.26). The repulsive steric interaction of R^a substituent on the catalyst and the aliphatic portion of the enol ether cycle is consistent with the observed (*S*)-stereochemistry of the products.

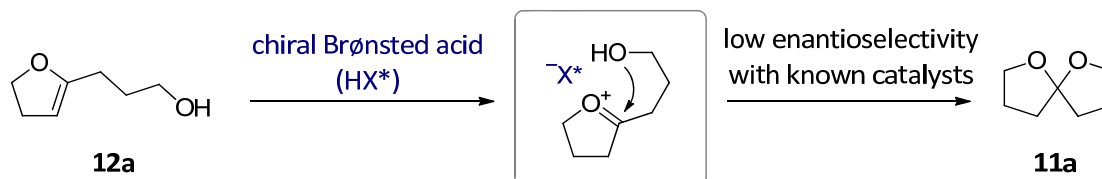


Scheme 4.26. Proposed stereochemical model for the spiroacetalization reaction.

4.4. Confined Brønsted acids

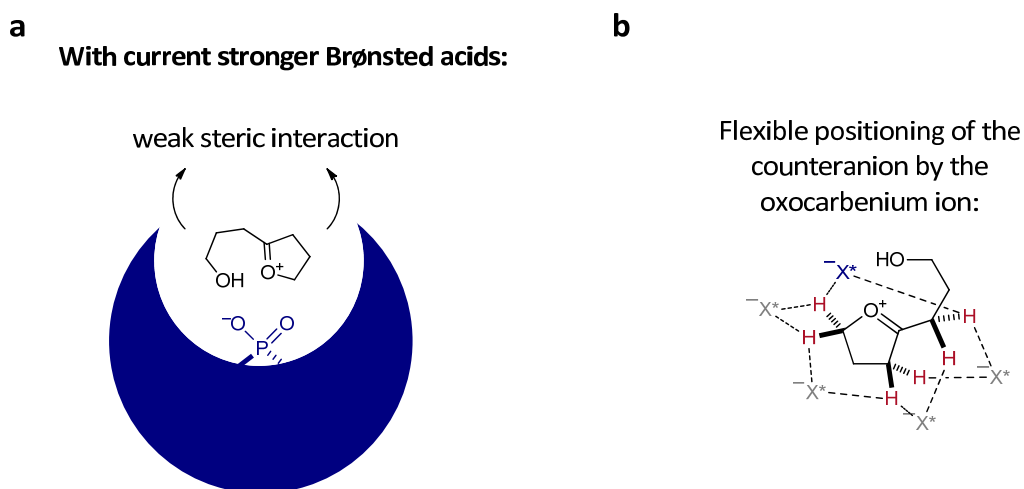
4.4.1. Design

During the attempts to develop the asymmetric spiroacetalization reaction we realized the limitations and deficiencies of current stronger Brønsted acid catalyst with small substrates (Scheme 4.27).



Scheme 4.27. Catalytic asymmetric spiroacetalization.

We hypothesized that the inability of the catalyst to impart efficient steric control for the small oxocarbenium ion intermediate is responsible for the lack of selectivity (Scheme 4.28a).



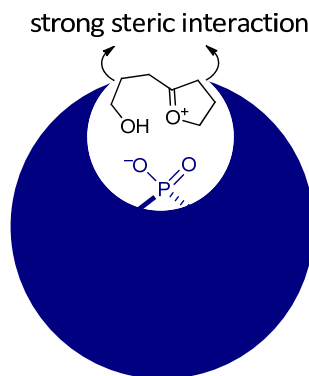
Scheme 4.28. Rationalization for the low selectivity in the spiroacetalization reaction.

In addition, the oxocarbenium ion lacks specific and sterically well defined interactions with its chiral anion, such as strong hydrogen bonding interaction (Scheme 4.28b). As a result the positioning of the anion relative to the oxocarbenium ion is not well determined leading to a number of possible orientations and lack of enantiocontrol (Scheme 4.28b).

While large active sites can accommodate various transition state geometries leading to different isomers, we reasoned that a confined space could limit this freedom and thereby increase selectivity (Scheme 4.29).^[138] On the basis of this hypothesis, we initiated modeling

studies towards sterically demanding acid catalysts for the envisioned spiroacetalization reaction.

Confined Brønsted acid:

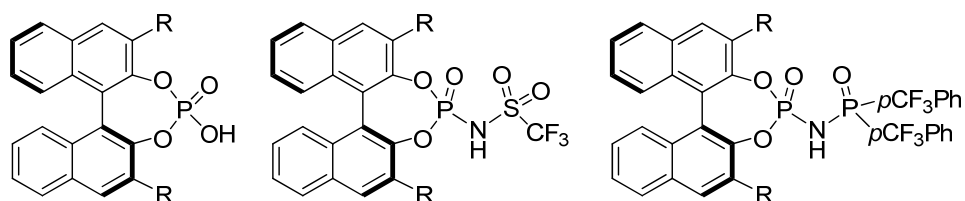


Scheme 4.29. New catalyst design.

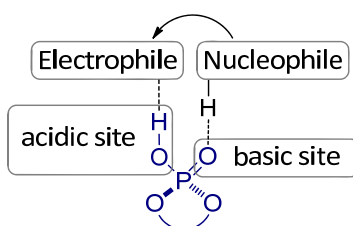
A solution to the spiroacetalization problem could potentially also tackle an important issue of broader significance in current Brønsted acid catalysis. Reactions of small aliphatic substrates that do not possess sterically demanding protecting groups, large aromatic or planar surfaces, or bulky substituents are still extremely rare.^[35-36, 147] We reasoned that a catalyst with compact chiral microenvironment could solve numerous other challenges in Brønsted acid catalysis. We speculated that such a catalyst could effectively restrict molecular motion, leading to efficient enantiodiscrimination even of substrates or intermediates, which lack spatially defined interactions such as hydrogen bonding with the catalyst. This design is inspired by enzymes that frequently display deep active site pockets constructed by the folding of the protein, and also by the architectures provided by artificial catalytic cavities.^[148-151] In the following we present the design of new, simple, and readily available synthetic Brønsted acid catalysts that display a sterically highly demanding and rigid chiral microenvironment around their active site.^[138]

Our design was based on the analysis of highly successful chiral phosphoric acids, in particular those based on the BINOL backbone,^[35-36, 58-59] their derivatives, *N*-triflyl phosphoramides introduced by Yamamoto,^[88] and the more recently developed *N*-phosphinyl phosphoramides and *C*₁-symmetric imidodiphosphoric acids (Scheme 4.30).^[92] The active site of a BINOL-derived phosphoric acid is composed of one Brønsted acidic (–OH) and one Brønsted basic site (=O). The remarkable success of phosphoric acids in asymmetric catalysis is

widely attributed to bifunctional activation, in which both of these sites are involved in the stabilization of a transition state (Scheme 4.31).^[35-36]

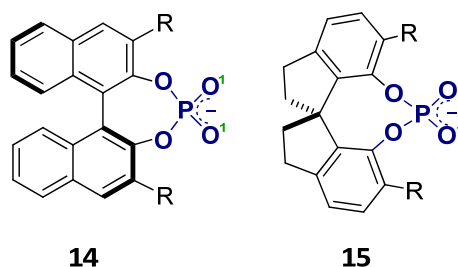


Scheme 4.30. Phosphoric acids, *N*-triflyl phosphoramides and *N*-phosphinyl phosphoramides.



Scheme 4.31. Bifunctional activation of reactants with Brønsted acid/base pair in phosphoric acid catalysis.

Although phosphates **14** and **15** have found wide application in asymmetric catalysis, it is challenging to further modify their steric environment because 3,3'-substituents on BINOL and SPINOL-backbones radiate away from the active site (Scheme 4.32).

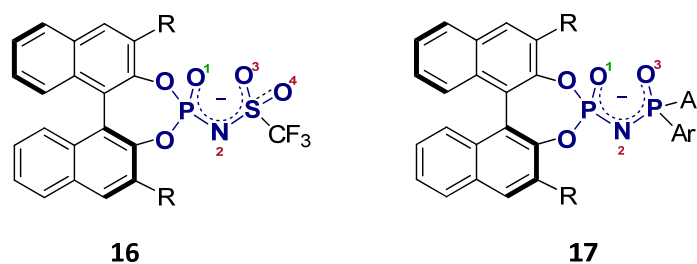


Feature: Single Brønsted acid/base pair (C_2 symmetry)
Issue: Bulky substituents radiate away from the active site

Scheme 4.32. C_2 -Symmetric anions of phosphoric acids.

C_1 -Symmetric anions **16** and particularly **17** seem to provide a simple alternative way of introducing additional steric demand close to the active site via the additional *N*-substituent (Scheme 4.33). However, both of these possess several different Brønsted basic sites potentially giving a large number of geometrically distinct acid/base pairs compared to only one such pair present in the phosphoric acid. The numbering of different Brønsted basic sites is

given in Scheme 4.32 and Scheme 4.33. This effectively leads to an ensemble of catalytically active species, which can stabilize different transition states, resulting in low selectivity.

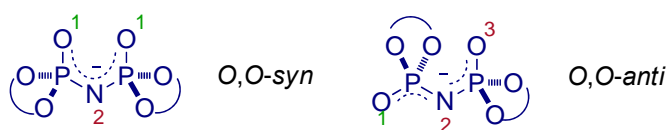


Feature: a simple way of introducing additional steric demand close to the active site
Issue: several different Brønsted basic sites, ensemble of catalytically active species

Scheme 4.33. C_1 -Symmetric anions of *N*-triflyl phosphoramides and *N*-phosphinoyl phosphoramides.

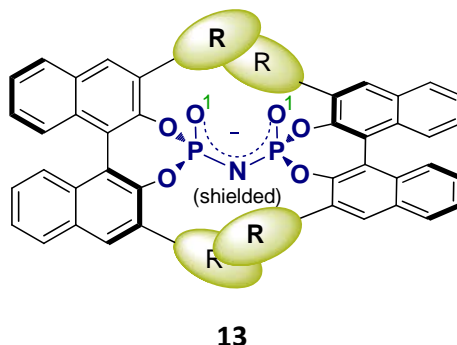
Furthermore, the rotational freedom around *P-N* and *N-S* bonds makes the relative positioning of acidic and basic site and therefore the entire chiral environment of anions **16** and **17** flexible. In some reactions only a reduced number of acid/base pairs could be catalytically relevant, due to steric or electronic factors. Indeed, while anions **16** and **17** display remarkable efficiency in a specific set of reactions, both of these structures lack the generality of phosphoric acids. However, in the case of *N*-triflyl phosphoramides this might be in part a consequence of their higher acidity. We reasoned that *only one distinct and geometrically fixed acid/base pair, translating into a single type of basic site in the corresponding anion is a prerequisite for the construction of a successful and broadly applicable Brønsted acid catalyst.*^[138]

Based on these considerations we designed a novel class of Brønsted acids, employing a C_2 -symmetric imidodiphosphate anion (Scheme 4.34). In principle, such a C_2 -symmetric imidodiphosphate moiety has two distinct Brønsted basic sites, *O* and *N*. The corresponding acid is expected to have a flexible relative positioning of acid/basic pairs due to rotation around *P-N* bonds, and would not satisfy the above mentioned criteria for the design of a general chiral Brønsted acid.



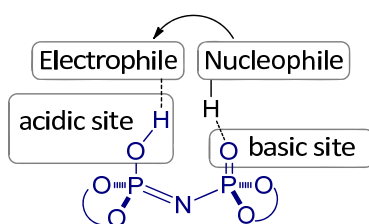
Scheme 4.34. General imidodiphosphate anion with numbering of different Brønsted basic sites.

However, our catalyst design aimed at restricting the imidodiphosphate moiety to a single *O,O*-*syn* conformation between two identical BINOL subunits with bulky 3,3'-substituents (Scheme 4.35).^[138]



Scheme 4.35. Conformationally locked *O,O*-*syn*-imidodiphosphate anion with C_2 -symmetry.

Based on the analysis of plastic ball and stick models we hypothesized that the inclusion of two BINOL subunits will result in their interlocking due to sterically demanding 3,3'-substituents as shown in Scheme 4.35. As a direct consequence, the BINOL subunits are unable to freely rotate and the resulting molecular structure possesses a very high rigidity. Importantly, such arrangement also resulted in the sterical blocking of the undesirable alternative Brønsted basic *N*-site. As the two BINOL subunits are identical, anion **13** is C_2 -symmetric, and has therefore two identical catalytically relevant Brønsted basic sites. Consequently, the corresponding Brønsted acid possesses a single catalytically active bifunctional acid/base pair with a fixed geometry (Scheme 4.36).^[138]

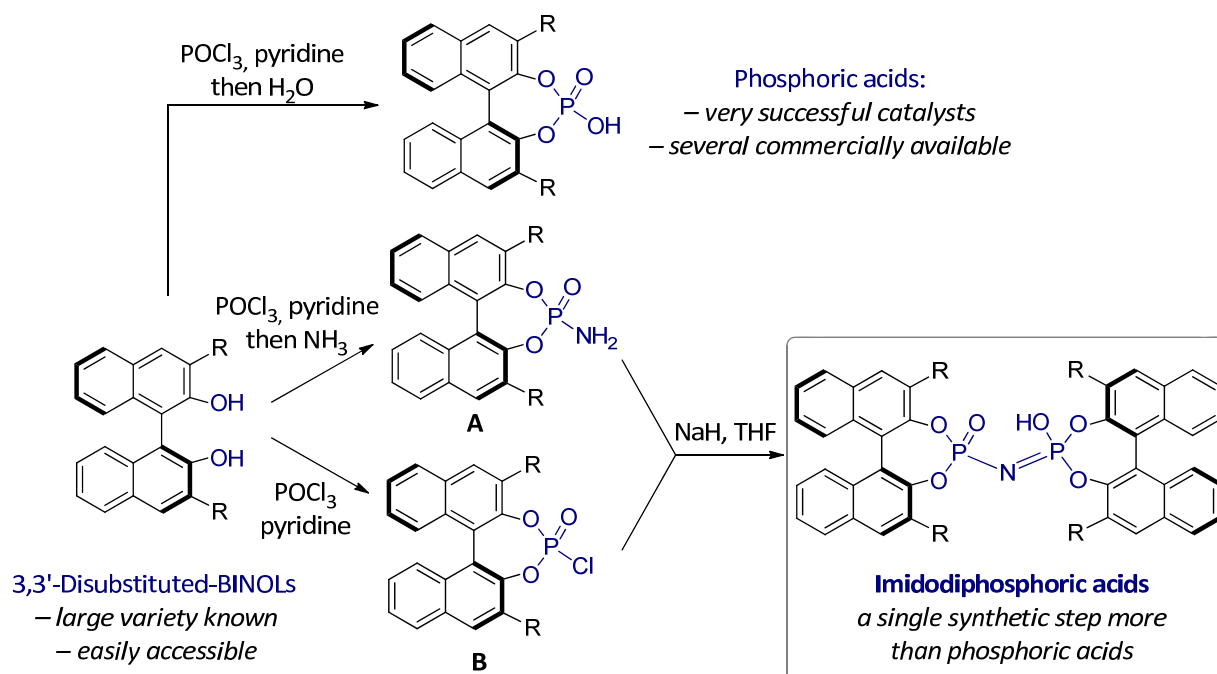


Scheme 4.36. Bifunctional activation of reactants with Brønsted acid/base pair in imidodiphosphoric acid catalysis.

The interlocking of BINOL-subunits could in principle also result in the conformational locking of the imidodiphosphate moiety in the *O,O*-*anti* conformation to give the *O,O*-*anti*-isomer of **13** (Scheme 4.34). However, based on our analysis of plastic models we expected that the formation of the corresponding *O,O*-*anti*-isomer will be disfavored with bulky 3,3'-substituents on BINOL backbones due to severe clashing of the substituents.

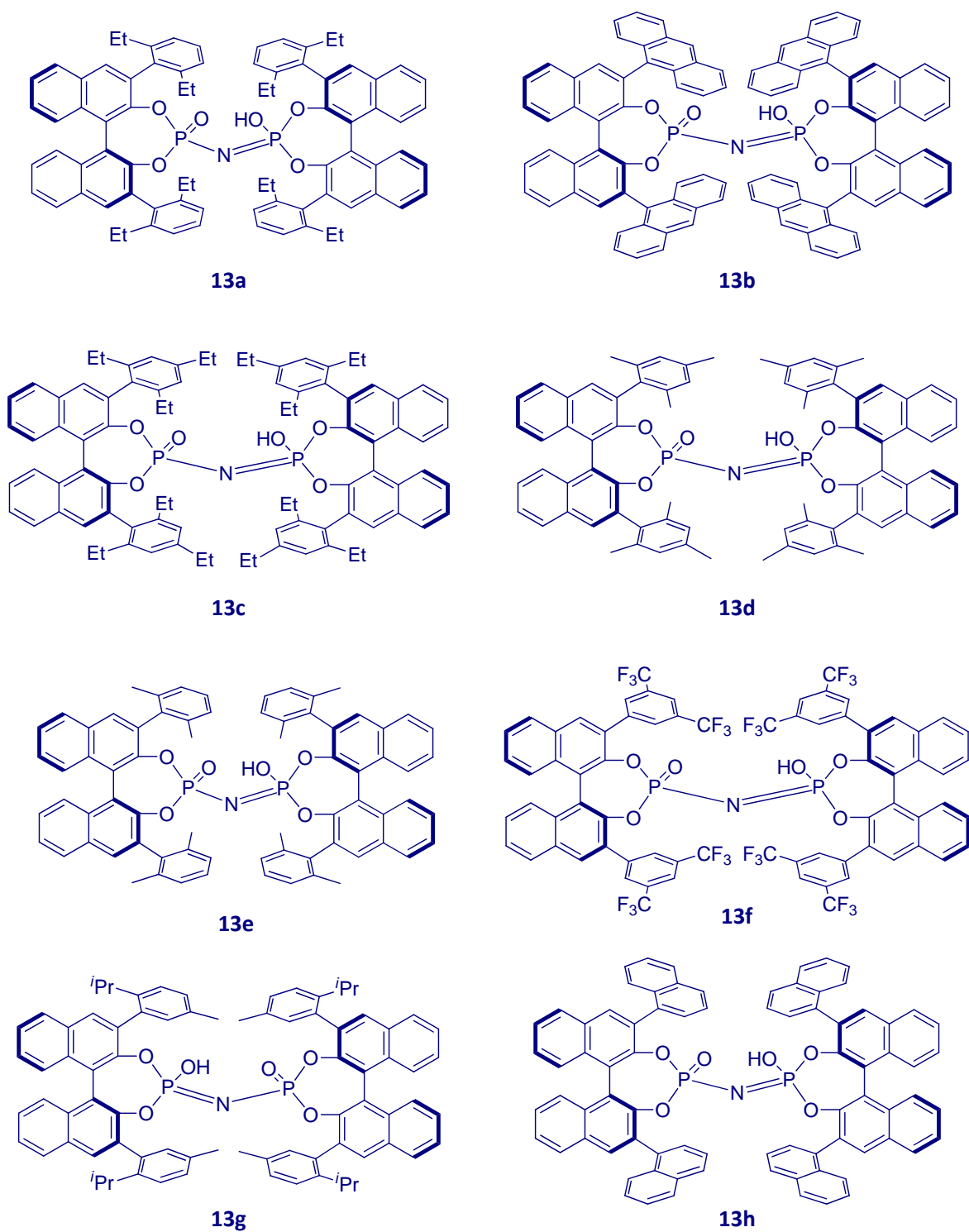
4.4.2. Synthesis

The structure of C_2 -symmetric imidodiphosphoric acids is based on interlocking of two identical BINOL subunits, enabling a highly convergent synthetic approach. In fact, their synthesis requires only a single additional synthetic step compared to the synthesis of the corresponding phosphoric acids (Scheme 4.37).^[138] Starting from readily available 3,3'-substituted BINOL-derivatives, synthetic intermediates **A** and **B** are obtained in a single step. Their coupling under basic conditions directly affords the desired C_2 -symmetric imidodiphosphoric acids (Scheme 4.37).^[138]



Scheme 4.37. Synthetic strategy for C_2 -symmetric imidodiphosphoric acids.

Based on this synthetic strategy we have obtained several imidodiphosphoric acids **13a-13h** with bulky substituents on the 3,3'-positions of the two BINOL backbones (Scheme 4.38). Acids were isolated after column chromatography and treatment with 3 N aqueous HCl to remove metal impurities and ensure the presence of pure Brønsted acids.^[60-61] Attempts to prepare the imidodiphosphoric acids with the very bulky 2,4,6-*i*-Pr₃C₆H₂- or 2,6-*i*-Pr₂C₆H₂-substituents on the BINOL backbones by this method were unsuccessful.



Scheme 4.38. Chiral C_2 -symmetric imidodiphosphoric acids.

4.4.3. X-Ray structures

Large crystals of C_2 -symmetric imidodiphosphoric acid **13c** were easily obtained by dissolving the acid in hot acetonitrile, adding a few drops of water and leaving the solution to freely cool to room temperature. The crystal structure of imidodiphosphoric acid **13c** reveals a confined active site deeply buried within a highly sterically demanding chiral environment (Figure 4.2).^[138]

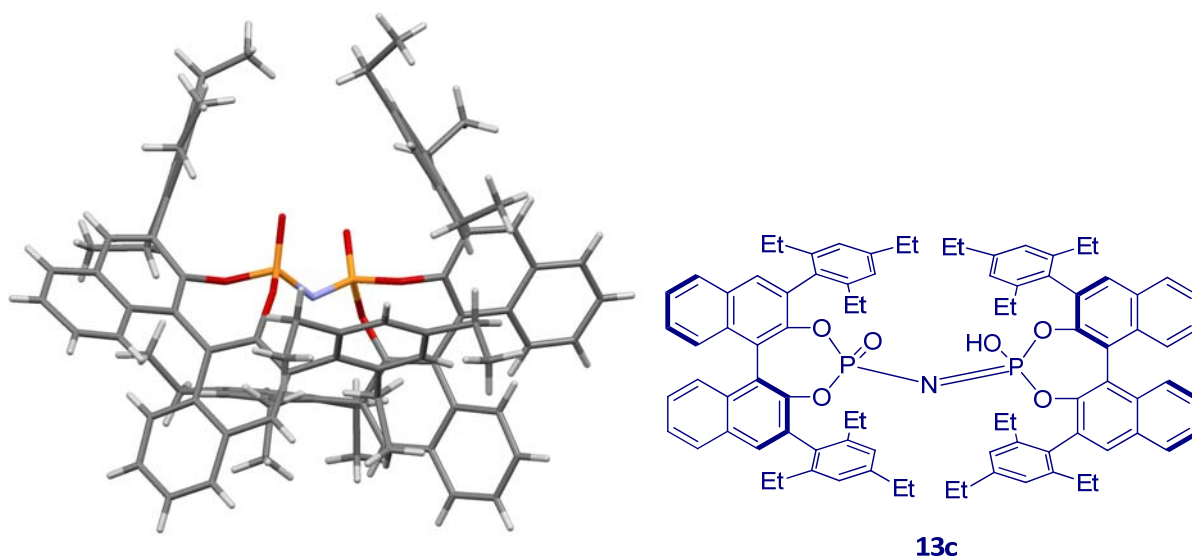


Figure 4.2. Crystal structure of the anion of **13c**, side view.^[138]

Viewing the catalytic moiety from the top illustrates how the two BINOL-substituents surround the active site from above (Figure 4.3a). Viewed from the bottom half, the catalyst demonstrates a tight arrangement of two remaining BINOL subunits units, which completely block access to the imidodiphosphate (Figure 4.3b).^[138]

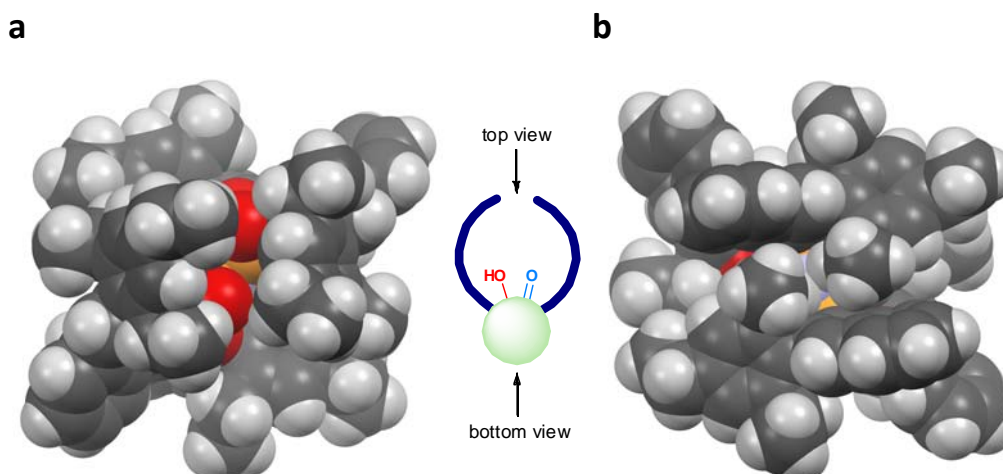


Figure 4.3. **13c**, Space filling models a) top view; b) bottom view.^[138]

4. RESULTS AND DISCUSSION

For comparison, the crystal structure of one of the most popular and sterically demanding phosphoric acids, TRIP (**1a**), is given in Figure 4.4.^[61] The active site of TRIP is placed inside a broad open cone, while that of the imidodiphosphate can better be described as a chiral pocket.

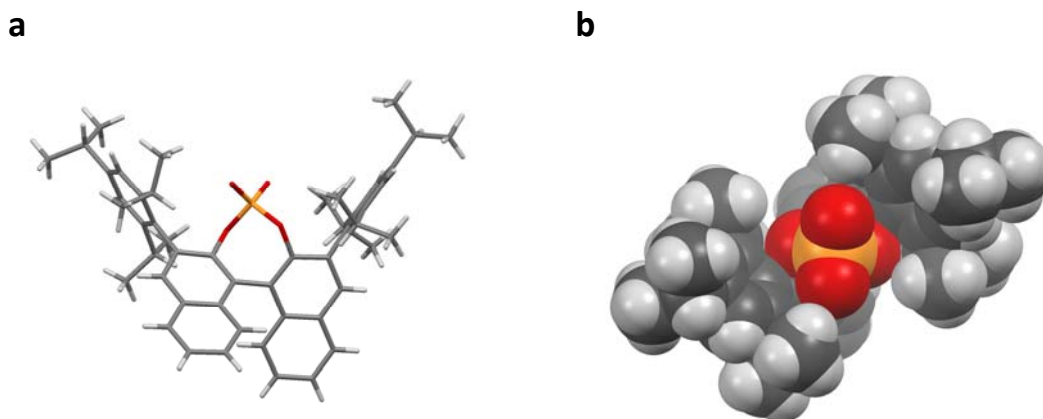


Figure 4.4. a) Crystal structure of TRIP anion; b) view at the active site, space filling model.

Crystals of imidodiphosphoric acids **13a** and **13b** were also obtained and their X-ray structures determined. Acid **13b** features a confined acid moiety similarly to catalyst **13c** (Figure 4.5). Two anthracenyl substituents surround the active site, while the remaining two substituents provide an aromatic “nest” below the catalytic moiety (Figure 4.6). Although acid **13a** (Figure 4.7) displays complete shielding of the imidodiphosphate from the bottom, compared to acids **13b** and **13c**, the active site is less shielded from the top (Figure 4.8).

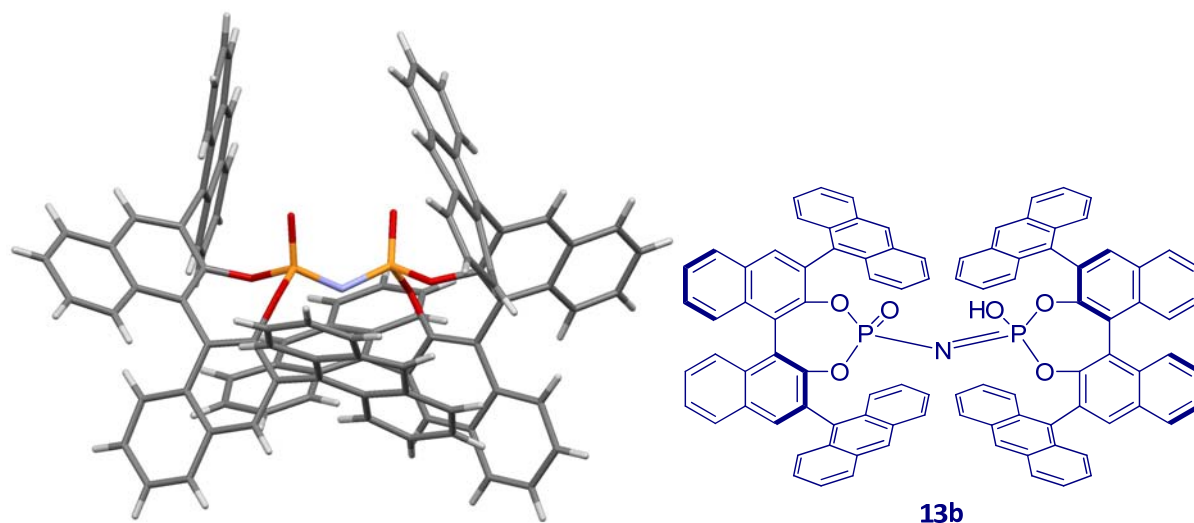


Figure 4.5. Crystal structure of the anion of **13b**, side view.

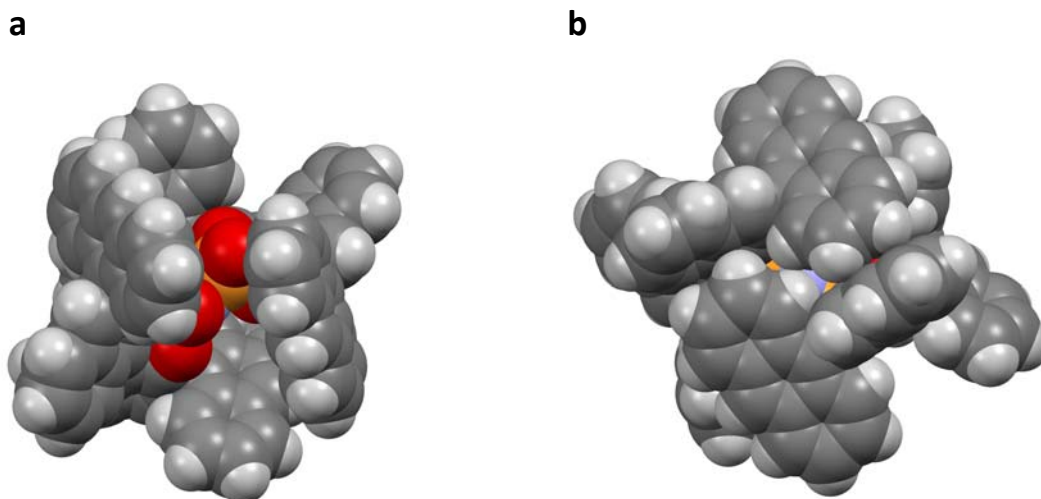


Figure 4.6. **13b**, Space filling models a) top view; b) bottom view.

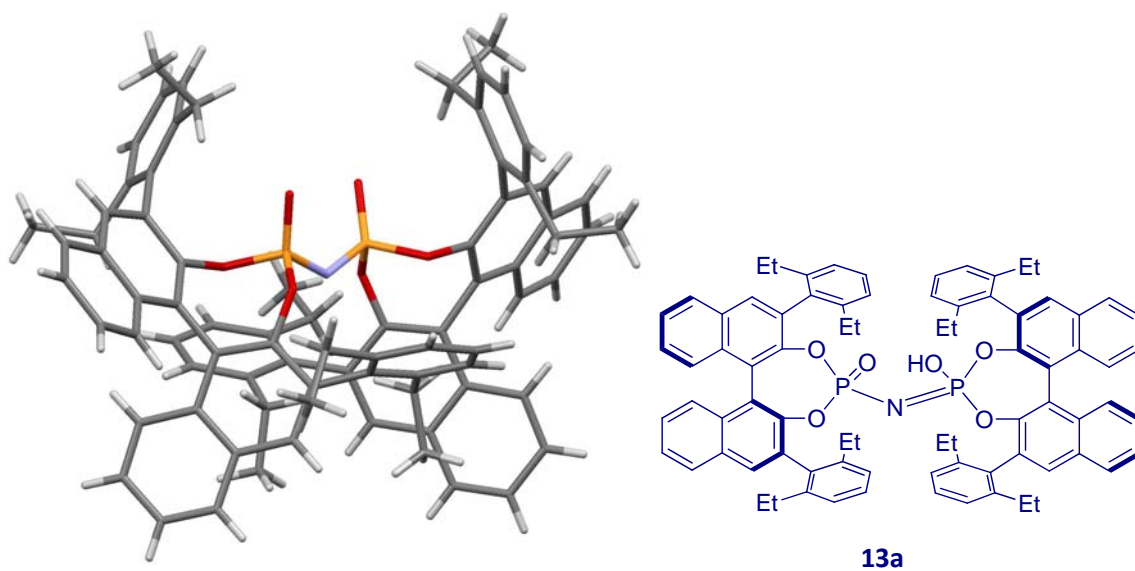


Figure 4.7. Crystal structure of the anion of **13a**, side view.

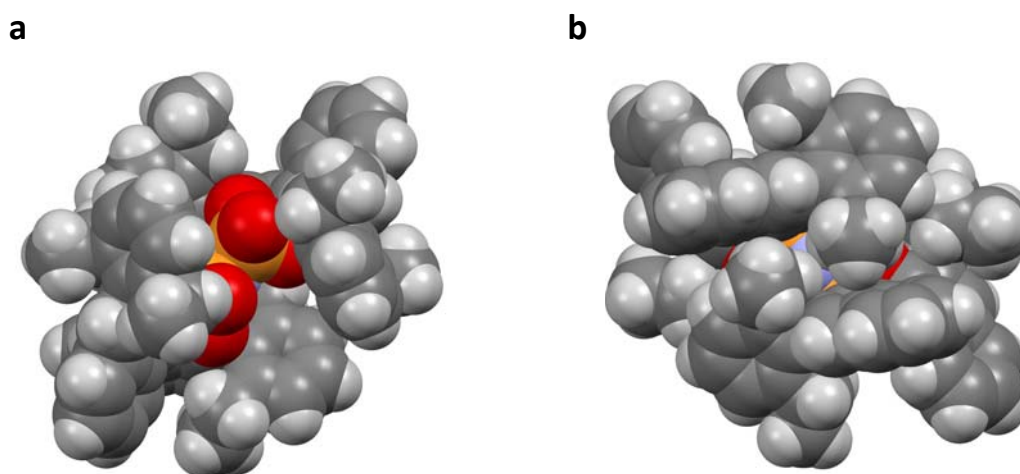


Figure 4.8. **13a**, Space filling models a) top view; b) bottom view.

4. RESULTS AND DISCUSSION

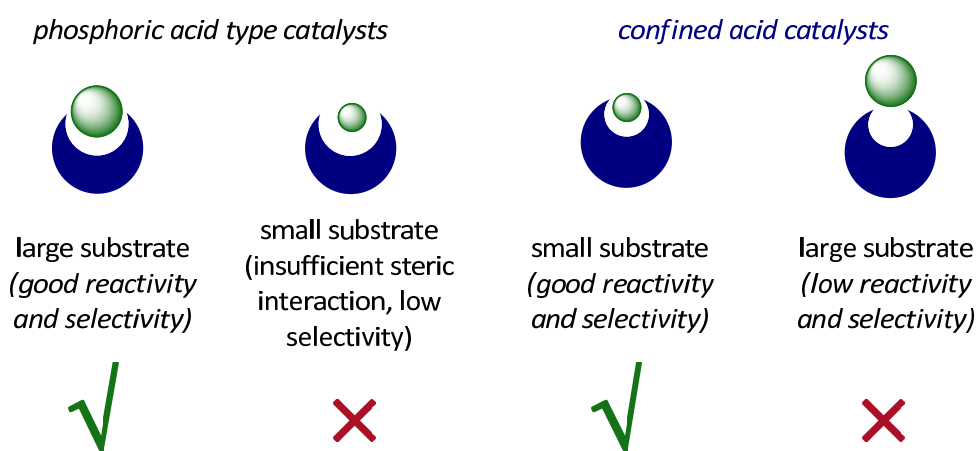
The geometrical parameters of the imidodiphosphoric acids, which co-crystallized with a molecule of water, are consistent with a hydronium ion bridging the two imidodiphosphate oxygen atoms. This supports proton location on oxygen rather than on nitrogen, as shown in Scheme 4.36.

4.4.4. Discussion

While recent developments in Brønsted acid catalysis have enabled an array of transformations to be performed asymmetrically,^[35-36, 87] substrates have typically been sterically or electronically biased. In principle any reaction can be performed asymmetrically if it is placed in a steric environment that is capable to accommodate one of the two enantiomeric transition states. For small molecules, and molecules or intermediates that have weak interactions with the catalyst's active moiety, a solution for high enantioselectivity could be provided by extremely sterically demanding environment of the catalyst that restricts the motion of the molecules. We have designed such acid catalysts, termed confined Brønsted acids that possess chiral pockets reminiscent of those found in enzymes.^[138] We believe that our concept opens the door for the development of various asymmetric reactions which include small aliphatic and/or loosely bound molecules.

Reactions with small and large substrates

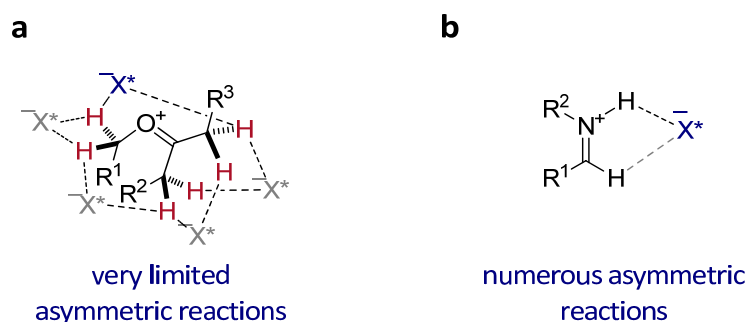
Phosphoric acid type catalysts are unable to impart selectivity to small substrates due to insufficient steric interaction with the catalyst structure (Scheme 4.39). On the other hand tight pockets of confined acids can overcome this issue, as demonstrated with the asymmetric spiroacetalization reaction (Scheme 4.39). However, chiral confined acids are not expected to efficiently accommodate large substrates as these cannot fit into the catalysts cavity. The performances of confined chiral acids and phosphoric acid type catalysts are expected to be complementary with the regard to the size of the substrate (Scheme 4.39).



Scheme 4.39. Schematic comparison of the expected performance of chiral confined acids and phosphoric acid type catalysts with large and small substrates.

Reactions with loosely bound molecules

Loosely bound molecules or intermediates are considered those lacking specific and sterically well defined interactions with the catalyst. A good example would be an oxocarbenium ion which possesses only very weakly acidic C-H bonds to bind the chiral anion of the catalyst (Scheme 4.40a). Furthermore, the oxocarbenium ion possesses a number of such C-H bonds giving multiple possibilities for anion binding. Such weak and geometrically unrestricted interaction with the chiral anion results in the presence of numerous transition state geometries for the nucleophilic attack leading to low enantioselectivity. Unlike oxocarbenium ions, iminium ions possess a strong $N^+ - H \cdots X^-$ hydrogen bond which fixes the position of the chiral anion, a scenario that rationalizes the success of numerous enantioselective additions of nucleophiles to imines (Scheme 4.40b).

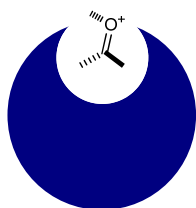


Scheme 4.40. a) Loose binding of oxocarbenium ion and a chiral counteranion; b) strong and restricted binding in the case of iminium ion.

If the loosely bound intermediate is placed within a tight chiral cavity, its motion could be restricted with shielding groups of the catalyst. Additionally, the catalyst architecture should also effect the nucleophile allowing the approach to the electrophile only from specific unblocked directions. These two effects result in an effective reduction of the number of available transition states leading to increased enantioselectivity. In addition to controlling reactions of small molecules, confined Brønsted acids were designed also to impart selectivity in the cases of weakly organized transition states (Scheme 4.41).

For the success of the asymmetric spiroacetalization reaction the ability of chiral confined acids to handle both small substrate and loosely bound intermediate might have been crucial.

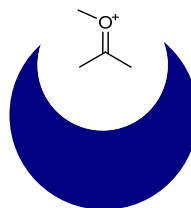
confined acid catalysts



loosely bound
intermediate
(*restricted motion in
tight space,
good selectivity*)



phosphoric acid type catalysts



loosely bound
intermediate
(*unrestricted motion,
low selectivity*)



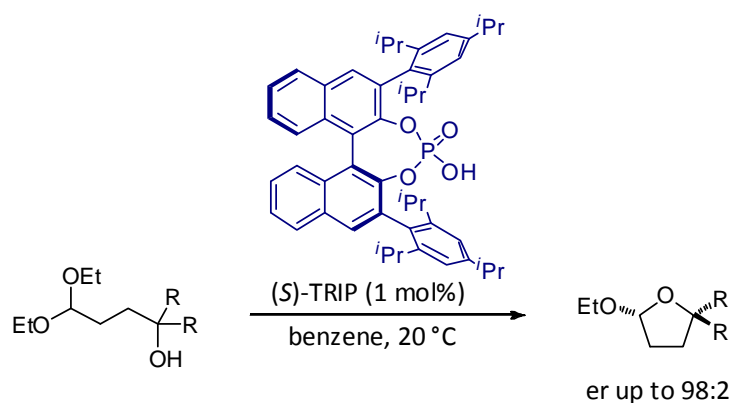
Scheme 4.41. Schematic comparison of the expected performance of chiral confined acids and phosphoric acid type catalysts with loosely bound intermediates.

5. SUMMARY

5.1. Catalytic asymmetric transacetalization

Chiral acetals are frequently encountered motifs in a variety of natural products as well as common functional groups in organic synthesis. Interestingly, the presence of an acetal in cellulose, the most abundant of all naturally occurring organic compounds, makes acetal stereocenters one of the most common organic stereocenters on Earth. However, methods for the enantioselective synthesis of chiral acetal carbon stereocenters are very limited. A single catalytic asymmetric formation of acetals was previously achieved via a metal-catalyzed hydroetherification of enol ethers with an er up to 93:7.

We have developed a catalytic asymmetric transacetalization reaction.^[107] For the first time catalytic asymmetric formation of an acetal stereocenters could be achieved with very high enantioselectivity (Scheme 5.1). In addition the reaction presents, to the best of our knowledge, a first example of phosphoric acid catalyzed enantioselective addition of nucleophiles to simple *O,O*-acetals.



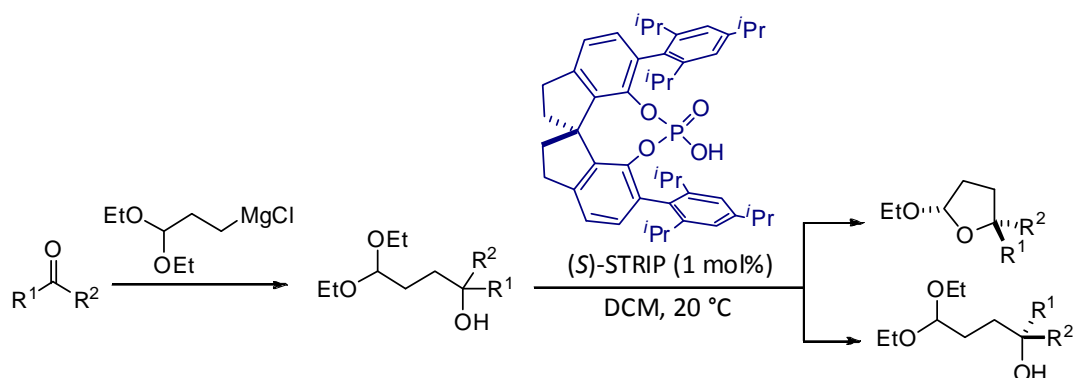
- *first catalytic highly enantioselective acetal formation*
- *first catalytic asymmetric substitution of acetals using Brønsted acids*

Scheme 5.1. Catalytic asymmetric transacetalization.

5.2. Kinetic resolution of homoaldols via catalytic asymmetric transacetalization

(with S. Müller)^[108]

Homoaldols are versatile motifs in organic synthesis that can be easily transformed into a vast array of important chiral compounds such as γ -lactones, tetrahydrofurans, pyrrolidines, and others. Due to problematic homoaldol disconnection these are not readily available in a catalytic asymmetric fashion. We have developed a highly enantioselective kinetic resolution of aldehyde protected homoaldols via a catalytic asymmetric transacetalization reaction.^[84] Our kinetic resolution represents a very atom economic method, forming ethanol as the only byproduct. The acetal group in cyclic acetals can be considered as a protecting group and as a functional group that can be directly modified, e.g. oxidized, reduced or substituted. Our method is applicable to the resolution of a wide range of secondary and tertiary homoaldols. The reaction represents the first examples of kinetic resolution of alcohols via acetal formation, and the first example of Brønsted acid catalyzed kinetic resolution of alcohols.

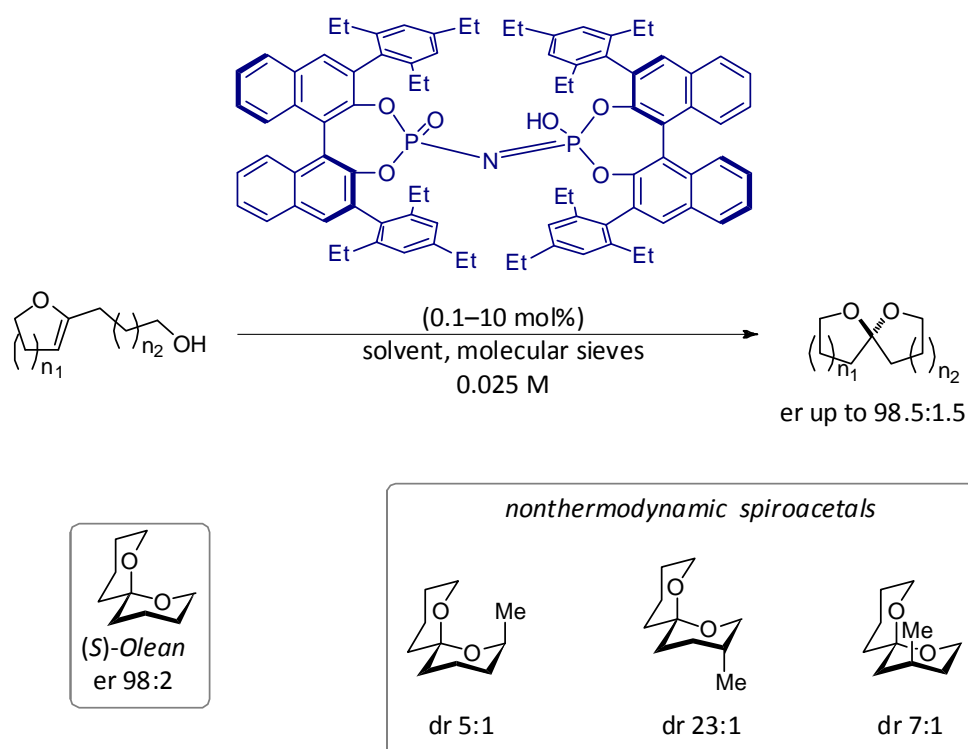


- first kinetic resolution of alcohols via catalytic asymmetric acetalization
- first Brønsted acid catalyzed kinetic resolution of alcohols
- rare example of a highly efficient kinetic resolution of tertiary alcohols
- no reagent required
- ethanol as the only byproduct

Scheme 5.2. Kinetic resolution of homoaldols.

5.3. Catalytic asymmetric spiroacetalization

Spiroacetals occur in many biologically active compounds ranging from small insect pheromones to complex macrocycles. We have developed the first catalytic asymmetric spiroacetalization reaction to access small unfunctionalized spiroacetals which are the cores of many natural products (Scheme 5.3).^[138] Additionally, our spiroacetalization reaction provides a direct catalyst controlled access to both nonthermodynamic and thermodynamic spiroacetals in mild kinetic conditions, a longstanding challenge in natural product synthesis (Scheme 5.3).^[2]



- Brønsted acid catalyzed synthesis of small unfunctionalized molecules
- first catalytic asymmetric synthesis of olean
- first catalytic synthesis of nonthermodynamic acetals
- asymmetric addition of heteroatom nucleophiles to oxocarbenium intermediates

Scheme 5.3. Catalytic asymmetric spiroacetalization.

5.4. Confined Brønsted acids

The field of Brønsted acid catalysis has acquired wide popularity and importance in recent years. However reactions of small molecules and/or loosely bound molecules or intermediates are largely undeveloped. We hypothesized that catalysts with truly compact chiral microenvironment could address these issues. We have rationally designed chiral confined Brønsted acids based on a C_2 -symmetric imidodiphosphoric acid motif.^[138] These catalysts feature extremely sterically demanding chiral environments around their active site and possess a single catalytically relevant and geometrically constrained bifunctional active site (Figure 5.1).

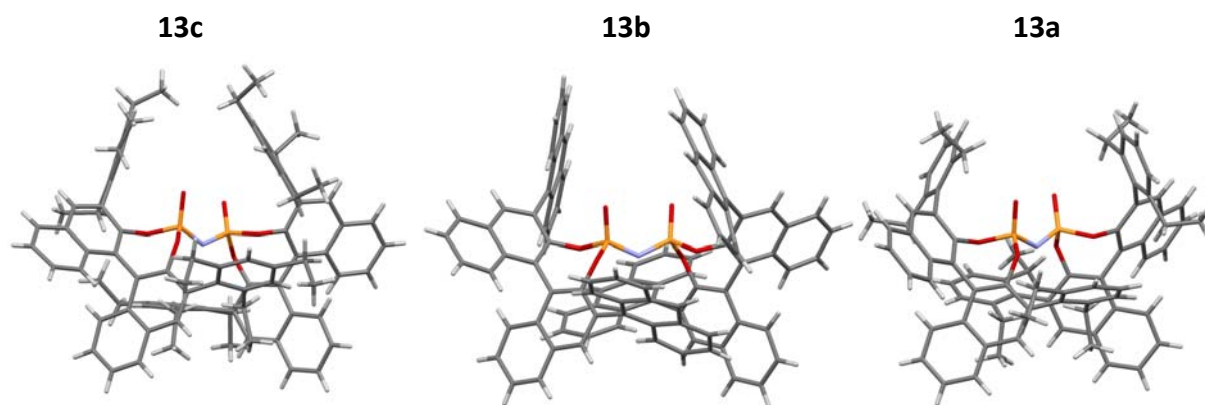


Figure 5.1. Confined Brønsted acids.

Confined Brønsted acid catalysts enabled the development of the first asymmetric spiroacetalization reaction to access natural product olefin and other small unfunctionalized spiroacetals.^[138]

Chiral cavities present in these catalysts are designed to induce enantioselectivity to the reactions with *transition states that are not well organized by noncovalent attractive interactions* and/or with *transitions states of small volume* (Figure 5.2).

It is noteworthy that diverse confined C_2 -symmetric imidodiphosphoric acids are easily accessible. Their synthesis requires only a single additional synthetic step compared to the corresponding phosphoric acids. Yet, they provide completely different active moiety and significant increase in the steric demand of the chiral environment, while retaining crucial features of the phosphoric acids: C_2 -symmetry of the anion and a single type of bifunctional active site (Scheme 5.4).

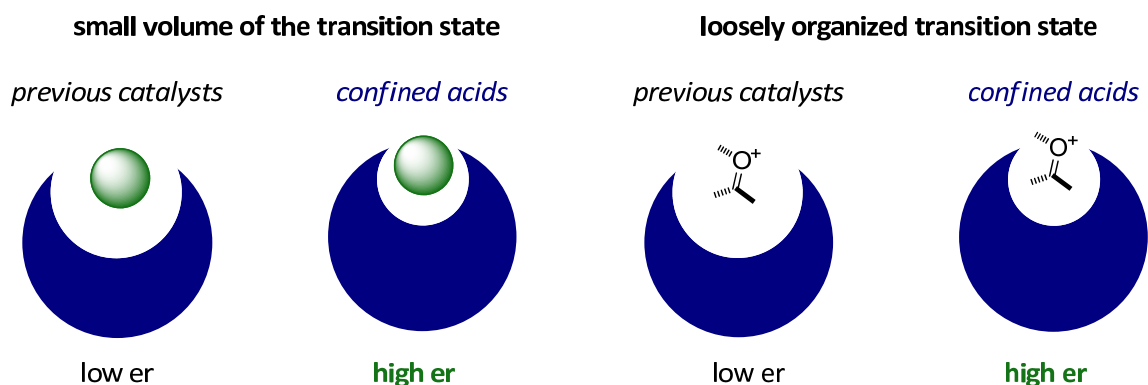
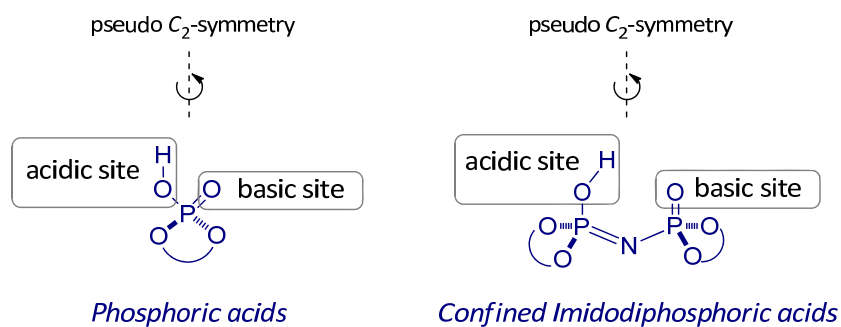


Figure 5.2. Influence of the size of the chiral environment on the catalyst performance.



Scheme 5.4. Pseudo C_2 -symmetry and a single type of bifunctional active site in phosphoric acids and imidodiphosphoric acids.

This work has been disclosed in part in the following publications:

“Asymmetric Spiroacetalization Catalysed by Confined Brønsted Acids”, I. Čorić, B. List, *Nature* **2012**, 483, 315.

“Kinetic Resolution of Homoaldols via Catalytic Asymmetric Transacetalization”, I. Čorić,[‡] S. Müller,[‡] B. List, *J. Am. Chem. Soc.* **2010**, 132, 17370. ([‡]equal contribution)

“N-Phosphinyl Phosphoramidate—A Chiral Brønsted Acid Motif for the Direct Asymmetric N,O-Acetalization of Aldehydes”, S. Vellalath, I. Čorić, B. List, *Angew. Chem. Int. Ed.* **2010**, 49, 9749.

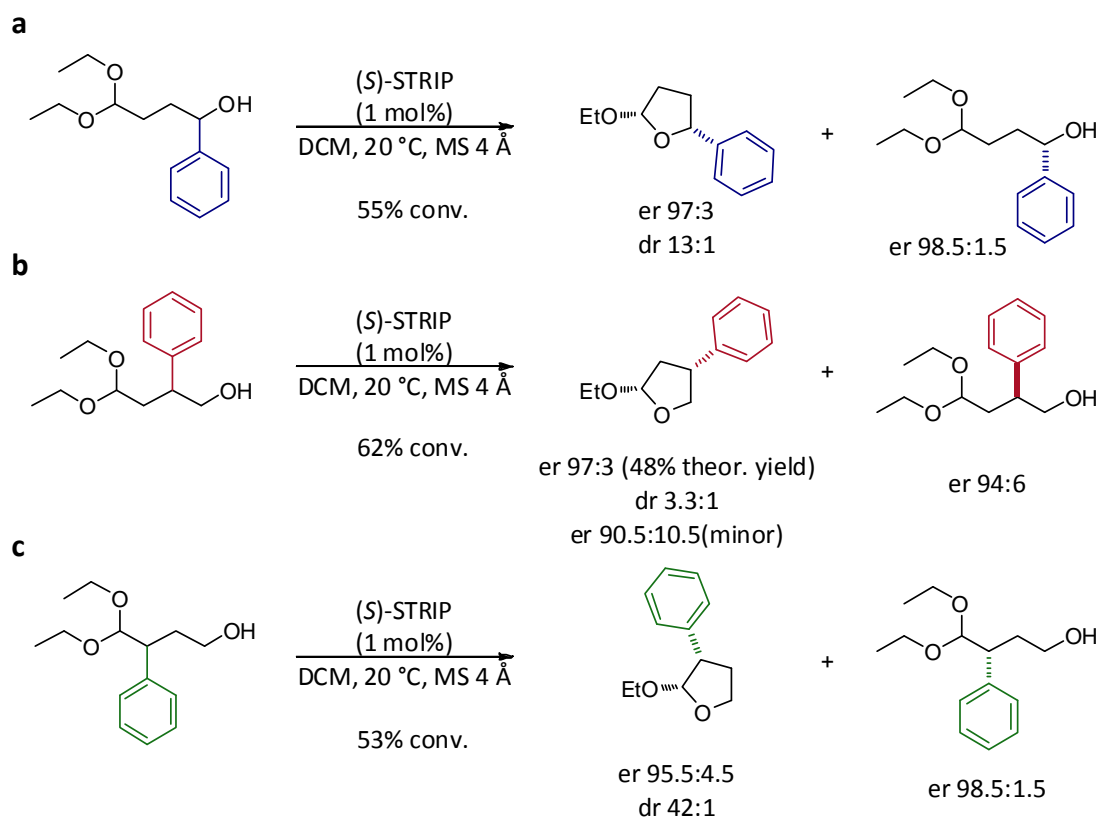
“Catalytic Asymmetric Transacetalization”, I. Čorić, S. Vellalath, B. List, *J. Am. Chem. Soc.* **2010**, 132, 8536. Erratum: *J. Am. Chem. Soc.* **2010**, 132, 12155.

6. OUTLOOK

6.1. Kinetic resolutions of homoaldols

(with S. Müller)^[108]

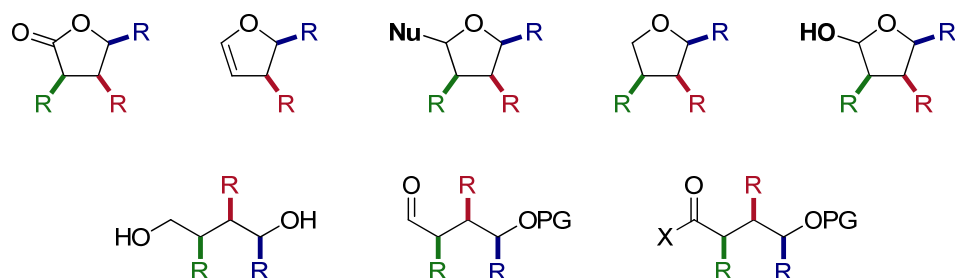
In our initial investigations on kinetic resolution of homoaldols via catalytic asymmetric transacetalization we have focused on the kinetic resolution of 4-substituted homoaldols (Scheme 6.1a).^[84] Due to the intramolecular nature of the reaction proceeding through an organized cyclic transition state we hypothesized that efficient kinetic resolution of substrates substituted anywhere in the chain might occur. Our initial studies in this regard show that 3-substituted primary alcohol substrates could be resolved to give cyclic acetals with high enantioselectivity, although with moderate diastereoselectivity (Scheme 6.1b). A 2-substituted acetal exhibited excellent kinetic resolution giving the cyclic product and enantioenriched alcohol with high enantioselectivity (Scheme 6.1c). Taken together these initial results demonstrate that our method could be used to access arbitrary substituted cyclic or acyclic acetal-protected homoaldols.



Scheme 6.1. Kinetic resolutions of arbitrary substituted homoaldol acetals.

6. OUTLOOK

All of these compounds are highly valuable synthetic intermediates that can be converted to numerous 1,4-dioxygenated compounds (Scheme 6.2).

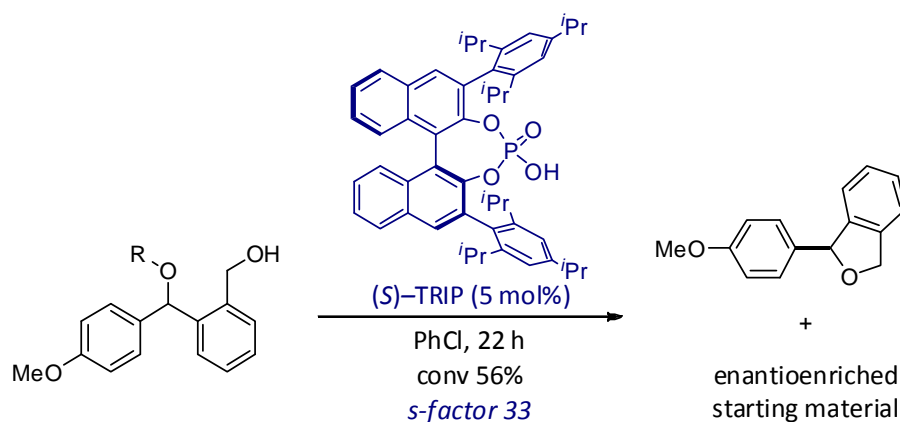


Scheme 6.2. Selection of compounds potentially accessible from our enantioenriched homoaldols.

6.2. Catalytic asymmetric transesterification

(with J. H. Kim and T. Vlaar)

With the catalytic asymmetric transacetalization it was demonstrated that chiral phosphoric acids are efficient catalysts for the activation of the acetal functionality.^[107] Encouraged by this discovery, we hypothesized that Brønsted acids of this type could potentially also activate resilient ether functionality and catalyze an asymmetric transesterification reaction. Initial results towards this goal show that this reaction is viable. The reaction of a secondary benzyl ether substrate proceeds with kinetic resolution and a selectivity factor of 33 (Scheme 6.3). This reaction represents the first example of Brønsted acid catalyzed asymmetric alkylation with ethers.



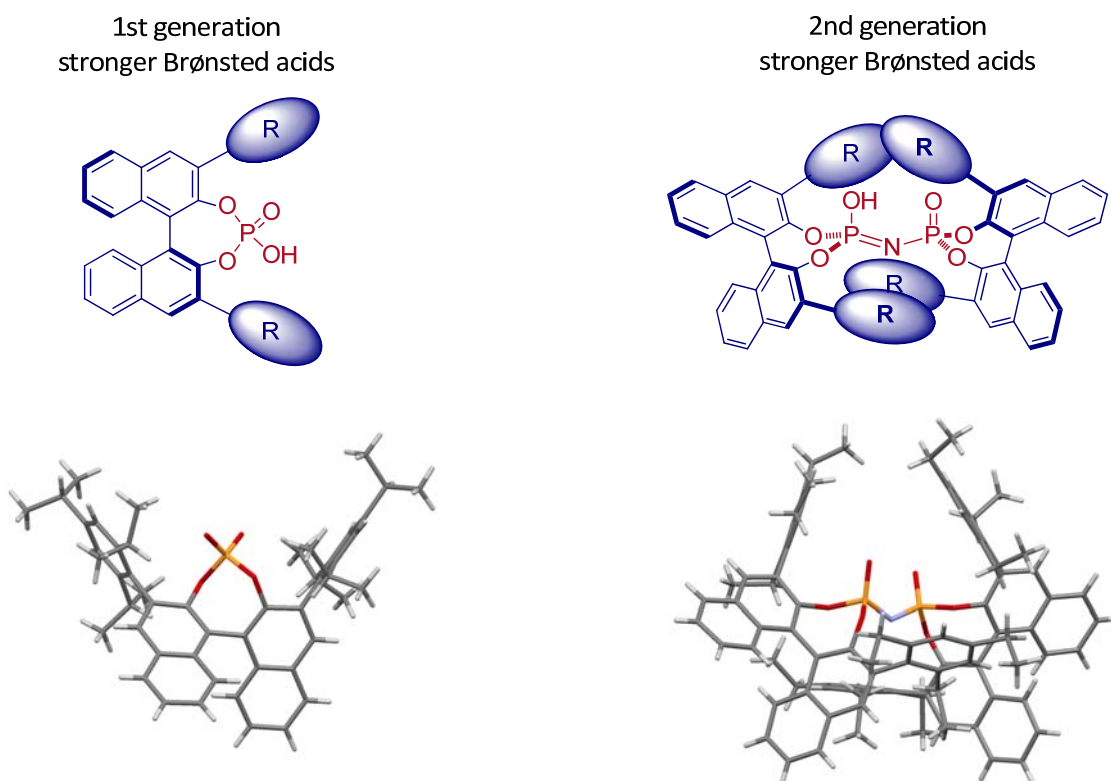
Scheme 6.3. Catalytic asymmetric transesterification.

6.3. Imidodiphosphoric acids as the second generation of stronger Brønsted acids

The first use of chiral stronger Brønsted acid catalysts, phosphoric acids, was described 8 years ago by Akiyama and Terada.^[58-59] Since then, a vast number of catalytic asymmetric reactions has been discovered.^[35-36] We believe that the imidodiphosphoric acids described here present a second generation of stronger Brønsted acid catalysts (Scheme 6.4).^[138] The steric demand of these catalysts can be controlled by desire allowing even extremely sterically demanding, tight chiral pockets to be accessed. These catalysts are expected to solve challenges in asymmetric Brønsted acid catalysis arising from:

- small volume of the transition states (e.g. small substrates)
- loosely bound intermediates and weakly organized transition states

Confined imidodiphosphates could also be widely applicable as anions, even beyond Brønsted acid catalysis.^[73-75] Confined imidodiphosphoric acid catalysts already showed excellent results, and we have recently resolved several longstanding challenges in our laboratory.

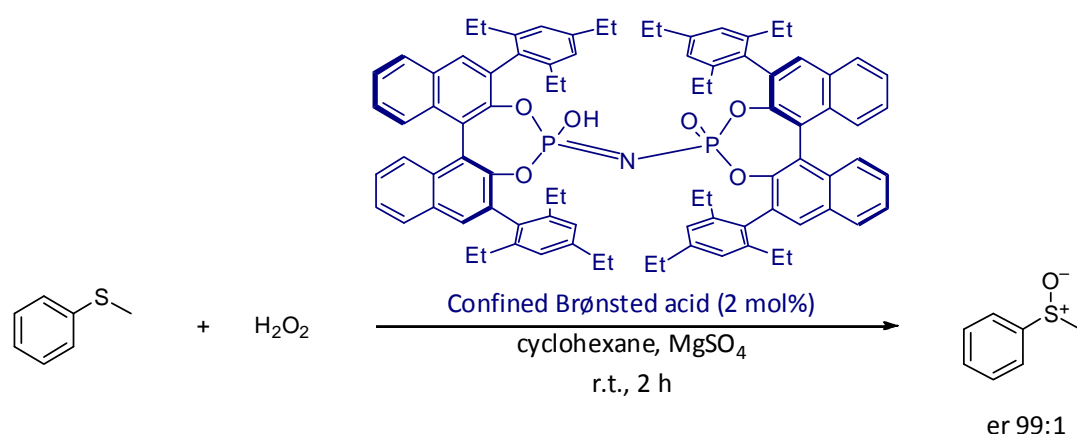


Scheme 6.4. Phosphoric and imidodiphosphoric acids.

Brønsted acid catalyzed sulfoxidation with H₂O₂

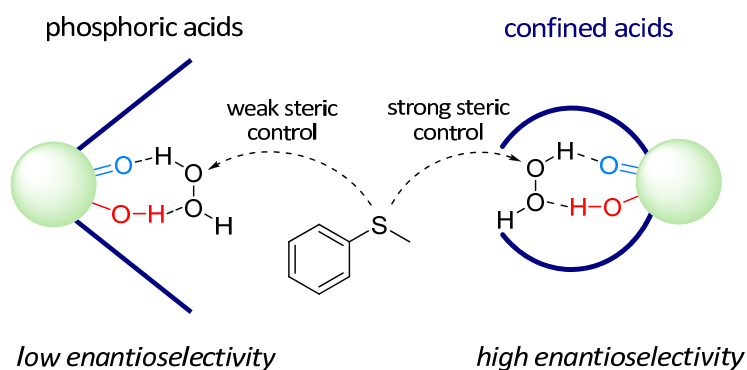
(with S. Liao)

One of the projects in our laboratory was directed towards developing Brønsted acid catalyzed asymmetric oxidation of sulfides with hydrogen peroxide. Although it was known that acids accelerate this reaction, no asymmetric version has been reported. Our attempts with a variety of known phosphoric acid catalysts resulted only in low enantioselectivity with an er of up to 78:22. Gratifyingly, confined imidodiphosphoric acids enabled a highly enantioselective sulfoxidation with H₂O₂ (Scheme 6.5).



Scheme 6.5. Confined acid catalyzed sulfoxidation.

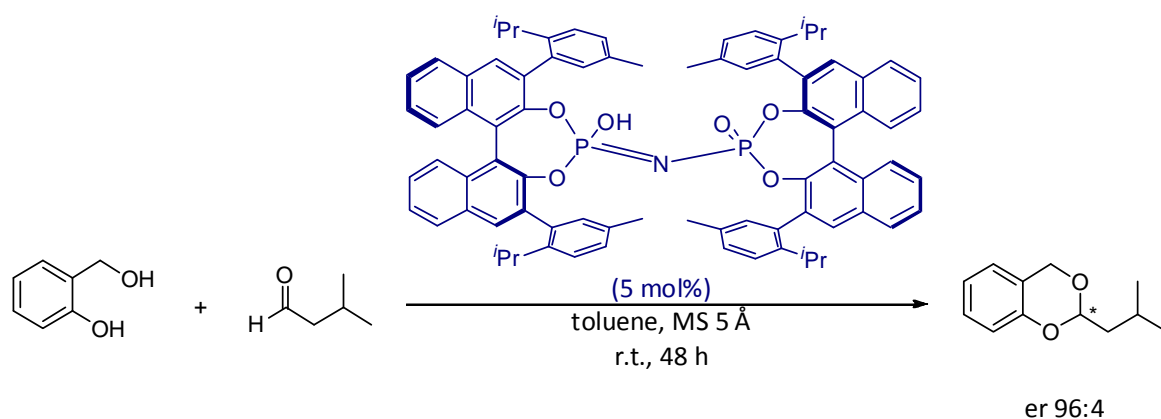
We hypothesize that with the confined Brønsted acid, H₂O₂ molecule is placed within a chiral cavity of the catalyst (Scheme 6.6). Such an environment severely restricts the approach geometry of the incoming substrate based solely on steric control. Such reactions including transition states that are not well organized with covalent or hydrogen bonding interactions between the catalyst and the substrates are very rare in current Brønsted acid catalysis.



Scheme 6.6. Activation of H₂O₂ with confined acids.

Catalytic asymmetric acetalization of aldehydes*(with J. H. Kim)*

The direct asymmetric acetalization of aldehydes has been a longstanding challenge in our laboratory. Our attempts with a variety of known phosphoric acids catalysts resulted only in low enantioselectivity with an er of up to 72:28. Gratifyingly, a novel imidodiphosphoric acid enabled the first highly enantioselective acetalization of aldehydes (Scheme 6.7).



Scheme 6.7. Asymmetric acetalization of aldehydes.

Although the substituents on the phosphoric acid can be readily modified, in practice only some very bulky substituents are effective in imparting good steric control. C_2 -Symmetric imidodiphosphoric acids possess much higher steric demand around the active site, enabling introduction of a variety of substituents without compromising the sterical demand of the active site. Consequently the architecture of the imidodiphosphoric acid enables the construction of much more diverse chiral environments than previous catalysts.

7. EXPERIMENTAL SECTION

7.1. General Experimental Conditions

Solvents and reagents

All solvents used in the standard procedures were purified by distillation. Absolute diethyl ether, tetrahydrofuran and toluene were obtained by distillation over sodium with benzophenone as indicator; absolute chloroform and dichloromethane were obtained by distillation over calcium hydride, and ethanol, isopropanol and methanol were dried by distillation over magnesium. Absolute 1,4-dioxane, MTBE and DCE were purchased from Sigma-Aldrich and used as received. Commercial reagents were obtained from various sources and used without further purification.

Known Brønsted acid catalysts

Chiral Brønsted acid catalysts in Table 4.7 and TRIP were kindly supplied by the coworkers from the List group and were prepared according to the literature procedures referenced in Table 4.7. VAPOL-derived phosphoric acid **1d** was purchased from Sigma-Aldrich and acidified by washing with aq. 4 N HCl before use. STRIP catalyst was developed and prepared by S. Müller.^[108]

Inert gas atmosphere

Air and moisture sensitive reactions were conducted under an atmosphere of argon (*Air Liquide*, >99.5% purity). Unless otherwise stated, all organocatalytic reactions were performed under an ambient atmosphere without the exclusion of moisture or air.

Thin layer chromatography (TLC)

Reactions were monitored by thin layer chromatography on silica gel or aluminum oxide pre-coated plastic sheets (0.2 mm, Machery-Nagel). Visualization was accomplished by irradiation with UV light at 254 nm and different staining reagents; phosphomolybdic acid (PMA) stain: PMA (10 g) in EtOH (100 ml); anisaldehyde stain: *p*-anisaldehyde (3.5 ml), glacial acetic acid (15 ml), EtOH (350 ml), conc. H₂SO₄ (50 ml).

Column chromatography

Column chromatography was performed under elevated pressure on silica gel (60, particle size 0.040-0.063 mm, Merck) or aluminum oxide (neutral, activated, Brockmann I, Sigma-Aldrich; Activity II with 3% H₂O; Activity III with 6% H₂O).

High pressure liquid chromatography (HPLC)

HPLC analyses on a chiral stationary phase were performed on a Shimadzu LC-2010C system equipped with a UV detector. Commercial HPLC-grade solvents were used, and measurements were conducted at 25 °C. The chiral stationary phase of the columns is specified in each experiment. The enantiomeric ratios were determined by comparing the samples with the appropriate racemic mixtures.

Gas chromatography (GC)

GC analyses on a chiral stationary phase were performed on HP 6890 and 5890 series instruments equipped with a split-mode capillary injection system and a flame ionization detector (FID) using hydrogen as a carrier gas. Detailed conditions are given in the individual experiment. The enantiomeric ratios were determined by comparing the samples with the appropriate racemic mixtures.

Nuclear magnetic resonance spectroscopy (NMR)

Proton, carbon, and phosphorus NMR spectra were recorded on Bruker AV-500 or Bruker AV-400 spectrometers in deuterated solvents at room temperature (298 K). Proton chemical shifts are reported in ppm (δ) relative to tetramethylsilane with the solvent resonance employed as the internal standard (C₆D₆, δ 7.16 ppm; DMSO-d₆, δ 2.49 ppm; CD₂Cl₂, δ 5.32 ppm; CDCl₃, δ 7.24 ppm; acetone-d₆, δ 2.04 ppm). ³¹P chemical shifts are reported in ppm relative to H₃PO₄ as the external standard. Data are reported as follows: chemical shift, multiplicity (s = singlet, d = doublet, t = triplet, q = quartet, m = multiplet), coupling constants (Hz) and integration. Slight shape deformation of the peaks in some cases due to weak coupling is not explicitly mentioned. ¹³C chemical shifts are reported in ppm from tetramethylsilane with the solvent resonance as the internal standard (C₆D₆, δ 128.06 ppm; DMSO-d₆, δ 39.5 ppm; CD₂Cl₂, 53.8 ppm; CDCl₃, δ 77.0 ppm; acetone-d₆, δ 206.0, 29.8 ppm).

Mass spectrometry (MS)

Mass spectra were measured on a Finnigan MAT 8200 (70 eV) or MAT 8400 (70 eV) by electron ionization, chemical ionization or fast atom/ion bombardment techniques. Electrospray ionization (ESI) mass spectra were recorded on a Bruker ESQ 3000 spectrometer. High resolution mass spectra were obtained on a Finnigan MAT 95 or Bruker APEX III FT-MS (7 T magnet). All masses are given in atomic units/elementary charge (m/z).

Specific rotation

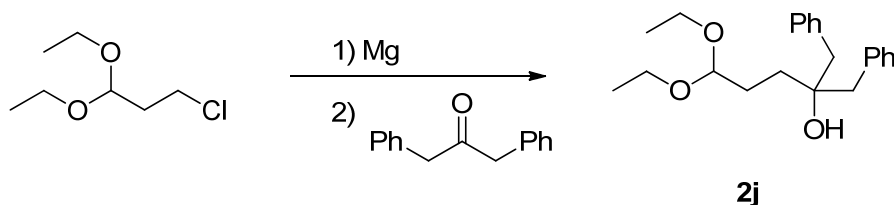
Optical rotations were determined with Autopol IV automatic polarimeter (Rudolph Research Analytical) using a 50 mm cell with temperature control. The measurements were performed at 25 °C at a wavelength $\lambda = 589$ nm (sodium D-line). Concentrations (c) are given in g/100 ml.

7.2. Catalytic asymmetric transacetalization

7.2.1. Starting materials

2a-l

Representative procedure for compounds 2a-l

*Preparation of the Grignard reagent*

A solution of freshly distilled 3-chloropropionaldehyde diethylacetal (5.0 g, 30.0 mmol) in THF (5 ml) was added to activatedⁱ magnesium turnings (1.46 g, 60 mmol). The temperature of the exothermic reaction mixture was kept between 15–25 °C by cooling with an ice bath.^{ii, iii} After heat development ceased, the mixture was diluted with toluene (10 ml) and the resulting solution (calculated ca. 1.5 mmol/ml) was used immediately.

Addition to ketones

A solution of the Grignard reagent prepared above (7.5 ml, 11.25 mmol)^{iv} was cooled to –30 °C and a solution of ketone (5.0 mmol) in toluene (1.25 ml) was added dropwise.^v The mixture was allowed to warm to 0 °C during 2–4 h. It was then quenched at 0 °C with concentrated aqueous NH₄Cl (5 ml) and H₂O (5 ml), and extracted with Et₂O (2 x 10 ml). The combined organic extracts were washed with conc. Na₂CO₃ (aq.) (5 ml), dried (MgSO₄), filtered, and concentrated directly prior to purification. Flash chromatography on silica gel yielded pure products.^{vi} The products were stored as 0.1–0.2 M solutions in EtOAc or Et₂O, or used immediately for transacetalization reaction.

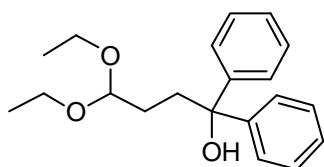
Notes:

- *i*) Activation was performed with a few drops of 1,2-dibromoethane.
- *ii*) For reactions on a larger scale a more efficient dry ice/acetone bath cooling is necessary.
- *iii*) If there is no exothermic reaction at this point, initiation is performed by adding more 1,2-dibromoethane and fast heating (with a heat gun) and cooling to 25 °C (repeated until reaction becomes exothermic after cooling).

7. EXPERIMENTAL SECTION

- iv) For all other reactions, except **2j** and **2d**, 1.5 equiv. of the Grignard reagent was used. However, incomplete conversion of the starting ketones was observed. This is probably a result of the decomposition of the Grignard reagent^[152] during preparation which leads to variable yields. Addition of more Grignard reagent (which was meanwhile kept at $-40\text{ }^{\circ}\text{C}$) has beneficial effect on conversion.
- v) Ketones that are solids were added in portions to the Grignard reagent diluted with 1.25 ml of toluene.
- vi) TLC visualization: UV (254 nm) and/or PMA stain.

4,4-Diethoxy-1,1-diphenylbutan-1-ol (**2a**)



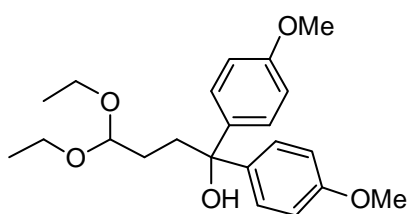
Purification: 10% EtOAc/hexane. Colorless oil, 2.12 g (from 10.0 mmol of ketone), 67%.

$^1\text{H NMR}$ (400 MHz, DMSO- d_6) δ 7.41 (dd, $J = 8.3, 1.2$ Hz, 4H), 7.26 (t, $J = 7.8$ Hz, 4H), 7.14 (tt, $J = 7.3, 1.2$ Hz, 2H), 5.50 (s, 1H), 4.42 (t, $J = 5.7$ Hz, 1 H) 3.51–3.43 (m, 2H), 3.38–3.30 (m, 2H), 2.24–2.20 (m, 2H), 1.47–1.41 (m, 2H), 1.06 (t, $J = 7.1$ Hz, 6H).

$^{13}\text{C NMR}$ (100 MHz, DMSO- d_6) δ 148.2, 127.7, 126.0, 125.7, 102.4, 76.1, 60.2, 36.0, 28.0, 15.3.

HRMS (ESI+) m/z calculated for $\text{C}_{20}\text{H}_{26}\text{O}_3\text{Na}$ ($\text{M}+\text{Na}^+$) 337.1774, found 337.1774.

4,4-Diethoxy-1,1-bis(4-methoxyphenyl)butan-1-ol (**2b**)

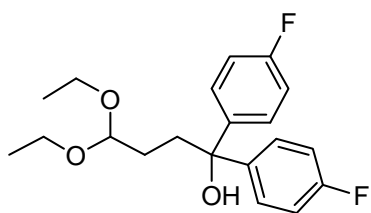


Purification: 20 % EtOAc/hexane (mixture loaded on the column as a solution in toluene). Colorless solid, 776 mg (from 5.0 mmol of ketone), 41%.

$^1\text{H NMR}$ (400 MHz, DMSO- d_6) δ 7.27 (d, $J = 8.9$ Hz, 4H), 6.81 (d, $J = 8.8$ Hz, 4H), 5.30 (s, 1H), 4.40 (t, $J = 5.6$ Hz, 1H), 3.69 (s, 6H), 3.51–3.43 (m, 2H), 3.38–3.30 (m, 2H), 2.16–2.12 (m, 2H), 1.45–1.40 (m, 2H), 1.06 (t, $J = 7.0$ Hz, 6H).

$^{13}\text{C NMR}$ (100 MHz, DMSO- d_6) δ 157.4, 140.7, 126.9, 112.9, 102.4, 75.6, 60.1, 54.9, 36.3, 28.1, 15.2.

HRMS (ESI+) m/z calculated for $\text{C}_{22}\text{H}_{30}\text{O}_5\text{Na}$ ($\text{M}+\text{Na}^+$) 397.1985, found 397.1982.

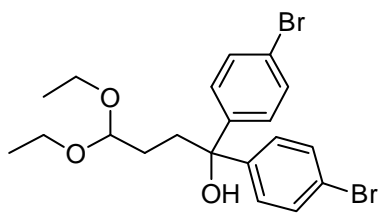
4,4-Diethoxy-1,1-bis(4-fluorophenyl)butan-1-ol (2c)

Purification: 20% EtOAc/hexane (mixture loaded on the column as a solution in toluene). Colorless oil, 781 mg (from 5.0 mmol of ketone), 45%.

$^1\text{H NMR}$ (400 MHz, DMSO- d_6) δ 7.43–7.38 (m, 4H), 7.11–7.05 (m, 4H), 5.64 (s, 1H), 4.41 (t, J = 5.6 Hz, 1H), 3.50–3.43 (m, 2H), 3.38–3.30 (m, 2H), 2.22–2.17 (m, 2H) 1.43–1.38 (m, 2H), 1.06 (t, J = 7.0 Hz, 6H).

$^{13}\text{C NMR}$ (100 MHz, DMSO- d_6) δ 160.6 (d, J = 242.3 Hz), 144.3 (d, J = 3.0 Hz), 127.7 (d, J = 7.9 Hz), 114.4 (d, J = 20.7 Hz), 102.3, 75.6, 60.2, 36.1, 28.0, 15.3.

HRMS (ESI+) m/z calculated for $\text{C}_{20}\text{H}_{24}\text{O}_3\text{F}_2\text{Na}$ ($\text{M}+\text{Na}^+$) 373.1586, found 373.1588.

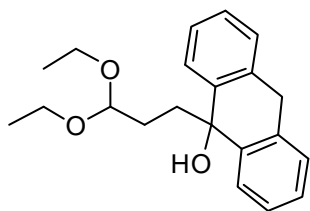
1,1-Bis(4-bromophenyl)-4,4-diethoxybutan-1-ol (2d)

Purification: CH_2Cl_2 /hexane/EtOAc 10:10:1. Colorless oil, 823 mg (from 3.15 mmol of ketone), 55%.

$^1\text{H NMR}$ (500 MHz, DMSO- d_6) δ 7.46 (d, J = 8.6 Hz, 4H), 7.33 (d, J = 8.5 Hz, 4H), 5.74 (s, 1H), 4.41 (t, J = 5.5 Hz, 1H), 3.50–3.43 (m, 2H), 3.37–3.31 (m, 2H), 2.20–2.17 (m, 2H), 1.41–1.37 (m, 2H), 1.06 (t, J = 7.0 Hz, 6H).

$^{13}\text{C NMR}$ (125 MHz, DMSO- d_6) δ 147.2, 130.8, 128.1, 119.5, 102.2, 75.7, 60.3, 35.5, 27.9, 15.3.

HRMS (ESI+) m/z calculated for $\text{C}_{20}\text{H}_{24}\text{O}_3\text{Br}_2\text{Na}$ ($\text{M}+\text{Na}^+$) 492.9985, found 492.9989.

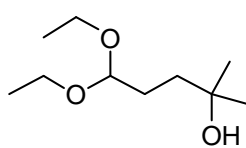
9-(3,3-Diethoxypropyl)-9,10-dihydroanthracen-9-ol (2e)

Purification: 15% EtOAc/hexane (crude product dissolved in 10 % EtOAc/hexane (5 ml), filtered and concentrated prior to chromatography). Colorless solid, 533 mg (from 5.0 mmol of ketone), 33%.

$^1\text{H NMR}$ (400 MHz, DMSO- d_6) δ 7.69 (dd, J = 7.6, 1.0 Hz, 2 H), 7.31–7.26 (m, 4H), 7.21 (td, J = 7.3, 1.2 Hz, 2H), 5.72 (s, 1H), 4.17 (t, J = 5.7 Hz, 1H), 3.94 (s, 2H), 3.39–3.31 (m, 2H), 3.26–3.18 (m, 2H), 1.57–1.53 (m, 2H), 1.38–1.32 (m, 2H), 0.98 (t, J = 7.0 Hz, 6H).

$^{13}\text{C NMR}$ (100 MHz, DMSO- d_6) δ 143.8, 133.7, 127.0, 126.3, 125.9, 125.1, 102.0, 72.6, 60.2, 37.6, 34.3, 28.1, 15.2.

HRMS (ESI+) m/z calculated for $\text{C}_{21}\text{H}_{26}\text{O}_3\text{Na}$ ($\text{M}+\text{Na}^+$) 349.1774, found 349.1776.

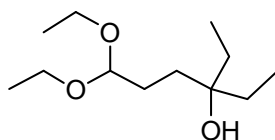
5,5-Diethoxy-2-methylpentan-2-ol (2f)

Purification: 30% EtOAc/hexane. Colorless oil, 473 mg (from 5.0 mmol of ketone), 50%.

$^1\text{H NMR}$ (500 MHz, DMSO- d_6) δ 4.39 (t, J = 5.7 Hz, 1H), 4.09 (s, 1H), 3.56–3.50 (m, 2H), 3.42–3.36 (m, 2H), 1.55–1.50 (m, 2H), 1.34–1.31 (m, 2H), 1.09 (t, J = 7.0 Hz, 6H), 1.04 (s, 6H).

$^{13}\text{C NMR}$ (125 MHz, DMSO- d_6) δ 102.7, 68.3, 60.2, 38.3, 29.2, 28.3, 15.2.

HRMS (ESI+) m/z calculated for $\text{C}_{10}\text{H}_{22}\text{O}_3\text{Na}$ ($\text{M}+\text{Na}^+$) 213.1461, found 213.1461.

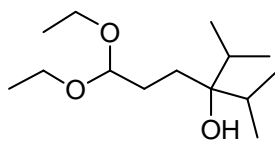
6,6-Diethoxy-3-ethylhexan-3-ol (2g)

Purification: 20% EtOAc/hexane. Colorless oil, 1.26 g (from 10 mmol of ketone), 58%.

$^1\text{H NMR}$ (400 MHz, DMSO- d_6) δ 4.38 (t, J = 5.6 Hz, 1H), 3.80 (s, 1H), 3.56–3.49 (m, 2H), 3.43–3.35 (m, 2H), 1.48–1.42 (m, 2H), 1.32–1.26 (m, 6H), 1.08 (t, J = 7.0 Hz, 6H), 0.74 (t, J = 7.5 Hz, 6H).

$^{13}\text{C NMR}$ (100 MHz, DMSO- d_6) δ 102.8, 72.1, 60.3, 32.5, 30.5, 27.5, 15.3, 7.8.

HRMS (CI (FE) *i*-butane) m/z calculated for $\text{C}_{12}\text{H}_{27}\text{O}_3$ ($\text{M}+\text{H}$) 219.1960, found 219.1962.

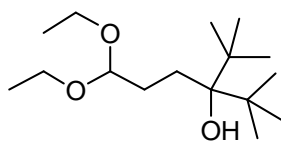
6,6-Diethoxy-3-isopropyl-2-methylhexan-3-ol (2h)

Purification: 15% EtOAc/hexane. Colorless oil, 645 mg (from 5.0 mmol of ketone), 52%.

$^1\text{H NMR}$ (500 MHz, DMSO- d_6) δ 4.35 (t, J = 5.4 Hz, 1H), 3.56–3.50 (m, 2H), 3.52 (s, 1H), 3.42–3.36 (m, 2H), 1.81–1.72 (m, 2H), 1.51–1.46 (m, 2H), 1.39–1.36 (m, 2H), 1.09 (t, J = 7.0 Hz, 6H), 0.85 (d, J = 6.9 Hz, 6H), 0.83 (d, J = 7.0 Hz, 6H).

$^{13}\text{C NMR}$ (125 MHz, DMSO- d_6) δ 103.0, 75.0, 60.4, 33.4, 28.4, 28.1, 17.6, 17.3, 15.3.

HRMS (ESI+) m/z calculated for $\text{C}_{14}\text{H}_{30}\text{O}_3\text{Na}$ ($\text{M}+\text{Na}^+$) 269.2087, found 269.2084.

3-(*tert*-Butyl)-6,6-diethoxy-2,2-dimethylhexan-3-ol (2i)

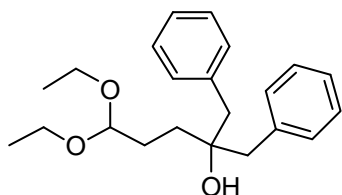
Purification: 5% EtOAc/hexane. Colorless oil, 231 mg (from 5.0 mmol of ketone), 17%.

$^1\text{H NMR}$ (500 MHz, DMSO- d_6) δ 4.40 (t, J = 5.0 Hz, 1H), 3.57–3.50 (m, 2H), 3.42–3.36 (m, 2H), 3.35 (s, 1H), 1.61–1.52 (m, 4H), 1.09 (t, J = 7.1 Hz, 6H), 0.97 (s, 18H).

^{13}C NMR (125 MHz, DMSO- d_6) δ 103.3, 78.1, 60.4, 42.2, 30.4, 28.6, 27.4, 15.3.

HRMS (ESI+) m/z calculated for $\text{C}_{16}\text{H}_{34}\text{O}_3\text{Na}$ ($\text{M}+\text{Na}^+$) 297.2400, found 297.2398.

2-Benzyl-5,5-diethoxy-1-phenylpentan-2-ol (2j)



Purification: 15% EtOAc/hexane. Colorless oil, 1.009 g (from 5.0 mmol of ketone), 59%.

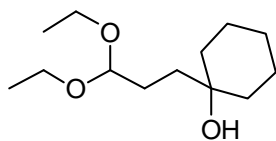
^1H NMR (500 MHz, DMSO- d_6) δ 7.24 (d, J = 4.4 Hz, 8H), 7.19–7.15 (m, 2H), 4.29 (s, 1H), 4.23 (t, J = 5.6 Hz, 1H), 3.47–3.41 (m, 2H),

3.35–3.28 (m, 2H), 2.67 (d, J = 13.6 Hz, 2H), 2.63 (d, J = 13.6 Hz, 2H), 1.64–1.60 (m, 2H), 1.20–1.17 (m, 2H), 1.02 (t, J = 7.0 Hz, 6H).

^{13}C NMR (125 MHz, DMSO- d_6) δ 138.3, 130.6, 127.5, 125.8, 102.8, 73.3, 60.4, 45.3, 32.3, 28.0, 15.2.

HRMS (ESI+) m/z calculated for $\text{C}_{22}\text{H}_{30}\text{O}_3\text{Na}$ ($\text{M}+\text{Na}^+$) 365.2087, found 365.2086.

1-(3,3-Diethoxypropyl)cyclohexanol (2k)



Purification: 25% EtOAc/hexane. Colorless oil, 656 mg (from 5.0 mmol of ketone), 57%.

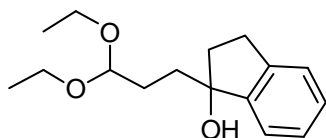
^1H NMR (500 MHz, DMSO- d_6) δ 4.38 (t, J = 5.6 Hz, 1H), 3.83 (s, 1H),

3.55–3.49 (m, 2H), 3.42–3.36 (m, 2H), 1.60–1.49 (m, 4H), 1.45–1.37 (m, 3H), 1.33–1.29 (m, 4H), 1.25–1.16 (m, 3H), 1.09 (t, J = 7.0 Hz, 6H).

^{13}C NMR (125 MHz, DMSO- d_6) δ 102.8, 68.8, 60.1, 37.0, 36.9, 27.0, 25.7, 21.8, 15.3.

HRMS (ESI+) m/z calculated for $\text{C}_{13}\text{H}_{26}\text{O}_3\text{Na}$ ($\text{M}+\text{Na}^+$) 253.1774, found 253.1772.

1-(3,3-Diethoxypropyl)-2,3-dihydro-1H-inden-1-ol (2l)



Purification: 25% EtOAc/hexane. Colorless oil, 684 mg (from 5.0 mmol of ketone), 52%.

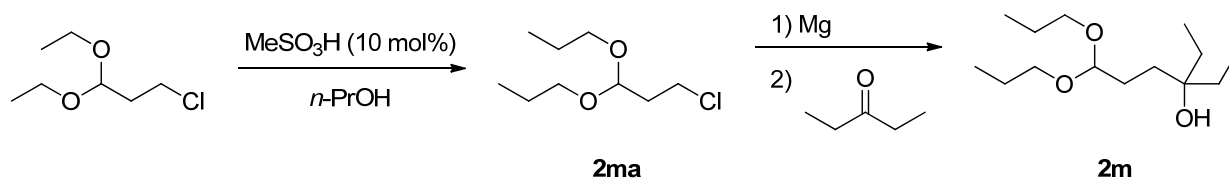
^1H NMR (500 MHz, DMSO- d_6) δ 7.26–7.23 (m, 1H), 7.19–7.17 (m,

3H), 4.92 (s, 1H), 4.40 (t, J = 5.2 Hz, 1H), 3.54–3.47 (m, 2H), 3.40–3.34 (m, 2H), 2.89–2.84 (m, 1H), 2.73–2.67 (m, 1H), 2.12–2.07 (m, 1H), 2.00–1.94 (m, 1H), 1.74–1.70 (m, 1H), 1.64–1.55 (m, 2H), 1.53–1.47 (m, 1H), 1.073 (t, J = 7.0 Hz, 3H), 1.068 (t, J = 7.0 Hz, 3H).

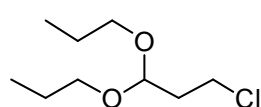
^{13}C NMR (125 MHz, DMSO- d_6) δ 148.7, 142.3, 127.3, 126.1, 124.5, 123.1, 102.5, 81.5, 60.5, 60.2, 39.4, 35.4, 29.0, 28.4, 15.3.

HRMS (ESI+) m/z calculated for $C_{16}H_{24}O_3Na$ ($M+Na^+$) 287.1618, found 287.1616.

2m



3-Chloro-1,1-dipropoxypropane (2ma)

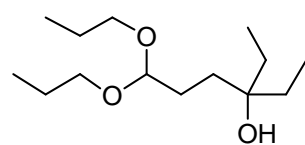


A solution of 3-chloropropionaldehyde diethylacetal (4.0 g, 24 mmol) and methanesulfonic acid (156 μ l, 2.4 mmol) in *n*-propanol was stirred at room temperature for 16 h. The volume of the mixture was slowly reduced to ca. 10 ml under reduced pressure at 42 °C. Sodium hydrogencarbonate (403 mg, 4.8 mmol) was then added and the remaining *n*-propanol removed under reduced pressure. Et₂O (20 ml) was added and the resulting solution washed with H₂O (3 x 10 ml), conc. aqueous Na₂CO₃ (5 ml), dried (MgSO₄), filtered, and the solvent was removed under reduced pressure. Purified by Kugelrohr distillation (80 °C, reduced pressure). Colorless oil, 3.80 g, 81%.

¹H NMR (400 MHz, CDCl₃) δ 4.66 (t, J = 5.6 Hz, 1H), 3.60–3.53 (m, 4 H), 3.42–3.37 (m, 2H), 2.05 (td, J = 6.6, 5.7 Hz, 2H), 1.63–1.54 (m, 4H), 0.92 (t, J = 7.4 Hz, 6H).

¹³C NMR (100 MHz, CDCl₃) δ 100.7, 68.4, 40.9, 36.8, 23.1, 10.7.

3-Ethyl-6,6-dipropoxyhexan-3-ol (2m)

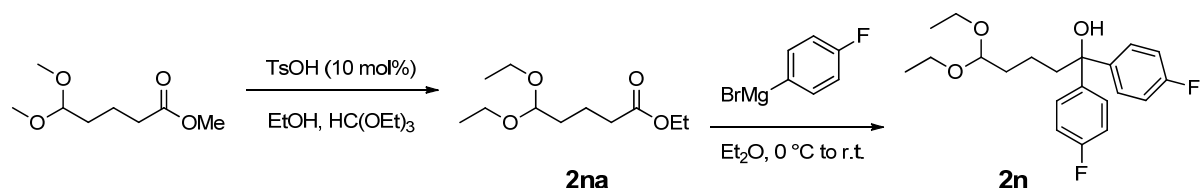
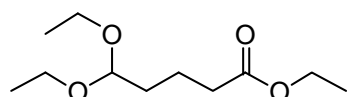


Representative procedure for compounds **2a–I** was followed using 3-chloro-1,1-dipropoxypropane (**2ma**) and 3-pentanone as substrates. Purification: 15% EtOAc/hexane. Colorless oil, 1.08 g (from 8.125 mmol of ketone), 54%.

¹H NMR (500 MHz, DMSO-*d*₆) δ 4.38 (t, J = 5.6 Hz, 1H), 3.79 (s, 1H), 3.44 (dt, J = 9.3, 6.6 Hz, 2H), 3.30 (dt, J = 9.3, 6.6 Hz, 2H), 1.52–1.45 (m, 6H), 1.32–1.27 (m, 6H), 0.86 (t, J = 7.5 Hz, 6H), 0.75 (t, J = 7.5 Hz, 6H).

¹³C NMR (125 MHz, DMSO-*d*₆) δ 103.0, 72.1, 66.4, 32.5, 30.5, 27.4, 22.7, 10.7, 7.8.

HRMS (ESI+) m/z calculated for $C_{14}H_{30}O_3Na$ ($M+Na^+$) 269.2087, found 269.2084.

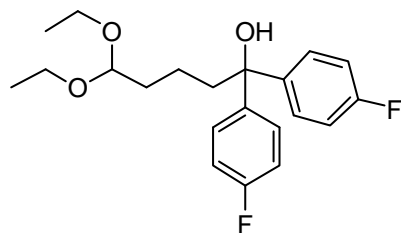
2n**Ethyl 5,5-diethoxypentanoate (2na)**

A solution of methyl 5,5-dimethoxypentanoate (1.76 g, 10 mmol), triethyl orthoformate (2 ml), and *p*-toluenesulfonic acid monohydrate (172 mg, 1 mmol) in ethanol (25 ml) was heated at reflux. The solvent was slowly distilled off to ca. 10 ml during 8 h. More ethanol (10 ml) was added and further 10 ml of solvent distilled off from the reaction mixture during 6 h. The reaction mixture was cooled to room temperature, sodium carbonate (106 mg, 1 mmol) added and solvent removed under reduced pressure. Diethyl ether (20 ml) was added to the residue, and the solution was washed with 0.5 M aqueous Na₂CO₃ solution (2 x 10 ml), water (3 x 10 ml), brine (10 ml), dried (MgSO₄), filtered, and concentrated under reduced pressure. Yellowish liquid, 2.17 g, 99%.

¹H NMR (500 MHz, DMSO-*d*₆) δ 4.43 (t, *J* = 4.9 Hz, 1H), 4.03 (q, *J* = 7.1 Hz, 2H), 3.57–3.50 (m, 2H), 3.42–3.36 (m, 2H), 2.28 (t, *J* = 6.8 Hz, 2H), 1.55–1.47 (m, 4H), 1.16 (t, *J* = 7.1 Hz, 3H), 1.08 (t, *J* = 7.1 Hz, 6H).

¹³C NMR (125 MHz, DMSO-*d*₆) δ 172.8, 101.8, 60.4, 59.6, 33.1, 32.4, 19.8, 15.3, 14.1.

HRMS (ESI+) *m/z* calculated for C₁₁H₂₂O₄Na (M+Na⁺) 241.1410, found 241.1409.

5,5-Diethoxy-1,1-bis(4-fluorophenyl)pentan-1-ol (2n)

A solution of ethyl 5,5-diethoxypentanoate (**2na**, 437 mg, 2.0 mmol) in Et₂O (5 ml) was added to the 2 M solution of (4-fluorophenyl)magnesium bromide (1196 mg, 6.0 mmol) in Et₂O at 0 °C. The reaction mixture was stirred for 1 h at 0 °C and 40 min at room temperature, then cooled to 0 °C and quenched with a concentrated ammonium chloride solution (5 ml). Diethyl ether (10 ml) and water (5 ml) were added to the mixture. The organic layer was separated, washed with concentrated sodium carbonate solution (5 ml), dried (MgSO₄), filtered, and concentrated under reduced pressure. Purification by silica gel chromatography (15% EtOAc/hexane) yielded a colorless oil, 541 mg, 74%.

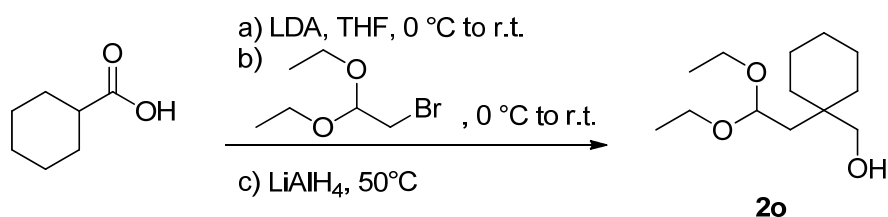
7. EXPERIMENTAL SECTION

¹H NMR (500 MHz, DMSO-*d*₆) δ 7.44–7.40 (m, 4H), 7.09–7.04 (m, 4H), 5.59 (s, 1H), 4.37 (t, *J* = 5.6 Hz, 1H), 3.51–3.45 (m, 2H), 3.39–3.31 (m, 2H), 2.21–2.17 (m, 2H), 1.50–1.46 (m, 2H), 1.23–1.16 (m, 2H), 1.03 (t, *J* = 7.0 Hz, 6H).

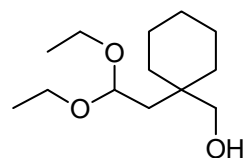
¹³C NMR (125 MHz, DMSO-*d*₆) δ 160.6 (d, *J* = 242.5 Hz), 144.5 (d, *J* = 2.5 Hz), 127.7 (d, *J* = 7.8 Hz), 114.4 (d, *J* = 20.9 Hz), 102.1, 75.9, 60.4, 41.0, 33.5, 18.7, 15.3.

HRMS (EI (DE)) *m/z* calculated for C₂₁H₂₆O₃F₂ (M) 364.1850, found 364.1849.

2o



(1-(2,2-Diethoxyethyl)cyclohexyl)methanol (2o)

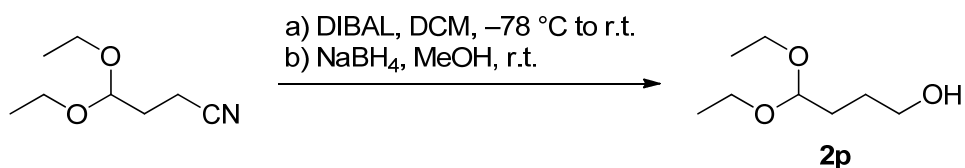
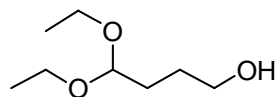


a) A 2.5 M solution of *n*-BuLi (11.8 ml, 29.4 mmol) in hexanes was added dropwise to a solution of diisopropyl amine (4.53 ml, 32.3 mmol) in dry THF (28 ml) at 0 °C and stirred for 30 min at 0 °C. Then a solution of cyclohexanecarboxylic acid (1.79 g, 14 mmol) in THF (3 ml) was added and the mixture stirred for 30 min at 0 °C and 2 h at room temperature. b) The mixture was cooled to 0 °C and bromoacetaldehyde diethyl acetal (2.32 ml, 3.03 g, 15.4 mmol) was added dropwise. The mixture was stirred for 30 min at 0 °C and 12 h at room temperature. c) Lithium aluminum hydride (1.06 g, 28 mmol) was added in small portions and the reaction mixture stirred at 50 °C for 2.5 h. The mixture was cooled to room temperature and poured slowly on the mixture of water (50 ml) and diethyl ether (150 ml). The organic layer was separated by decantation, and the aqueous slurry extracted with diethyl ether (6 x 25 ml). The combined organic extracts were washed with concentrated aqueous sodium carbonate solution (2 x 25 ml), dried (MgSO₄), filtered, and concentrated directly prior to purification. Purification by silica gel chromatography (hexane/EtOAc/MeOH 9:1:0.2) yielded a colorless oil, 1.31 g, 41%.

¹H NMR (500 MHz, DMSO-*d*₆) δ 4.56 (t, *J* = 5.3 Hz, 1H), 4.26 (t, *J* = 5.3 Hz, 1H), 3.56–3.50 (m, 2H), 3.42–3.36 (m, 2H), 3.23 (d, *J* = 5.4 Hz, 2H), 1.51 (d, *J* = 5.3 Hz, 2H), 1.39–1.34 (m, 5H), 1.29–1.22 (m, 5H), 1.08 (t, *J* = 7.0 Hz, 6H).

¹³C NMR (125 MHz, DMSO-*d*₆) δ 100.3, 66.8, 60.2, 38.2, 36.0, 32.5, 26.0, 21.2, 15.3.

HRMS (ESI+) *m/z* calculated for C₁₃H₂₆O₃Na (M+Na⁺) 253.1774, found 253.1774.

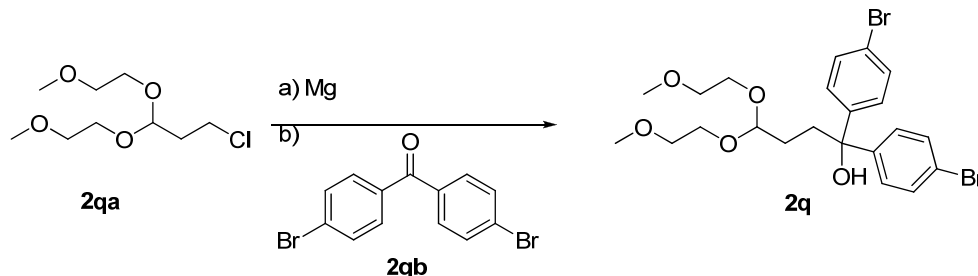
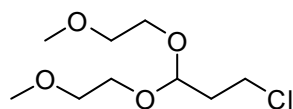
2p**4,4-Diethoxybutan-1-ol (2p)**

a) A 1.0 M solution of DIBAL (6 ml, 6.0 mmol) in toluene was added to a solution of 3-cyanopropionaldehyde diethyl acetal (943 mg, 6.0 mmol) in dry DCM (30 ml) at $-78\text{ }^{\circ}\text{C}$ and stirred for 1.5 h at $-78\text{ }^{\circ}\text{C}$. The mixture was allowed to warm to room temperature, treated with concentrated aqueous ammonium chloride solution (10 ml) and water (10 ml), and extracted with DCM (3 x 20 ml). The combined organic extracts were washed with brine (2 x 20 ml), dried (MgSO_4), filtered, and concentrated. b) The oily residue was dissolved in methanol (10 ml), NaBH_4 (227 mg, 6 mmol) was added and the mixture was stirred at room temperature. After 1 h water (10 ml) was added to the mixture, methanol was removed under reduced pressure, and the resulting mixture was extracted with ethyl acetate (3 x 20 ml). The combined organic extracts were washed with concentrated aqueous sodium carbonate solution (10 ml), dried (MgSO_4), filtered, and concentrated. Purification by silica gel chromatography (50% EtOAc/hexane) yielded a colorless oil, 407 mg, 42%.

$^1\text{H NMR}$ (500 MHz, DMSO-d_6) δ 4.43 (t, $J = 5.6$ Hz, 1H), 4.37 (t, $J = 5.2$ Hz, 1H), 3.56–3.50 (m, 2H), 3.43–3.35 (m, 4H), 1.53–1.48 (m, 2H), 1.43–1.38 (m, 2H), 1.09 (t, $J = 7.1$ Hz, 6H).

$^{13}\text{C NMR}$ (125 MHz, DMSO-d_6) δ 102.1, 60.5, 60.3, 29.9, 27.8, 15.3.

HRMS (CI (FE) *i*-butane) m/z calculated for $\text{C}_8\text{H}_{19}\text{O}_3$ (M+H) 163.1334, found 163.1332.

2q**6-(2-chloroethyl)-2,5,7,10-tetraoxaundecane (2qa)**

The mixture of 3-chloropropionaldehyde diethylacetal (4.0 g, 24 mmol), 2-methoxyethanol (20 ml) and methanesulfonic acid (156 μl , 2.4 mmol) was stirred at $40\text{ }^{\circ}\text{C}$ under reduced pressure (reflux of 2-

7. EXPERIMENTAL SECTION

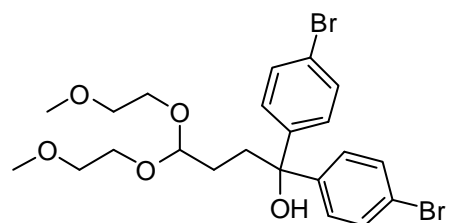
methoxyethanol) for 24 h. After cooling to room temperature the mixture was treated with solid sodium carbonate (1 g), diluted with diethyl ether (20 ml), filtered, and concentrated under reduced pressure. Purification by silica gel chromatography (40% EtOAc/hexane) yielded a colorless oil, 3.02 g.

$^1\text{H NMR}$ (400 MHz, DMSO- d_6) δ 4.69 (t, J = 5.6 Hz, 1H), 3.68-3.59 (m, 4H), 3.56-3.51 (m, 2H), 3.44 (t, J = 4.7 Hz, 4H), 3.24 (s, 6H), 1.99-1.95 (m, 2H).

$^{13}\text{C NMR}$ (100 MHz, CDCl_3) δ 100.1, 71.2, 64.8, 58.0, 40.9, 36.2.

HRMS (ESI+) m/z calculated for $\text{C}_9\text{H}_{19}\text{O}_4\text{NaCl}$ ($\text{M}+\text{Na}$) 249.0864, found 249.0864.

1,1-bis(4-bromophenyl)-4,4-bis(2-methoxyethoxy)butan-1-ol (**2q**)

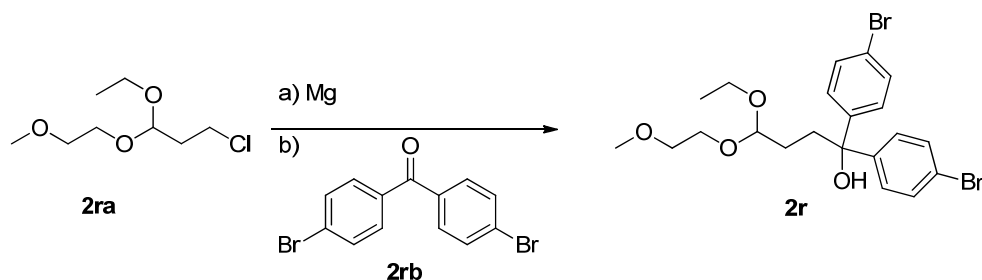
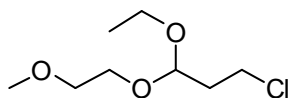


A solution of **2qa** (1.4 g, 6.2 mmol) in THF (1.5 ml) was added to activated Mg turnings (370 mg, 12.4 mmol, activated with 0.1 ml of 1,2-dibromoethane) in THF (1.5 ml).

After the temperature of the weakly exothermic reaction mixture reached room temperature, the mixture was diluted with toluene (3 ml) and the resulting solution was transferred via syringe to a new flask and cooled to $-30\text{ }^\circ\text{C}$. To the solution, ketone **2qb** (422 mg, 1.24 mmol) was added as a solid, and the mixture was allowed to warm to $0\text{ }^\circ\text{C}$ during 2 h. It was then quenched at $0\text{ }^\circ\text{C}$ with concentrated aqueous NH_4Cl (5 ml) and H_2O (5 ml), and extracted with EtOAc (20 ml, 2 \cdot 10 ml). The combined organic extracts were washed with conc. Na_2CO_3 (aq.) (10 ml), dried (MgSO_4), filtered, and concentrated. The residue was purified by silica gel chromatography (50% EtOAc/hexane). Colorless oil, 358 mg, containing **2qa** as an impurity.

$^1\text{H NMR}$ (500 MHz, C_6D_6) δ 7.27-7.24 (m, 4H), 7.13-7.10 (m, 4H), 4.60 (t, J = 5.4 Hz, 1H), 3.61-3.56 (m, 2H), 3.47-3.39 (m, 2H), 3.29-3.19 (m, 4H), 3.31 (s, 1H), 3.02 (s, 6H), 2.21-2.18 (m, 2H), 1.69-1.65 (m, 2H).

$^{13}\text{C NMR}$ (125 MHz, DMSO- d_6) δ 146.9, 131.4, 121.0, 103.7, 76.9, 72.3, 65.5, 58.6, 35.8, 28.1.

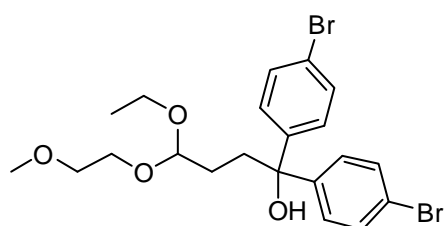
2r**3-chloro-1-ethoxy-1-(2-methoxyethoxy)propane (2ra)**

The mixture of 3-chloropropionaldehyde diethylacetal (6.33 g, 38 mmol), 2-methoxyethanol (3.0 ml, 2.89 g, 38 mmol) and methanesulfonic acid (246 μl , 3.8 mmol) was stirred at 100 °C under argon flow for 30 min. After cooling to room temperature the mixture was treated with concentrated aqueous sodium carbonate solution (10 ml) and extracted with Et₂O (2 · 25 ml), dried (MgSO₄), and the solvent was removed under reduced pressure. Purification by silica gel chromatography (10% EtOAc/hexane) yielded a pale yellow oil, 1.53 g.

¹H NMR (500 MHz, DMSO-d₆) δ 4.65 (t, *J* = 5.6 Hz, 1H), 3.65-3.57 (m, 4H), 3.55-3.51 (m, 1H), 3.48-3.42 (m, 3H), 3.24 (s, 3H), 1.98-1.94 (m, 2H), 1.10 (t, *J* = 7.0 Hz, 3H).

¹³C NMR (125 MHz, CDCl₃) δ 99.9, 71.3, 64.7, 61.2, 58.1, 41.1, 36.3, 15.2.

HRMS (CI (FE) *i*-butane) *m/z* calculated for C₈H₁₈O₃Cl (M+H) 197.0944, found 197.0942.

1,1-bis(4-bromophenyl)-4-ethoxy-4-(2-methoxyethoxy)butan-1-ol (2r)

A solution of **2ra** (1.5 g, 7.6 mmol) in THF (1.5 ml) was added to activated Mg turnings (370 mg, 15.2 mmol, activated with 0.1 ml of 1,2-dibromoethane) in THF (1.5 ml).

The temperature of the weakly exothermic reaction mixture was kept between 30–32 °C by cooling with water. After 1 h the mixture was diluted with toluene (3 ml) and the resulting solution was transferred via syringe to a new flask and cooled to –30 °C. To the solution, ketone **2rb** (861 mg, 2.53 mmol) was added as a solid, and the mixture was allowed to warm to 0 °C during 1 h. It was then quenched at 0 °C with concentrated aqueous NH₄Cl (5 ml) and H₂O (5 ml), and extracted with EtOAc (20 ml, 2 · 10 ml). The combined organic extracts were washed with conc. Na₂CO₃ (aq.) (5 ml), dried (MgSO₄), filtered, and concentrated. The residue was treated with hexane, the precipitate was discarded

7. EXPERIMENTAL SECTION

and the solution loaded onto silica gel and chromatographed (30% EtOAc/hexane). Colorless oil, 266 mg, 21%.

¹H NMR (500 MHz, C₆D₆) δ 7.27-7.23 (m, 4H), 7.12-7.08 (m, 4H), 4.46 (dd, *J* = 5.6, 4.7 Hz, 1H), 3.54-3.45 (m, 2H), 3.37-3.33 (m, 1H), 3.27-3.16 (m, 3H, overlapped), 3.21 (s, 1H), 2.99 (s, 3H), 2.17 (t, *J* = 7.8 Hz, 2H), 1.72-1.66 (m, 1H), 1.62-1.55 (m, 1H), 1.07 (t, *J* = 7.0 Hz, 3H).

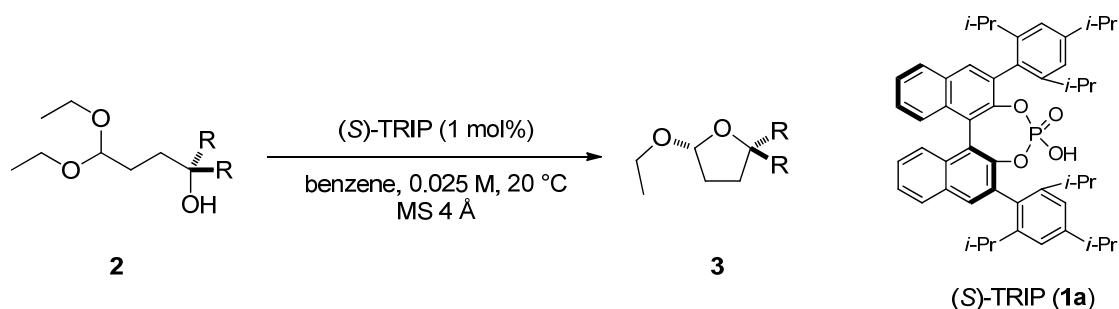
¹³C NMR (125 MHz, DMSO-*d*₆) δ 146.8, 146.8, 131.5, 121.1, 103.4, 76.9, 72.3, 65.4, 61.9, 58.6, 35.9, 28.3, 15.4.

HRMS (ESI+) *m/z* calculated for C₂₁H₂₆O₄Br₂Na (M+Na) 523.0090, found 523.0086.

Enantiomers of the compound were separated by HPLC on a chiral stationary phase Chiralpak IA, 20 μm (196 x 48 mm NW 50, 08/18) using iso-hexane/2-propanol 98:2 as the mobile phase.

7.2.2. Products

General procedure for the catalytic asymmetric transacetalization



Molecular sieves 4 Å (150 mg) and a solution of (S)-TRIP (2.38 mg, 0.003 mmol, co-crystallized with CH₃CN 1:1) in dry benzene (4 ml), were added to the solution of **2** (0.3 mmol) in dry benzene (8 ml) and stirred at 20 °C. Et₃N (42 μl) was added to the reaction mixture after complete conversion of the starting material (in most cases within 9–24 h).ⁱ

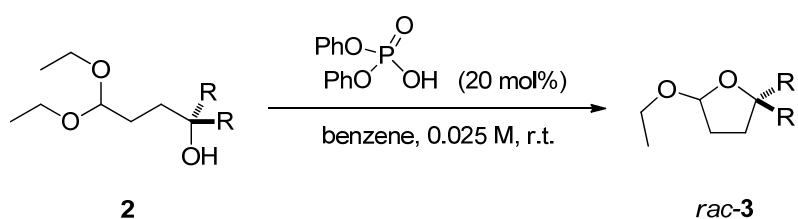
– For non-volatile products:ⁱⁱ The reaction mixture was concentrated under reduced pressure and the product was purified by silica gel (5 g) chromatography with EtOAc/hexane as the eluent.ⁱⁱⁱ

– For volatile products:ⁱⁱ The reaction mixture was directly loaded on silica gel (5 g, preconditioned with pentane) column. The crude mixture was first eluted with some pentane to remove benzene, and then with Et₂O/pentane to isolate the product.ⁱⁱⁱ

Notes:

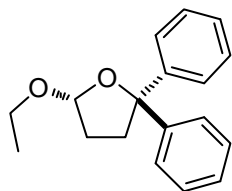
- *i*) Reaction progress monitored by TLC (EtOAc/hexane), visualization: UV (254 nm) and/or PMA stain.
- *ii*) Use of DCM or CHCl₃ as a solvent during sample preparation for the chiral GC might lead to product epimerization as these solvents tend to contain HCl as an impurity.
- *iii*) Molecular sieves hinder solvent flow when the crude reaction mixture is loaded onto the column. For reactions on a larger scale, a small pad of celite on top of the silica column was used to prevent column clogging.

Preparation of the racemates



Diphenyl phosphate (1.25 mg, 0.005 mmol) was added to the solution of **2** (0.025 mmol) in benzene (1 ml). After 1 h sample of the product for HPLC was isolated by TLC (eluent as used for purification of enantioenriched products).

(*R*)-5-Ethoxy-2,2-diphenyltetrahydrofuran (**3a**)



Reaction time: 24 h. Purification: 3% EtOAc/hexane. Colorless oil, 76.7 mg, 95%.

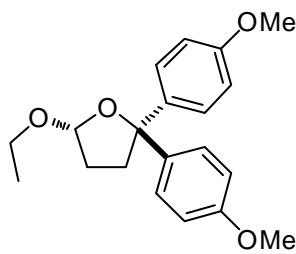
$^1\text{H NMR}$ (400 MHz, CD_2Cl_2) δ 7.46–7.41 (m, 4H), 7.31–7.27 (m, 4H), 7.22–7.17 (m, 2H), 5.35 (dd, $J = 5.0, 1.9$ Hz, 1H), 3.87–3.80 (m, 1H), 3.57–3.49 (m, 1H), 2.72–2.65 (m, 1H), 2.61–2.55 (m, 1H) 2.04–1.90 (m, 2H), 1.13 (t, $J = 7.1$ Hz, 3H).

$^{13}\text{C NMR}$ (100 MHz, CD_2Cl_2) δ 147.8, 147.2, 128.35, 128.25, 126.94, 126.92, 126.4, 126.0, 104.5, 89.3, 63.3, 37.5, 32.9, 15.3.

HRMS (ESI+) m/z calculated for $\text{C}_{18}\text{H}_{20}\text{O}_2\text{Na}$ ($\text{M}+\text{Na}^+$) 291.1356, found 291.1358.

HPLC (OJ-H), *n*-heptane/*i*-PrOH 90:10, 0.5 ml/min, $\lambda = 210$ nm, $t_{\text{minor}} = 15.3$ min, $t_{\text{major}} = 28.2$ min, er 94.5:5.5.

(*R*)-5-Ethoxy-2,2-bis(4-methoxyphenyl)tetrahydrofuran (**3b**)



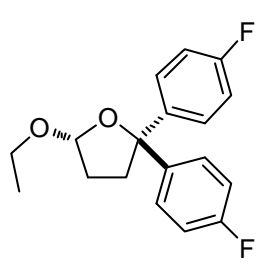
Reaction time: 24 h. Purification: 10% EtOAc/hexane. Colorless oil, 94.1 mg, 96%.

$^1\text{H NMR}$ (400 MHz, CD_2Cl_2) δ 7.34–7.27 (m, 4H), 6.83–6.79 (m, 4H) 5.31 (dd, $J = 5.2, 2.0$ Hz, 1H), 3.86–3.78 (m, 1H), 3.77 (s, 3H), 3.76 (s, 3H), 3.55–3.48 (m, 1H), 2.65–2.58 (m, 1H), 2.53–2.47 (m, 1H), 2.03–1.88 (m, 2H), 1.15 (t, $J = 7.1$ Hz, 3 H).

$^{13}\text{C NMR}$ (100 MHz, CD_2Cl_2) δ 158.70, 158.68, 140.2, 127.7, 127.2, 113.55, 113.45, 104.5, 88.9, 63.2, 55.5, 37.8, 33.0, 15.4.

HRMS (ESI+) m/z calculated for $\text{C}_{20}\text{H}_{24}\text{O}_4\text{Na}$ ($\text{M}+\text{Na}^+$) 351.1567, found 351.1563.

HPLC (OJ-H), *n*-heptane/*i*-PrOH 60:40, 0.5 ml/min, $\lambda = 210$ nm, $t_{\text{minor}} = 22.5$ min, $t_{\text{major}} = 32.9$ min, er 95.5:4.5.

(R)-5-Ethoxy-2,2-bis(4-fluorophenyl)tetrahydrofuran (3c)

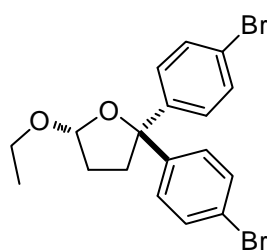
Reaction time: 24 h. Purification: 5% EtOAc/hexane. Colorless oil, 89.4 mg, 98%.

$^1\text{H NMR}$ (400 MHz, CD_2Cl_2) δ 7.42–7.34 (m, 4H), 7.01–6.95 (m, 4H), 5.33 (dd, $J = 5.1, 2.2$ Hz, 1H), 3.84–3.76 (m, 1H), 3.55–3.48 (m, 1H), 2.69–2.62 (m, 1H), 2.55–2.49 (m, 1H), 2.03–1.90 (m, 2H), 1.12 (t, $J = 7.1$ Hz, 3H).

$^{13}\text{C NMR}$ (100 MHz, CD_2Cl_2) δ 162.0 (d, $J = 244.1$ Hz), 143.5 (d, $J = 3.2$ Hz), 142.8 (d, $J = 3.1$ Hz), 128.2 (d, $J = 8.0$ Hz), 127.8 (d, $J = 8.0$ Hz), 115.0 (d, $J = 21.3$ Hz), 114.9 (d, $J = 21.2$ Hz), 104.6, 88.5, 63.4, 37.9, 32.9, 15.3.

HRMS (ESI+) m/z calculated for $\text{C}_{18}\text{H}_{18}\text{O}_2\text{F}_2\text{Na}$ ($\text{M}+\text{Na}^+$) 327.1167, found 327.1168.

HPLC (OJ-H), *n*-heptane/*i*-PrOH 98:2, 0.5 ml/min, $\lambda = 210$ nm, $t_{\text{minor}} = 12.3$ min, $t_{\text{major}} = 14.8$ min, er 97:3.

(R)-2,2-Bis(4-bromophenyl)-5-ethoxytetrahydrofuran (3d)

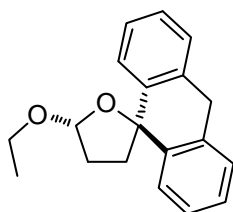
Reaction performed on 0.9 mmol scale. Reaction time: 24 h. Purification: 5% EtOAc/hexane. Colorless oil, 381 mg, 99% (Crystallizes at -20 °C, remains solid when reheated to room temperature).

$^1\text{H NMR}$ (500 MHz, CD_2Cl_2) δ 7.43–4.41 (m, 4H), 7.32–7.26 (m, 4H), 5.33 (dd, $J =$ (overlap), 2.0 Hz, 1H), 3.81–3.75 (m, 1H), 3.54–3.48 (m, 1H), 2.68–2.62 (m, 1H), 2.53–2.48 (m, 1H), 2.01–1.90 (m, 2H), 1.12 (t, $J = 7.0$ Hz, 3H).

$^{13}\text{C NMR}$ (125 MHz, CD_2Cl_2) δ 146.4, 145.8, 131.5, 131.4, 128.3, 127.9, 121.0, 104.6, 88.4, 63.4, 37.5, 32.8, 15.3.

HRMS (ESI+) m/z calculated for $\text{C}_{18}\text{H}_{18}\text{O}_2\text{Na}$ ($\text{M}+\text{Na}^+$) 446.9566, found 446.9570.

HPLC (OJ-H), *n*-heptane/*i*-PrOH 98:2, 0.5 ml/min, $\lambda = 220$ nm, $t_{\text{minor}} = 11.8$ min, $t_{\text{major}} = 13.0$ min, er 97:3.

(R)-5'-Ethoxy-4',5'-dihydro-3'H,10H-spiro[anthracene-9,2'-furan] (3e)

Reaction time: 7 days. Purification: 30% CH_2Cl_2 /hexane. Colorless oil, 72.1 mg, 86%.

$^1\text{H NMR}$ (500 MHz, CD_2Cl_2) δ 7.76 (d, $J = 7.8$ Hz, 1H), 7.45 (dd, $J = 7.8, 1.2$ Hz, 1H), 7.34–7.21 (m, 6H), 5.68 (d, $J = 5.0$ Hz, 1H), 4.22–4.15 (m, 1H), 4.01 (d, $J = 17.9$ Hz, 1H), 3.92 (d, $J = 17.9$ Hz, 1H), 3.79–3.73 (m, 1H), 2.17–2.10 (m,

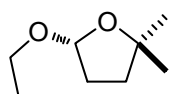
1H), 2.10–2.02 (m, 1H), 2.02–1.96 (m, 2H), 1.37 (t, $J = 7.1$ Hz, 3H) .

^{13}C NMR (125 MHz, CD_2Cl_2) δ 144.3, 143.4, 134.7, 134.6, 127.7, 127.2, 126.9, 126.8, 126.3, 124.2, 124.0, 105.8, 86.1, 64.0, 37.9, 36.0, 32.0, 15.5.

HRMS (ESI+) m/z calculated for $\text{C}_{19}\text{H}_{20}\text{O}_2\text{Na}$ ($\text{M}+\text{Na}^+$) 303.1355, found 303.1355.

HPLC (OD-3), *n*-heptane/*i*-PrOH 90:10, 0.5 ml/min, $\lambda = 210$ nm, $t_{\text{minor}} = 5.50$ min, $t_{\text{major}} = 6.58$ min, er 95.5:4.5.

(*R*)-5-Ethoxy-2,2-dimethyltetrahydrofuran (3f)



Reaction time: 10 h. Purification: 10% Et_2O /pentane. Colorless oil, 38.3 mg, 84%.

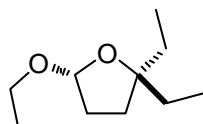
^1H NMR (500 MHz, CD_2Cl_2) δ 5.01 (d, $J = 4.9$ Hz, 1H), 3.71–3.65 (m, 1H), 3.38–3.32 (m, 1H), 2.05–1.98 (m, 1H), 1.91–1.84 (m, 2H), 1.71–1.66 (m, 1H), 1.31 (s, 3H), 1.17 (s, 3H), 1.14 (t, $J = 7.0$ Hz, 3H).

^{13}C NMR (125 MHz, CD_2Cl_2) δ 104.2, 82.1, 62.3, 36.6, 33.4, 30.1, 28.9, 15.4.

HRMS (EI (FE) *i*-butane) m/z calculated for $\text{C}_8\text{H}_{17}\text{O}_2$ ($\text{M}+\text{H}$) 145.1228, found 145.1227.

GC (Column: 29.5 m BGB-176 SE/SE52 (2,3-dimethyl-6-*tert*-butyldimethylsilyl- β -cyclodextrin), i.D. 0.25 mm, df. 0.15 μm ; Detector: FID; Temperature: injector 230 $^\circ\text{C}$, detector 350 $^\circ\text{C}$, oven 60 $^\circ\text{C}$; gas: 0.6 bar H_2), $t_{\text{minor}} = 4.76$ min, $t_{\text{major}} = 5.57$ min, er 94.5:5.5.

(*R*)-5-Ethoxy-2,2-diethyltetrahydrofuran (3g)



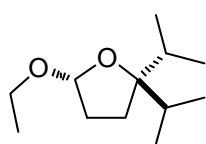
Reaction time: 16 h. Purification: 3% EtOAc/hexane. Colorless oil, 47.6 mg, 92%.

^1H NMR (500 MHz, CD_2Cl_2) δ 5.02 (d, $J = 4.9$ Hz, 1H), 3.73–3.66 (m, 1H), 2.38–3.32 (m, 1H), 1.98–1.90 (m, 1H), 1.86–1.75 (m, 2H), 1.69–1.51 (m, 3H), 1.51–1.38 (m, 2), 1.13 (t, $J = 7.1$ Hz, 3H), 0.87 (t, $J = 7.5$ Hz, 3H), 0.82 (t, $J = 7.5$ Hz, 3H).

^{13}C NMR (125 MHz, CD_2Cl_2) δ 104.0, 87.6, 62.3, 33.3, 33.0, 32.5, 30.8, 15.4, 8.9, 8.7.

HRMS (EI (FE) *i*-butane) m/z calculated for $\text{C}_{10}\text{H}_{21}\text{O}_2$ ($\text{M}+\text{H}$) 173.1542, found 173.1540.

GC (Column: 29.5 m BGB-176 SE/SE52 (2,3-dimethyl-6-*tert*-butyldimethylsilyl- β -cyclodextrin), i.D. 0.25 mm, df. 0.15 μm ; Detector: FID; Temperature: injector 220 $^\circ\text{C}$, detector 320 $^\circ\text{C}$, oven 90 $^\circ\text{C}$; gas: 0.8 bar H_2), $t_{\text{minor}} = 5.49$ min, $t_{\text{major}} = 5.98$ min, er 97:3.

(R)-5-Ethoxy-2,2-diisopropyltetrahydrofuran (3h)

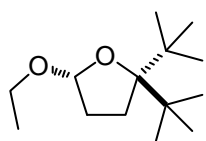
Reaction time: 12 h. Purification: 10% Et₂O/pentane. Colorless oil, 55.8 mg, 93%.

¹H NMR (500 MHz, CD₂Cl₂) δ 5.05 (d, *J* = 5.8 Hz, 1H), 3.75–3.69 (m, 1H), 3.39–3.33 (m, 1H), 2.06–1.99 (m, 1H), 2.00–1.85 (m, 2H), 1.85–1.73 (m, 2H), 1.62–1.57 (m, 1H), 1.14 (t, *J* = 7.1 Hz, 3H), 0.91 (t, *J* = 7.6 Hz, 6H), 0.83 (t, *J* = 6.7 Hz, 6H).

¹³C NMR (125 MHz, CD₂Cl₂) δ 105.3, 93.1, 62.9, 34.7, 34.3, 33.9, 26.4, 18.4, 18.2, 17.9, 17.7, 15.3.

HRMS (ESI+) *m/z* calculated for C₁₂H₂₄O₂Na (M+Na⁺) 223.1669, found 223.1667.

GC (Column: 29.5 m BGB-176 SE/SE52 (2,3-dimethyl-6-*tert*-butyldimethylsilyl-β-cyclodextrin), i.D. 0.25 mm, df. 0.15 μm; Detector: FID; Temperature: injector 250 °C, detector 350 °C, oven 100 °C; gas: 0.6 bar H₂), *t*_{minor} = 9.02 min, *t*_{major} = 9.28 min, er 98:2.

(R)-2,2-Di-*tert*-butyl-5-ethoxytetrahydrofuran (3i)

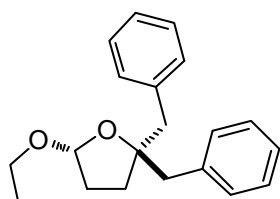
Reaction time: 9 h. Purification: 2% EtOAc/hexane. Colorless oil, 61.7 mg, 90%.

¹H NMR (500 MHz, CD₂Cl₂) δ 5.13 (dd, *J* = 6.5 Hz, 4.0 Hz, 1H), 3.79–3.73 (m, 1H), 3.45–3.39 (m, 1H), 2.17–2.10 (m, 1H), 1.98–1.92 (m, 1H), 1.86–1.80 (m, 1H), 1.78–1.71 (m, 1H), 1.16 (t, *J* = 7.1 Hz, 3 H), 1.06 (s, 9H), 1.00 (s, 9H).

¹³C NMR (125 MHz, CD₂Cl₂) δ 107.0, 96.8, 63.7, 42.5, 41.0, 34.7, 29.6, 29.2, 28.7, 15.5.

HRMS (ESI+) *m/z* calculated for C₁₄H₂₈O₂Na (M+Na⁺) 251.1981, found 251.1977.

GC (Column: 30 m BGB-176 SE/SE52 (2,3-dimethyl-6-*tert*-butyldimethylsilyl-β-cyclodextrin), i.D. 0.25 mm, df. 0.25 μm; Detector: FID; Temperature: injector 230 °C, detector 350 °C, oven 90 °C; gas: 0.5 bar H₂), *t*_{minor} = 65.11 min, *t*_{major} = 66.38 min, er 98:2.

(R)-2,2-Dibenzyl-5-ethoxytetrahydrofuran (3j)

Reaction time: 14 h. Purification: 5% EtOAc/hexane. Colorless oil, 87.2 mg, 98%.

¹H NMR (500 MHz, CD₂Cl₂) δ 7.34–7.29 (m, 4H), 7.25–7.17 (m, 6H), 4.90 (d, *J* = 5.0 Hz, 1H), 3.85–3.78 (m, 1H), 3.44–3.37 (m, 1H), 3.04 (d, *J* = 13.6 Hz, 1H), 2.94 (d, *J* = 13.6 Hz, 1H), 2.73 (d, *J* = 13.6 Hz, 1H), 2.56 (d, *J* = 13.6 Hz, 1H), 1.99–1.93 (m, 1H), 1.79–1.75 (m, 1H), 1.56–1.52 (m, 1H), 1.14 (t, *J* = 7.1 Hz, 3H), 1.02–0.94 (m, 1H).

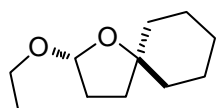
7. EXPERIMENTAL SECTION

^{13}C NMR (125 MHz, CD_2Cl_2) δ 138.9, 138.6, 131.0, 130.9, 128.2, 128.1, 126.5, 126.4, 104.8, 87.3, 62.8, 49.2, 45.3, 33.1, 32.4, 15.4.

HRMS (ESI+) m/z calculated for $\text{C}_{20}\text{H}_{24}\text{O}_2\text{Na}$ ($\text{M}+\text{Na}^+$) 319.1668, found 319.1668.

HPLC (OJ-H), *n*-heptane/*i*-PrOH 98:2, 0.5 ml/min, $\lambda = 220$ nm, $t_{\text{minor}} = 9.6$ min, $t_{\text{major}} = 11.9$ min, er 97:3.

(*R*)-2-Ethoxy-1-oxaspiro[4.5]decane (3k)



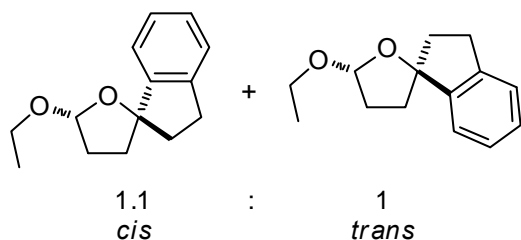
Reaction time: 12 h. Purification: 10% Et_2O /pentane. Colorless oil, 52.0 mg, 94%.

^1H NMR (500 MHz, CD_2Cl_2) δ 5.01 (d, $J = 4.9$ Hz, 1H), 3.72–3.66 (m, 1H), 3.39–3.32 (m, 1H), 1.99–1.91 (m, 1H), 1.88–1.83 (m, 1H), 1.81–1.75 (m, 1H), 1.72–1.68 (m, 1H), 1.68–1.61 (m, 3H), 1.59–1.54 (m, 1H), 1.50–1.46 (m, 1H), 1.43–1.36 (m, 5H), 1.13 (t, $J = 7.1$ Hz, 3H).

^{13}C NMR (125 MHz, CD_2Cl_2) δ 103.6, 84.2, 62.2, 40.1, 38.2, 34.4, 32.8, 26.0, 24.3, 15.5.

HRMS (EI (FE)) m/z calculated for $\text{C}_{11}\text{H}_{20}\text{O}_2$ (M) 184.1463, found 184.1465.

GC (Column: 29.5 m BGB-176 SE/SE52 (2,3-dimethyl-6-*tert*-butyldimethylsilyl- β -cyclodextrin), i.D. 0.25 mm, df. 0.25 μm ; Detector: FID; Temperature: injector 220 $^\circ\text{C}$, detector 320 $^\circ\text{C}$, oven 90 $^\circ\text{C}$; gas: 0.8 bar H_2), $t_{\text{minor}} = 10.06$ min, $t_{\text{major}} = 10.34$ min, er 97:3.

(1'S,5R)-5-Ethoxy-2',3',4,5-tetrahydro-3H-spiro[furan-2,1'-indene] + (1'R,5R)-5-ethoxy-2',3',4,5-tetrahydro-3H-spiro[furan-2,1'-indene] (3l)

Reaction time: 20 h. Purification: 8% EtOAc/hexane.

Colorless oil, 62.9 mg, 96%.

¹H NMR (500 MHz, CD₂Cl₂) δ 7.36–7.33 (m, 0.49H, major isomer), 7.25–7.18 (m, 3.26H), 5.26 (dd, *J* = 5.3, 2.0 Hz, 0.45H, minor isomer), 5.17 (dd, *J* = 4.1, 0.9 Hz,

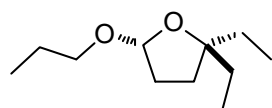
0.50H, major isomer), 3.80–3.73 (m, 1H), 3.48–3.40 (m, 1H), 3.00–2.91 (m, 1H), 2.85–2.76 (m, 1H), 2.36–2.27 (m, 1H), 2.25–2.01 (m, 5H), 1.23 (t, *J* = 7.1 Hz, 1.56H, major isomer), 1.19 (t, *J* = 7.1 Hz, 1.41H, minor isomer).

¹³C NMR (125 MHz, CD₂Cl₂) δ 147.8, 147.1, 143.6, 143.2, 128.3, 128.0, 127.1, 126.9, 125.0, 124.8, 124.0, 123.0, 104.6, 103.9, 93.8, 92.8, 63.0, 62.7, 41.4, 40.7, 36.3, 36.1, 33.9, 33.8, 30.2, 29.7, 15.5, 15.4.

Diastereomeric ratio = 1.1:1, determined by ¹H NMR, protons on acetal carbon stereocenter, δ 5.26 (0.4519H) and δ 5.17 (0.4957H). Relative stereochemistry of diastereomers determined by NOESY experiment: only one of the acetal protons, the one of minor diastereomer (δ 5.26) has a cross-peak with aromatic proton indicating *trans* relationship between OEt and aromatic substituent.

HRMS (ESI+) *m/z* calculated for C₁₄H₁₈O₂Na (M+Na⁺) 241.1199, found 241.1198.

GC for *cis* diastereomer (Column: 30 m ChiralDex G-BP (gamma-cyclodextrin-butryl), i.D. 0.25 mm, df. 0.25 μm; Detector: FID; Temperature: injector 220 °C, detector 350 °C, oven 80 °C; gas: 0.9 bar H₂), *t*_{major} = 211.3 min, *t*_{minor} = 225.1 min, er (*cis*) 91:9. **GC** for *trans* diastereomer (Column: 24.8 m Hydrodex-B-TBDAC-CD (Heptakis-(2,3-di-*O*-acetyl-6-*O*-*t*-butyldimethyl-silyl)-β-cyclodextrin), i.D. 0.25 mm; Detector: FID; Temperature: injector 220 °C, detector 350 °C, oven 100 °C; gas: 0.5 bar H₂), *t*_{major} = 109.0 min, *t*_{minor} = 112.4 min, er (*trans*) 96:4.

(R)-2,2-diethyl-5-propoxytetrahydrofuran (3m)

Reaction time: 24 h. Purification: 10% Et₂O/pentane. Colorless oil, 54.5 mg, 95%.

¹H NMR (400 MHz, CD₂Cl₂) δ 5.01 (dd, *J* = 4.9, 1.1 Hz, 1H), 3.60 (dt, *J* =

7. EXPERIMENTAL SECTION

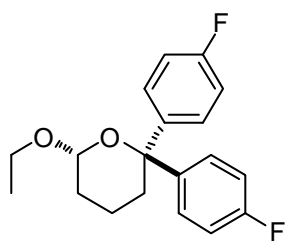
9.4, 6.8 Hz, 1H), 3.25 (dt, $J = 9.4, 6.6$ Hz, 1H), 1.99–1.90 (m, 1H), 1.88–1.82 (m, 1H), 1.82–1.74 (m, 1H), 1.70–1.51 (m, 5H), 1.51–1.38 (m, 2H), 0.90 (t, $J = 7.4$ Hz, 3H), 0.87 (t, $J = 7.5$ Hz, 3H), 0.82 (t, $J = 7.5$ Hz, 3H).

^{13}C NMR (100 MHz, CD_2Cl_2) δ 104.4, 87.7, 68.8, 33.4, 33.0, 32.7, 30.8, 23.4, 10.9, 9.0, 8.7.

HRMS (CI (FE) *i*-butane) m/z calculated for $\text{C}_{11}\text{H}_{23}\text{O}_2$ (M+H) 187.1698, found 187.1697.

GC (Column: 30 m BGB-177/BGB-15 (2,6-dimethyl-3-pentyl- β -cyclodextrin), i.D. 0.25 mm, df. 0.25 μm ; Detector: FID; Temperature: injector 220 $^\circ\text{C}$, detector 350 $^\circ\text{C}$, oven 115 $^\circ\text{C}$; gas: 0.6 bar H_2), $t_{\text{minor}} = 7.06$ min, $t_{\text{major}} = 7.34$ min, er 95:5.

(*R*)-6-Ethoxy-2,2-bis(4-fluorophenyl)tetrahydro-2H-pyran (3n)



Reaction time: 4 days. Purification: 5% EtOAc/hexane. Colorless oil, 92.1 mg, 96%.

^1H NMR (500 MHz, CD_2Cl_2) δ 7.43–7.39 (m, 2H), 7.32–7.28 (m, 2H), 7.09–7.04 (m, 2H), 6.97–6.92 (m, 2H), 4.46 (dd, $J = 9.7, 2.1$ Hz, 1H), 4.07–4.01 (m, 1H), 3.51–3.44 (m, 1H), 2.61–2.57 (m, 1H), 1.86–1.81 (m,

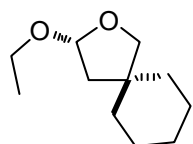
1H), 1.79–1.66 (m, 3H), 1.54–1.46 (m, 1H), 1.21 (t, $J = 7.0$ Hz, 3H).

^{13}C NMR (125 MHz, CD_2Cl_2) δ 162.1 (d, $J = 246.2$ Hz), 161.7 (d, $J = 243.9$ Hz), 145.2 (d, $J = 2.7$ Hz), 139.4 (d, $J = 3.3$ Hz), 129.2 (d, $J = 8.1$ Hz), 126.9 (d, $J = 7.7$ Hz), 115.7 (d, $J = 21.8$ Hz), 114.9 (d, $J = 21.1$ Hz), 97.9, 80.3, 64.1, 34.9, 31.5, 20.1, 15.5.

HRMS (EI (DE)) m/z calculated for $\text{C}_{19}\text{H}_{20}\text{O}_2\text{F}_2$ (M) 318.1431, found 318.1431.

HPLC (OJ-H), *n*-heptane/*i*-PrOH 99.7:0.3, 0.5 ml/min, $\lambda = 220$ nm, $t_{\text{minor}} = 13.9$ min, $t_{\text{major}} = 17.3$ min, er 82:18.

(*R*)-3-Ethoxy-2-oxaspiro[4.5]decane (3o)



Reaction time: 30 min. Purification: 10% Et_2O /pentane. Colorless oil, 51.9 mg, 94%.

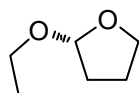
^1H NMR (500 MHz, CD_2Cl_2) δ 5.07 (dd, $J = 5.8$ Hz, 2.6 Hz, 1H), 3.70–3.64 (m, 1H), 3.60 (d, $J = 8.3$ Hz, 1H), 3.56 (d, $J = 8.3$ Hz, 1H), 3.41–3.34 (m, 1H), 1.89 (dd, $J = 13.3, 5.7$ Hz, 1H), 1.60 (dd, $J = 13.3, 2.6$ Hz, 1H), 1.53–1.36 (m, 10 H), 1.15 (t, $J = 7.1$ Hz, 3H).

^{13}C NMR (125 MHz, CD_2Cl_2) δ 104.7, 77.1, 63.1, 45.5, 43.1, 37.2, 36.4, 26.3, 24.5, 23.9, 15.5.

HRMS (ESI+) m/z calculated for $\text{C}_{11}\text{H}_{20}\text{O}_2\text{Na}$ (M+ Na^+) 207.1356, found 207.1355.

GC (Column: 29.5m BGB-176 SE/SE52 (2,3-dimethyl-6-*tert*-butyldimethylsilyl- β -cyclodextrin), i.D. 0.25 mm, df. 0.15 μ m; Detector: FID; Temperature: injector 220 °C, detector 350 °C, oven 110 °C; gas: 0.5 bar H₂), $t_{\text{minor}} = 14.64$ min, $t_{\text{major}} = 15.19$ min, er 82.5:17.5.

(R)-2-Ethoxytetrahydrofuran (3p)



Reaction time: 7 h. Purification: product is highly volatile but it can be isolated as a solution in organic solvent (e.g. dichloromethane): (1/6 (2 ml) of the reaction mixture was directly loaded on silica gel (0.5 g, preconditioned with pentane) column and product eluted with CD₂Cl₂). Yield 76%: determined by ¹H NMR using Ph₃CH (0.05 mmol) as internal standard and comparing relative area of Ph₃CH and proton on acetal carbon stereocenter.

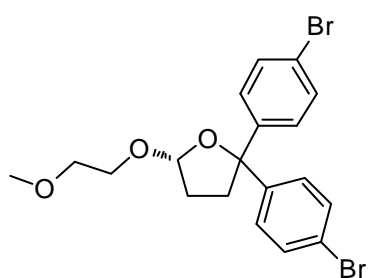
¹H NMR (500 MHz, CD₂Cl₂) δ 5.08 (dd, $J = 4.7, 1.4$ Hz, 1H), 3.85–3.78 (m, 2H), 3.69–3.63 (m, 1H), 3.42–3.36 (m, 1H), 1.97–1.86 (m, 2H), 1.84–1.76 (m, 2H), 1.14 (t, $J = 7.0$ Hz, 3H).

¹³C NMR (125 MHz, CD₂Cl₂) δ 103.9, 67.0, 62.7, 32.7, 23.9, 15.4.

GC-MS (EI) m/z 116.

GC (Column: 30 m BGB-176 SE/SE52 (2,3-dimethyl-6-*tert*-butyldimethylsilyl- β -cyclodextrin), i.D. 0.25 mm, df. 0.25 μ m; Detector: FID; Temperature: injector 220 °C, detector 320 °C, oven 70 °C; gas: 0.5 bar H₂), $t_{\text{minor}} = 5.20$ min, $t_{\text{major}} = 5.79$ min, er 79:21.

(R)-2,2-bis(4-bromophenyl)-5-(2-methoxyethoxy)tetrahydrofuran (3q)



Catalyst loading: 10 mol%. Reaction time: 3 days. Purification: 20% EtOAc/hexane. Colorless oil, 94%, corrected for impurity **2qa** in the starting material.

¹H NMR (500 MHz, C₆D₆) δ 7.28-7.23 (m, 4H), 7.10-7.07 (m, 2H), 6.98-6.95 (m, 2H), 5.11 (dd, $J = 5.1, 1.1$ Hz, 1H), 3.79-3.75 (m, 1H), 3.55-3.50 (m, 1H), 3.30-3.21 (m, 2H), 3.05 (s, 3H), 2.42-2.36 (m, 1H), 2.00-1.96 (m, 1H), 1.83-1.78 (m, 1H), 1.57-1.50 (m, 1H).

¹³C NMR (125 MHz, C₆D₆) δ 146.3, 145.6, 131.5, 131.4, 128.4, 121.3, 121.2, 104.8, 88.5, 72.1, 67.1, 58.6, 37.3, 32.7.

HRMS (ESI+) m/z calculated for C₁₉H₂₀O₃Br₂Na (M+Na) 476.9672, found 476.9674.

HPLC (OD-3), *n*-heptane/*i*-PrOH 90:10, 1.0 ml/min, $\lambda = 220$ nm, $t_{\text{minor}} = 2.85$ min, $t_{\text{major}} = 78.84$ min, er 79:21.

7.2.3. X-Ray data for compound **3d**

Absolute configuration determination of **3d** by X-ray single-crystal structure analysis

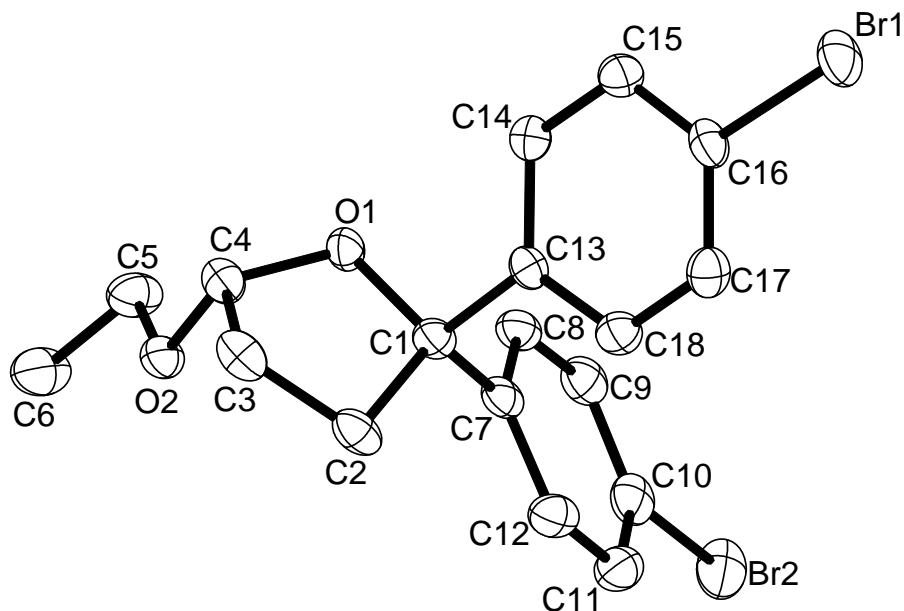


Figure 7.1. Crystal structure of **3d**, showing the absolute configuration of the sample. Anisotropic displacement parameters are drawn at the 50% probability level and hydrogen atoms omitted for clarity.

Crystals of **3d** were obtained as fine needles after keeping the oil in the freezer at $-20\text{ }^{\circ}\text{C}$. The compound remains solid when warmed up to room temperature. More crystals in the form of prisms were obtained by dissolving a few milligrams of the product in dichloromethane, evaporating the solvent, and keeping the remaining oil at $-20\text{ }^{\circ}\text{C}$ overnight. The absolute configurations of four crystals picked at random from the sample were investigated, and all showed the configuration shown in Figure 7.1. The Flack parameter x and the Hooft factor y for the four crystals were as follows: (1) $x = -0.018(12)$ (3048 reflections), $y = -0.026(4)$ (1447 Bijvoet pairs)(Cu); (2) $x = -0.009(11)$ (6792 reflections), $y = -0.0120(1)$ (3304 Bijvoet pairs)(Mo); (3) $x = -0.07(4)$ (2168 reflections), $y = -0.096(22)$ (1036 Bijvoet pairs)(Cu); (4) $x = -0.003(20)$ (2797 reflections), $y = -0.004(12)$ (1226 Bijvoet pairs)(Cu).

X-ray Crystal Structure Analysis of 3d: $[\text{C}_{18}\text{H}_{18}\text{Br}_2\text{O}_2]$, $M_r = 426.14\text{ g}\cdot\text{mol}^{-1}$, colorless prism, crystal size $0.060 \times 0.204 \times 0.573\text{ mm}^3$, tetragonal, space group $P4_1$, $a = 10.8373(9)\text{ \AA}$, $c = 14.8921(13)\text{ \AA}$, $V = 1749.0(3)\text{ \AA}^3$, $T = 100\text{ K}$, $Z = 4$, $D_{\text{calc}} = 1.618\text{ g}\cdot\text{cm}^{-3}$, $\lambda = 1.54178\text{ \AA}$, $\mu = 5.909$

7. EXPERIMENTAL SECTION

mm^{-1} , Gaussian absorption correction ($T_{\min} = 0.10636$, $T_{\max} = 0.70728$), scaling SADABS, Bruker AXS ProteumX8 diffractometer, $4.08 < \theta < 66.52^\circ$, 40020 measured reflections, 3048 independent reflections, 3046 reflections with $I > 2\sigma(I)$, $R_{\text{int}} = 0.0405$. Structure solved by direct methods and refined by full-matrix least-squares against F^2 to $R_1 = 0.0168$ [$I > 2\sigma(I)$], $wR_2 = 0.0407$, 200 parameters.^[153] The Flack parameter is $-0.018(12)$.^[154] The Hooft factor γ based on 1447 Bijvoet pairs is $-0.026(4)$.^[155] H atoms riding, $S = 1.133$, residual electron density $+0.26 / -0.22 \text{ e } \text{\AA}^{-3}$. CCDC 771853.

Crystal data and structure refinement.

Empirical formula	$\text{C}_{18} \text{H}_{18} \text{Br}_2 \text{O}_2$
Color	colorless
Formula weight	$426.14 \text{ g} \cdot \text{mol}^{-1}$
Temperature	100 K
Wavelength	1.54178 \AA
Crystal system	Tetragonal
Space group	P4₁, (no. 76)
Unit cell dimensions	$a = 10.8373(9) \text{ \AA}$ $\alpha = 90^\circ$. $b = 10.8373(9) \text{ \AA}$ $\beta = 90^\circ$. $c = 14.8921(13) \text{ \AA}$ $\gamma = 90^\circ$.
Volume	$1749.0(3) \text{ \AA}^3$
Z	4
Density (calculated)	$1.618 \text{ Mg} \cdot \text{m}^{-3}$
Absorption coefficient	5.909 mm^{-1}
F(000)	848 e
Crystal size	$0.973 \times 0.204 \times 0.060 \text{ mm}^3$
θ range for data collection	4.08 to 66.52° .
Index ranges	$-12 \leq h \leq 12$, $-12 \leq k \leq 12$, $-17 \leq l \leq 17$
Reflections collected	40020
Independent reflections	3048 [$R_{\text{int}} = 0.0405$]
Reflections with $I > 2\sigma(I)$	3046

7. EXPERIMENTAL SECTION

Completeness to $\theta = 66.52^\circ$	99.6 %	
Absorption correction	Gaussian	
Max. and min. transmission	0.71 and 0.11	
Refinement method	Full-matrix least-squares on F^2	
Data / restraints / parameters	3048 / 1 / 200	
Goodness-of-fit on F^2	1.133	
Final R indices [$I > 2\sigma(I)$]	$R_1 = 0.0168$	$wR^2 = 0.0407$
R indices (all data)	$R_1 = 0.0168$	$wR^2 = 0.0407$
Absolute structure parameter	-0.018(12)	
Largest diff. peak and hole	0.256 and -0.216 e · Å ⁻³	

Atomic coordinates and equivalent isotropic displacement parameters (Å²).

U_{eq} is defined as one third of the trace of the orthogonalized U_{ij} tensor.

	x	y	z	U_{eq}
Br(1)	0.0872(1)	-0.3557(1)	1.1153(1)	0.033(1)
Br(2)	0.3290(1)	0.1452(1)	0.5970(1)	0.036(1)
C(1)	0.2644(2)	0.1691(2)	1.0105(2)	0.022(1)
C(2)	0.1805(2)	0.2743(2)	1.0443(2)	0.026(1)
C(3)	0.2454(2)	0.3136(2)	1.1306(2)	0.028(1)
C(4)	0.3788(2)	0.2997(2)	1.1047(2)	0.024(1)
C(5)	0.5412(2)	0.4053(2)	1.0296(2)	0.033(1)
C(6)	0.5751(2)	0.5339(2)	1.0007(2)	0.038(1)
C(7)	0.2797(2)	0.1664(2)	0.9089(2)	0.023(1)
C(8)	0.3915(2)	0.1288(2)	0.8713(2)	0.024(1)
C(9)	0.4060(2)	0.1220(2)	0.7788(2)	0.027(1)
C(10)	0.3082(2)	0.1537(2)	0.7241(2)	0.028(1)
C(11)	0.1959(2)	0.1907(2)	0.7589(2)	0.031(1)

7. EXPERIMENTAL SECTION

C(12)	0.1829(2)	0.1961(2)	0.8519(2)	0.027(1)
C(13)	0.2198(2)	0.0419(2)	1.0420(1)	0.020(1)
C(14)	0.2959(2)	-0.0374(2)	1.0902(2)	0.024(1)
C(15)	0.2555(2)	-0.1547(2)	1.1144(2)	0.026(1)
C(16)	0.1389(2)	-0.1914(2)	1.0901(1)	0.025(1)
C(17)	0.0600(2)	-0.1141(2)	1.0436(2)	0.026(1)
C(18)	0.1011(2)	0.0015(2)	1.0195(2)	0.025(1)
O(1)	0.3837(1)	0.1913(1)	1.0508(1)	0.023(1)
O(2)	0.4137(1)	0.4050(1)	1.0552(1)	0.025(1)

Bond lengths [Å] and angles [°].

Br(1)-C(16)	1.9047(19)	Br(2)-C(10)	1.908(2)
C(1)-O(1)	1.446(2)	C(1)-C(7)	1.523(3)
C(1)-C(13)	1.534(3)	C(1)-C(2)	1.543(3)
C(2)-C(3)	1.526(3)	C(3)-C(4)	1.504(3)
C(4)-O(2)	1.411(3)	C(4)-O(1)	1.424(3)
C(5)-O(2)	1.434(3)	C(5)-C(6)	1.504(3)
C(7)-C(12)	1.387(3)	C(7)-C(8)	1.395(3)
C(8)-C(9)	1.389(4)	C(9)-C(10)	1.379(3)
C(10)-C(11)	1.382(3)	C(11)-C(12)	1.394(4)
C(13)-C(14)	1.390(3)	C(13)-C(18)	1.399(3)
C(14)-C(15)	1.392(3)	C(15)-C(16)	1.374(3)
C(16)-C(17)	1.383(3)	C(17)-C(18)	1.377(3)
O(1)-C(1)-C(7)	108.57(16)	O(1)-C(1)-C(13)	107.74(16)
C(7)-C(1)-C(13)	108.74(17)	O(1)-C(1)-C(2)	105.59(17)
C(7)-C(1)-C(2)	113.69(17)	C(13)-C(1)-C(2)	112.25(17)
C(3)-C(2)-C(1)	102.06(17)	C(4)-C(3)-C(2)	101.53(18)
O(2)-C(4)-O(1)	111.24(18)	O(2)-C(4)-C(3)	108.08(16)

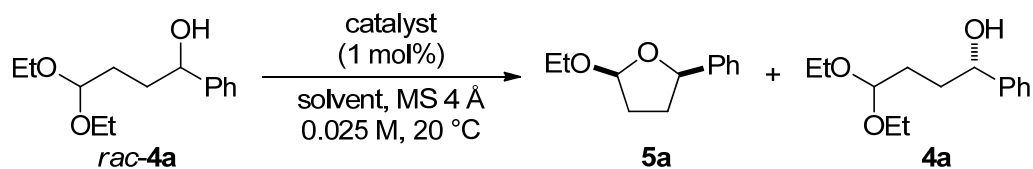
7. EXPERIMENTAL SECTION

O(1)-C(4)-C(3)	105.23(16)	O(2)-C(5)-C(6)	108.22(18)
C(12)-C(7)-C(8)	118.6(2)	C(12)-C(7)-C(1)	121.41(19)
C(8)-C(7)-C(1)	119.90(19)	C(9)-C(8)-C(7)	120.8(2)
C(10)-C(9)-C(8)	119.0(2)	C(9)-C(10)-C(11)	121.8(2)
C(9)-C(10)-Br(2)	118.83(18)	C(11)-C(10)-Br(2)	119.32(18)
C(10)-C(11)-C(12)	118.3(2)	C(7)-C(12)-C(11)	121.4(2)
C(14)-C(13)-C(18)	118.39(18)	C(14)-C(13)-C(1)	121.73(18)
C(18)-C(13)-C(1)	119.84(18)	C(13)-C(14)-C(15)	120.78(19)
C(16)-C(15)-C(14)	119.03(19)	C(15)-C(16)-C(17)	121.70(18)
C(15)-C(16)-Br(1)	119.33(16)	C(17)-C(16)-Br(1)	118.89(15)
C(18)-C(17)-C(16)	118.79(19)	C(17)-C(18)-C(13)	121.3(2)
C(4)-O(1)-C(1)	109.78(14)	C(4)-O(2)-C(5)	113.50(15)

7.3. Kinetic resolution of homoaldols via catalytic asymmetric transacetalization

(with S. Müller)^[108]

7.3.1. Optimization of the reaction conditions

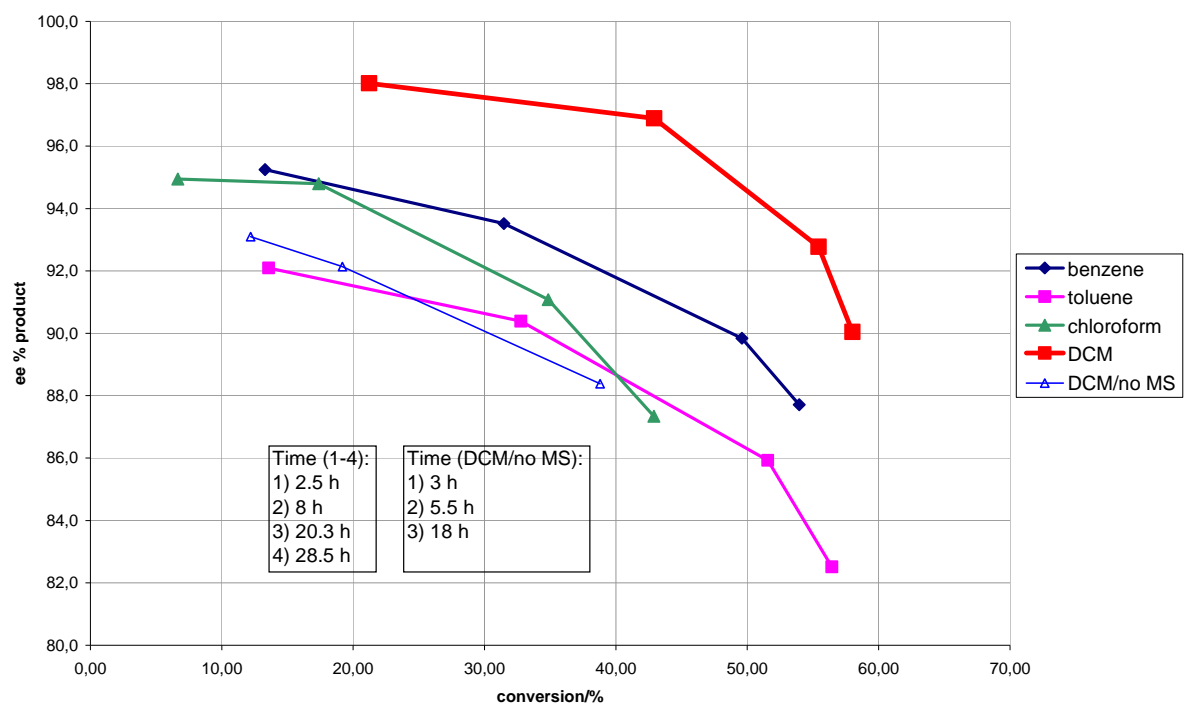


Molecular sieves 4 Å (12.5 mg) and a solution of catalyst (0.00025 mmol) in dry solvent (0.5 mL), were added to the solution of *rac*-**4a** (0.025 mmol) in dry solvent (0.5 mL) and stirred at 20 °C. Samples (ca. 100 µL) were removed from the reaction mixture, quenched with a drop of Et₃N, and diluted with ⁱPrOH (200 µL). The enantiomeric ratios of **5a**, 5-*epi*-**5a**, and **4a** were determined by HPLC analysis of these crude mixtures using Daicel Chiralcel OJ-H column: *n*-heptane/*i*-PrOH 90:10, flow rate 0.5 mL/min, λ = 220 nm.ⁱ Conversions were calculated from the enantiomeric excesses of products and starting material.ⁱⁱ

Notes:

- *i*) In these conditions enantiomers of **5a**, 5-*epi*-**5a**, and **4a** are separated (see details in Substrates and Products sections).
- *ii*) See “Determination of conversion and dr” in Products section

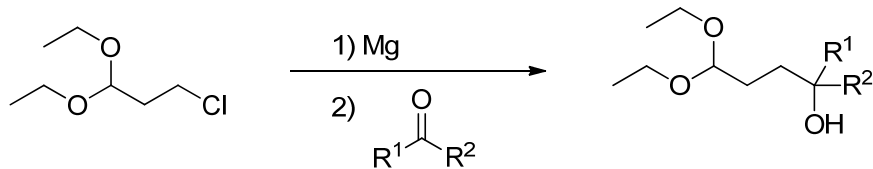
Solvent Screening with STRIP catalyst



7.3.2. Substrates

rac-4a-i and rac-4m-r

Representative procedure for compounds rac-4a-i and rac-4m-r

*Preparation of the Grignard reagent*

A solution of freshly distilled 3-chloropropionaldehyde diethylacetal (8.0 g, 48.0 mmol) in THF (10 mL) was added to activatedⁱ magnesium turnings (1.46 g, 60 mmol). The temperature of the exothermic reaction mixture was kept between 15-25 °C by cooling with an ice bath.^{ii, iii} After heat development ceased, the mixture was diluted with THF (15 mL) and the resulting solution was used immediately.

Addition to aldehydes and ketones

One quarter of the solution of the Grignard reagent prepared above (\approx 8 mL, 12.0 mmol) was added dropwise to a solution of the corresponding aldehyde or ketone (3.0 mmol) in THF (4 mL) at -40 °C. The mixture was stirred at -40 °C for 30 min and then allowed to warm to 0 °C within 2 h. It was then quenched at 0 °C with saturated aqueous NaHCO₃ (5 mL) and H₂O (5 mL), and extracted with Et₂O (3 x 10 mL). The combined organic extracts were dried over Na₂CO₃, filtered, and concentrated directly prior to purification. Flash chromatography on silica gel yielded pure products.^{iv} The products were stored as 0.1-0.2 M solutions in EtOAc or Et₂O, or used immediately in the transacetalization reaction.^v

Notes:

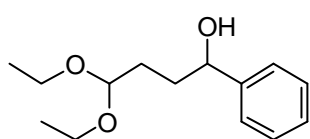
- *i*) Activation was performed with a few drops of 1,2-dibromoethane.
- *ii*) Depending on the purity of the starting materials and the activity of the magnesium sometimes a dry ice/acetone bath is necessary for sufficient cooling.
- *iii*) If there is no exothermic reaction at this point, initiation is performed by adding more 1,2-dibromoethane and fast short heating to reflux (with a heat gun) before cooling again to 25 °C (repeated until reaction becomes exothermic after cooling).
- *iv*) TLC visualization: UV (254 nm) and/or PMA stain.

7. EXPERIMENTAL SECTION

- v) A slow spontaneous intramolecular transacetalization can be observed in neat samples.

In the following, next to the NMR data for *rac*-**4**, HPLC and GC analysis information and optical rotation values for enantioenriched samples are given.

4,4-Diethoxy-1-phenylbutan-1-ol (*rac*-**4a**)



Purification: Pentane/Et₂O 2:1. Colorless oil 657 mg (2.76 mmol, 92%).

¹H NMR (500 MHz, C₆D₆) δ = 7.29 (d, *J* = 7.3 Hz, 2H), 7.19-7.16 (m, 2H), 7.10-7.07 (m, 1H), 4.51-4.48 (m, 1H), 4.40-4.38 (m, 1H), 3.51-3.44 (m, 2H), 3.32-3.24 (m, 2H), 2.06 (br, 1H), 1.88-1.80 (m, 3H), 1.75-1.71 (m, 1H), 1.69-1.05 (m, 6H) ppm.

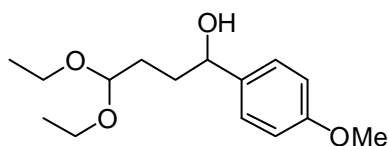
¹³C NMR (125 MHz, C₆D₆) δ 145.9, 128.5, 127.4, 126.2, 103.1, 74.1, 61.1, 60.9, 34.9, 30.4, 15.5 ppm.

HRMS (ESI+) *m/z* calculated for C₁₄H₂₂O₃Na (M+Na⁺) 261.146115, found 261.145833.

HPLC analysis using Daicel Chiralcel OJ-H column: *n*-heptane/*i*-PrOH 90:10, flow rate 0.5 mL/min, λ = 220 nm: *t*₁ = 13.17 min, *t*₂ = 14.95 min.

$\alpha_D^{25} = -31.2^\circ$ (*c* = 0.50, CH₂Cl₂) for (*S*)-**4a** with er 96.5:3.5.

4,4-Diethoxy-1-(4-methoxyphenyl)butan-1-ol (*rac*-**4b**)



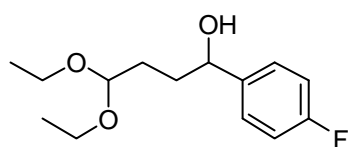
Purification: Pentane/Et₂O 2:1. Colorless oil 764 mg (2.85 mmol, 95%).

¹H NMR (500 MHz, C₆D₆) δ 7.23 (d, *J* = 8.6 Hz, 2H), 6.80 (d, *J* = 8.6 Hz, 2H), 4.55-4.52 (m, 1H), 4.43 (t, *J* = 5.2 Hz, 1H), 3.51-3.45 (m, 2H), 3.34 (s, 3H), 3.33-3.28 (m, 2H), 2.46 (br, 1H), 1.93-1.83 (m, 3H), 1.77-1.72 (m, 1H), 1.09 (m, 6H) ppm.

¹³C NMR (125 MHz, C₆D₆) δ 159.4, 138.0, 127.4, 114.0, 103.1, 73.8, 61.0, 60.9, 54.8, 35.0, 30.5, 15.6 ppm.

HRMS (ESI+) *m/z* calculated for C₁₅H₂₄O₄Na (M+Na⁺) 291.156679, found 291.156687.

HPLC analysis using Daicel Chiralcel OJ-H column: *n*-heptane/*i*-PrOH 80:20, flow rate 0.5 mL/min, λ = 220 nm: *t*₁ = 12.93 min, *t*₂ = 14.13 min.

4,4-Diethoxy-1-(4-fluorophenyl)butan-1-ol (*rac*-4c)

Purification: Pentane/Et₂O 2:1. Colorless oil 689 mg (2.69 mmol, 90%).

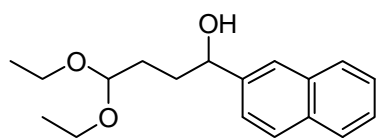
¹H NMR (500 MHz, C₆D₆) δ 7.07-7.04 (m, 2H), 6.84-6.80 (m, 2H), 4.40-4.36 (m, 2H), 3.51-3.44 (m, 2H), 3.32-3.24 (m, 2H), 2.18 (d, br, *J* = 3.5 Hz, 1H), 1.80-1.65 (m, 4H), 1.10-1.05 (m, 6H) ppm.

¹³C NMR (125 MHz, C₆D₆) δ 162.4 (d, *J* = 244.5 Hz), 141.6 (d, *J* = 2.9 Hz), 127.7 (d, *J* = 7.6 Hz), 115.2 (d, *J* = 21.2 Hz), 103.0, 73.4, 61.2, 61.1, 34.9, 30.4, 15.5 ppm.

HRMS (ESI+) *m/z* calculated for C₁₄H₂₁FO₃Na (M+Na⁺) 279.136689, found 279.136498.

HPLC analysis using Daicel Chiralcel OJ-H column: *n*-heptane/*i*-PrOH 95:5, flow rate 0.5 mL/min, λ = 220 nm: t₁ = 16.99 min, t₂ = 22.95 min.

α_D²⁵ = -28.8° (c = 0.50, CH₂Cl₂) for (*S*)-4c with er 97.5:2.5.

4,4-Diethoxy-1-(naphthalen-2-yl)butan-1-ol (*rac*-4d)

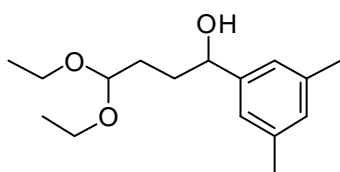
Purification: Pentane/Et₂O 1:1. Colorless oil 817 mg (2.83 mmol, 94%).

¹H NMR (500 MHz, C₆D₆) δ 7.74 (s, 1H), 7.68-7.63 (m, 3H), 7.42 (dd, *J* = 8.5, 1.6 Hz, 1H), 7.30-7.25 (m, 2H), 4.67-4.65 (m, 1H), 4.43-4.41 (m, 1H), 3.50-3.45 (m, 2H), 3.31-3.26 (m, 2H), 2.37 (d, *J* = 3.5 Hz, 1H), 1.95-1.87 (m, 3H), 1.80-1.77 (m, 1H), 1.11-1.06 (m, 6H) ppm.

¹³C NMR (125 MHz, C₆D₆) δ 143.4, 134.0, 133.5, 128.4, 128.3, 128.0, 126.3, 125.8, 124.8, 124.7, 103.1, 74.3, 61.1, 61.0, 34.7, 30.5, 15.6 ppm.

HRMS (ESI+) *m/z* calculated for C₁₈H₂₄O₃Na (M+Na⁺) 311.161768, found 311.161760.

HPLC analysis using Daicel Chiralcel OJ-H column: *n*-heptane/*i*-PrOH 80:20, flow rate 0.5 mL/min, λ = 220 nm: t₁ = 14.13 min, t₂ = 18.58 min.

1-(3,5-Dimethylphenyl)-4,4-diethoxybutan-1-ol (*rac*-4e)

Purification: Pentane/Et₂O 2:1. Colorless oil 771 mg (2.90 mmol, 97%).

¹H NMR (500 MHz, C₆D₆) δ 7.00 (s, 2H), 6.76 (s, 1H), 4.54-4.53 (m, 1H), 4.44-4.42 (m, 1H), 3.51-3.47 (m, 2H), 3.33-3.27 (m, 2H), 2.34 (br, 1H), 2.17 (s, 6H), 1.95-1.87 (m, 3H), 1.80-1.78 (m, 1H), 1.10-1.06 (m, 6H) ppm.

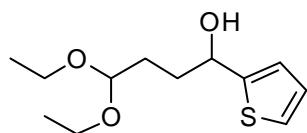
7. EXPERIMENTAL SECTION

^{13}C NMR (125 MHz, C_6D_6) δ 146.0, 137.8, 129.1, 124.1, 103.1, 74.3, 61.0, 60.9, 35.0, 30.6, 21.4, 15.6 ppm.

HRMS (ESI+) m/z calculated for $\text{C}_{16}\text{H}_{26}\text{O}_3\text{Na}$ ($\text{M}+\text{Na}^+$) 289.177416, found 289.177500.

HPLC analysis using Daicel Chiralcel AD-3 column: *n*-heptane/*i*-PrOH 99:1, flow rate 1.0 mL/min, $\lambda = 220$ nm: $t_1 = 17.74$ min, $t_2 = 20.90$ min.

4,4-Diethoxy-1-(thiophen-2-yl)butan-1-ol (*rac*-4f)



Purification: Pentane/ Et_2O 2:1. Yellowish oil 714 mg (2.93 mmol, 97%).

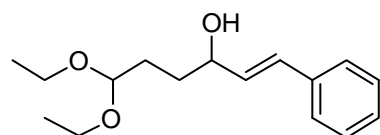
^1H NMR (500 MHz, C_6D_6) δ 6.87 (dd, $J = 5.0, 1.2$ Hz, 1H), 6.78-6.77 (m, 1H), 6.73 (dd, $J = 5.0, 3.5$ Hz, 1H), 4.77-4.74 (m, 1H), 4.37 (t, $J = 5.5$ Hz, 1H), 3.49-3.43 (m, 2H), 3.30-3.23 (m, 2H), 2.67 (d, $J = 4.3$ Hz, 1H), 1.96-1.90 (m, 2H), 1.86-1.80 (m, 1H), 1.76-1.72 (m, 1H), 1.08-1.05 (m, 6H) ppm.

^{13}C NMR (125 MHz, C_6D_6) δ 150.2, 126.7, 124.2, 123.4, 102.9, 70.2, 61.1, 61.1, 35.1, 30.3, 15.5 ppm.

HRMS (ESI+) m/z calculated for $\text{C}_{12}\text{H}_{21}\text{O}_3\text{S}$ ($\text{M}+\text{H}^+$) 267.102536, found 267.102704.

HPLC analysis using Daicel Chiralcel OJ-H column: *n*-heptane/*i*-PrOH 90:10, flow rate 0.5 mL/min, $\lambda = 220$ nm: $t_1 = 14.34$ min, $t_2 = 15.48$ min.

(*E*)-6,6-Diethoxy-1-phenylhex-1-en-3-ol (*rac*-4g)



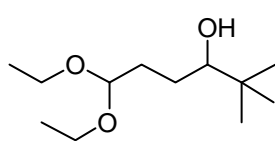
Purification: Pentane/ Et_2O 2:1. Colorless oil 641 mg (2.43 mmol, 81%).

^1H NMR (500 MHz, C_6D_6) δ 7.25 (d, $J = 7.3$ Hz, 2H), 7.13 (dd, $J = 7.3, 7.3$ Hz, 2H), 7.05 (t, $J = 7.3$ Hz, 1H), 6.54 (d, $J = 15.9$ Hz, 1H), 6.15 (dd, $J = 15.9, 6.2$ Hz, 1H), 4.46 (t, $J = 5.5$ Hz, 1H), 4.15-4.14 (m, 1H), 3.55-3.49 (m, 2H), 3.37-3.30 (m, 2H), 2.11 (d, $J = 3.0$ Hz, 1H), 1.89-1.81 (m, 2H), 1.74-1.70 (m, 2H), 1.12-1.09 (m, 6H) ppm.

^{13}C NMR (125 MHz, C_6D_6) δ 137.5, 133.5, 129.9, 128.8, 127.6, 126.9, 103.1, 72.5, 61.1, 61.0, 32.9, 30.1, 15.6 ppm.

HRMS (ESI+) m/z calculated for $\text{C}_{16}\text{H}_{24}\text{O}_3\text{Na}$ ($\text{M}+\text{Na}^+$) 287.161765, found 287.161872.

HPLC analysis using Daicel Chiralcel AD-3 column: *n*-heptane/*i*-PrOH 95:5, flow rate 1.0 mL/min, $\lambda = 220$ nm: $t_1 = 8.85$ min, $t_2 = 9.58$ min.

6,6-Diethoxy-2,2-dimethylhexan-3-ol (*rac*-4h)

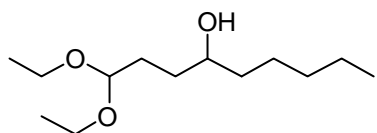
Purification: Pentane/Et₂O 2:1. Colorless oil 504 mg (2.31 mmol, 77%).

¹H NMR (500 MHz, C₆D₆) δ 4.46 (t, *J* = 5.5 Hz, 1H), 3.58-3.50 (m, 2H), 3.38-3.32 (m, 2H), 3.11-3.09 (m, 1H), 2.07 (d, *J* = 3.9 Hz, 1H), 1.99-1.92 (m, 1H), 1.77-1.70 (m, 1H), 1.65-1.58 (m, 1H), 1.40-1.32 (m, 1H), 1.11 (t, *J* = 7.1 Hz, 6H), 0.90 (s, 9H) ppm.

¹³C NMR (125 MHz, C₆D₆) δ 103.4, 79.5, 61.1, 61.0, 35.2, 31.7, 27.0, 26.0, 15.6, 15.6 ppm.

HRMS (ESI+) *m/z* calculated for C₁₂H₂₆O₃Na (M+Na⁺) 241.177415, found 241.177430.

GC analysis using BGB-176 column (30 m, 2,3-dimethyl-6-*tert*-butyldimethylsilyl-β-cyclodextrin), Detector: FID; Temperature: injector 220 °C, detector 320 °C, oven 110 °C; gas: 0.5 bar H₂. *t*₁ = 17.23 min, *t*₂ = 18.80 min.

1,1-Diethoxynonan-4-ol (*rac*-4i)

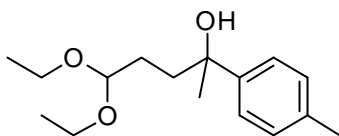
Purification: Pentane/Et₂O 2:1. Colorless oil 555 mg (2.39 mmol, 80%).

¹H NMR (500 MHz, C₆D₆) δ 4.47 (t, *J* = 5.4 Hz, 1H), 3.57-3.51 (m, 2H), 3.50-3.48 (m, 1H), 3.39-3.32 (m, 2H), 2.00 (br, 1H), 1.90-1.84 (m, 1H), 1.79-1.75 (m, 1H), 1.60-1.53 (m, 1H), 1.51-1.10 (m, 9H), 1.14-1.10 (m, 6H), 0.89 (t, *J* = 7.1 Hz, 3H) ppm.

¹³C NMR (125 MHz, C₆D₆) δ 103.3, 71.4, 61.1, 60.9, 38.2, 33.0, 32.4, 30.5, 25.9, 23.1, 15.6, 15.6, 14.3 ppm.

HRMS (ESI+) *m/z* calculated for C₁₃H₂₈O₃Na (M+Na⁺) 255.193064, found 255.192881.

GC analysis using BGB-176 column (30 m, 2,3-dimethyl-6-*tert*-butyldimethylsilyl-β-cyclodextrin), Detector: FID; Temperature: injector 220 °C, detector 320 °C, oven: 105 °C, 0.25 °C/min until 125 °C; gas: 0.4 bar H₂. *t*₁ = 65.99 min, *t*₂ = 66.77 min.

5,5-Diethoxy-2-(*p*-tolyl)pentan-2-ol (*rac*-4m)

Purification: Pentane/Et₂O 2:1. Colorless oil 656 mg (2.46 mmol, 82%).

¹H NMR (500 MHz, C₆D₆) δ 7.37 (d, *J* = 8.2 Hz, 2H), 7.04 (d, *J* = 8.0 Hz, 2H), 4.37 (t, *J* = 5.4 Hz, 1H), 3.48-3.45 (m, 1H), 3.43-3.39 (m, 1H), 3.28-3.23 (m, 2H), 2.30 (s, 1H), 2.15 (s, 3H), 1.96-1.90 (m, 2H), 1.79-1.75 (m, 1H), 1.65-1.62 (m, 1H), 1.43 (s, 3H), 1.09-1.04 (m, 6H) ppm.

7. EXPERIMENTAL SECTION

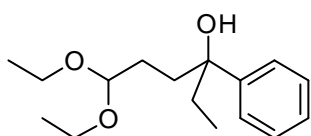
^{13}C NMR (125 MHz, C_6D_6) δ 145.9, 135.7, 129.0, 125.4, 103.3, 73.9, 61.1, 60.7, 39.2, 31.3, 28.8, 21.0, 15.5, 15.5 ppm.

HRMS (ESI+) m/z calculated for $\text{C}_{16}\text{H}_{26}\text{O}_3\text{Na}$ ($\text{M}+\text{Na}^+$) 289.177412, found 289.177404.

HPLC analysis using Daicel Chiralcel OD-3 column: *n*-heptane/*i*-PrOH 99:1, flow rate 1.0 mL/min, $\lambda = 220$ nm: $t_1 = 8.53$ min, $t_2 = 9.34$ min.

$\alpha_D^{25} = -9.1^\circ$ ($c = 0.837$ in CH_2Cl_2 , er 96:4).

6,6-Diethoxy-3-phenylhexan-3-ol (*rac*-4n)



Purification: Pentane/ Et_2O 2:1. Colorless oil 773 mg (2.90 mmol, 97%).

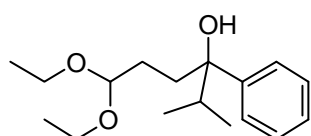
^1H NMR (500 MHz, C_6D_6) δ 7.41 (dd, $J = 8.3, 1.0$ Hz, 2H), 7.21 (dd, $J = 8.3, 7.4$ Hz, 2H), 7.08 (t, $J = 7.4$ Hz, 1H), 4.33 (t, $J = 5.3$ Hz, 1H), 3.48-3.42 (m, 1H), 3.40-3.34 (m, 1H), 3.27-3.19 (m, 2H), 2.55 (s br, 1H), 1.96-1.89 (m, 2H), 1.77-1.68 (m, 3H), 1.57-1.51 (m, 1H), 1.07 (t, $J = 7.0$ Hz, 3H), 1.04 (t, $J = 7.0$ Hz, 3H), 0.78 (t, $J = 7.4$ Hz, 3H) ppm.

^{13}C NMR (125 MHz, C_6D_6) δ 146.8, 128.26, 126.4, 126.0, 103.3, 76.5, 61.3, 60.7, 37.6, 36.8, 28.3, 15.5, 15.5, 8.1 ppm.

HRMS (ESI+) m/z calculated for $\text{C}_{16}\text{H}_{26}\text{O}_3\text{Na}$ ($\text{M}+\text{Na}^+$) 289.177412, found 289.177328.

HPLC analysis using Daicel Chiralcel OJ-H column: *n*-heptane/*i*-PrOH 80:20, flow rate 0.5 mL/min, $\lambda = 220$ nm: $t_1 = 7.38$ min, $t_2 = 12.83$ min.

6,6-Diethoxy-2-methyl-3-phenylhexan-3-ol (*rac*-4o)



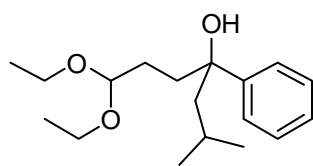
Purification: Pentane/ Et_2O 5:1. Colorless oil 812 mg (2.89 mmol, 96%).

^1H NMR (500 MHz, C_6D_6) δ 7.42 (dd, $J = 8.3, 1.0$ Hz, 2H), 7.21 (dd, $J = 8.3, 7.3$ Hz, 2H), 7.08 (t, $J = 7.3$ Hz, 1H), 4.31 (t, $J = 5.3$ Hz, 1H), 3.46-3.40 (m, 1H), 3.37-3.31 (m, 1H), 3.24-3.16 (m, 2H), 2.66 (s br, 1H), 2.04-1.98 (m, 1H), 1.96-1.91 (m, 1H), 1.90-1.86 (m, 1H), 1.67-1.61 (m, 1H), 1.49-1.44 (m, 1H), 1.07-1.01 (m, 6H), 1.00 (d, $J = 6.8$ Hz, 3H), 0.77 (d, $J = 6.8$ Hz, 3H) ppm.

^{13}C NMR (125 MHz, C_6D_6) δ 146.6, 128.1, 126.4, 126.3, 103.3, 78.4, 61.6, 60.7, 39.0, 34.5, 28.6, 17.9, 17.0, 15.5, 15.4 ppm.

HRMS (ESI+) m/z calculated for $\text{C}_{17}\text{H}_{28}\text{O}_3\text{Na}$ ($\text{M}+\text{Na}^+$) 303.193065, found 303.192836.

HPLC analysis using Daicel Chiralcel OJ-H column: *n*-heptane/*i*-PrOH 90:10, flow rate 0.5 mL/min, $\lambda = 220$ nm: $t_1 = 8.25$ min, $t_2 = 10.46$ min.

1,1-diethoxy-6-methyl-4-phenylheptan-4-ol (*rac*-4p)

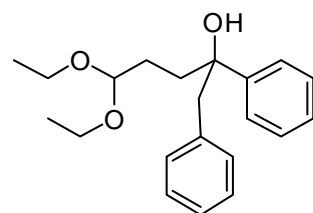
Purification: 10% EtOAc/hexane. Colorless oil 838 mg (2.85 mmol, 95%).

$^1\text{H NMR}$ (500 MHz, C_6D_6) δ 7.42 (dd, $J = 8.4, 1.2$ Hz, 2H), 7.21 (t, $J = 7.7$ Hz, 2H), 7.07 (dt, $J = 7.4, 1.1$ Hz, 1H), 4.32 (t, $J = 5.3$ Hz, 1H), 3.48-3.42 (m, 1H), 3.38-3.32 (m, 1H), 3.26-3.18 (m, 2H), 2.45 (s, 1H), 1.96-1.86 (m, 2H), 1.74-1.67 (m, 3H), 1.63-1.58 (m, 1H), 1.53-1.46 (m, 1H), 1.08 (t, $J = 7.0$ Hz, 3H), 1.04 (t, $J = 7.0$ Hz, 3H), 0.99 (d, $J = 6.5$ Hz, 3H), 0.69 (d, $J = 6.4$ Hz, 3H) ppm.

$^{13}\text{C NMR}$ (125 MHz, C_6D_6) δ 147.3, 126.3, 126.0, 103.3, 76.9, 61.5, 60.7, 52.9, 39.1, 28.2, 24.8, 24.7, 24.5, 15.47, 15.45 ppm.

HRMS (ESI+) m/z calculated for $\text{C}_{18}\text{H}_{30}\text{O}_3\text{Na}$ ($\text{M}+\text{Na}^+$) 317.2087, found 317.2083.

HPLC analysis using Daicel Chiralcel AD-3 column: *n*-heptane/*i*-PrOH 99.5:0.5, flow rate 1.0 mL/min, $\lambda = 210$ nm: $t_1 = 14.74$ min, $t_2 = 16.58$ min.

5,5-Diethoxy-1,2-diphenylpentan-2-ol (*rac*-4q)

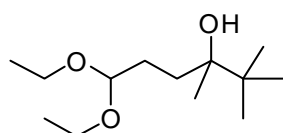
Purification: Pentane/Et₂O 4:1. Colorless oil 673 mg (2.05 mmol, 68%).

$^1\text{H NMR}$ (500 MHz, C_6D_6) δ 7.31 (dd, $J = 8.3, 1.1$ Hz, 2H), 7.16-7.13 (m, 2H), 7.07-7.00 (m, 4H), 6.99-6.96 (m, 2H), 4.30 (t, $J = 5.4$ Hz, 1H), 3.45-3.39 (m, 1H), 3.37-3.31 (m, 1H), 3.22-3.16 (m, 2H), 3.03 (d, $J = 13.3$ Hz, 1H), 2.95 (d, $J = 13.3$ Hz, 1H), 2.55 (s, 1H), 2.10-2.04 (m, 1H), 1.97-1.91 (m, 1H), 1.81-1.74 (m, 1H), 1.58-1.51 (m, 1H), 1.06-1.01 (m, 6H) ppm.

$^{13}\text{C NMR}$ (125 MHz, C_6D_6) δ 146.7, 137.3, 131.2, 128.2, 128.1, 126.7, 126.5, 126.1, 103.2, 76.5, 61.3, 60.6, 50.8, 36.8, 28.3, 15.5, 15.4 ppm.

HRMS (ESI+) m/z calculated for $\text{C}_{21}\text{H}_{28}\text{O}_3\text{Na}$ ($\text{M}+\text{Na}^+$) 351.193062, found 351.193062.

HPLC analysis using Daicel Chiralcel OJ-H column: *n*-heptane/*i*-PrOH 90:10, flow rate 0.5 mL/min, $\lambda = 220$ nm: $t_1 = 10.07$ min, $t_2 = 11.72$ min.

6,6-diethoxy-2,2,3-trimethylhexan-3-ol (*rac*-4r)

Purification: 15% EtOAc/hexane. Colorless oil 453 mg (1.95 mmol, 65%).

$^1\text{H NMR}$ (500 MHz, C_6D_6) δ 4.46-4.43 (m, 1H), 3.60-3.50 (m, 2H), 3.41-3.31 (m, 2H), 2.00-1.91 (m, 1H), 1.77-1.68 (m, 2H), 1.53-1.45 (m, 2H),

7. EXPERIMENTAL SECTION

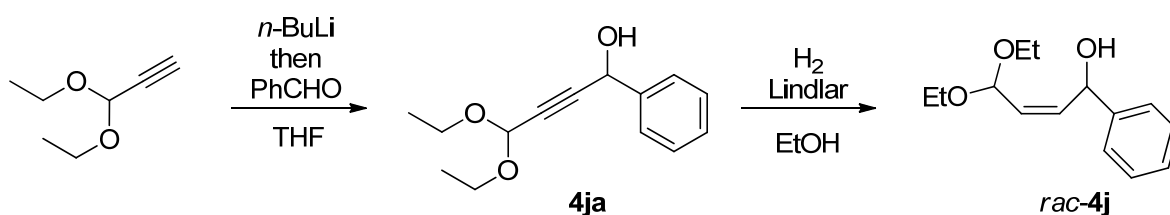
1.121 (t, $J = 7.0$ Hz, 3H, overlapped), 1.117 (t, $J = 7.0$ Hz, 3H, overlapped), 0.99 (s, 3H), 0.93 (s, 9H) ppm.

^{13}C NMR (125 MHz, C_6D_6) δ 103.9, 75.3, 61.2, 60.8, 38.4, 30.9, 28.5, 25.5, 21.4, 15.7, 15.6 ppm.

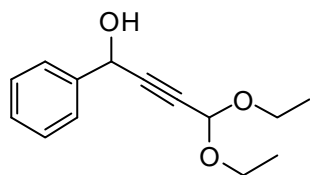
HRMS (ESI+) m/z calculated for $\text{C}_{13}\text{H}_{28}\text{O}_3\text{Na}$ ($\text{M}+\text{Na}^+$) 255.1931, found 255.1930.

GC analysis using BGB-176 column SE/SE52 (30 m, 2,3-dimethyl-6-*tert*-butyldimethylsilyl- β -cyclodextrin, i.D. 0.25 mm, df. 0.25 μm), Detector: FID; Temperature: injector 220 $^\circ\text{C}$, detector 350 $^\circ\text{C}$, oven: 125 $^\circ\text{C}$; gas: 0.5 bar H_2 . $t_1 = 25.11$ min, $t_2 = 26.26$ min.

rac-4j



4,4-Diethoxy-1-phenylbut-2-yn-1-ol (4ja)

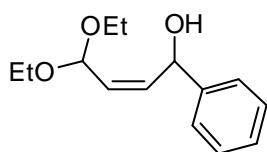


n-BuLi (1.32 mL, 3.30 mmol, 2.5 M solution in hexanes) was added dropwise to a solution of 3,3-diethoxyprop-1-yne (385 mg, 3.0 mmol) in THF (10 mL) at -78 $^\circ\text{C}$. The mixture was stirred at -78 $^\circ\text{C}$ for 30 min, before benzaldehyde (350 mg, 3.3 mmol) was added. After being stirred at -78 $^\circ\text{C}$ for 2 h the mixture was warmed up to -40 $^\circ\text{C}$ within 1h and was then quenched with saturated NaHCO_3 -solution (10 mL) and water (10 mL). The layers were separated, the aqueous layer extracted with Et_2O (3x30 mL) and the combined organic layers dried over MgSO_4 and filtered. The solvent was removed under reduced pressure and the residue purified by silica gel chromatography with pentane/ Et_2O (3:1) as the eluent to give the title compound (663 mg, 2.83 mmol, 94%) as a colorless oil.

^1H NMR (500 MHz, CDCl_3) δ 7.52 (d, $J = 7.2$ Hz, 2H), 7.39-7.37 (m, 2H), 7.34-7.31 (m, 1H), 5.52 (s, 1H), 5.34 (d, $J = 1.2$ Hz, 1H), 3.77-3.71 (m, 2H), 3.63-3.56 (m, 2H), 2.62 (s br, 1H), 1.24-1.21 (m, 6H) ppm.

^{13}C NMR (125 MHz, CDCl_3) δ 140.1, 128.7, 128.6, 126.8, 91.4, 85.2, 82.0, 64.5, 61.1, 61.1, 15.2 ppm.

HRMS (ESI+) m/z calculated for $\text{C}_{14}\text{H}_{18}\text{O}_3\text{Na}$ ($\text{M}+\text{Na}^+$) 257.114813, found 257.114561.

(Z)-4,4-Diethoxy-1-phenylbut-2-en-1-ol (*rac*-4j)

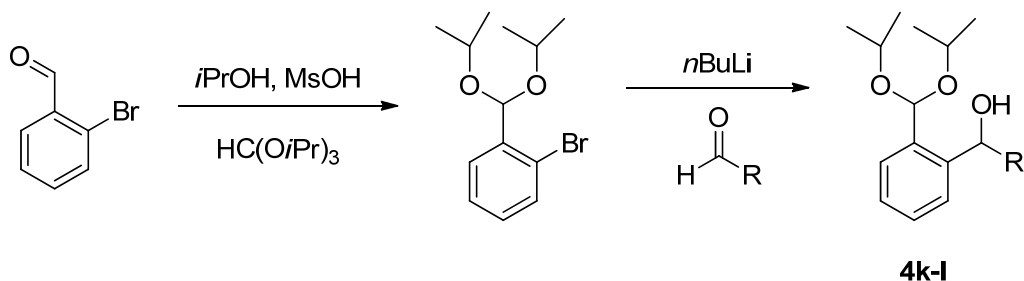
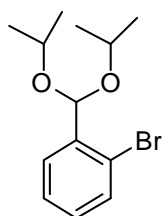
A mixture of **4ja** (442 mg, 1.89 mmol) and Lindlar catalyst (19 mg) in EtOH (7 mL) was stirred under 1 atm of H₂ at 20 °C for 1h. After complete conversion of the starting material (indicated by TLC), the mixture was filtered over celite, concentrated and purified by silica gel chromatography with pentane/Et₂O (2:1) as the eluent to give ***rac*-4j** (389 mg, 1.64 mmol, 87%) as a colorless oil.

¹H NMR (500 MHz, C₆D₆) δ 7.49 (d, *J* = 7.3 Hz, 2H), 7.20 (dd, *J* = 7.3, 7.3 Hz, 2H), 7.09 (t, *J* = 7.3 Hz, 1H), 5.73 (ddd, *J* = 11.3, 8.3, 1.3 Hz, 1H), 5.62 (ddd, *J* = 11.3, 8.3, 1.0 Hz, 1H), 5.59 (dd, *J* = 8.3, 3.3 Hz, 1H), 5.38 (d, *J* = 5.5, 1.2 Hz, 1H), 3.60-3.54 (m, 1H), 3.47-3.42 (m, 1H), 3.41-3.31 (m, 2H), 2.56 (d, *J* = 3.7 Hz, 1H), 1.10 (t, *J* = 7.1 Hz, 3H), 1.05 (t, *J* = 7.1 Hz, 3H) ppm.

¹³C NMR (125 MHz, C₆D₆) δ 143.9, 137.1, 129.1, 128.6, 127.6, 126.5, 98.0, 70.2, 60.6, 60.0, 15.5, 15.4 ppm.

HRMS (ESI+) *m/z* calculated for C₁₄H₂₀O₃Na (M+Na⁺) 259.130461, found 259.130377.

HPLC analysis using Daicel Chiralcel OJ-H column: *n*-heptane/*i*-PrOH 98:2, flow rate 0.5 mL/min, λ = 220 nm: t₁ = 29.00 min, t₂ = 31.35 min.

***rac*-4k-l****1-Bromo-2-(diisopropoxymethyl)benzene**

A solution of 2-bromobenzaldehyde (2.78 g, 15.00 mmol), triisopropyl orthoformate (5 mL), and methanesulfonic acid (97 μL, 144mg, 1.5 mmol, 10 mol%) in isopropanol (20 mL) was stirred at room temperature. After 24 hours, sodium carbonate (2 g) was added, mixture stirred for 5 min, filtered and concentrated. Product was purified by silica gel chromatography with 5% EtOAc/hexane as the eluent. Colorless oil, 3.89 g, 90%.

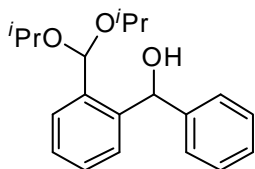
¹H NMR (500 MHz, DMSO-*d*₆) δ 7.57 (dd, *J* = 7.8, 1.4 Hz, 2H), 7.39 (td, *J* = 6.5, 0.9 Hz, 1H), 7.26 (td, *J* = 7.7, 1.8 Hz, 1H), 5.67 (s, 1H), 3.82 (sept, *J* = 6.1 Hz, 2H), 1.13 (d, *J* = 6.2 Hz, 6H), 1.08 (d, *J* = 6.2 Hz, 6H) ppm.

7. EXPERIMENTAL SECTION

^{13}C NMR (125 MHz, DMSO- d_6) δ 139.1, 132.4, 130.2, 128.5, 127.6, 122.0, 98.1, 68.3, 22.8, 22.3 ppm.

HRMS (ESI+) m/z calculated for $\text{C}_{13}\text{H}_{19}\text{BrO}_2\text{Na}$ ($\text{M}+\text{Na}^+$) 309.0461, found 309.0457.

(2-(Diisopropoxymethyl)phenyl)(phenyl)methanol (*rac*-4k)



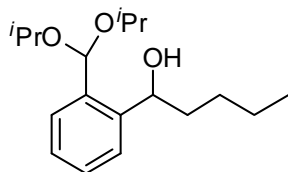
2.5 M solution of *n*BuLi in hexanes (1.32 mL, 3.3 mmol) was added dropwise to the solution of 1-bromo-2-(diisopropoxymethyl)benzene (prepared above, 1.034 g, 3.6 mmol) in THF (5 mL) at -78°C . After 2.5 hours at -78°C to the mixture a solution of benzaldehyde (303 μl , 318 mg, 3 mmol) in THF (1 mL) was added dropwise at -78°C . The solution was stirred at -78°C for 3 hours, and then allowed to warm to 0°C . Water (10 mL) was added and mixture extracted with diethyl ether (20 mL, 2x10 mL). Combined organic extracts were washed with concentrated aqueous sodium carbonate solution (10 mL), dried (MgSO_4), filtered, and concentrated. Product was purified by silica gel chromatography with 10% EtOAc/hexane as the eluent. Colorless oil, 824 mg, 87%, stored as a solution in EtOAc.

^1H NMR (500 MHz, C_6D_6) δ 7.61 (d, $J = 7.9$ Hz, 2H), 7.54 (dd, $J = 7.4, 1.3$ Hz, 1H), 7.25 (dd, $J = 7.4, 1.3$ Hz, 1H), 7.20 (t, $J = 7.8$ Hz, 2H), 7.10 (t, $J = 7.30$ Hz, 1H), 7.08 (td, $J = 7.5, 1.5$ Hz, 1H), 7.03 (td, $J = 7.3, 1.5$ Hz, 1H), 6.58 (d, $J = 4.5$ Hz, 1H), 5.63 (s, 1H), 3.82 (sept, $J = 6.1$ Hz, 1H), 3.76 (d, $J = 4.6$ Hz, 1H), 3.69 (sept, $J = 6.3$ Hz, 1H), 1.05 (d, $J = 6.2$ Hz, 3H), 1.03 (d, $J = 6.2$ Hz, 3H), 0.97 (d, $J = 6.1$ Hz, 3H), 0.93 (d, $J = 6.1$ Hz, 3H) ppm.

^{13}C NMR (125 MHz, C_6D_6) δ 144.3, 143.5, 138.5, 129.8, 128.9, 128.4, 127.5, 127.2, 127.1, 99.2, 72.7, 68.6, 68.3, 23.2, 22.8, 22.4 ppm.

HRMS (ESI+) m/z calculated for $\text{C}_{20}\text{H}_{26}\text{O}_3\text{Na}$ ($\text{M}+\text{Na}^+$) 337.1774, found 337.1773.

HPLC analysis using Daicel Chiralcel OJ-H column: *n*-heptane/*i*-PrOH 98:2, flow rate 0.5 mL/min, $\lambda = 210$ nm: $t_1 = 12.40$ min, $t_2 = 16.19$ min.

1-(2-(Diisopropoxymethyl)phenyl)pentan-1-ol (*rac*-4I)

Procedure as for *rac*-4k. Colorless oil, 671 mg (from 3.0 mmol of pentanal), 76%, stored as a solution in EtOAc.

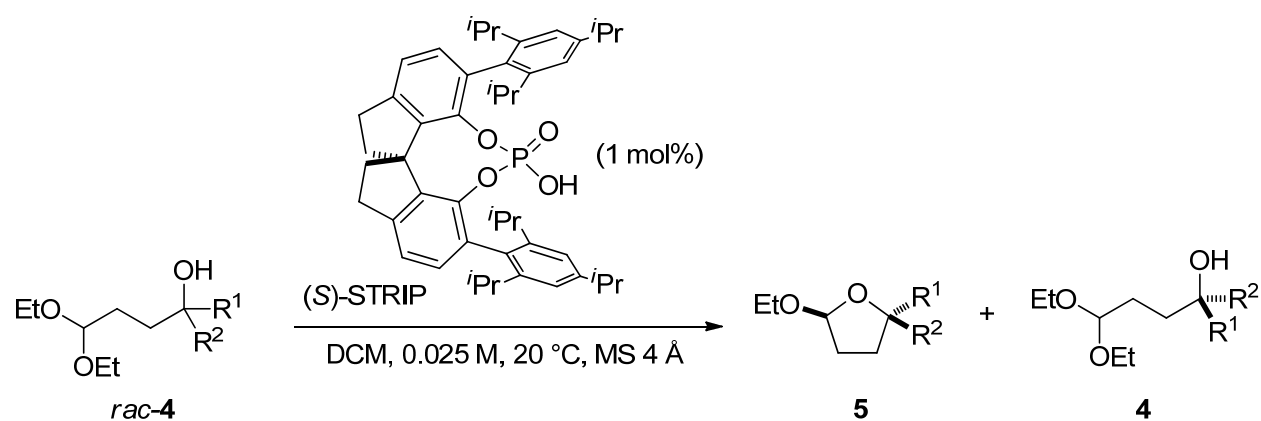
$^1\text{H NMR}$ (500 MHz, C_6D_6) δ 7.56 (t, $J = 8.6$ Hz, 2H), 7.19 (td, $J = 7.5$, 1.4 Hz, 1H), 7.12 (td, $J = 7.5$, 1.3 Hz, 1H), 5.71 (s, 1H), 5.41-5.38 (m, 1H), 3.80 (sept d, $J = 6.2$, 1.6 Hz, 2H), 2.52 (d, $J = 3.1$ Hz, 1H), 2.03-1.96 (m, 1H), 1.93-1.86 (m, 1H), 1.72-1.63 (m, 1H), 1.52-1.43 (m, 1H), 1.42-1.34 (m, 2H), 1.12 (d, $J = 6.1$ Hz, 3H), 1.10 (d, $J = 6.1$ Hz, 3H), 1.05 (d, $J = 6.2$ Hz, 3H), 1.00 (d, $J = 6.1$ Hz, 3H), 0.90 (t, $J = 7.3$ Hz, 3H) ppm.

$^{13}\text{C NMR}$ (125 MHz, C_6D_6) δ 144.1, 137.9, 128.9, 127.7, 127.0, 126.9, 99.5, 69.6, 68.7, 68.2, 37.4, 29.2, 23.22, 23.15, 22.6, 22.4, 14.4 ppm.

HRMS (ESI+) m/z calculated for $\text{C}_{18}\text{H}_{30}\text{O}_3\text{Na}$ ($\text{M}+\text{Na}^+$) 317.2087, found 317.2085.

HPLC analysis using Daicel Chiralcel AD-3 column: *n*-heptane/*i*-PrOH 99:1, flow rate 1.0 mL/min, $\lambda = 210$ nm: $t_1 = 7.28$ min, $t_2 = 9.54$ min.

$\alpha_D^{25} = +15.2^\circ$ ($c = 0.475$, CH_2Cl_2) for (*R*)-4I with er 97.5:2.5.

7.3.3. Products**General procedure for STRIP-catalyzed kinetic resolution of homoaldols via asymmetric transacetalization**

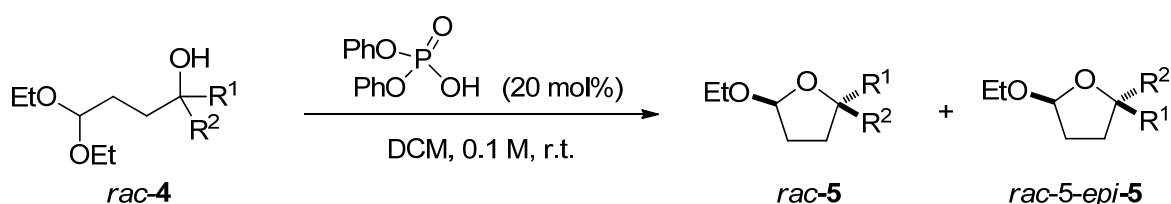
Molecular sieves 4 Å (50 mg) and a solution of (*S*)-STRIP (0.72 mg, 0.001 mmol) in dry dichloromethane (1 mL), were added to the solution of *rac*-4 (0.1 mmol) in dry dichloromethane (3 mL) and stirred at 20 °C. Samples (ca. 300 μL) were removed from the reaction mixture, quenched by a few drops of Et_3N . Subsequently, the product and remaining starting material were isolated by silica gel chromatography using Et_2O /pentane as the eluent,

and analyzed by HPLC or GC on a chiral stationary phase.ⁱ Conversions were calculated from the enantiomeric excesses of products and starting material.ⁱⁱ

Notes:

- i) All fractions containing product were combined together (important for correct dr determination) and solvent carefully evaporated to prevent loss of volatile products. TLC (EtOAc/hexane or Et₂O/pentane), visualization: PMA stain.
- ii) See below

Preparation of the racemates



Diphenyl phosphate (10 mg, 0.04 mmol) was added to the solution of *rac-4* (0.2 mmol) in dichloromethane (2 mL). After 15 min at room temperature, the reaction was quenched with Et₃N (ca. 50 μ L). The mixture was concentrated and products were isolated by silica gel chromatography using Et₂O/pentane or EtOAc/hexane as the eluents. (For substrate *rac-4j*, 0.5 mg of diphenyl phosphate was used)

Determination of conversion and dr

Conversions were calculated from ee and dr values. The corresponding formula was derived from two simple and reasonable assumptions:

- a) Since the reactions are very clean and no significant byproducts are formed, the conversion can be represented by Eq 1.
- b) The preformed alcohol stereocenter is not racemizing under the reaction conditions. The absolute configuration of this stereocenter of the major product was found to be opposite to the configuration of the minor diastereoisomer and the starting material (this finding is further supported by the significant formation of the minor diastereoisomer at higher levels of conversion). The sum of ee-values with respect to this stereocenter has to be zero at every time (Eq 4). Consequently the conversion can easily be calculated by using Eq 5, derived from Eq 1, Eq 2 and Eq 4.

7. EXPERIMENTAL SECTION

$$\text{conversion} = 1 - y_{\text{SM}} = y_{\text{maj}} + y_{\text{min}} \quad (\text{eq 1})$$

$$\text{dr} = \frac{y_{\text{maj}}}{y_{\text{min}}} = F \times \frac{\text{Area}_{\text{maj}}}{\text{Area}_{\text{min}}} \quad (\text{eq 2})$$

$$F = \frac{\text{dr}_{\text{NMR}}(\text{racemate})}{\text{dr}_{\text{HPLC}}(\text{racemate})} \quad (\text{eq 3})$$

$$y_{\text{SM}} \times ee_{\text{SM}} - y_{\text{maj}} \times ee_{\text{maj}} + y_{\text{min}} \times ee_{\text{min}} = 0 \quad (\text{eq 4})$$

$$\text{conversion} = \frac{1}{1 + \frac{ee_{\text{maj}} - ee_{\text{min}}/\text{dr}}{ee_{\text{SM}} \times (1 + 1/\text{dr})}} \quad (\text{eq 5})$$

y_{SM} = yield of the starting material

y_{maj} = yield of the major diastereoisomer

y_{min} = yield of the minor diastereoisomer

Area_{maj} = HPLC or GC area of major diastereomer peaks

Area_{min} = HPLC or GC area of minor diastereomer peaks

ee = enantiomeric excess

dr = diastereomeric ratio

F = correction factor for different responses of the HPLC detector for two diastereomers

As the diastereomeric ratio determined by HPLC depends on detector responses for two diastereomers, the correction factor (F) must be added to calculate the real dr value (Eq 2). This factor F was determined by comparing NMR (real dr) and HPLC diastereomeric ratios of prepared mixtures of both diastereoisomers (Eq 3). In cases where it was not possible to determine the response factor, it was assumed to be $F = 1$ (small variations of F value have little influence on calculated conversion). For GC traces with FID detection F factor is taken as 1.

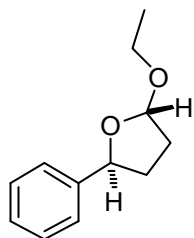
Product	5a	5b	5c	5d	5e	5f	5g	5h
F	0.79	1	0.71	1.05	1	1.06	1	1

Product	5i	5j	5k	5l	5m	5n	5o	5p
F	1	n.d. (1)	0.96	1.05	n.d. (1)	n.d. (1)	1	1

Product	5q	5r
F	0.80	1

In the following, next to the NMR data for *rac-5* and *rac-5-epi-5*, HPLC and GC analysis information and optical rotation values for enantioenriched samples are given.

***trans*-2-Ethoxy-5-phenyltetrahydrofuran (*rac-5-epi-5a*)**



Purification: Pentane/Et₂O 9:1. Colorless oil.

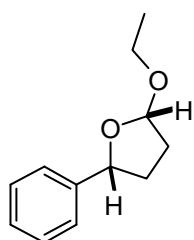
¹H NMR (500 MHz, C₆D₆) δ 7.30 (d, *J* = 7.4 Hz, 2H), 7.18 (dd, *J* = 7.4, 7.3 Hz, 2H), 7.09 (t, *J* = 7.3 Hz, 1H), 5.22 (dd, *J* = 4.8, 2.6 Hz, 1H), 5.10 (t, *J* = 7.2 Hz, 1H), 3.88-3.82 (m, 1H), 3.41-3.35 (m, 1H), 2.18-2.13 (m, 1H), 1.87-1.82 (m, 2H), 1.52-1.44 (m, 1H), 1.15 (t, *J* = 7.1 Hz, 3H) ppm.

¹³C NMR (125 MHz, C₆D₆) δ 143.6, 128.5, 127.4, 126.1, 104.5, 79.4, 63.1, 33.4, 32.7, 15.6 ppm.

HRMS (EI) *m/z* calculated for C₁₂H₁₆O₂ 192.115034, found 192.115255.

HPLC analysis using Daicel Chiralcel OJ-H column: *n*-heptane/*i*-PrOH 90:10, flow rate 0.5 mL/min, λ = 220 nm: *t*₁ = 23.49 min, *t*₂ = 27.89 min.

***cis*-2-Ethoxy-5-phenyltetrahydrofuran (*rac-5a*)**



Purification: Pentane/Et₂O 9:1. Colorless oil.

¹H NMR (500 MHz, C₆D₆) δ 7.44 (d, *J* = 7.3 Hz, 2H), 7.23 (dd, *J* = 7.4, 7.3 Hz, 2H), 7.11 (t, *J* = 7.4 Hz, 1H), 5.09 (d, *J* = 5.1 Hz, 1H), 4.87 (dd, *J* = 9.1, 6.4 Hz, 1H), 3.94-3.88 (m, 1H), 3.38-3.32 (m, 1H), 2.00-1.92 (m, 2H), 1.88-1.83 (m, 1H), 1.67-1.63 (m, 1H), 1.15 (t, *J* = 7.1 Hz, 3H) ppm.

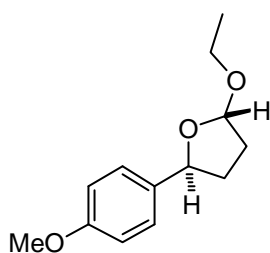
¹³C NMR (125 MHz, C₆D₆) δ 144.5, 128.6, 127.5, 126.7, 104.3, 82.8, 62.9, 34.2, 33.5, 15.5 ppm.

HRMS (EI) *m/z* calculated for C₁₂H₁₆O₂ (M) 192.115033, found 192.115079.

HPLC analysis using Daicel Chiralcel OJ-H column: *n*-heptane/*i*-PrOH 90:10, flow rate 0.5 mL/min, λ = 220 nm: *t*₁ = 12.24 min, *t*₂ = 19.58 min.

$\alpha_D^{25} = +148.7^\circ$ (*c* = 0.39, CH₂Cl₂) for (2*S*,5*R*)-**5a** with er 97.5:2.5.

***trans*-2-Ethoxy-5-(4-methoxyphenyl)tetrahydrofuran (*rac-5-epi-5b*)**



Purification: Pentane/Et₂O 3:1. Colorless oil.

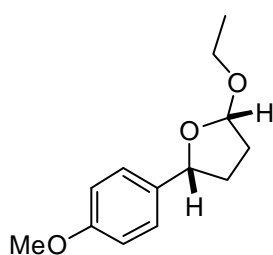
¹H NMR (500 MHz, C₆D₆) δ 7.25 (d, *J* = 8.6 Hz, 2H), 6.82 (d, *J* = 8.6 Hz, 2H), 5.25 (t, *J* = 3.7 Hz, 1H), 5.11 (t, *J* = 7.2 Hz, 1H), 3.90-3.85 (m, 1H), 3.42-3.38 (m, 1H), 3.31 (s, 3H), 2.19-2.15 (m, 1H), 1.92-1.88 (m, 2H), 1.56-1.50 (m, 1H), 1.16 (t, *J* = 7.1 Hz, 3H) ppm.

^{13}C NMR (125 MHz, C_6D_6) δ 159.5, 135.4, 127.4, 114.0, 104.4, 79.2, 63.1, 54.8, 33.6, 32.9, 15.6 ppm.

HRMS (EI) m/z calculated for $\text{C}_{13}\text{H}_{18}\text{O}_3$ 222.125593, found 222.125441.

HPLC analysis using Daicel Chiralcel OJ-H column: *n*-heptane/*i*-PrOH 80:20, flow rate 0.5 mL/min, $\lambda = 220$ nm: $t_1 = 31.16$ min, $t_2 = 37.79$ min.

***cis*-2-Ethoxy-5-(4-methoxyphenyl)tetrahydrofuran (*rac*-5b)**



Purification: Pentane/ Et_2O 3:1. Colorless oil.

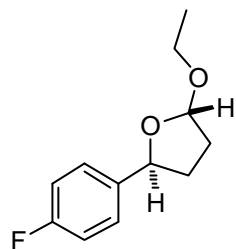
^1H NMR (500 MHz, C_6D_6) δ 7.38 (d, $J = 8.6$ Hz, 2H), 6.86 (d, $J = 8.6$ Hz, 2H), 5.10 (d, $J = 5.0$ Hz, 1H), 4.89 (dd, $J = 9.5, 6.3$ Hz, 1H), 3.95-3.89 (m, 1H), 3.40-3.33 (m, 1H), 3.32 (s, 3H), 2.05-1.96 (m, 2H), 1.90-1.85 (m, 1H), 1.71-1.65 (m, 1H), 1.17 (t, $J = 7.1$ Hz, 3H) ppm.

^{13}C NMR (125 MHz, C_6D_6) δ 159.6, 136.4, 114.1, 104.1, 82.6, 62.8, 54.8, 34.3, 33.4, 30.5, 15.5 ppm.

HRMS (EI) m/z calculated for $\text{C}_{13}\text{H}_{18}\text{O}_3$ 222.125593, found 222.125385.

HPLC analysis using Daicel Chiralcel OJ-H column: *n*-heptane/*i*-PrOH 80:20, flow rate 0.5 mL/min, $\lambda = 220$ nm: $t_1 = 17.51$ min, $t_2 = 25.17$ min.

***trans*-2-Ethoxy-5-(4-fluorophenyl)tetrahydrofuran (*rac*-5-*epi*-5c)**



Purification: Pentane/ Et_2O 4:1. Colorless oil.

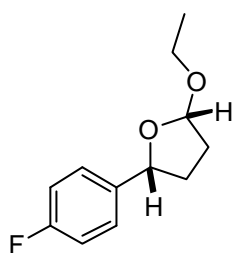
^1H NMR (500 MHz, C_6D_6) δ 7.06-7.03 (m, 2H), 6.84-6.80 (m, 2H), 5.17 (dd, $J = 5.2, 2.2$ Hz, 1H), 5.00 (t, $J = 7.2$ Hz, 1H), 3.86-3.80 (m, 1H), 3.40-3.33 (m, 1H), 2.10-2.05 (m, 1H), 1.85-1.78 (m, 2H), 1.37-1.31 (m, 1H), 1.15 (t, $J = 7.1$ Hz, 3H) ppm.

^{13}C NMR (125 MHz, C_6D_6) δ 162.5 (d, $J = 244.5$ Hz), 139.2 (d, $J = 2.9$ Hz), 127.7 (d, $J = 7.7$ Hz), 115.2 (d, $J = 21.2$ Hz), 104.5, 78.7, 63.1, 33.4, 32.7, 15.6 ppm.

HRMS (EI) m/z calculated for $\text{C}_{12}\text{H}_{15}\text{O}_2\text{F}$ 210.105606, found 210.105423.

HPLC analysis using Daicel Chiralcel OJ-H column: *n*-heptane/*i*-PrOH 95:5, flow rate 0.5 mL/min, $\lambda = 220$ nm: $t_1 = 18.69$ min, $t_2 = 23.85$ min.

$\alpha_D^{25} = +59.1^\circ$ ($c = 0.45$, CH_2Cl_2) for (2*S*,5*S*)-5c with er 99.5:0.5.

***cis*-2-Ethoxy-5-(4-fluorophenyl)tetrahydrofuran (*rac*-5c)**

Purification: Pentane/Et₂O 4:1. Colorless oil.

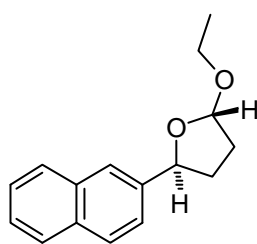
¹H NMR (500 MHz, C₆D₆) δ 7.23-7.20 (m, 2H), 6.88-6.84 (m, 2H), 5.04 (d, *J* = 5.0 Hz, 1H), 4.74 (dd, *J* = 9.1, 6.6 Hz, 1H), 3.86-3.79 (m, 1H), 3.35-3.29 (m, 1H), 1.93-1.76 (m, 3H), 1.65-1.59 (m, 1H), 1.12 (t, *J* = 7.1 Hz, 3H) ppm.

¹³C NMR (125 MHz, C₆D₆) δ 162.6 (d, *J* = 244.6 Hz), 140.2 (d, *J* = 2.7 Hz), 128.4 (d, *J* = 7.7 Hz), 115.3 (d, *J* = 21.2 Hz), 104.3, 82.0, 62.9, 34.1, 33.4, 24.5, 15.4 ppm.

HRMS (EI) *m/z* calculated for C₁₂H₁₅O₂F 210.105611, found 210.105474.

HPLC analysis using Daicel Chiralcel OJ-H column: *n*-heptane/*i*-PrOH 95:5, flow rate 0.5 mL/min, λ = 220 nm: *t*₁ = 12.50 min, *t*₂ = 13.49 min.

α_D^{25} = +137.1° (*c* = 0.75, CH₂Cl₂) for (2*S*,5*R*)-5c with er 97.5:2.5.

***trans*-2-Ethoxy-5-(naphthalen-2-yl)tetrahydrofuran (*rac*-5-*epi*-5d)**

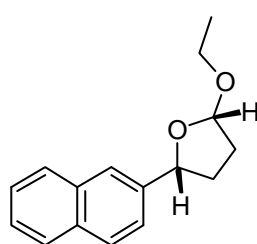
Purification: Pentane/Et₂O 4:1. Colorless oil.

¹H NMR (500 MHz, C₆D₆) δ 7.81 (s, 1H), 7.70-7.64 (m, 3H), 7.38 (dd, *J* = 8.5, 1.6 Hz, 1H), 7.29-7.24 (m, 2H), 5.30 (dd, *J* = 4.9, 2.3 Hz, 1H), 5.26 (t, *J* = 7.2 Hz, 1H), 3.94-3.88 (m, 1H), 3.46-3.39 (m, 1H), 2.28-2.21 (m, 1H), 1.95-1.85 (m, 2H), 1.60-1.53 (m, 1H), 1.19 (t, *J* = 7.1 Hz, 3H) ppm.

¹³C NMR (125 MHz, C₆D₆) δ 141.0, 133.9, 133.4, 128.4, 128.3, 128.1, 126.3, 125.9, 124.7, 124.5, 104.7, 79.5, 63.2, 33.3, 32.8, 15.6 ppm.

HRMS (ESI+) *m/z* calculated for C₁₆H₁₈O₂Na (M+Na⁺) 265.119896, found 265.119713.

HPLC analysis using Daicel Chiralcel AD-3 column: *n*-heptane/*i*-PrOH 99:1, flow rate 1.0 mL/min, λ = 220 nm: *t*₁ = 3.60 min, *t*₂ = 4.12 min.

***cis*-2-Ethoxy-5-(naphthalen-2-yl)tetrahydrofuran (*rac*-5d)**

Purification: Pentane/Et₂O 4:1. Colorless solid.

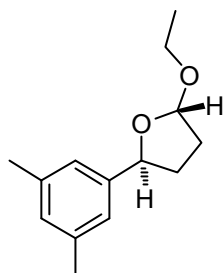
¹H NMR (500 MHz, C₆D₆) δ 7.80 (s, 1H), 7.71-7.70 (m, 2H), 7.66-7.63 (m, 2H), 7.31-7.25 (m, 2H), 5.14 (d, *J* = 5.0 Hz, 1H), 5.03 (dd, *J* = 9.6, 6.5 Hz, 1H), 4.01-3.95 (m, 1H), 3.43-3.37 (m, 1H), 2.10-2.04 (m, 1H), 2.02-1.98 (m, 1H), 1.95-1.89 (m, 1H), 1.74-1.67 (m, 1H), 1.20 (t, *J* = 7.1 Hz, 3H) ppm.

¹³C NMR (125 MHz, C₆D₆) δ 141.8, 133.9, 133.5, 128.6, 128.3, 128.1, 126.3, 125.9, 125.6, 125.1, 104.4, 83.0, 62.9, 34.3, 33.3, 15.5 ppm.

HRMS (ESI+) m/z calculated for $C_{16}H_{18}O_2Na$ ($M+Na^+$) 265.119901, found 265.119634.

HPLC analysis using Daicel Chiralcel AD-3 column: *n*-heptane/*i*-PrOH 99:1, flow rate 1.0 mL/min, $\lambda = 220$ nm: $t_1 = 6.79$ min, $t_2 = 7.46$ min.

***trans*-5-(3,5-Dimethylphenyl)-2-ethoxytetrahydrofuran (*rac*-5-*epi*-5e)**



Purification: Pentane/Et₂O 9:1. Colorless oil.

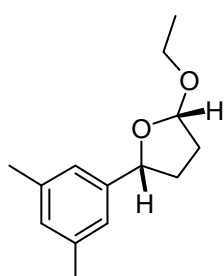
¹H NMR (500 MHz, C₆D₆) δ 7.03 (s, 2H), 6.77 (s, 1H), 5.27 (t, $J = 3.7$ Hz, 1H), 5.13 (t, $J = 7.2$ Hz, 1H), 3.93-3.86 (m, 1H), 3.44-3.38 (m, 1H), 2.24-2.19 (m, 1H), 2.17 (s, 6H), 1.93-1.89 (m, 2H), 1.60-1.53 (m, 1H), 1.17 (t, $J = 7.1$ Hz, 3H) ppm.

¹³C NMR (125 MHz, C₆D₆) δ 143.5, 137.7, 129.1, 124.0, 104.5, 79.5, 63.1, 33.6, 32.9, 21.4, 15.6 ppm.

HRMS (ESI+) m/z calculated for $C_{14}H_{20}O_2Na$ ($M+Na^+$) 243.135551, found 243.135330.

HPLC analysis using Daicel Chiralcel OJ-RH column: MeOH/H₂O 80:20, flow rate 1.0 mL/min, $\lambda = 220$ nm: $t_1 = 11.20$ min, $t_2 = 12.34$ min.

***cis*-5-(3,5-Dimethylphenyl)-2-ethoxytetrahydrofuran (*rac*-5e)**



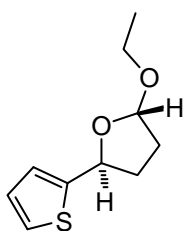
Purification: Pentane/Et₂O 9:1. Colorless oil.

¹H NMR (500 MHz, C₆D₆) δ 7.13 (s, 2H), 6.79 (s, 1H), 5.11 (d, $J = 5.0$ Hz, 1H), 4.91 (dd, $J = 9.5, 6.4$ Hz, 1H), 4.00-3.94 (m, 1H), 3.41-3.35 (m, 1H), 2.21 (s, 6H), 2.09-1.89 (m, 3H), 1.72-1.64 (m, 1H), 1.20 (t, $J = 7.1$ Hz, 3H) ppm.

¹³C NMR (125 MHz, C₆D₆) δ 144.5, 137.7, 129.1, 124.8, 104.3, 83.0, 62.7, 34.3, 33.5, 21.5, 15.5 ppm.

HRMS (ESI+) m/z calculated for $C_{14}H_{20}O_2Na$ ($M+Na^+$) 243.135548, found 243.135342.

HPLC analysis using Daicel Chiralcel OJ-RH column: MeOH/H₂O 80:20, flow rate 1.0 mL/min, $\lambda = 220$ nm: $t_1 = 5.68$ min, $t_2 = 9.96$ min.

***trans*-2-Ethoxy-5-(thiophen-2-yl)tetrahydrofuran (*rac*-5-*epi*-5f)**

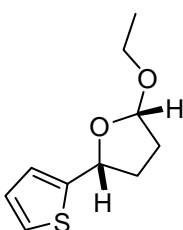
Purification: Pentane/Et₂O 15:1. Colorless oil.

¹H NMR (500 MHz, C₆D₆) δ 6.86 (dd, *J* = 5.0, 1.2 Hz, 1H), 6.77-6.76 (m, 1H), 6.72 (dd, *J* = 5.0, 3.5 Hz, 1H), 5.29 (t, *J* = 6.9 Hz, 1H), 5.14 (dd, *J* = 5.2, 2.0 Hz, 1H), 3.83-3.77 (m, 1H), 3.34-3.28 (m, 1H), 2.16-2.11 (m, 1H), 1.88-1.79 (m, 2H), 1.68-1.61 (m, 1H), 1.11 (t, *J* = 7.1 Hz, 3H) ppm.

¹³C NMR (125 MHz, C₆D₆) δ 147.3, 126.7, 124.5, 123.8, 104.3, 75.9, 63.2, 33.7, 32.7, 15.5 ppm.

HRMS (EI) *m/z* calculated for C₁₀H₁₄O₂S 198.071450, found 198.071412.

HPLC analysis using Daicel Chiralcel OJ-H column: *n*-heptane/*i*-PrOH 50:50, flow rate 0.5 mL/min, λ = 220 nm: *t*₁ = 15.58 min, *t*₂ = 21.64 min.

***cis*-2-Ethoxy-5-(thiophen-2-yl)tetrahydrofuran (*rac*-5f)**

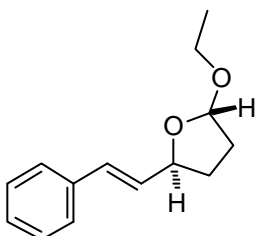
Purification: Pentane/Et₂O 15:1. Colorless oil.

¹H NMR (500 MHz, C₆D₆) δ 6.91 (dd, *J* = 5.1, 1.1 Hz, 1H), 6.84-6.83 (m, 1H), 6.73 (dd, *J* = 5.1, 3.5 Hz, 1H), 5.07 (dd, *J* = 9.3, 6.6 Hz, 1H), 5.01 (d, *J* = 4.9 Hz, 1H), 3.96-3.90 (m, 1H), 3.34-3.28 (m, 1H), 2.17-2.10 (m, 1H), 1.95-1.91 (m, 1H), 1.89-1.83 (m, 1H), 1.61-1.53 (m, 1H), 1.16 (t, *J* = 7.1 Hz, 3H) ppm.

¹³C NMR (125 MHz, C₆D₆) δ 148.7, 126.6, 125.0, 124.4, 104.0, 78.0, 62.8, 34.2, 33.6, 15.4 ppm.

HRMS (EI) *m/z* calculated for C₁₀H₁₄O₂S 198.071450, found 198.071343.

HPLC analysis using Daicel Chiralcel OJ-H column: *n*-heptane/*i*-PrOH 50:50, flow rate 0.5 mL/min, λ = 220 nm: *t*₁ = 12.43 min, *t*₂ = 18.87 min.

***trans*-2-Ethoxy-5-((*E*)-styryl)tetrahydrofuran (*rac*-5-*epi*-5g)**

Purification: Pentane/Et₂O 6:1. Colorless oil.

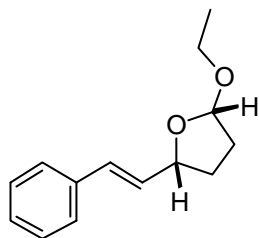
¹H NMR (500 MHz, C₆D₆) δ 7.25 (d, *J* = 7.3 Hz, 2H), 7.11 (dd, *J* = 7.3, 7.3 Hz, 2H), 7.04 (t, *J* = 7.3 Hz, 1H), 6.60 (d, *J* = 15.8 Hz, 1H), 6.16 (d, *J* = 15.8, 6.4 Hz, 1H), 5.16 (dd, *J* = 5.1, 2.1 Hz, 1H), 4.71-4.67 (m, 1H), 3.91-3.85 (m, 1H), 3.41-3.35 (m, 1H), 2.04-1.98 (m, 1H), 1.89-1.81 (m, 2H), 1.43-1.36 (m, 1H), 1.16 (t, *J* = 7.1 Hz, 3H) ppm.

¹³C NMR (125 MHz, C₆D₆) δ 137.5, 130.8, 130.4, 128.8, 127.7, 126.9, 104.4, 78.5, 63.0, 32.7, 31.0, 15.6 ppm.

HRMS (ESI+) *m/z* calculated for C₁₄H₁₈O₂Na (M+Na⁺) 241.119900, found 241.119709.

HPLC analysis using Daicel Chiralcel OJ-H column: *n*-heptane/*i*-PrOH 95:5, flow rate 0.5 mL/min, $\lambda = 220$ nm: $t_1 = 18.93$ min, $t_2 = 21.46$ min.

***cis*-2-Ethoxy-5-((*E*)-styryl)tetrahydrofuran (*rac*-5g)**



Purification: Pentane/Et₂O 6:1. Colorless oil.

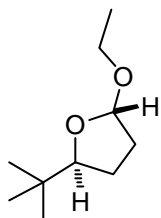
¹H NMR (500 MHz, C₆D₆) δ 7.27 (d, $J = 7.3$ Hz, 2H), 7.11 (dd, $J = 7.3, 7.3$ Hz, 2H), 7.04 (t, $J = 7.3$ Hz, 1H), 6.53 (d, $J = 15.9$ Hz, 1H), 6.35 (d, $J = 15.8, 7.4$ Hz, 1H), 5.07 (d, $J = 4.9$ Hz, 1H), 4.54-4.50 (m, 1H), 3.92-3.86 (m, 1H), 3.39-3.33 (m, 1H), 1.96-1.93 (m, 1H), 1.91-1.83 (m, 1H), 1.77-1.71 (m, 1H), 1.66-1.61 (m, 1H), 1.15 (t, $J = 7.1$ Hz, 3H) ppm.

¹³C NMR (125 MHz, C₆D₆) δ 137.5, 132.9, 130.8, 128.8, 127.7, 126.9, 104.1, 81.3, 62.7, 33.8, 30.7, 15.6 ppm.

HRMS (ESI+) m/z calculated for C₁₄H₁₈O₂Na (M+Na⁺) 241.119900, found 241.120167.

HPLC analysis using Daicel Chiralcel OJ-H column: *n*-heptane/*i*-PrOH 95:5, flow rate 0.5 mL/min, $\lambda = 220$ nm: $t_1 = 11.25$ min, $t_2 = 13.75$ min.

***trans*-5-(*tert*-Butyl)-2-ethoxytetrahydrofuran (*rac*-5-*epi*-5h)**



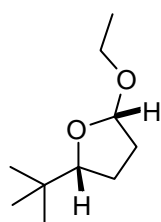
Purification: Pentane/Et₂O 15:1. Colorless oil.

¹H NMR (500 MHz, C₆D₆) δ 5.06 (dd, $J = 4.9, 1.6$ Hz, 1H), 3.82-3.76 (m, 2H), 3.38-3.33 (m, 1H), 1.86-1.82 (m, 1H), 1.73-1.67 (m, 2H), 1.34-1.32 (m, 1H), 1.15 (t, $J = 7.1$ Hz, 3H), 0.91 (s, 9H) ppm.

¹³C NMR (125 MHz, C₆D₆) δ 104.1, 85.5, 62.6, 33.5, 33.0, 25.9, 24.7, 15.7 ppm.

HRMS (CI) m/z calculated for C₁₀H₂₁O₂ (M+H) 173.1542, found 173.1540.

GC analysis using BGB-176 column (30 m, 2,3-dimethyl-6-*tert*-butyldimethylsilyl- β -cyclodextrin), Detector: FID; Temperature: injector 220 °C, detector 350 °C, oven: 60 °C, 1 °C/min until 85 °C, 8 °C/min until 220 °C; gas: 0.4 bar H₂. $t_1 = 13.89$ min, $t_2 = 15.86$ min.

***cis*-5-(*tert*-Butyl)-2-ethoxytetrahydrofuran (*rac*-5h)**

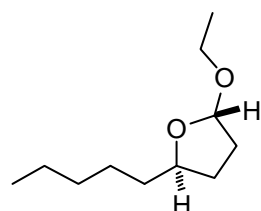
Purification: Pentane/Et₂O 15:1. Colorless oil.

¹H NMR (500 MHz, C₆D₆) δ 4.95 (d, *J* = 5.0 Hz, 1H), 3.83-3.78 (m, 1H), 3.60 (dd, *J* = 10.6, 5.8 Hz, 1H), 3.30-3.24 (m, 1H), 1.88 (dd, *J* = 12.1, 7.0 Hz, 1H), 1.74-1.67 (m, 1H), 1.62-1.57 (m, 1H), 1.38-1.33 (m, 1H), 1.12 (t, *J* = 7.1 Hz, 3H), 0.96 (s, 9H) ppm.

¹³C NMR (125 MHz, C₆D₆) δ 103.4, 89.3, 62.3, 33.9, 33.6, 26.2, 24.7, 15.4 ppm.

HRMS (CI) *m/z* calculated for C₁₀H₂₁O₂ (M+H) 173.154153, found 173.153985.

GC analysis using BGB-176 column (30 m, 2,3-dimethyl-6-*tert*-butyldimethylsilyl-β-cyclodextrin), Detector: FID; Temperature: injector 220 °C, detector 350 °C, oven: 60 °C, 1 °C/min until 85 °C, 8 °C/min until 220 °C; gas: 0.4 bar H₂. *t*₁ = 14.39 min, *t*₂ = 16.69 min.

***trans*-2-Ethoxy-5-pentyltetrahydrofuran (*rac*-5-*epi*-5i)**

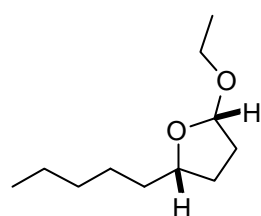
Purification: Pentane/Et₂O 20:1. Colorless oil.

¹H NMR (500 MHz, C₆D₆) δ 5.10 (dd, *J* = 5.1, 1.5 Hz, 1H), 4.11-4.06 (m, 1H), 3.87-3.81 (m, 1H), 3.39-3.33 (m, 1H), 1.93-1.77 (m, 3H), 1.63-1.57 (m, 1H), 1.47-1.17 (m, 8H), 1.15 (t, *J* = 7.1 Hz, 3H), 0.87 (t, *J* = 7.0 Hz, 3H) ppm.

¹³C NMR (125 MHz, C₆D₆) δ 104.0, 77.9, 62.8, 36.1, 32.7, 32.3, 30.0, 26.3, 23.1, 15.6, 14.3 ppm.

HRMS (CI) *m/z* calculated for C₁₁H₂₃O₂ (M+H) 187.169801, found 187.169618.

GC analysis using BGB-176/SE column (30 m, 2,3-dimethyl-6-*tert*-butyldimethylsilyl-β-cyclodextrin), Detector: FID; Temperature: injector 220 °C, detector 320 °C, oven: 90 °C; gas: 0.4 bar H₂. *t*₁ = 25.85 min, *t*₂ = 27.73 min.

***cis*-2-Ethoxy-5-pentyltetrahydrofuran (*rac*-5i)**

Purification: Pentane/Et₂O 20:1. Colorless oil.

¹H NMR (500 MHz, C₆D₆) δ 5.02 (d, *J* = 4.3, 1H), 3.97-3.91 (m, 1H), 3.87-3.81 (m, 1H), 3.36-3.30 (m, 1H), 1.94-1.91 (m, 1H), 1.76-1.70 (m, 1H), 1.67-1.62 (m, 3H), 1.51-1.44 (m, 2H), 1.38-1.23 (m, 5H), 1.14 (t, *J* = 7.1 Hz, 3H), 0.89 (t, *J* = 6.9 Hz, 3H) ppm.

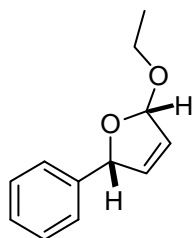
¹³C NMR (125 MHz, C₆D₆) δ 103.7, 80.6, 62.3, 38.2, 33.7, 32.3, 29.8, 26.6, 23.1, 15.6, 14.3 ppm.

HRMS (CI) *m/z* calculated for C₁₁H₂₃O₂ (M+H) 187.169803, found 187.169651.

7. EXPERIMENTAL SECTION

GC analysis using BGB-176/SE column (30 m, 2,3-dimethyl-6-*tert*-butyldimethylsilyl- β -cyclodextrin), Detector: FID; Temperature: injector 220 °C, detector 320 °C, oven: 90 °C; gas: 0.4 bar H₂. $t_1 = 26.53$ min, $t_2 = 27.13$ min.

cis-2-Ethoxy-5-phenyl-2,5-dihydrofuran (*rac*-5j)



Prepared with 1 mol% of diphenyl phosphate. Purification: Pentane/Et₂O 20:1.
Colorless solid.

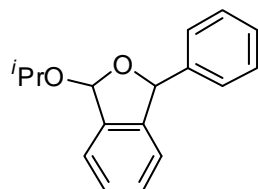
¹H NMR (500 MHz, C₆D₆) δ 7.41 (d, $J = 7.1$ Hz, 2H), 7.18 (dd, $J = 7.4, 7.1$ Hz, 2H), 7.07 (d, $J = 7.4$ Hz, 1H), 5.81 (m, 1H), 5.73-5.71 (m, 1H), 5.62-5.60 (m, 1H), 5.57 (br, 1H), 3.89-3.82 (m, 1H), 3.46-3.40 (m, 1H), 1.13 (t, $J = 7.1$ Hz, 3H) ppm.

¹³C NMR (125 MHz, C₆D₆) δ 141.6, 135.4, 128.6, 128.0, 127.4, 126.3, 109.2, 88.1, 63.9, 15.7 ppm.

HRMS (ESI+) m/z calculated for C₁₂H₁₄O₂Na (M+Na⁺) 213.088601, found 213.088364.

HPLC analysis using Daicel Chiralcel OJ-H column: *n*-heptane/*i*-PrOH 98:2, flow rate 0.5 mL/min, $\lambda = 220$ nm: $t_1 = 19.43$ min, $t_2 = 22.95$ min.

1-Isopropoxy-3-phenyl-1,3-dihydroisobenzofuran (*rac*-5k)



cis-5k/*trans*-5k
dr = 2.59:1

Purification: 10% EtOAc/hexane. Diastereomers were not separated.

Colorless oil, 47.9 mg, 94%. Diastereomeric ratio *cis/trans* 2.59:1 by ¹H NMR. Relative configuration determined from NOESY spectra.

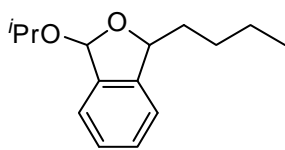
¹H NMR (500 MHz, C₆D₆) δ 7.46-7.45 (m, 2H_{maj}), 7.30 (d, $J = 7.5$ Hz, 1H_{maj} + 1H_{min}), 7.24-7.22 (m, 2H_{min}), 7.15-7.12 (m, 2H_{maj} + 2H_{min}), 7.09-7.03 (m, 2H_{maj} + 2H_{min}), 7.00-6.97 (m, 1H_{maj} + 1H_{min}), 6.83-6.78 (m, 1H_{maj} + 1H_{min}),

6.49 (d, $J = 1.9$ Hz, 1H_{min}), 6.38 (s, 1H_{maj}), 6.27 (s, 1H_{min}), 6.05 (s, 1H_{maj}), 4.10 (sept, $J = 6.2$ Hz, 1H_{maj} + 1H_{min}), 1.31 (d, $J = 6.2$ Hz, 3H_{min}), 1.26 (d, $J = 6.2$ Hz, 3H_{maj}), 1.20 (d, $J = 6.2$ Hz, 3H_{min}), 1.17 (d, $J = 6.2$ Hz, 3H_{maj}) ppm.

¹³C NMR (125 MHz, C₆D₆) δ 144.2, 143.8, 143.1, 142.0, 139.5, 138.8, 129.3, 129.2, 128.7, 128.6, 127.6, 123.4, 123.2, 122.5, 122.4, 105.8, 105.6, 86.3, 84.9, 71.1, 70.6, 24.1, 24.0, 22.6, 22.5 ppm.

HRMS (ESI+) m/z calculated for C₁₇H₁₈O₂Na (M+Na⁺) 277.1199, found 277.1196.

HPLC analysis using Daicel Chiralcel OJ-H column: *n*-heptane/*i*-PrOH 60:40, flow rate 0.5 mL/min, $\lambda = 210$ nm: $t_{1(cis)} = 10.05$ min, $t_{1(trans)} = 12.89$ min, $t_{2(cis)} = 12.12$ min, $t_{2(trans)} = 20.05$ min.

1-Butyl-3-isopropoxy-1,3-dihydroisobenzofuran (*rac*-5I)

cis-5I/*trans*-5I
dr = 1:1.14

Purification: 5% EtOAc/hexane. Diastereomers were not separated.

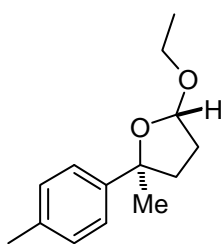
Colorless oil, 44.9 mg, 92%. Diastereomeric ratio *cis/trans* 1:1.14 by ^1H NMR. Relative configuration determined from NOESY spectra.

^1H NMR (500 MHz, C_6D_6) δ 7.29-7.26 (m, $1\text{H}_{\text{maj}} + 1\text{H}_{\text{min}}$), 7.13-7.07 (m, $2\text{H}_{\text{maj}} + 2\text{H}_{\text{min}}$), 6.93-6.89 (m, $1\text{H}_{\text{maj}} + 1\text{H}_{\text{min}}$), 6.33 (s, 1H_{maj}), 6.26 (s, 1H_{min}), 5.34 (t, $J = 3.4$ Hz, 1H_{maj}), 5.10 (dd, $J = 7.4, 4.8$ Hz, 1H_{min}), 4.07 (sept, $J = 6.2$ Hz, $1\text{H}_{\text{maj}} + 1\text{H}_{\text{min}}$), 1.83-1.71 (m, 3H), 1.63-1.52 (m, 3H), 1.50-1.40 (m, 2H), 1.36-1.23 (m, 10H), 1.17 (t, $J = 5.7$ Hz, 6H), 0.89-0.84 (m, 6H) ppm.

^{13}C NMR (125 MHz, C_6D_6) δ 144.1, 144.0, 140.0, 128.9, 128.8, 127.68, 127.66, 123.5, 123.4, 121.4, 121.1, 105.2, 104.9, 83.7, 82.4, 70.4, 70.1, 38.0, 35.8, 28.3, 27.7, 24.2, 24.1, 23.2, 23.1, 22.64, 22.59, 14.3 ppm.

HRMS (ESI+) m/z calculated for $\text{C}_{15}\text{H}_{22}\text{O}_2\text{Na}$ ($\text{M}+\text{Na}^+$) 257.1512, found 257.1511.

HPLC analysis using Daicel Chiralcel AD-3 column: *n*-heptane/*i*-PrOH 99.9:0.1, flow rate 1.0 mL/min, $\lambda = 210$ nm: $t_{1(\text{trans})} = 3.11$ min, $t_{2(\text{trans})} = 3.72$ min, $t_{1(\text{cis})} = 5.60$ min, $t_{2(\text{cis})} = 6.55$ min. *cis*-Diastereomer is the major product in the asymmetric reaction, opposite to the racemic reaction.

***trans*-2-Ethoxy-5-methyl-5-(*p*-tolyl)tetrahydrofuran (*rac*-5-*epi*-5m)**

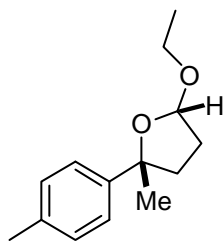
Purification: Pentane/ Et_2O 20:1. Colorless oil.

^1H NMR (500 MHz, C_6D_6) δ 7.34 (d, $J = 8.2$ Hz, 2H), 7.05 (d, $J = 7.9$ Hz, 2H), 5.16 (d, $J = 5.2$ Hz, 1H), 3.95-3.89 (m, 1H), 3.44-3.38 (m, 1H), 2.20-2.14 (m, 1H), 2.16 (s, 3H), 1.95-1.86 (m, 2H), 1.73-1.66 (m, 1H), 1.67 (s, 3H), 1.18 (t, $J = 7.1$ Hz, 3H) ppm.

^{13}C NMR (125 MHz, C_6D_6) δ 146.2, 135.8, 129.0, 125.1, 104.4, 85.7, 62.7, 38.6, 32.9, 31.6, 21.0, 15.6 ppm.

HRMS (ESI+) m/z calculated for $\text{C}_{14}\text{H}_{20}\text{O}_2\text{Na}$ ($\text{M}+\text{Na}^+$) 243.135547, found 243.135715.

HPLC analysis using Daicel Chiralcel OJ-H column: *n*-heptane/*i*-PrOH 90:10, flow rate 0.5 mL/min, $\lambda = 220$ nm: $t_1 = 16.35$ min, $t_2 = 29.00$ min.

***cis*-2-Ethoxy-5-methyl-5-(*p*-tolyl)tetrahydrofuran (*rac*-5m)**

Purification: Pentane/Et₂O 20:1. Colorless oil.

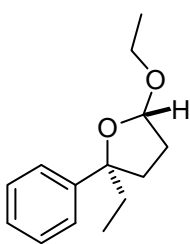
¹H NMR (500 MHz, C₆D₆) δ 7.45 (d, *J* = 8.2 Hz, 2H), 7.07 (d, *J* = 7.9 Hz, 2H), 5.15 (dd, *J* = 4.8; 1:5 Hz, 1H), 3.94-3.88 (m, 1H), 3.40-3.34 (m, 1H), 2.31-2.22 (m, 1H), 2.16 (s, 3H), 1.93-1.88 (m, 1H), 1.87-1.81 (m, 1H), 1.80-1.75 (m, 1H), 1.42 (s, 3H), 1.08 (t, *J* = 7.1 Hz, 3H) ppm.

¹³C NMR (125 MHz, C₆D₆) δ 146.9, 135.7, 128.9, 125.3, 104.5, 85.7, 62.9, 37.7, 33.1, 30.7, 21.0, 15.4 ppm.

HRMS (ESI+) *m/z* calculated for C₁₄H₂₀O₂Na (M+Na⁺) 243.135546, found 243.135668.

HPLC analysis using Daicel Chiralcel OJ-H column: *n*-heptane/*i*-PrOH 90:10, flow rate 0.5 mL/min, λ = 220 nm: *t*₁ = 7.39 min, *t*₂ = 9.95 min.

α_D²⁵ = +102.8 ° (c = 0.876 in CH₂Cl₂, er 98.5:1.5).

***trans*-2-Ethoxy-5-ethyl-5-phenyltetrahydrofuran (*rac*-5-*epi*-5n)**

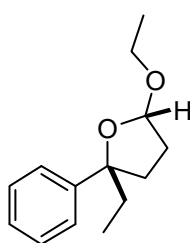
Purification: Pentane/Et₂O 20:1. Colorless oil.

¹H NMR (500 MHz, C₆D₆) δ 7.37 (dd, *J* = 8.1, 1.0 Hz, 2H), 7.21 (dd, *J* = 8.1, 7.4 Hz, 2H), 7.10 (t, *J* = 7.4 Hz, 1H), 5.12 (d, *J* = 5.1 Hz, 1H), 3.93-3.87 (m, 1H), 3.42-3.36 (m, 1H), 2.21-2.15 (m, 1H), 1.99-1.90 (m, 2H), 1.89-1.81 (m, 2H), 1.64-1.57 (m, 1H), 1.17 (t, *J* = 7.1 Hz, 3H), 0.90 (t, *J* = 7.4 Hz, 3H) ppm.

¹³C NMR (125 MHz, C₆D₆) δ 147.3, 128.2, 126.5, 125.7, 104.1, 88.7, 62.7, 37.0, 36.6, 32.4, 15.6, 9.2 ppm.

HRMS (ESI+) *m/z* calculated for C₁₄H₂₀O₂Na (M+Na⁺) 243.135553, found 243.135812.

HPLC analysis using Daicel Chiralcel OJ-H column: *n*-heptane/*i*-PrOH 90:10, flow rate 0.5 mL/min, λ = 220 nm: *t*₁ = 21.42 min, *t*₂ = 26.68 min.

***cis*-2-Ethoxy-5-ethyl-5-phenyltetrahydrofuran (*rac*-5n)**

Purification: Pentane/Et₂O 20:1. Colorless oil.

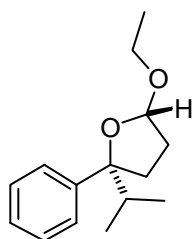
¹H NMR (500 MHz, C₆D₆) δ 7.45 (dd, *J* = 8.3, 1.1 Hz, 2H), 7.23 (dd, *J* = 8.3, 7.4 Hz, 2H), 7.11 (t, *J* = 7.4 Hz, 1H), 5.13-5.12 (m, 1H), 3.91-3.85 (m, 1H), 3.40-3.33 (m, 1H), 2.27-2.21 (m, 1H), 1.90-1.75 (m, 3H), 1.69-1.61 (m, 2H), 1.03 (t, *J* = 7.1 Hz, 3H), 0.82 (t, *J* = 7.4 Hz, 3H) ppm.

^{13}C NMR (125 MHz, C_6D_6) δ 148.3, 128.0, 126.4, 125.8, 104.5, 88.4, 63.0, 36.5, 36.2, 33.1, 15.4, 8.9 ppm.

HRMS (ESI+) m/z calculated for $\text{C}_{14}\text{H}_{20}\text{O}_2\text{Na}$ ($\text{M}+\text{Na}^+$) 243.135546, found 243.135714.

HPLC analysis using Daicel Chiralcel OJ-H column: *n*-heptane/*i*-PrOH 90:10, flow rate 0.5 mL/min, $\lambda = 220$ nm: $t_1 = 8.29$ min, $t_2 = 9.57$ min.

***trans*-2-Ethoxy-5-isopropyl-5-phenyltetrahydrofuran (*rac*-5-*epi*-5o)**



Purification: Pentane/ Et_2O 50:1. Colorless oil.

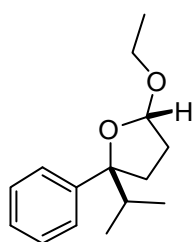
^1H NMR (500 MHz, C_6D_6) δ 7.38 (dd, $J = 8.3, 1.1$ Hz, 2H), 7.20 (dd, $J = 8.3, 7.4$ Hz, 2H), 7.10 (t, $J = 7.4$ Hz, 1H), 5.04 (d, $J = 5.1$ Hz, 1H), 3.93-3.87 (m, 1H), 3.39-3.33 (m, 1H), 2.28-2.22 (m, 1H), 2.11-2.05 (m, 1H), 1.88 (ddd, $J = 11.9, 7.6, 1.5$ Hz, 1H), 1.79 (dd, $J = 12.4, 7.1$ Hz, 1H), 1.55-1.48 (m, 1H), 1.17 (t, $J = 7.1$ Hz, 3H), 1.02 (d, $J = 6.7$ Hz, 3H), 0.87 (d, $J = 6.7$ Hz, 3H) ppm.

^{13}C NMR (125 MHz, C_6D_6) δ 145.7, 127.8, 126.6, 126.6, 103.5, 91.4, 62.7, 38.6, 33.8, 32.6, 18.8, 17.9, 15.5 ppm.

HRMS (ESI+) m/z calculated for $\text{C}_{15}\text{H}_{22}\text{O}_2\text{Na}$ ($\text{M}+\text{Na}^+$) 257.151196, found 257.151410.

HPLC analysis using Daicel Chiralcel OJ-H column: *n*-heptane/*i*-PrOH 95:5, flow rate 0.5 mL/min, $\lambda = 220$ nm: $t_1 = 12.57$ min, $t_2 = 48.83$ min.

***cis*-2-Ethoxy-5-isopropyl-5-phenyltetrahydrofuran (*rac*-5o)**



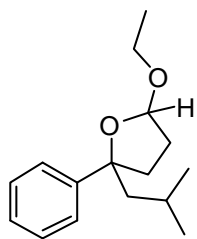
Purification: Pentane/ Et_2O 50:1. Colorless oil.

^1H NMR (500 MHz, C_6D_6) δ 7.41 (dd, $J = 8.2, 1.1$ Hz, 2H), 7.22 (dd, $J = 8.2, 7.4$ Hz, 2H), 7.11 (t, $J = 7.4$ Hz, 1H), 5.12 (dd, $J = 5.0, 2.0$ Hz, 1H), 3.85-3.79 (m, 1H), 3.36-3.30 (m, 1H), 2.27-2.21 (m, 1H), 1.96-1.91 (m, 1H), 1.86-1.73 (m, 3H), 0.97 (t, $J = 7.1$ Hz, 3H), 0.87 (d, $J = 6.7$ Hz, 3H), 0.80 (d, $J = 6.9$ Hz, 3H) ppm.

^{13}C NMR (125 MHz, C_6D_6) δ 147.5, 127.5, 126.6, 126.4, 104.7, 90.6, 62.9, 39.2, 33.8, 33.5, 18.4, 17.6, 15.3 ppm.

HRMS (ESI+) m/z calculated for $\text{C}_{15}\text{H}_{22}\text{O}_2\text{Na}$ ($\text{M}+\text{Na}^+$) 257.151198, found 257.151435.

HPLC analysis using Daicel Chiralcel OJ-H column: *n*-heptane/*i*-PrOH 95:5, flow rate 0.5 mL/min, $\lambda = 220$ nm: $t_1 = 7.33$ min, $t_2 = 8.47$ min.

5-Ethoxy-2-isobutyl-2-phenyltetrahydrofuran (*rac*-5p)

cis-5p/*trans*-5p
dr = 3.3:1

Purification: 2% EtOAc/hexane. Diastereomers were not separated. Colorless oil, 44.4 mg, 89%. Diastereomeric ratio *cis/trans* 3.3:1 by ^1H NMR.

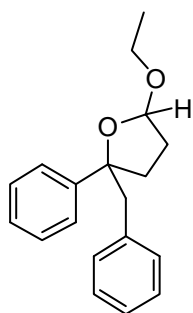
^1H NMR (500 MHz, C_6D_6) δ 7.47-7.45 (m, 2H_{maj}), 7.35-7.33 (m, 2H_{min}), 7.25-7.19 (m, 2H_{maj} + 2H_{min}), 7.11-7.07 (m, 1H_{maj} + 1H_{min}), 5.13-5.12 (m, 1H_{maj} + 1H_{min}), 3.96-3.87 (m, 1H_{maj} + 1H_{min}), 3.42-3.35 (m, 1H_{maj} + 1H_{min}), 2.25-2.16 (m, 1H_{maj} + 1H_{min}), 1.95 (dd, $J = 14.0, 4.6$ Hz, 1H_{min}), 1.88 (ddd, $J = 11.8, 7.8, 1.9$ Hz, 1H_{min}), 1.85-1.76 (m, 3H_{maj} + 2H_{min}), 1.69-1.51 (m, 3H_{maj} + 2H_{min}), 1.19 (t, $J =$

7.1 Hz, 3H_{min}), 1.07 (t, $J = 7.1$ Hz, 3H_{maj}, overlapped), 1.07 (d, $J = 6.6$ Hz, 3H_{min}, overlapped), 1.01 (d, $J = 6.4$ Hz, 3H_{maj}), 0.75 (d, $J = 6.7$ Hz, 3H_{min}), 0.73 (d, $J = 6.3$ Hz, 3H_{maj}) ppm.

^{13}C NMR (125 MHz, C_6D_6) δ (major *cis* diastereomer) 148.5, 126.4, 125.8, 104.9, 88.5, 63.3, 52.3, 38.4, 32.7, 24.9, 24.7, 24.4, 15.4 ppm; δ (minor *trans* diastereomer) 147.5, 126.5, 125.7, 104.4, 88.8, 62.7, 52.5, 39.3, 31.8, 25.3, 24.7, 23.9, 15.6 ppm.

HRMS (ESI+) m/z calculated for $\text{C}_{16}\text{H}_{24}\text{O}_2\text{Na}$ ($\text{M}+\text{Na}^+$) 271.1668, found 271.1664.

GC analysis using Astek G-DA column (30 m, dialkyl- γ -cyclodextrin, i.D. 0.25 mm), Detector: FID; Temperature: injector 220 °C, detector 320 °C, oven: 130 °C; gas: 0.5 bar H_2 . $t_{1(\text{cis})} = 37.36$ min, $t_{2(\text{cis})} = 38.38$ min, $t_{1(\text{trans})} = 40.37$ min, $t_{2(\text{trans})} = 42.03$ min.

5-Benzyl-2-ethoxy-5-phenyltetrahydrofuran (*rac*-5q)

cis-5q/*trans*-5q
dr = 3.57:1

Purification: Pentane/ Et_2O 15:1. Colorless oil. Diastereoisomers were not separated (diastereomeric ratio 3.57:1 by ^1H NMR).

^1H NMR (500 MHz, C_6D_6) δ 7.38 (dd, $J = 8.2, 1.1$ Hz, 2H_{maj}), 7.22-7.17 (m, 2H_{maj} + 2H_{min}), 7.13-7.01 (m, 6H_{maj} + 8H_{min}), 5.07-5.05 (m, 1H_{maj} + 1H_{min}), 3.98-3.92 (m, 1H_{min}), 3.83-3.77 (m, 1H_{maj}), 3.41-3.36 (m, 1H_{min}), 3.34-3.28 (m, 1H_{maj}), 3.18 (d, $J = 13.6$ Hz, 1H_{min}), 3.16 (d, $J = 13.6$ Hz, 1H_{min}), 2.97 (d, $J = 13.4$ Hz, 1H_{maj}), 2.81 (d, $J = 13.4$ Hz, 1H_{maj}), 2.29-2.23 (m, 1H_{maj} + 1H_{min}), 2.04-1.99 (m,

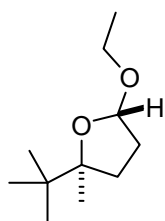
1H_{maj}), 1.94-1.90 (m, 1H_{min}), 1.83-1.78 (m, 1H_{min}), 1.73-1.69 (m, 1H_{maj}), 1.60-1.53 (m, 1H_{min}), 1.33-1.28 (m, 1H_{maj}), 1.16 (t, $J = 7.1$ Hz, 3H_{min}), 0.97 (t, $J = 7.1$ Hz, 3H_{maj}) ppm.

^{13}C NMR (125 MHz, C_6D_6) δ 149.0, 146.6, 138.1, 138.0, 131.1, 131.0, 128.3, 128.0, 127.9, 127.8, 126.7, 126.6, 126.5, 126.4, 126.1, 125.8, 104.7, 104.2, 88.7, 88.4, 63.1, 62.9, 50.4, 50.0, 36.5, 35.0, 33.0, 32.2, 15.5, 15.3 ppm.

HRMS (ESI+) m/z calculated for $\text{C}_{19}\text{H}_{22}\text{O}_2\text{Na}$ ($\text{M}+\text{Na}^+$) 305.151203, found 305.150760.

HPLC analysis. The diastereoisomers were separated on a Zorbax Eclipse Plus C18 column (50 mm, 1.8 μm particle size): MeOH/H₂O 70:30, flow rate 1.0 mL/min, $\lambda = 220$ nm: $t_{\text{maj}} = 9.69$ min, $t_{\text{min}} = 10.09$ min. The enantiomeric ratio of the major diastereoisomer was determined by using a column-switching technique, switching to a Kromasil AmyCoat RP column (150 mm) while the separated diastereoisomer is being eluted: MeCN/H₂O 65:35, flow rate 1.0 mL/min, $\lambda = 220$ nm: $t_1 = 13.48$ min, $t_2 = 14.23$ min.

***trans*-2-(*tert*-Butyl)-5-ethoxy-2-methyltetrahydrofuran (*rac*-5-*epi*-5r)**



Purification: Hexane/EtOAc 50:1. Colorless oil.

¹H NMR (500 MHz, C₆D₆) δ 5.03 (d, $J = 5.2$ Hz, 1H), 3.85-3.79 (m, 1H), 3.34-3.28 (m, 1H), 1.97-1.92 (m, 1H), 1.79-1.66 (m, 2H), 1.61-1.56 (m, 1H), 1.37 (s, 3H), 1.14 (t, $J = 7.0$ Hz, 3H), 0.93 (s, 9H) ppm.

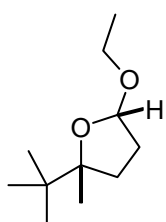
rac-5-*epi*-5r

¹³C NMR (125 MHz, C₆D₆) δ 104.7, 89.0, 62.2, 37.6, 34.3, 31.9, 25.7, 25.1, 15.6 ppm.

HRMS (CI (FE) *i*-butane) m/z calculated for C₁₁H₂₃O₂ (M+H⁺) 187.1698, found 187.1696.

GC analysis using BGB-176 column SE/SE52 (30 m, 2,3-dimethyl-6-*tert*-butyldimethylsilyl- β -cyclodextrin, i.D. 0.25 mm, df. 0.25 μm), Detector: FID; Temperature: injector 220 $^{\circ}\text{C}$, detector 350 $^{\circ}\text{C}$, oven: 105 $^{\circ}\text{C}$; gas: 0.5 bar H₂. $t_1 = 8.41$ min, $t_2 = 8.76$ min.

***cis*-2-(*tert*-Butyl)-5-ethoxy-2-methyltetrahydrofuran (*rac*-5r)**



Purification: Hexane/EtOAc 50:1. Colorless oil.

¹H NMR (500 MHz, C₆D₆) δ 4.96 (d, $J = 5.1$ Hz, 1H), 3.83-3.76 (m, 1H), 3.28-3.22 (m, 1H), 2.08-2.02 (m, 1H), 1.87-1.80 (m, 2H), 1.16-1.10 (m, 1H, overlapped), 1.12 (t, $J = 7.1$ Hz, 3H, overlapped), 1.05 (s, 3H), 1.03 (s, 9H) ppm.

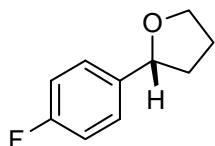
¹³C NMR (125 MHz, C₆D₆) δ 103.7, 90.0, 62.4, 36.8, 32.9, 30.3, 26.3, 22.6, 15.3 ppm.

HRMS (CI (FE) *i*-butane) m/z calculated for C₁₁H₂₃O₂ (M+H⁺) 187.1698, found 187.1697.

GC analysis using BGB-176 column SE/SE52 (30 m, 2,3-dimethyl-6-*tert*-butyldimethylsilyl- β -cyclodextrin, i.D. 0.25 mm, df. 0.25 μm), Detector: FID; Temperature: injector 220 $^{\circ}\text{C}$, detector 350 $^{\circ}\text{C}$, oven: 105 $^{\circ}\text{C}$; gas: 0.5 bar H₂. $t_1 = 9.26$ min, $t_2 = 10.64$ min.

7.3.4. Transformations of 5c, determination of absolute configurations, and natural product syntheses

(R)-2-(4-Fluorophenyl)tetrahydrofuran (6)



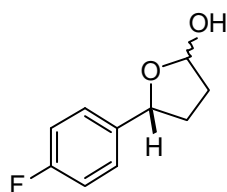
$\text{BF}_3 \cdot \text{OEt}_2$ (38 μL , 0.30 mmol) was added dropwise to the solution of *cis*-2-ethoxy-5-(4-fluorophenyl)tetrahydrofuran (**5c**, 21.0 mg, 0.1 mmol, er 97.5:2.5) and Et_3SiH (162 μL , 116 mg, 1.0 mmol,) in dry CH_2Cl_2 (1 mL) at -30°C under argon atmosphere. The mixture was allowed to warm to -10°C during 1.5 hours. Then saturated aqueous sodium bicarbonate solution (1 ml) was added and mixture extracted with diethyl ether (10 mL), dried (MgSO_4) and filtered. Product was purified by silica gel chromatography with 10% Et_2O /pentane as the eluent. Colorless oil, (15.3 mg, 92%).

$^1\text{H NMR}$ (500 MHz, CDCl_3) δ 7.10-7.06 (m, 2H), 6.86-6.81 (m, 2H), 4.59 (t, $J = 7.1$ Hz, 1H), 3.81 (td, $J = 7.7, 6.2$ Hz, 1H), 3.64 (td, $J = 7.9, 6.3$ Hz, 1H), 1.84-1.77 (m, 1H), 1.56-1.42 (m, 2H), 1.40-1.33 (m, 1H) ppm.

$^{13}\text{C NMR}$ (125 MHz, CDCl_3) δ 162.4 (d, $J = 244$ Hz), 140.0 (d, $J = 3.1$ Hz), 127.5 (d, $J = 7.5$ Hz), 115.2 (d, $J = 21.2$ Hz), 80.0, 68.4, 34.9, 26.0 ppm.

HRMS (EI (FE)) m/z calculated for $\text{C}_{10}\text{H}_{11}\text{O}_1\text{F}_1$ 166.0794, found 166.0793.

HPLC analysis using Daicel Chiralcel OJ-H column: *n*-heptane/*i*-PrOH 80:20, flow rate 0.5 mL/min, $\lambda = 210$ nm: $t_1 = 12.15$ min, $t_2 = 13.90$ min, er = 98:2. $\alpha_D^{25} = +37.9^\circ$ ($c = 0.75$ in CH_2Cl_2).

(5R)-5-(4-Fluorophenyl)tetrahydrofuran-2-ol (7)

A solution of **5c** (21.0 mg, 0.10 mmol, er 97.5:2.5) in MeCN (3 mL) was treated with 1M HCl (1 mL). After being stirred at room temperature for 90 min the mixture was diluted with H₂O and extracted with CH₂Cl₂ (3 x 10 mL).

The combined organic layers were dried over MgSO₄, filtered, concentrated under reduced pressure and the residue was purified by silica gel column chromatography using hexane/EtOAc (2:1) as the eluent to give the title compound (16.6 mg, 0.091 mmol, 91%, 1.2:1 mixture of anomers) as a colorless oil.

Major diastereoisomer:

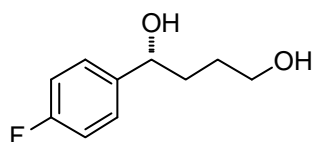
¹H NMR (500 MHz, C₆D₆) δ 7.01-6.98 (m, 2H), 6.84-6.78 (m, 2H), 5.42 (dd, *J* = 6.9, 3.4 Hz, 1H), 5.02 (dd, *J* = 7.1, 7.1 Hz, 1H), 2.74 (d, *J* = 3.1 Hz, 1H), 2.09-2.02 (m, 1H), 1.83-1.75 (m, 1H), 1.74-1.67 (m, 1H), 1.35-1.28 (m, 1H) ppm.

Minor diastereoisomer:

¹H NMR (500 MHz, C₆D₆) δ 7.23-7.19 (m, 2H), 6.89-6.84 (m, 2H), 5.31 (dd, *J* = 4.6, 3.5 Hz, 1H), 4.65 (dd, *J* = 9.2, 6.4 Hz, 1H), 2.83 (dd, *J* = 3.2, 1.5 Hz, 1H), 1.83-1.75 (m, 1H), 1.74-1.67 (m, 2H), 1.56-1.49 (m, 1H) ppm.

¹³C NMR (125 MHz, C₆D₆) δ 162.6 (d, *J* = 244.7 Hz), 162.5 (d, *J* = 244.6 Hz), 139.7 (d, *J* = 3.1 Hz), 139.0 (d, *J* = 3.0 Hz), 128.4 (d, *J* = 8.0 Hz), 127.6 (d, *J* = 8.2 Hz), 115.4, 115.2, 99.1, 98.8, 82.2, 78.9, 34.7, 33.2, 33.2 ppm.

HRMS (EI (DE)) *m/z* calculated for C₁₀H₁₁O₂F₁ 182.0743, found 182.0744.

(R)-1-(4-Fluorophenyl)butane-1,4-diol (8)

At 0 °C NaBH₄ (18.7mg, 0.494 mmol) was added to a solution of **7** (15.0 mg, 0.082 mmol) in MeOH (2 mL). The mixture was stirred at 0 °C for 30 min, then silica gel (500 mg) was added and the solvent was removed in vacuo. The residue was loaded onto a pad of silica gel and eluted with hexane/EtOAc/MeOH (1:3:0.2) to give the title compound as a colorless solid (13.6 mg, 0.0738 mmol, 90%).

¹H NMR (500 MHz, CDCl₃) δ 7.33-7.30 (m, 2H), 7.04-7.00 (m, 2H), 4.71 (t, *J* = 6.3 Hz, 1H), 3.73-3.64 (m, 2H), 2.53 (s, 2H), 1.85-1.81 (m, 2H), 1.70-1.63 (m, 2H) ppm.

7. EXPERIMENTAL SECTION

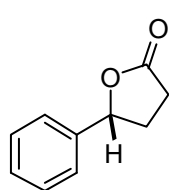
^{13}C NMR (125 MHz, CDCl_3) δ 162.2 (d, $J = 245.6$ Hz), 140.5 (d, $J = 3.0$ Hz), 127.5 (d, $J = 7.7$ Hz), 115.4 (d, $J = 21.4$ Hz), 73.9, 63.0, 36.6, 29.2 ppm.

HRMS (EI (DE)) m/z calculated for $\text{C}_{10}\text{H}_{13}\text{O}_2\text{F}_1$ 184.0900, found 182.0898.

HPLC analysis using Daicel Chiralcel OB-H column: *n*-heptane/*i*-PrOH 90:10, flow rate 0.5 mL/min, $\lambda = 220$ nm: $t_1 = 21.66$ min, $t_2 = 23.29$ min.

$\alpha_D^{25} = +44.1$ ($c = 0.200$, CH_2Cl_2)

(*R*)-5-Phenyldihydrofuran-2(3H)-one



To determine the absolute configurations of secondary homoaldol products a sample of **5a** was oxidized as described below for **5m** \rightarrow **9a** to give the title compound as a colorless oil.

^1H NMR (500 MHz, C_6D_6) δ 7.10-7.02 (m, 3H), 7.01-6.99 (m, 2H), 4.72 (t, $J = 7.5$ Hz, 1H), 1.97-1.91 (m, 1H), 1.86-1.79 (m, 1H), 1.61-1.54 (m, 1H), 1.39-1.28 (m, 1H) ppm.

^{13}C NMR (125 MHz, C_6D_6) δ 175.6, 140.4, 128.8, 128.3, 125.5, 80.4, 30.9, 28.6 ppm.

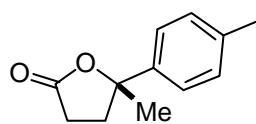
HRMS (EI) m/z calculated for $\text{C}_{10}\text{H}_{10}\text{O}_2$ 162.068082, found 162.068013.

HPLC analysis using Daicel Chiralcel OB-H column: *n*-heptane/*i*-PrOH 60:40, flow rate 1.0 mL/min, $\lambda = 220$ nm: $t_1 = 12.94$ min, $t_2 = 16.89$ min.

$\alpha_D^{25} = +31.1^\circ$ ($c = 0.135$, CHCl_3)

Absolute configuration was assigned as (*R*) by comparison of optical rotation with a literature reported value.^[156]

(*S*)-5-Methyl-5-(*p*-tolyl)dihydrofuran-2(3H)-one ((*S*)-Boivinain A, *ent*-9a)



CrO_3 (60.0 mg, 0.60 mmol) and conc. H_2SO_4 (2 drops) were subsequently added to a vigorously stirred solution of (*S*)-5,5-diethoxy-2-(*p*-tolyl)pentan-2-ol ((*S*)-**4m**, 26.6 mg, 0.10 mmol) in acetone/ H_2O (3:1, 2 mL) at ambient temperature. The mixture was stirred for 24 h before quenched with *i*-PrOH (0.5 mL) and diluted with H_2O (5 mL) and CH_2Cl_2 (10 mL). The layers were separated and the green aqueous layer extracted with CH_2Cl_2 (3 x 10 mL). The combined organic layers were dried (MgSO_4), filtered, and concentrated under reduced pressure. Purification of the residue by column chromatography on silica gel using pentane/ Et_2O (1:1) as the eluent afforded the title compound as a colorless oil (17.0 mg, 0.089 mmol, 89%).

7. EXPERIMENTAL SECTION

$^1\text{H NMR}$ (500 MHz, C_6D_6) δ 7.09 (d, $J = 8.2$ Hz, 2H), 6.92 (d, $J = 8.0$ Hz, 2H), 2.07 (s, 3H), 2.02-1.88 (m, 2H), 1.76-1.70 (m, 1H), 1.57-1.51 (m, 1H), 1.28 (s, 3H) ppm.

$^{13}\text{C NMR}$ (125 MHz, C_6D_6) δ 175.3, 142.4, 137.1, 129.4, 124.4, 85.8, 36.0, 29.2, 28.8, 20.9 ppm.

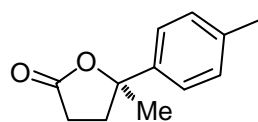
HRMS (EI) m/z calculated for $\text{C}_{12}\text{H}_{14}\text{O}_2$ 190.099378, found 190.099233.

HPLC analysis using Daicel Chiralcel OJ-H column: *n*-heptane/*i*-PrOH 70:30, flow rate 0.5 mL/min, $\lambda = 220$ nm: $t_1 = 12.34$ min, $t_2 = 15.30$ min.

$\alpha_D^{25} = -49.0^\circ$ ($c = 0.204$, CHCl_3)

Absolute configuration assigned as (*S*) by comparison of optical rotation with a literature reported value.^[157]

(*R*)-5-Methyl-5-(*p*-tolyl)tetrahydrofuran-2(3H)-one ((*R*)-Boiviniain A, **9a**)



Following the same procedure as described for *ent*-**9a** and using 30.0 mg (0.30 mmol) of CrO_3 the title compound was obtained from (2*R*,5*S*)-2-ethoxy-5-methyl-5-(*p*-tolyl)tetrahydrofuran (**5m**, 22.0 mg, 0.10 mmol) as a colorless oil (18.2 mg (0.096 mmol, 96%).

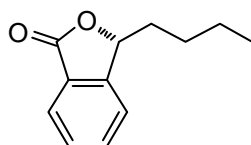
HPLC analysis using Daicel Chiralcel OJ-H column: *n*-heptane/*i*-PrOH 70:30, flow rate 0.5 mL/min, $\lambda = 220$ nm: $t_1 = 12.34$ min, $t_2 = 15.30$ min.

$\alpha_D^{25} = +50.8^\circ$ ($c = 0.370$, CHCl_3)

Absolute configuration assigned as (*R*) by comparison of optical rotation with a literature reported value.^[157]

When a sample of (2-*epi*-**5m**) was oxidized under identical conditions, (*S*)-Boiviniain A (*ent*-**9a**) was obtained (absolute configuration assigned by comparison of the previously obtained HPLC retention time).

(*R*)-3-Butylisobenzofuran-1(3H)-one (**9b**)



CrO_3 (30 mg, 0.3 mmol) and two drops of conc. H_2SO_4 were added to the solution of **5I** (19.4 mg, 0.066 mmol, er 97.5:2.5) in acetone/water 3:1 (1.33 mL) at 0°C . After 40 min at 0°C , excess of *i*-PrOH was added to the mixture, and stirring continued for 20 min more at 0°C . Then water was

added and mixture extracted with diethyl ether. Combined extracts were washed with concentrated aqueous sodium carbonate solution, dried (MgSO_4) and filtered. The product was

7. EXPERIMENTAL SECTION

purified by silica gel chromatography with 15% Et₂O/pentane as the eluent. Colorless oil, (10.7 mg, 85%).

¹H NMR (500 MHz, CDCl₃) δ 7.88 (d, *J* = 7.6 Hz, 1H), 7.65 (td, *J* = 7.6, 0.8 Hz, 1H), 7.50 (t, *J* = 7.5 Hz, 1H), 7.41 (dd, *J* = 7.6, 0.6 Hz, 1H), 5.46 (dd, *J* = 7.8, 4.1 Hz, 1H), 2.06-1.99 (m, 1H), 1.78-1.71 (m, 1H), 1.50-1.31 (m, 4H), 0.89 (t, *J* = 7.3 Hz, 3H) ppm.

¹³C NMR (125 MHz, CDCl₃) δ 170.7, 150.1, 133.9, 129.0, 126.1, 125.7, 121.7, 81.4, 34.4, 26.9, 22.4, 13.8 ppm.

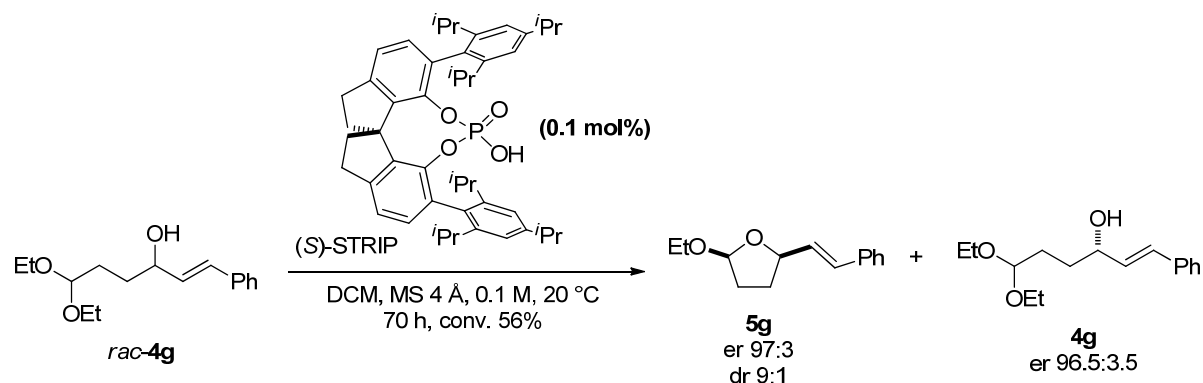
HRMS (EI (DE)) *m/z* calculated for C₁₂H₁₄O₂ (M) 190.0994, found 190.0993.

HPLC analysis using Daicel Chiralcel OD-3 column: *n*-heptane/*i*-PrOH 98:2, flow rate 1.0 mL/min, λ = 254 nm: *t*₁ = 5.88 min, *t*₂ = 6.76 min.

α_D²⁵ = +63.3 ° (*c* = 0.495 in CHCl₃).

Absolute configuration assigned as (*R*) by comparison of optical rotation with a literature reported value.^[158]

Experiment with 0.1 mol% catalyst loading



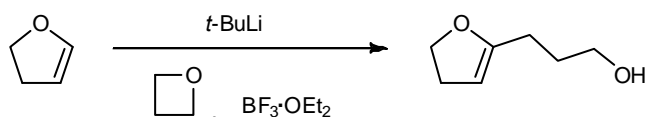
Molecular sieves 4 Å (50 mg) and a solution of (*S*)-STRIP (0.072 mg, 0.0001 mmol) in dry dichloromethane (0.5 mL), were added to the solution of *rac*-**4g** (26.4 mg, 0.1 mmol) in dry dichloromethane (0.5 mL) and stirred at 20 °C. Samples (ca. 100 μL) were removed from the reaction mixture, quenched by a few drops of Et₃N. Subsequently, the product and remaining starting material were isolated by column chromatography (silica gel, 2 g) using Et₂O/pentane (20%, then 50%) as the eluent, and analyzed by HPLC on a chiral stationary phase.

7.4. Catalytic asymmetric spiroacetalization

7.4.1. Substrates

The synthesized substrates were used immediately for the spiroacetalization reaction or stored as solutions in Et₂O or EtOAc.

3-(4,5-Dihydrofuran-2-yl)propan-1-ol (12a)



A 1.7 M solution of *tert*-butyl lithium in pentane (2.94 ml, 5 mmol) was added dropwise to a solution of dihydrofuran (378

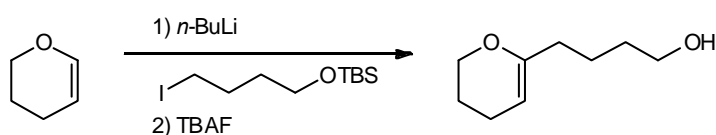
μl, 350 mg, 5 mmol) in THF (2 ml) at –78 °C under argon atmosphere. After being stirred at 0 °C for 30 min, the mixture was cooled to –78 °C and diluted with THF (3 ml). Oxetane (650 μl, 581 mg, 10 mmol) was added to this mixture followed by the dropwise addition of BF₃·OEt₂ (634 μl, 710 mg, 5 mmol). The mixture was stirred for 15 min at –78 °C, and Et₃N (2 ml) was added dropwise and the mixture was allowed to warm to room temperature. The mixture was filtered through aluminum oxide (10 g, activity III, preconditioned with Et₂O) using 5% MeOH/Et₂O as eluent. The solvent was removed under reduced pressure and the residue was purified by column chromatography on aluminum oxide (activity III) using 20% EtOAc/hexane as the eluent giving a colorless oil, 483 mg, 97 %.

¹H-NMR (400 MHz, DMSO-d₆): δ 4.59-4.57 (m, 1H), 4.39 (t, *J* = 5.2 Hz, 1H), 4.20 (t, *J* = 9.4 Hz, 2H), 3.38 (q, *J* = 6.0 Hz, 2H), 2.54-2.49 (m, 2H, overlap with solvent), 2.07-2.03 (m, 2H), 1.59-1.52 (m, 2H);

¹³C-NMR (100 MHz, DMSO-d₆): δ 158.2, 93.3, 69.0, 60.1, 29.6, 29.4, 23.9;

HRMS (EI (FE)) (*m/z*): [M] calcd for C₇H₁₂O₂, 128.0837; found, 128.0836.

4-(3,4-Dihydro-2H-pyran-6-yl)butan-1-ol (12b)



A 2.5 M solution of *n*-butyl lithium in hexane (2 ml, 5 mmol) was added dropwise to a solution of 3,4-dihydro-

2H-pyran (457 μl, 420 mg, 5 mmol) in THF (2 ml) at 0 °C under argon atmosphere. After being stirred at 50 °C for 1 h, the mixture was cooled to –10 °C. A solution of *tert*-butyl(4-iodobutoxy)dimethylsilane (5 mmol) in THF (2 ml) was added to the mixture at –10 °C. The

7. EXPERIMENTAL SECTION

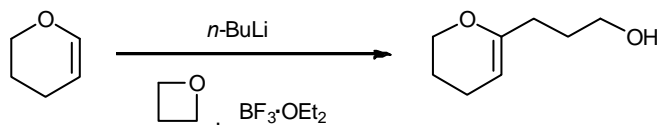
mixture was heated to 50 °C for 1.5 h, cooled to room temperature, and filtered through celite and aluminum oxide (5 g, activity III) using hexane as the eluent. The solvent was removed under reduced pressure and the residue was treated with 1 M solution of tetrabutylammonium fluoride in THF (6 mmol, 6 ml) for 1 h 45 min at room temperature. The mixture was then diluted with hexane (10 ml) and filtered through celite and aluminum oxide (5 g, activity III) using Et₂O as the eluent. The solvent was removed under reduced pressure and the residue was purified by column chromatography on aluminum oxide (activity III) using 10% EtOAc/hexane as the eluent giving a colorless oil, 349 mg, 45 %.

¹H-NMR (500 MHz, C₆D₆): δ 4.45 (t, *J* = 3.7 Hz, 1H), 3.77-3.75 (m, 2H), 3.37-3.34 (m, 2H), 2.06 (t, *J* = 7.5 Hz, 2H), 1.83-1.80 (m, 2H), 1.60-1.54 (m, 2H), 1.49-1.45 (m, 2H), 1.44-1.39 (m, 2H), 0.69 (t, *J* = 5.2 Hz, 1H);

¹³C-NMR (125 MHz, C₆D₆): δ 154.8, 95.3, 66.0, 62.6, 34.6, 32.6, 23.7, 22.8, 20.6;

HRMS (EI (FE)) (*m/z*): [M] calcd for C₉H₁₆O₂, 156.1150; found, 156.1149.

3-(3,4-Dihydro-2H-pyran-6-yl)propan-1-ol (12c)

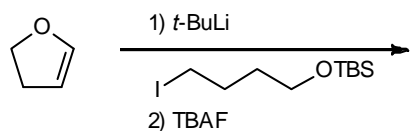


A 2.5 M solution of *n*-butyl lithium in hexane (2 ml ml, 5 mmol) was added dropwise to a solution of 3,4-dihydro-2H-pyran (457 μl, 420 mg, 5 mmol) in THF (2 ml) at 0 °C under argon atmosphere. After being stirred at 50 °C for 1 h, the mixture was cooled to -78 °C and diluted with THF (3 ml). Oxetane (650 μl, 581 mg, 10 mmol) was added to this mixture followed by the dropwise addition of BF₃·OEt₂ (634 μl, 710 mg, 5 mmol). The mixture was stirred for 15 min at -78 °C, then Et₃N (2 ml) was added dropwise and mixture allowed to warm to room temperature. The mixture was filtered through aluminum oxide (10 g, activity III, preconditioned with Et₂O) using 5% MeOH/Et₂O as eluent. The solvent was removed under reduced pressure and the residue was purified by column chromatography on aluminum oxide (activity III) using 20% EtOAc/hexane as the eluent giving a colorless oil, 365 mg, 51 %.

¹H-NMR (400 MHz, DMSO-*d*₆): δ 4.42 (t, *J* = 3.6, 1H), 4.33 (t, *J* = 5.2 Hz, 1H), 3.89-3.86 (m, 2H), 3.38-3.33 (m, 2H), 1.98-1.89 (m, 4H), 1.71-1.65 (m, 2H), 1.54-1.47 (m, 2H);

¹³C-NMR (100 MHz, DMSO-*d*₆): δ 153.7, 94.7, 65.3, 60.2, 30.3, 30.0, 22.0, 19.7;

HRMS (EI (FE)) (*m/z*): [M] calcd for C₈H₁₄O₂, 142.0994; found, 142.0993.

4-(4,5-Dihydrofuran-2-yl)butan-1-ol (12d)

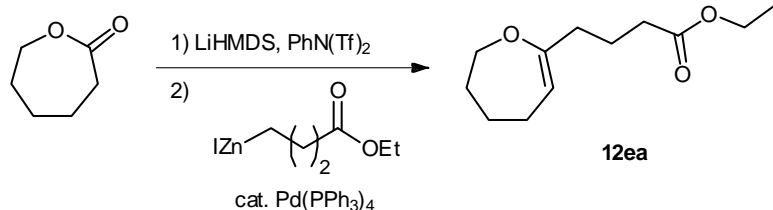
A 1.7 M solution of *tert*-butyl lithium in pentane (2.94 ml, 5 mmol) was added dropwise to a solution of dihydrofuran

(378 μ l, 350 mg, 5 mmol) in THF (2 ml) at -78 $^{\circ}$ C under argon atmosphere. After being stirred at 0 $^{\circ}$ C for 30 min, the mixture was cooled to -78 $^{\circ}$ C and diluted with THF (3 ml). A solution of *tert*-butyl(4-iodobutoxy)dimethylsilane (7.5 mmol) in THF (2 ml) was added dropwise to the mixture at -78 $^{\circ}$ C. The cooling bath (dry ice/acetone) was allowed to warm to room temperature overnight. To the mixture, water (10 ml) was added and the mixture extracted with hexane. The combined organic extracts were washed with water (2 x 10 ml) and brine (10 ml), and dried (MgSO_4). After filtration the solvent was removed under reduced pressure and the residue treated with 1 M solution of tetrabutylammonium fluoride in THF (10 mmol, 10 ml) for 1 h 30 min at room temperature. Water was added and the mixture extracted with Et_2O . The combined organic extracts were washed with saturated aqueous Na_2CO_3 , and dried (MgSO_4). After filtration, the solvent was removed under reduced pressure and the residue was purified by column chromatography on aluminum oxide (activity III) using 20% EtOAc /hexane as the eluent giving a colorless oil, 356 mg, 50 %.

$^1\text{H-NMR}$ (500 MHz, DMSO-d_6): δ 4.58 (s, 1H), 4.35 (t, $J = 5.2$ Hz, 1H), 4.20 (t, $J = 9.3$ Hz, 2H), 3.36 (q, $J = 5.8$ Hz, 2H), 2.53-2.49 (m, 2H, overlap with solvent), 2.03-2.05 (m, 2H), 1.47-1.38 (m, 4H);

$^{13}\text{C-NMR}$ (125 MHz, DMSO-d_6): δ 158.3, 93.5, 69.0, 60.4, 32.1, 29.5, 27.1, 22.7;

HRMS (EI (FE)) (m/z): [M] calcd for $\text{C}_8\text{H}_{14}\text{O}_2$, 142.0994; found, 142.0993.

Ethyl 4-(4,5,6,7-tetrahydrooxepin-2-yl)butanoate (12ea)

1) A 1 M solution of LiHMDS in THF (12.5 mmol, 12.5 ml) was diluted with THF (40 ml), and cooled to -78 $^{\circ}$ C. To the solution HMPA (2.24 g, 12.5 mmol) was

added, followed by a solution of the lactone (1.11 ml, 1.14 g, 10 mmol) in THF (13 ml). After being stirred for 90 min at -78 $^{\circ}$ C, a solution of $\text{PhN}(\text{Tf})_2$ in THF (10 ml) was added dropwise. After 90 min at -78 $^{\circ}$ C, the cooling bath was removed and the mixture was allowed to warm to 0° C. 10 % Aqueous sodium hydroxide solution was added (60 ml) and the mixture extracted

7. EXPERIMENTAL SECTION

with Et₂O (3 x 60 ml). The combined organic extracts were washed with water (2 x 20 ml) and dried over K₂CO₃. The resulting solution of enol triflate was concentrated to 5 ml and diluted with benzene (30 ml) and used immediately for coupling reactions.

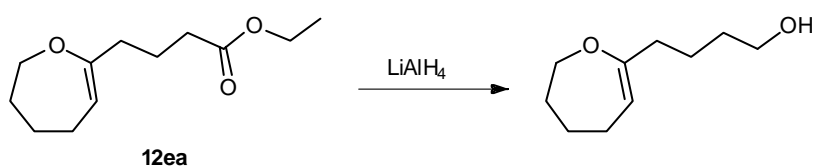
2) In a separate flask, ethyl 4-iodobutanoate (2.42 g, 10 mmol) was added to a suspension of Zn-Cu couple (1.31 g, 20 mmol) in benzene (13 ml) and *N,N*-dimethylacetamide (1.7 ml) under argon and the mixture was refluxed for 2 h. After cooling to room temperature, half of the above prepared solution of enol triflate in benzene (5 mmol in 15 ml benzene) was added, followed by a solution of Pd(PPh₃)₄ (289 mg, 0.25 mmol, 5 mol%) in benzene (15 ml). After 1 h 20 min at room temperature Et₃N (3 ml) was added, and the mixture was filtered through silica gel (20 g) using Et₂O as the eluent, and concentrated under reduced pressure. The residue was purified by column chromatography on silica gel using 2-4% EtOAc/hexane as the eluent giving colorless oil, 466 mg, 44 %.

¹H-NMR (400 MHz, DMSO-d₆): δ 4.66 (t, *J* = 5.7 Hz, 1H), 4.03 (q, *J* = 7.1 Hz, 2H), 3.85-3.83 (m, 2H), 2.25 (t, *J* = 7.4 Hz, 2H), 2.03-1.99 (m, 2H), 1.93 (t, *J* = 7.3 Hz, 2H), 1.76-1.71 (m, 2H), 1.65-1.60 (m, 2H), 1.58-1.51 (m, 2H), 1.16 (t, *J* = 7.1 Hz, 3H);

¹³C-NMR (100 MHz, DMSO-d₆): δ 172.7, 158.6, 105.2, 71.1, 59.6, 34.5, 32.7, 31.1, 25.6, 25.2, 22.0, 14.1;

HRMS (ESI+) (*m/z*): [M+Na] calcd for C₁₂H₂₀O₃Na, 235.1305; found, 235.1303.

4-(4,5,6,7-Tetrahydrooxepin-2-yl)butan-1-ol (12e)



LiAlH₄ (159 mg, 4.20 mmol) was added to a solution of ester **12ea** (406 mg, 1.91 mmol) in THF (4 ml) under

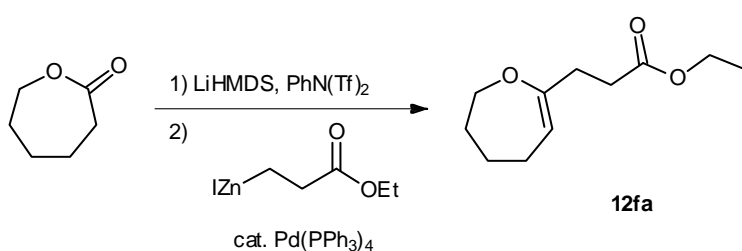
argon. The mixture was stirred without heating for 1 h, then heated shortly to reflux with a heat gun, and left to cool to room temperature. Excess LiAlH₄ was destroyed with a minimum amount of brine, and the solution separated from the inorganic precipitate which was washed with Et₂O (5 x 10 ml). The combined organic extracts were dried (MgSO₄), filtered, and the solvent was removed under reduced pressure. The residue was purified by column chromatography on aluminum oxide (activity III) using 20% EtOAc/hexane as the eluent giving colorless oil, 307 mg, 94 %.

¹H-NMR (500 MHz, DMSO-*d*₆): δ 4.66 (t, *J* = 5.8 Hz, 1H), 4.32 (t, *J* = 5.2 Hz, 1H), 3.84-3.82 (m, 2H), 3.37-3.34 (m, 2H), 2.02-1.99 (m, 2H), 1.92-1.88 (m, 2H), 1.75-1.71 (m, 2H), 1.56-1.51 (m, 2H), 1.41-1.34 (m, 4H);

¹³C-NMR (125 MHz, DMSO-*d*₆): δ 159.6, 104.7, 71.0, 60.5, 35.1, 32.0, 31.2, 25.7, 25.2, 23.1;

HRMS (EI (FE)) (*m/z*): [M] calcd for C₁₀H₁₈O₂, 170.1307; found, 170.1305.

Ethyl 3-(4,5,6,7-tetrahydrooxepin-2-yl)propanoate (12fa)



1) A 1 M solution of LiHMDS in THF (12.5 mmol, 12.5 ml) was diluted with THF (40 ml), and cooled to –78 °C. HMPA (2.24 g, 12.5 mmol) was added followed by a solution of

the lactone (1.11 ml, 1.14 g, 10 mmol) in THF (13 ml). After being stirred for 90 min at –78 °C, a solution of PhN(Tf)₂ in THF (10 ml) was added dropwise. After 90 min at –78 °C, the cooling bath was removed and the mixture was allowed to warm to 0°C. 10 % Aqueous sodium hydroxide solution was added (60 ml) and the mixture was extracted with Et₂O (3 x 60 ml). The combined organic extracts were washed with water (2 x 20 ml) and dried over K₂CO₃. The resulting solution of enol triflate was concentrated to 5 ml and diluted with benzene (30 ml) and used immediately for coupling reactions.

2) In a separate flask, ethyl 3-iodopropanoate (2.28 g, 10 mmol) was added to a suspension of Zn-Cu couple (1.31 g, 20 mmol) in benzene (13 ml) and *N,N*-dimethylacetamide (1.7 ml) under argon, and the mixture was refluxed for 2 h. After cooling to room temperature, half of the above prepared solution of enol triflate in benzene (5 mmol in 15 ml benzene) was added, followed by a solution of Pd(PPh₃)₄ (289 mg, 0.25 mmol, 5 mol%) in benzene (15 ml). After 1h 20 min at room temperature Et₃N (3 ml) was added, and the mixture filtered thorough silica gel (20 g) using Et₂O as the eluent, and concentrated under reduced pressure. The residue was purified by column chromatography on silica gel using 2-4% EtOAc/hexane as the eluent giving colorless oil, 572 mg, 58 %.

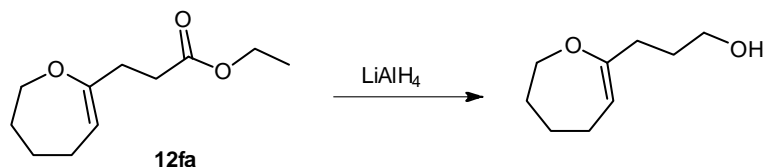
¹H-NMR (400 MHz, DMSO-*d*₆): δ 4.73-4.69 (m, 1H), 4.03 (q, *J* = 7.1 Hz, 2H), 3.82-3.81 (m, 2H), 2.36-2.33 (m, 2H), 2.21-2.17 (m, 2H), 2.02-1.99 (m, 2H), 1.76-1.70 (m, 2H), 1.55-1.49 (2H), 1.16 (t, *J* = 7.1 Hz, 3H);

7. EXPERIMENTAL SECTION

$^{13}\text{C-NMR}$ (100 MHz, DMSO-d_6): δ 172.2, 157.9, 105.4, 71.3, 59.7, 31.7, 31.1, 30.8, 25.5, 25.2, 14.1;

HRMS (ESI+) (m/z): $[M+\text{Na}]$ calcd for $\text{C}_{11}\text{H}_{18}\text{O}_3\text{Na}$, 221.1148; found, 221.1144.

3-(4,5,6,7-Tetrahydrooxepin-2-yl)propan-1-ol (12f)



LiAlH_4 (195 mg, 5.13 mmol) was added to a solution of ester **12fa** (462 mg, 2.33 mmol) in THF (6 ml) under Argon. The mixture was

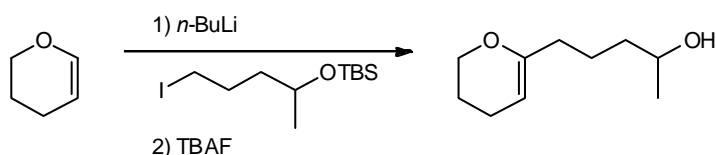
stirred without heating for 1 h, then heated shortly to reflux with a heat gun, and left to cool to room temperature. Excess LiAlH_4 was destroyed with a minimum amount of brine, and the solution separated from the inorganic precipitate which was washed with Et_2O (5 x 10 ml). The combined organic extracts were dried (MgSO_4), filtered, and the solvent was removed under reduced pressure. The residue was purified by column chromatography on aluminum oxide (activity III) using 20% EtOAc /hexane as the eluent giving colorless oil, 330 mg, 91 %.

$^1\text{H-NMR}$ (500 MHz, DMSO-d_6): δ 4.66 (t, $J = 5.8$ Hz, 1H), 4.34 (t, $J = 5.2$ Hz, 1H), 3.84-3.81 (m, 2H), 3.37-3.33 (m, 2H), 2.02-1.98 (m, 2H), 1.93 (t, $J = 7.5$ Hz, 2H), 1.75-1.71 (m, 2H), 1.55-1.47 (m, 4H);

$^{13}\text{C-NMR}$ (125 MHz, DMSO-d_6): δ 159.5, 104.7, 71.1, 60.3, 31.9, 31.3, 30.2, 25.7, 25.3;

HRMS (EI (FE)) (m/z): $[M]$ calcd for $\text{C}_9\text{H}_{16}\text{O}_2$, 156.1150; found, 156.1150.

5-(3,4-Dihydro-2H-pyran-6-yl)pentan-2-ol (12g)



A 2.5 M solution of *n*-butyl lithium in hexane (2 ml, 5 mmol) was added dropwise to a solution of 3,4-dihydro-2H-pyran (457 μl , 420 mg, 5 mmol) in

THF (2 ml) at 0 °C under argon atmosphere. After being stirred at 50 °C for 1 h, the mixture was cooled to -10 °C. A solution of *tert*-butyl((5-iodopentan-2-yl)oxy)dimethylsilane (5.5 mmol, obtained by opening of 2-Me-THF with TBSCl and $\text{NaI}^{[159]}$) in THF (2 ml) was added to the mixture at -10 °C. The mixture was heated to 50 °C for 2 h, cooled to room temperature, and filtered through celite and aluminum oxide (5 g, activity III) using hexane as the eluent. The solvent was removed under reduced pressure and the residue was treated with 1 M solution of

7. EXPERIMENTAL SECTION

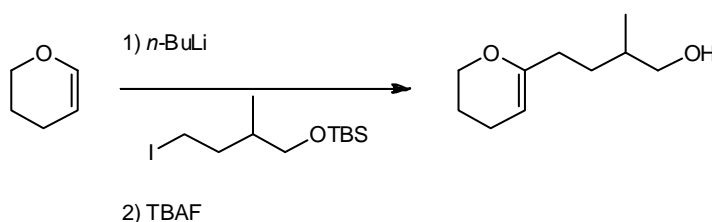
tetrabutylammonium fluoride in THF (10 mmol, 10 ml) for 18 h at reflux temperature. The mixture was then diluted with hexane (20 ml) and filtered through celite and aluminum oxide (10 g, activity III) using Et₂O as the eluent. The solvent was removed under reduced pressure and the residue was purified by column chromatography on aluminum oxide (activity III) using 5-20% EtOAc/hexane as the eluent giving a colorless oil, 422 mg, 50 %.

¹H-NMR (500 MHz, C₆D₆): δ 7.47 (t, *J* = 3.7 Hz, 1H), 3.79-3.77 (m, 2H), 3.58-3.51 (m, 1H), 2.12-2.03 (m, 2H), 1.84-1.81 (m, 2H), 1.71-1.62 (m, 1H), 1.60-1.51 (m, 1H), 1.50-1.46 (m, 2H), 1.39-1.25 (m, 2H), 0.99 (d, *J* = 6.2 Hz, 3H), 0.87 (d, *J* = 4.2 Hz, 1H);

¹³C-NMR (125 MHz, C₆D₆): δ 154.9, 95.3, 67.6, 66.0, 39.2, 34.9, 23.8, 23.7, 22.8, 20.7;

HRMS (EI (FE)) (*m/z*): [M] calcd for C₁₀H₁₈O₂, 170.1307; found, 170.1305.

4-(3,4-Dihydro-2H-pyran-6-yl)-2-methylbutan-1-ol (**12i**)



A 2.5 M solution of *n*-butyl lithium in hexane (2 ml, 5 mmol) was added dropwise to a solution of 3,4-dihydro-2H-pyran (457 μl, 420 mg, 5 mmol) in THF (2 ml) at 0 °C under argon

atmosphere. After being stirred at 50 °C for 1 h, the mixture was cooled to -10 °C. A solution of *tert*-butyl(4-iodo-2-methylbutoxy)dimethylsilane and *tert*-butyl(4-iodo-3-methylbutoxy)dimethylsilane (1.2:1, 5.5 mmol, obtained by opening of 3-Me-THF with TBSCl and NaI^[159]) in THF (2 ml) was added to the mixture at -10 °C. The mixture was heated to 50 °C for 1.5 h. After cooling to room temperature, water was added and the mixture extracted with hexane. The combined organic extracts were washed with brine, and dried (MgSO₄). After filtration the solvent was removed under reduced pressure and the residue treated with a 1 M solution of tetrabutylammonium fluoride in THF (10 mmol, 10 ml) for 2 h at room temperature. Water was added and the mixture was extracted with Et₂O. The combined organic extracts were washed with saturated aqueous Na₂CO₃, and dried (MgSO₄). After filtration, the solvent was removed under reduced pressure and the residue was purified by column chromatography on aluminum oxide (activity III) using 5-40% Et₂O/pentane as the eluent. Some of **12i** was isolated as pure material, colorless oil, 46 mg. The rest was collected as a mixture **12i/12k** 2:1, colorless oil, 173 mg.

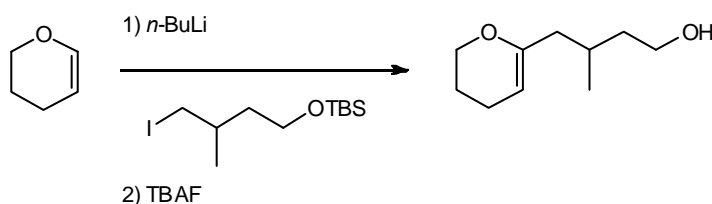
7. EXPERIMENTAL SECTION

¹H-NMR (500 MHz, C₆D₆): δ 4.47 (t, *J* = 3.7 Hz, 1H), 3.78-3.76 (m, 2H), 3.28-3.24 (m, 1H), 3.20-3.16 (m, 1H), 2.18-2.12 (m, 1H), 2.08-2.02 (m, 1H), 1.84-1.80 (m, 2H), 1.73-1.66 (m, 1H), 1.54-1.46 (m, 3H), 1.37-1.30 (m, 1H), 0.84 (d, *J* = 6.7 Hz, 3H), 0.72 (t, *J* = 4.6 Hz, 1H);

¹³C-NMR (125 MHz, C₆D₆): δ 155.2, 95.1, 67.9, 66.1, 35.6, 32.4, 30.9, 22.8, 20.7, 16.8:

HRMS (EI (FE)) (*m/z*): [M] calcd for C₁₀H₁₈O₂, 170.1307; found, 170.1306.

4-(3,4-Dihydro-2H-pyran-6-yl)-3-methylbutan-1-ol (**12k**)



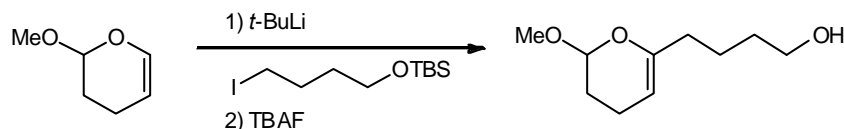
A 2.5 M solution of *n*-butyl lithium in hexane (1.78 ml, 4.45 mmol) was added dropwise to a solution of 3,4-dihydro-2H-pyran (407 μl, 374 mg, 4.45 mmol) in THF (1.8 ml) at 0 °C under argon atmosphere. After being stirred at 50 °C for 1 h, the mixture was cooled to -10 °C. A solution of *tert*-butyl(4-iodo-3-methylbutoxy)dimethylsilane (4.45 mmol, containing <10% of *tert*-butyl(4-iodo-2-methylbutoxy)dimethylsilane, obtained from 1:1.2 mixture^[159] by chromatography on silica gel using 0-10% EtOAc/hexane as eluent) in THF (1.8 ml) was added to the mixture at -10 °C. The mixture was heated to 50 °C for 2 h. After cooling to room temperature, water was added and the mixture extracted with hexane. The combined organic extracts were washed with brine, and dried (MgSO₄). As a significant amount of iodide remained unconsumed, the unpurified residue was again treated with lithiated 3,4-dihydro-2H-pyran (407 μl, 374 mg, 4.45 mmol) as described above. The workup was repeated as above and after filtration the solvent was removed under reduced pressure and the residue treated with 1 M solution of tetrabutylammonium fluoride in THF (10 mmol, 10 ml) for 2 h at room temperature. Water was added and the mixture extracted with MTBE. The combined organic extracts were washed with saturated aqueous Na₂CO₃, and dried (MgSO₄). After filtration, the solvent was removed under reduced pressure and the residue was purified by column chromatography on aluminum oxide (activity III) using 5-50% Et₂O/pentane as the eluent giving a colorless oil, 146 mg (containing <10% of **12i**).

¹H-NMR (500 MHz, C₆D₆): δ 4.44 (t, *J* = 3.7 Hz, 1H), 3.78-3.70 (m, 2H), 3.50-3.40 (m, 2H), 2.09-1.96 (m, 2H), 1.88-1.80 (m, 3H), 1.57-1.50 (m, 1H), 1.49-1.43 (m, 2H), 1.29-1.22 (m, 1H), 0.90 (d, *J* = 6.5 Hz, 3H), 0.68 (t, *J* = 4.7 Hz, 1H);

¹³C-NMR (125 MHz, C₆D₆): δ 153.8, 96.7, 66.0, 61.0, 42.7, 40.0, 27.9, 22.8, 20.7, 19.9;

HRMS (EI (FE)) (m/z): [M] calcd for $C_{10}H_{18}O_2$, 170.1307; found, 170.1307.

4-(2-Methoxy-3,4-dihydro-2H-pyran-6-yl)butan-1-ol (12m)



A 1.7 M solution of *t*-butyl lithium in pentane (11.8 ml, 20 mmol) was added

dropwise to a solution of 2-methoxy-3,4-dihydro-2H-pyran (1.14 g, 10 mmol) in THF (4 ml) at $-78\text{ }^{\circ}\text{C}$ under argon atmosphere. After being stirred for 15 min at $-78\text{ }^{\circ}\text{C}$ and for 30 min at $0\text{ }^{\circ}\text{C}$, the mixture was diluted with THF (5 ml). After being stirred for additional 10 min at $0\text{ }^{\circ}\text{C}$, the mixture was cooled to $-78\text{ }^{\circ}\text{C}$. A solution of *tert*-butyl(4-iodobutoxy)dimethylsilane (10 mmol) in THF (2 ml) was added dropwise at $-78\text{ }^{\circ}\text{C}$, and the mixture allowed to warm slowly to room temperature overnight. The mixture was filtered through celite and aluminum oxide (activity III) using hexane as the eluent. The solvent was removed under reduced pressure and the residue was treated with 1 M solution of tetrabutylammonium fluoride in THF (12 mmol, 12 ml) for 7 h at room temperature. The mixture was then diluted with hexane (30 ml) and filtered through celite and aluminum oxide (20 g, activity III) using Et_2O as the eluent. The solvent was removed under reduced pressure and the residue was purified by column chromatography on aluminum oxide (activity III) using 10-30% EtOAc /hexane as the eluent giving a colorless oil, 646 mg, 35 %.

The characterization as for the enantioenriched sample.

7.4.2. Products

Racemates

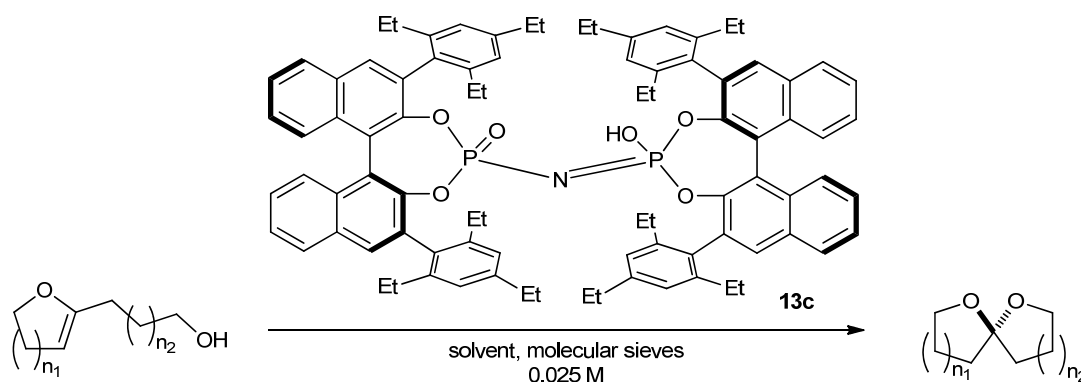
Racemic products were prepared by mixing a solution of substrate in Et₂O or EtOAc with aqueous HCl for few minutes. Samples for GC analysis were isolated by thin layer chromatography on aluminum oxide using EtOAc/hexane as eluent.

For chiral substrates, racemates were prepared both under kinetic and thermodynamic conditions as described for individual case.

General procedure for small scale optimizations

To a solution of substrate **12** (0.025 mmol) in solvent (0.5 ml) was added (dropwise at temperatures below r.t.) a solution of catalyst in solvent (0.5 ml). The reaction was quenched with 2-3 drops of Et₃N. Samples for GC analysis were isolated by thin layer chromatography on aluminum oxide using EtOAc/hexane as eluent.

General procedure for the catalytic asymmetric spiroacetalization



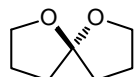
Solvent (7 ml) and molecular sieves were cooled to the reaction temperature in a vial closed with a septum. A solution of substrate **12** (0.25 mmol) in solvent (2 ml) was added, and the mixture stirred for 5-10 min allowing it to reach the reaction temperature. To the mixture a solution of catalyst **13c** in solvent (1 ml) was added dropwise. After designated time at the designated temperature the reaction was quenched with Et₃N (50 μ l).

Purification was performed by chromatography as described for individual case. Solutions of products after chromatography were carefully concentrated to ca. <0.1 ml, and immediately dissolved in C₆D₆ (3 ml). Yield was determined by ¹H NMR analysis using 1 ml of this solution and Ph₃CH (20.4 mg, 0.0833 mmol) as internal standard, integration of Ph₃CH vs. product –

CH_2O -. NMR spectra without remaining solvent are obtained after concentrating the other 2 ml of the C_6D_6 solution (previously used for optical rotation measurement) to < 0.3 ml and diluting with C_6D_6 . Alternatively, after chromatography the solution was concentrated to <50 mg, part of the sample was directly used for optical rotation measurement, and the rest immediately used for NMR analysis, and yield corrected for residual solvent by integration in ^1H NMR spectrum. Due to the volatility of the products some imprecision in the determination of yields and optical rotation values is expected.

Absolute configuration of (*S*)-**11b** was determined by comparison with literature value,^[27] and configurations of other products were assigned by analogy.

(*S*)-1,6-Dioxaspiro[4.4]nonane (**11a**)



Reaction conditions: catalyst loading, 0.1 mol%; solvent, CH_2Cl_2 ; molecular sieves, 3 Å (125 mg); temperature, $-55\text{ }^\circ\text{C}$, 12 h. *Purification:* To the mixture Et_3N (0.5 ml) was added, mixture concentrated to <1 ml, silica gel column using 10% Et_2O /pentane as eluent. Colorless liquid, yield 62%;

$^1\text{H-NMR}$ (400 MHz, C_6D_6): δ 3.93-3.87 (m, 2H), 3.74-3.68 (m, 2H), 2.01-1.83 (m, 4H), 1.69-1.61 (m, 2H), 1.58-1.48 (m, 2H);

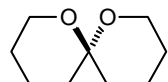
$^{13}\text{C-NMR}$ (100 MHz, C_6D_6): δ 114.6, 66.9, 34.8, 25.0;

HRMS (EI (FE)) (m/z): [M] calcd for $\text{C}_7\text{H}_{12}\text{O}_2$, 128.0837; found, 128.0838;

$[\alpha]_D^{25} = +182.4\text{ }^\circ$ ($c = 0.44$ in pentane, er 96:4);

GC (Column: 25 m Lipodex-G (octakis-(2,3-di-*O*-pentyl-6-*O*-methyl)- γ -cyclodextrin), i.D. 0.25 mm; Detector: FID; Temperature: injector $230\text{ }^\circ\text{C}$, detector $350\text{ }^\circ\text{C}$, oven $95\text{ }^\circ\text{C}$; gas: 0.5 bar H_2), $t_{\text{minor}} = 2.82$ min, $t_{\text{major}} = 3.00$ min, er 96:4.

(*S*)-1,7-Dioxaspiro[5.5]undecane ((*S*)-**11b**)



Reaction conditions: catalyst loading, 5 mol%; solvent, *tert*-butyl-methyl ether; molecular sieves, 4 Å (50 mg); temperature, $-25\text{ }^\circ\text{C}$, 24 h. *Purification:* mixture concentrated to <1 ml, silica gel column using 5% Et_2O /pentane as eluent. Colorless liquid, yield 77%.

$^1\text{H-NMR}$ (400 MHz, C_6D_6): δ 3.71-3.64 (m, 2H), 3.57-3.52 (m, 2H), 2.03-1.91 (m, 2H), 1.68-1.62 (m, 2H), 1.51-1.30 (m, 6H), 1.27-1.22 (m, 2H);

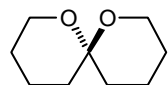
$^{13}\text{C-NMR}$ (100 MHz, C_6D_6): δ 94.9, 60.2, 36.3, 25.8, 19.1;

HRMS (EI (FE)) (m/z): [M] calcd for $C_9H_{16}O_2$, 156.1150; found, 156.1151;

$[\alpha]_D^{25} = +121.5^\circ$ ($c = 0.85$ in pentane, er 98:2) (Literature value for (*R*)-**11b**: $[\alpha]_D^{19} = -122.8^\circ$, $c = 3.2$ in pentane, er > 97.5:2.5)^[27];

GC (Column: 25 m Lipodex-G (octakis-(2,3-di-*O*-pentyl-6-*O*-methyl)- γ -cyclodextrin), i.D. 0.25 mm; Detector: FID; Temperature: injector 230 °C, detector 350 °C, oven 100 °C; gas: 0.5 bar H_2), $t_{\text{minor}} = 4.86$ min, $t_{\text{major}} = 5.36$ min, er 98:2.

(*R*)-1,7-Dioxaspiro[5.5]undecane ((*R*)-11b)



Reaction conditions: catalyst loading, 5 mol%; solvent, *tert*-butyl-methyl ether;

molecular sieves, 4 Å (50 mg); temperature, – 25 °C, 12 h. *Purification*: mixture concentrated to <1 ml, silica gel column using 5% Et_2O /pentane as eluent. Colorless liquid, yield 70%.

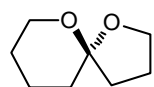
¹H-NMR (500 MHz, C_6D_6): δ 3.70-3.65 (m, 2H), 3.57-3.53 (m, 2H), 2.02-1.92 (m, 2H), 1.67-1.63 (m, 2H), 1.50-1.30 (m, 6H), 1.27-1.22 (m, 2H);

¹³C-NMR (125 MHz, C_6D_6): δ 94.9, 60.2, 36.3, 25.8, 19.1;

$[\alpha]_D^{25} = -96.3^\circ$ ($c = 0.91$ in C_6D_6 , er 97.5:2.5);

GC (Column: 25 m Lipodex-G (octakis-(2,3-di-*O*-pentyl-6-*O*-methyl)- γ -cyclodextrin), i.D. 0.25 mm; Detector: FID; Temperature: injector 230 °C, detector 350 °C, oven 100 °C; gas: 0.5 bar H_2), $t_{\text{major}} = 4.53$ min, $t_{\text{minor}} = 5.05$ min, er 97.5:2.5.

(*S*)-1,6-Dioxaspiro[4.5]decane (11c) (obtained from substrate 12c)



Reaction conditions: catalyst loading, 1 mol%; solvent, 1,2-dichloroethane;

molecular sieves, 3 Å (125 mg); temperature, – 35 °C, 12 h. *Purification*: Reaction mixture loaded onto pentane preconditioned silica gel column, product eluted using 10% Et_2O /pentane as eluent. Colorless liquid, yield 81%.

¹H-NMR (400 MHz, C_6D_6): δ 3.96-3.90 (m, 1H), 3.88-3.83 (m, 1H), 3.77-3.72 (m, 1H), 3.60-3.55 (m, 1H), 2.02-1.82 (m, 3H), 1.68-1.58 (m, 2H), 1.55-1.37 (m, 4H), 1.29-1.21 (m, 1H);

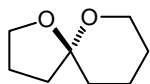
¹³C-NMR (100 MHz, C_6D_6): δ 105.5, 67.0, 61.5, 38.2, 34.0, 25.8, 24.2, 20.8;

HRMS (EI (FE)) (m/z): [M] calcd for $C_8H_{14}O_2$, 142.0994; found, 142.0995;

$[\alpha]_D^{25} = +130.9^\circ$ ($c = 0.88$ in pentane, er 95.5:4.5);

GC (Column: 25 m Lipodex-G (octakis-(2,3-di-*O*-pentyl-6-*O*-methyl)- γ -cyclodextrin), i.D. 0.25 mm; Detector: FID; Temperature: injector 230 °C, detector 350 °C, oven 100 °C; gas: 0.5 bar H₂), $t_{\text{minor}} = 3.30$ min, $t_{\text{major}} = 3.47$ min, er 95.5:4.5.

(S)-1,6-Dioxaspiro[4.5]decane (11c) (obtained from substrate 12d)



Reaction conditions: catalyst loading, 1 mol%; solvent, *tert*-butyl-methyl ether; molecular sieves, 4 Å (50 mg); temperature, -35 °C, 12 h. *Purification:* To the mixture Et₃N (0.5 ml) was added, mixture concentrated to <1 ml, silica gel column using 5% Et₂O/pentane as eluent. Colorless liquid, yield 69%.

¹H-NMR (500 MHz, C₆D₆): δ 3.96-3.91 (m, 1H), 3.89-3.83 (m, 1H), 3.76-3.72 (m, 1H), 3.59-3.56 (m, 1H), 2.01-1.83 (m, 3H), 1.67-1.61 (m, 2H), 1.54-1.38 (m, 4H), 1.27-1.22 (m, 1H);

¹³C-NMR (125 MHz, C₆D₆): δ 105.5, 67.0, 61.4, 38.2, 34.0, 25.8, 24.2, 20.8;

HRMS (EI (FE)) (m/z): [M] calcd for C₈H₁₄O₂, 142.0994; found, 142.0993;

$[\alpha]_D^{25} = +103.1^\circ$ ($c = 0.83$ in C₆D₆, er 96:4);

GC (Column: 25 m Lipodex-G (octakis-(2,3-di-*O*-pentyl-6-*O*-methyl)- γ -cyclodextrin), i.D. 0.25 mm; Detector: FID; Temperature: injector 230 °C, detector 350 °C, oven 100 °C; gas: 0.5 bar H₂), $t_{\text{minor}} = 3.31$ min, $t_{\text{major}} = 3.46$ min, er 96.0:4.0.

(S)-1,7-Dioxaspiro[5.6]dodecane (11e)



Reaction conditions: catalyst loading, 1 mol%; solvent, *tert*-butyl-methyl ether; molecular sieves, 4 Å (50 mg); temperature, -25 °C, 12 h. *Purification:* To the mixture Et₃N (0.5 ml) was added, mixture concentrated to <1 ml, silica gel column using 5% Et₂O/pentane as eluent. Colorless liquid, yield 78%.

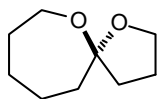
¹H-NMR (500 MHz, C₆D₆): δ 3.84-3.79 (m, 1H), 3.76-3.71 (m, 1H), 3.60-3.52 (m, 2H), 1.99-1.79 (m, 4H), 1.67-1.62 (m, 1H), 1.61-1.54 (m, 1H), 1.52-1.32 (m, 5H), 1.31-1.24 (m, 2H), 1.16-1.07 (m, 1H);

¹³C-NMR (125 MHz, C₆D₆): δ 99.9, 61.4, 61.0, 42.1, 36.1, 31.2, 30.3, 26.1, 22.8, 19.5;

HRMS (EI (FE)) (m/z): [M] calcd for C₁₀H₁₈O₂, 170.1307; found, 170.1305;

$[\alpha]_D^{25} = +111.8^\circ$ ($c = 1.11$ in C₆D₆, er 96:4);

GC (Column: 25 m Lipodex-G (octakis-(2,3-di-*O*-pentyl-6-*O*-methyl)- γ -cyclodextrin), i.D. 0.25 mm; Detector: FID; Temperature: injector 220 °C, detector 350 °C, oven 105 °C; gas: 0.5 bar H₂), $t_{\text{minor}} = 7.05$ min, $t_{\text{major}} = 7.29$ min, er 96:4.

(S)-1,6-Dioxaspiro[4.6]undecane (11f)

Reaction conditions: catalyst loading, 1 mol%; solvent, *tert*-butyl-methyl ether; molecular sieves, 4 Å (50 mg); temperature, -35 °C, 12 h. *Purification:* To the mixture Et₃N (0.5 ml) was added, mixture concentrated to <1 ml, silica gel column using 5% Et₂O/pentane as eluent. Colorless liquid, yield 88%.

¹H-NMR (500 MHz, C₆D₆): δ 3.88-3.74 (m, 3H), 3.60-3.56 (m, 1H), 2.09-2.01 (m, 2H), 1.91-1.82 (m, 2H), 1.66-1.35 (m, 7H), 1.20-1.11 (m, 1H);

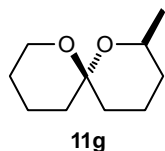
¹³C-NMR (125 MHz, C₆D₆): δ 110.6, 66.7, 62.5, 39.1, 38.7, 31.3, 30.0, 25.2, 23.9;

HRMS (EI (FE)) (*m/z*): [M] calcd for C₉H₁₆O₂, 156.1150; found, 156.1152;

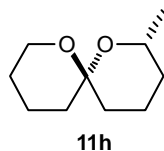
[α]_D²⁵ = + 121.7 ° (c = 1.15 in C₆D₆, er 98.5:1.5);

GC (Column: 25 m Ivadex-1/PS086 (dimethyl-pentyl-β-cyclodextrin), i.D. 0.25 mm, df. 0.15 μm; Detector: FID; Temperature: injector 220 °C, detector 320 °C, oven 105 °C; gas: 0.5 bar H₂), t_{minor} = 6.25 min, t_{major} = 6.60 min, er 98.5:1.5.

(2S,6S)-2-Methyl-1,7-dioxaspiro[5.5]undecane (11g) and (2R,6S)-2-Methyl-1,7-dioxaspiro[5.5]undecane (11h)



11g



11h

Reaction conditions: catalyst loading, 5 mol%; solvent, *tert*-butyl-methyl ether; molecular sieves, 3 Å (125 mg); temperature, -35 °C, 60 h. *Purification:* The product was isolated by passing the reaction mixture through Amberlyst

A26 hydroxide form (washed with MeOH and Et₂O prior to use) and washing the resin with Et₂O. Colorless liquid, combined yield 86%, **11g/11h** 1:1, dr(**11g**) 5:1, dr(**11h**) 65:1.

¹H-NMR (500 MHz, C₆D₆): δ 4.21-4.16 (m, 1Ha), 3.78-3.72 (m, 1Hb), 3.67-3.58 (m, 1Ha+1Hb), 3.56-3.52 (m, 1Hb), 3.48-3.42 (m, 1Ha), 2.06-1.95 (m, 2Hb), 1.94-1.90 (m, 1Ha), 1.76-1.24 (m, 10Ha+9Hb), 1.21 (d, *J* = 6.3 Hz, 3Ha), 1.16 (d, *J* = 6.3 Hz, 3Hb), 1.15-1.07 (m, 1Ha+1Hb);

¹³C-NMR (125 MHz, C₆D₆): 96.5, 95.5, 68.5, 65.3, 61.0, 60.2, 36.4, 36.3, 35.7, 33.2, 32.6, 31.0, 26.1, 25.9, 22.22, 22.20, 19.4, 19.13, 19.07, 18.9;

HRMS (EI (FE)) (*m/z*): [M] calcd for C₁₀H₁₈O₂, 170.1307; found, 170.1305;

[α]_D²⁵ = +51.5 ° (c = 1.22 in C₆D₆, dr(**11g**) 5:1, dr(**11h**) 65:1, **11g/11h** 1:1);

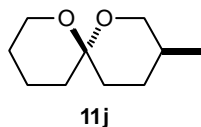
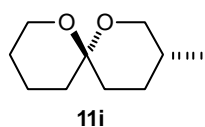
GC (Column: 25 m Lipodex-G (octakis-(2,3-di-*O*-pentyl-6-*O*-methyl)-γ-cyclodextrin), i.D. 0.25 mm; Detector: FID; Temperature: injector 220 °C, detector 350 °C, oven 60 to 90 °C, 1 °C/min; gas: 0.5 bar H₂), t_{minor}(**11g**) = 17.39 min, t_{major}(**11h**) = 20.49 min, t_{minor}(**11h**) = 24.92 min,

$t_{\text{major}}(\mathbf{11g}) = 27.15$ min, $\text{dr}(\mathbf{11g})$ 5:1, $\text{dr}(\mathbf{11h})$ 65:1, $\mathbf{11g}/\mathbf{11h}$ 48.5:51.5. (dr values are in respect to spiroacetal stereocenters, minor and major designations refer to minor and major diastereomer). Peaks in the GC spectra are assigned as follows: major peaks in the thermodynamic racemate are assigned as thermodynamic (*trans*) products. In the enantioenriched sample major enantiomers are assigned (*S*)-configurations at the spiroacetal center according to analogy with other spiroacetal products. This allows for the complete assignment of the peaks.

Racemic sample under kinetic control was prepared by treating a *tert*-butyl-methyl ether solution with 5 mol% of $(\text{PhO})_2\text{PO}_2\text{H}$ at -25 °C for 12 h. Low conversion, $\text{dr}(\mathbf{11g}/\mathbf{11h}) = 1:1$.

Racemic sample under thermodynamic control was prepared by treating an ethyl acetate solution with 3 N HCl at room temperature for 10 min. $\text{dr}(\mathbf{11g}/\mathbf{11h}) = 1:124$.

(3*R*,6*S*)-3-Methyl-1,7-dioxaspiro[5.5]undecane (11i) and (3*S*,6*S*)-3-methyl-1,7-dioxaspiro[5.5]undecane (11j)



Reaction conditions: catalyst loading, 5 mol%; solvent, *tert*-butyl-methyl ether; molecular sieves, 3 Å (125 mg); temperature, -35 °C, 60 h. The mixture was

concentrated to <1 ml, silica gel column using 5% Et_2O /pentane as eluent. Colorless liquid, yield 70%, $\mathbf{11i}/\mathbf{11j}$ 1:1, $\text{dr}(\mathbf{11i})$ 23:1, $\text{dr}(\mathbf{11j})$ 50:1. Analysis of the sample isolated by TLC prior to purification: $\text{dr}(\mathbf{11i})$ 20:1, $\text{dr}(\mathbf{11j})$ 43:1.

$^1\text{H-NMR}$ (500 MHz, C_6D_6): δ 3.86 (dd, $J = 11, 3.0$ Hz, 1H), 3.71-3.66 (m, 2H), 3.56-3.51 (m, 3H), 3.34 (t, $J = 10.9$ Hz, 1H), 3.26-3.24 (m, 1H), 2.21-2.13 (m, 1H), 2.02-1.91 (m, 2H), 1.72-1.62 (m, 4H), 1.61-1.53 (m, 2H), 1.50-1.35 (m, 9H), 1.34-1.22 (m, 3H), 1.20-1.15 (m, 1H), 1.03 (d, $J = 7.1$ Hz, 3H), 0.64 (d, $J = 6.5$ Hz, 3H);

$^{13}\text{C-NMR}$ (125 MHz, C_6D_6): δ 95.1, 94.5, 66.6, 64.9, 60.4, 60.3, 36.4, 36.0, 35.8, 31.2, 30.8, 27.82, 27.80, 25.8, 24.9, 19.2, 19.1, 17.4, 16.6;

HRMS (EI (FE)) (m/z): [M] calcd for $\text{C}_{10}\text{H}_{18}\text{O}_2$, 170.1307; found, 170.1305;

$[\alpha]_D^{25} = +88.4$ ° ($c = 0.99$ in C_6D_6 , $\text{dr}(\mathbf{11i})$ 23:1, $\text{dr}(\mathbf{11j})$ 50:1, $\mathbf{11i}/\mathbf{11j}$ 1:1);

GC (Column: 30 m BGB-176SE/SE52 (2,3-dimethyl-6-*tert*-butyldimethylsilyl- β -cyclodextrin), i.D. 0.25 mm, df. 0.25 μm ; Detector: FID; Temperature: injector 220 °C, detector 320 °C, oven 60 to 150 °C, 1 °C/min; gas: 0.5 bar H_2), $t_{\text{major}}(\mathbf{11i}) = 38.04$ min, $t_{\text{major}}(\mathbf{11j}) = 38.81$ min, $t_{\text{minor}}(\mathbf{11i}) = 42.43$ min, $t_{\text{minor}}(\mathbf{11j}) = 44.87$ min, $\text{dr}(\mathbf{11i})$ 23:1, $\text{dr}(\mathbf{11j})$ 50:1. (dr values are in respect to

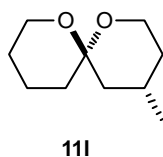
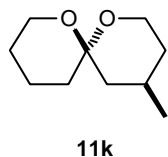
7. EXPERIMENTAL SECTION

spiroacetal stereocenters, minor and major designations refer to minor and major diastereomer). Peaks in the GC spectra are assigned as follows: major peaks in the thermodynamic racemate are assigned as thermodynamic (*cis*) products. In the enantioenriched sample major enantiomers are assigned (*S*)-configurations at the spiroacetal center according to analogy with other spiroacetal products. This allows for the complete assignment of the peaks.

Racemic sample under kinetic control was prepared by treating a *tert*-butyl-methyl ether solution with 5 mol% of (PhO)₂PO₂H at room temperature for 1 h. dr(**11i**/**11j**) = 1:1.

Racemic sample under thermodynamic control was prepared by treating a *tert*-butyl-methyl ether solution with 3 N HCl at room temperature for 1.5 h. dr(**11i**/**11j**) = 1:9.

(4*R*,6*S*)-4-Methyl-1,7-dioxaspiro[5.5]undecane (**11k**) and (4*S*,6*S*)-4-methyl-1,7-dioxaspiro[5.5]undecane (**11l**)



Reaction conditions: catalyst loading, 5-10 mol%; solvent, *tert*-butyl-methyl ether; molecular sieves, 3 Å (125 mg); temperature, -35 °C, 72 h with 5 mol% of the catalyst, then more catalyst (5 mol% in 1 ml MTBE) was added and

the mixture stirred for additional 48 h. *Purification:* The mixture was concentrated to <1 ml, silica gel column using 5% Et₂O/pentane as eluent. Colorless liquid, combined yield 81%, **11k**/**11l** 1:1.15, dr(**11k**) 7:1, dr(**11l**) 100:1. Analysis of the sample isolated by TLC prior to purification: dr(**11k**) 7:1, dr(**11l**) 99:1.

¹H-NMR (500 MHz, C₆D₆): δ 3.88-3.79 (m, 2Ha), 3.70-3.64 (m, 2Hb), 3.59 (ddd, *J* = 10.9, 5.0, 1.3 Hz, 1Hb), 3.56-3.52 (m, 1Ha+1Hb), 3.38 (dt, *J* = 11.5, 4.9 Hz, 1Ha), 2.10-1.94 (m, 2Hb), 1.92-1.83 (m, 1Ha), 1.75-1.63 (m, 2Ha+2Hb), 1.59-1.53 (m, 2Ha), 1.50-1.22 (4Ha+6Hb), 1.13-1.02 (m, 2Ha), 1.10 (d, *J* = 7.0 Hz, 3Ha), 0.95 (t, *J* = 12.6 Hz, 1Hb), 0.77 (d, *J* = 6.6 Hz, 3Hb);

¹³C-NMR (125 MHz, C₆D₆): δ 96.3, 95.4, 60.6, 60.3, 60.2, 57.8, 45.0, 42.5, 36.2, 34.5, 34.2, 32.1, 25.9, 25.8, 25.7, 25.2, 22.5, 21.1, 19.2, 19.1;

HRMS (EI (FE)) (*m/z*): [M] calcd for C₁₀H₁₈O₂, 170.1307; found, 170.1305;

[α]_D²⁵ = +83.5 ° (*c* = 1.15 in C₆D₆, dr(**11k**) 7:1, dr(**11l**) 100:1, **11k**/**11l** 1:1.15);

GC (Column: 30 m BGB-176/BGB-15 (2,3-dimethyl-6-*tert*-butyldimethylsilyl-β-cyclodextrin), i.D. 0.25 mm, df. 0.25 μm; Detector: FID; Temperature: injector 220 °C, detector 320 °C, oven 60 to 100 °C, 0.5 °C/min; gas: 0.5 bar H₂), t_{major}(**11l**) = 60.48 min, t_{major}(**11k**) = 68.95 min, t_{minor}(**11k**) =

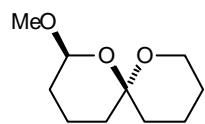
7. EXPERIMENTAL SECTION

70.27 min, $t_{\text{minor}}(\mathbf{11l}) = 75.97$ min, $\text{dr}(\mathbf{11k})$ 7:1, $\text{dr}(\mathbf{11l})$ 100:1. (dr values are in respect to spiroacetal stereocenters, minor and major designations refer to minor and major diastereomer). Peaks in the GC spectra are assigned as follows: major peaks in the thermodynamic racemate are assigned as thermodynamic (*trans*) products. In the enantioenriched sample major enantiomers are assigned (*S*)-configurations at the spiroacetal center according to analogy with other spiroacetal products. This allows for the complete assignment of the peaks. Minor impurities in the GC traces were **11i** and **11j** formed from **12i** which was the minor impurity in the starting material.

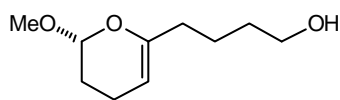
Racemic sample under kinetic control was prepared by treating a *tert*-butyl-methyl ether solution with 5 mol% of $(\text{PhO})_2\text{PO}_2\text{H}$ at room temperature for 1 h. $\text{dr}(\mathbf{11k}/\mathbf{11l}) = 1:2.5$.

Racemic sample under thermodynamic control was prepared by treating a *tert*-butyl-methyl ether solution with 3 N HCl at room temperature for 1.5 h. $\text{dr}(\mathbf{11k}/\mathbf{11l}) = 1:60$.

(2*S*,6*S*)-2-Methoxy-1,7-dioxaspiro[5.5]undecane (**11n**) and (*R*)-4-(2-methoxy-3,4-dihydro-2*H*-pyran-6-yl)butan-1-ol ((*R*)-**12m**)



11n



(*R*)-**12m**

Reaction conditions: catalyst loading, 5 mol%; solvent, *tert*-butyl-methyl ether; molecular sieves, 4 Å (50 mg); temperature, -25 °C, 36 h. *Purification:* reaction mixture

was filtered through Amberlyst A26 hydroxide form (washed with MeOH and Et₂O prior to use). The resin was washed with Et₂O to give a solution mostly containing the spiroacetal product. The resin was then washed with MeOH to elute the remaining starting material. The solutions were concentrated, and separately purified by silica gel chromatography using 5-60% Et₂O/pentane as eluent. Spiroacetal **11n**, colorless liquid, yield 70%. Alcohol (*R*)-**12m**, colorless liquid, 20 mg, 86%.

11n:

¹H-NMR (500 MHz, C₆D₆): δ 4.63 (dd, $J = 9.7, 2.3$ Hz, 1H), 3.69-3.64 (m, 1H), 3.55-3.51 (m, 1H), 3.39 (s, 3H), 1.99-1.88 (m, 2H), 1.78-1.74 (m, 1H), 1.69-1.75 (m, 1H), 1.54-1.30 (m, 6H), 1.27-1.19 (m, 2H);

¹³C-NMR (125 MHz, C₆D₆): δ 97.9, 97.3, 60.6, 55.5, 36.1, 35.4, 31.2, 25.8, 19.1, 18.2;

HRMS (EI (FE)) (m/z): [M] calcd for C₁₀H₁₈O₃, 186.1256; found, 186.1254;

7. EXPERIMENTAL SECTION

$[\alpha]_D^{25} = +92.3^\circ$ (c = 0.54 in C_6D_6 , er 97.5:2.5, dr 82:1);

GC (Column: 30 m BGB-178/BGB-15 (2,3-diethyl-6-*tert*-butyldimethylsilyl- β -cyclodextrin), i.D. 0.25 mm, df. 0.25 μ m; Detector: FID; Temperature: injector 220 $^\circ$ C, detector 320 $^\circ$ C, oven 115 $^\circ$ C; gas: 0.5 bar H_2), $t_{major} = 15.87$ min, $t_{minor} = 16.75$ min, minor diastereomer ($t_{major} = 17.91$ min, $t_{minor} = 18.97$ min) er = 97.5:2.5, dr = 82:1.

(R)-12m:

1H -NMR (500 MHz, C_6D_6): δ 4.74 (t, $J = 2.9$ Hz, 1H), 4.54-4.52 (m, 1H), 3.37-3.34 (m, 2H), 3.29 (s, 3H), 2.26-2.18 (m, 1H), 2.11-2.00 (m, 2H), 1.77-1.68 (m, 2H), 1.60-1.53 (m, 3H), 1.46-1.38 (m, 2H), 0.64 (bs, 1H);

^{13}C -NMR (125 MHz, C_6D_6): δ 150.9, 98.5, 96.4, 62.5, 55.3, 34.4, 32.5, 26.7, 23.7, 16.9; HRMS (EI (FE)) (m/z): [M] calcd for $C_{10}H_{18}O_3$, 186.1256; found, 186.1254;

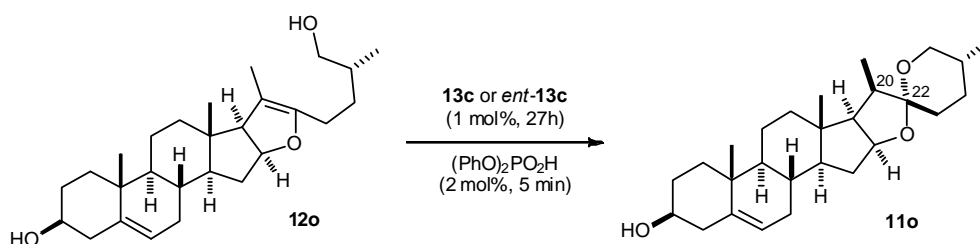
$[\alpha]_D^{25} = -83.3^\circ$ (c = 0.67 in C_6D_6 , er 97:3);

For determination of the enantiomeric ratio of **(R)-12m**, a sample in C_6D_6 /EtOAc 1:2 (1 ml) was treated with 10 mol% of $(PhO)_2PO_2H$ at room temperature for 15 min. A sample of the major diastereomer of the product spiroacetal was isolated for GC analysis by thin layer chromatography on aluminum oxide using EtOAc/hexane as eluent.

GC (Column: 30 m BGB-178/BGB-15 (2,3-diethyl-6-*tert*-butyldimethylsilyl- β -cyclodextrin), i.D. 0.25 mm, df. 0.25 μ m; Detector: FID; Temperature: injector 220 $^\circ$ C, detector 320 $^\circ$ C, oven 115 $^\circ$ C; gas: 0.5 bar H_2), $t_{minor} = 15.84$ min, $t_{major} = 16.70$ min, er 97:3.

Racemic sample under kinetic control was prepared by treating a *tert*-butyl-methyl ether solution with 5 mol% of $(PhO)_2PO_2H$ at -25° C for 12 h. dr = 2.4:1 (thermodynamic spiroacetal major).

Racemic sample under thermodynamic control was prepared by treating an ethyl acetate solution with 3 N HCl at room temperature for 10 min. dr = 70:1.

20-*epi*-Diosgenin (11o)^[145-146]

Reaction conditions: scale, 0.025 mmol, catalyst loading, 1 mol%; solvent, DCE (1 ml); molecular sieves, 4 Å (12.5 mg); temperature, 20 °C, 27 h. *Purification:* silica gel column using MTBE as eluent. Colorless solid, yield 89%. Reaction performed with *ent*-**13c** as the catalyst gave similar reactivity and yield of 88%.

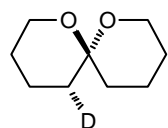
The reaction with achiral catalyst (PhO)₂PO₂H (2 mol%) gave full conversion in 5 min (yield 87%). For small substrates (PhO)₂PO₂H seems to be a less reactive catalyst than **13c**. The (PhO)₂PO₂H-catalyzed racemate preparation with substrate **12g** proceeded slower than the reaction with catalyst **13c**.

All three reactions gave only **11o** with dr>20:1:1:1.

¹H-NMR (500 MHz, CD₂Cl₂ + K₂CO₃(s) to neutralize any acid impurity): δ 5.35-5.34 (m, 1H), 4.41-4.37 (m, 1H), 3.49-3.42 (m, 1H), 4.40 (d, *J* = 8.5 Hz, 2H), 2.46-4.0 (m, 1H), 2.28-2.16 (m, 2H), 2.04-1.96 (m, 3H), 1.91-1.73 (m, 4H), 1.65-1.37 (m, 10H), 1.31 (td, *J* = 13.0, 3.8 Hz, 1H), 1.86-1.13 (m, 1H, overlapped), 1.13 (d, *J* = 8.0 Hz, 3H, overlapped), 1.09-0.99 (m, 2H, overlapped), 1.01 (s, 3H), 0.96 (s, 3H), 0.91 (td, *J* = 11.3, 5.3 Hz, 1H), 0.77 (d, *J* = 6.3 Hz, 3H);

¹³C-NMR (125 MHz, CD₂Cl₂ + K₂CO₃(s) to neutralize any acid impurity): δ 141.4, 121.6, 108.6, 81.3, 72.0, 68.3, 60.9, 58.0, 50.5, 46.8, 42.7, 42.1, 40.2, 37.6, 36.9, 32.4, 32.2, 32.0, 31.6, 31.0, 29.0, 20.8, 19.6, 17.3, 16.3, 11.5;

HRMS (ESI+) (*m/z*): [M+Na] calcd for C₂₇H₄₂O₃Na, 437.3026; found, 437.3031.

(5*R*,6*S*)-5-deutero-1,7-Dioxaspiro[5.5]undecane

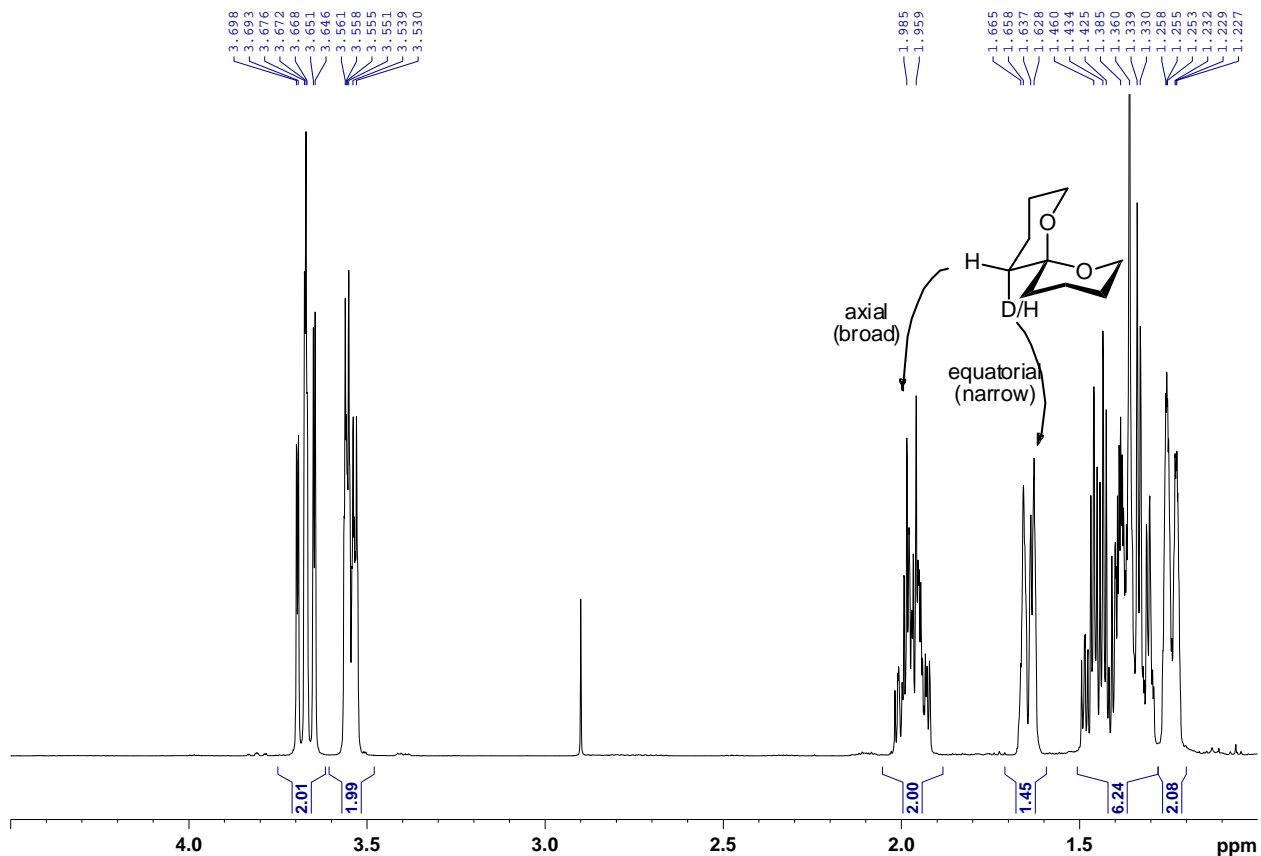
Deuterated starting material was obtained by washing EtOAc solution with D₂O.

Reaction conditions: catalyst loading, 1 mol%; solvent, DCE; molecular sieves, 4 Å (50 mg); temperature, r.t., 2 h. *Purification:* mixture concentrated to <1 ml, silica gel column using 5% Et₂O/pentane as eluent. Colorless liquid, yield 83%.

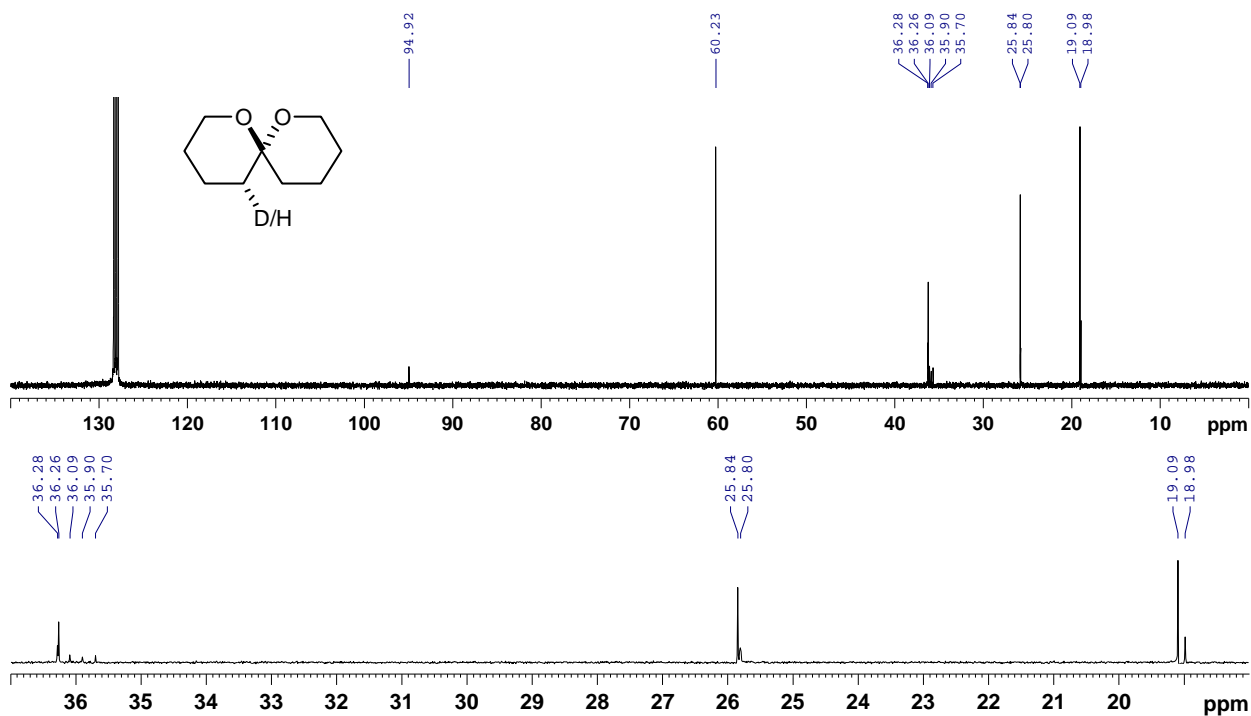
7. EXPERIMENTAL SECTION

Based on the ^1H NMR given below the incorporation of the deuterium at the equatorial position of the product could be observed (ca. 50%). The equatorial proton possess broader signal, compared to the axial proton, due to the smaller sum of ^1H - ^1H coupling constants.

^1H NMR (500 MHz, C_6D_6)

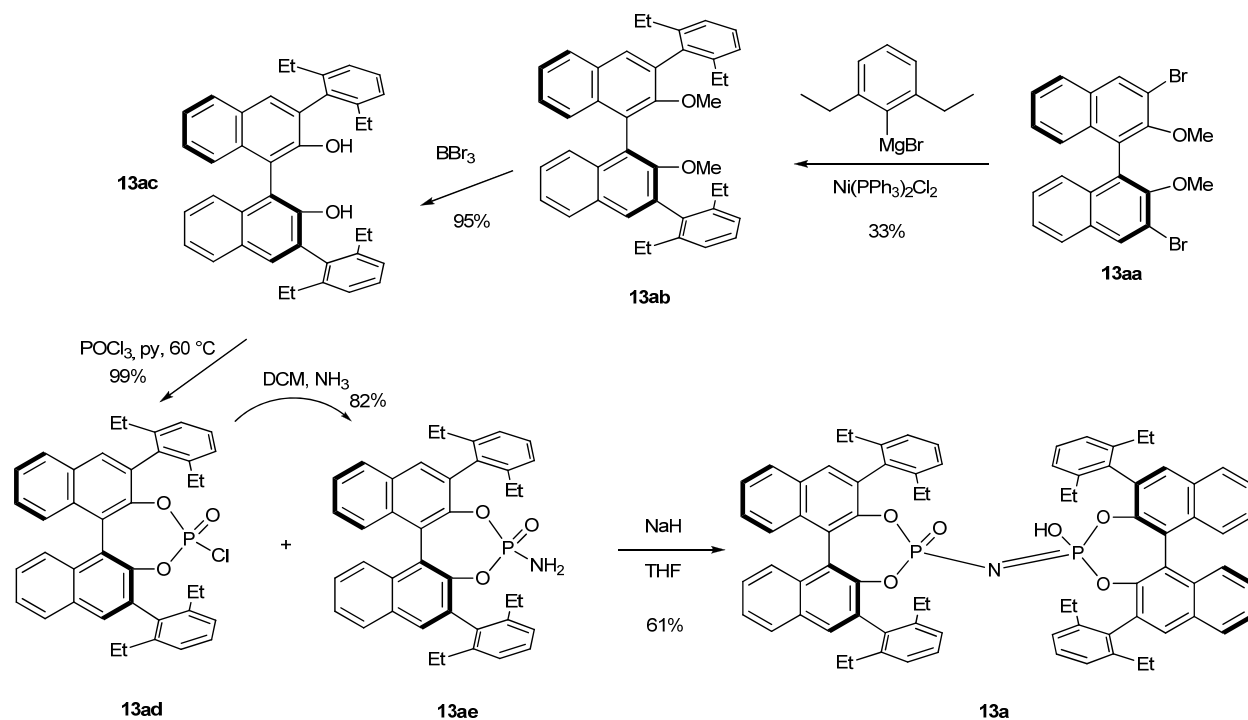
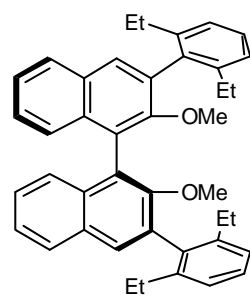


^{13}C NMR (100 MHz, C_6D_6)



7.5. Confined Brønsted acids

7.5.1. Synthesis

13a**(S)-2,2'-Dimethoxy-3,3'-bis(2,6-diethylphenyl)-1,1'-binaphthalene (13ab)**

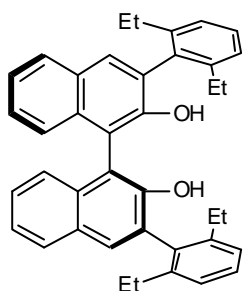
To magnesium turnings (168 mg, 6.9 mmol) activated with 1,2-dibromoethane in diethyl ether (1 ml), 2-bromo-1,3-diethylbenzene (980 mg, 4.6 mmol) and diethylether (5 ml) were added alternately. After complete addition the mixture was refluxed (oil bath heating) for 17 h. After cooling to ambient temperature, the solution was diluted with Et_2O (10 ml), and added to a mixture of (*S*)-3,3'-dibromo-2,2'-dimethoxy-1,1'-binaphthalene (**13aa**, 543 mg, 1.15 mmol) and $\text{Ni}(\text{PPh}_3)_2\text{Cl}_2$ (113 mg, 0.173 mmol) in anhydrous diethyl ether (10 mL). The reaction mixture was refluxed for 24 h, cooled to ambient temperature, carefully treated with saturated aqueous NH_4Cl solution (10 ml) and water (10 ml), and extracted with CH_2Cl_2 (2 · 25 ml). The combined organic layers were dried (MgSO_4), filtered, and the solvent removed under reduced pressure. The residue was purified by column chromatography on silica gel using 20% CH_2Cl_2 /hexane as the eluent yielding the title compound as a colorless solid (222 mg, 33%).

¹H-NMR (500 MHz, CD₂Cl₂): δ 7.90 (d, *J* = 8.2 Hz, 2H), 7.75 (s, 2H), 7.44-7.41 (m, 2H), 7.34-7.26 (m, 6H), 7.21 (t, *J* = 6.6 Hz, 4H), 3.09 (s, 6H), 2.52 (q, *J* = 7.6 Hz, 4H), 2.47 (q, *J* = 7.6 Hz, 4H), 1.16 (t, *J* = 7.6 Hz, 6H), 1.08 (t, *J* = 7.6 Hz, 6H);

¹³C-NMR (125 MHz, CD₂Cl₂): δ 154.8, 143.1, 142.9, 137.5, 134.21, 134.18, 131.2, 130.8, 128.3, 128.1, 126.4, 125.9, 125.8, 125.3, 125.1, 60.1, 27.4, 27.2, 15.5, 15.3;

HRMS (ESI+) (*m/z*): [M+Na] calcd for C₄₂H₄₂O₂Na, 601.3077; found, 601.3080.

(S)-3,3'-Bis(2,6-diethylphenyl)-[1,1'-binaphthalene]-2,2'-diol (13ac)



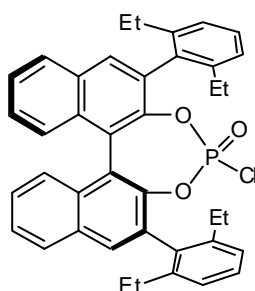
A 1 M solution of BBr₃ in CH₂Cl₂ (1.48 ml, 1.48 mmol) was added dropwise to the solution of (S)-**13ab** (214 mg, 0.37 mmol) in CH₂Cl₂ (5 ml) at 0 °C under argon. After 17 h at room temperature, the solution was cooled to 0 °C, water (25 ml) was carefully added, and the mixture was extracted with CH₂Cl₂ (50 ml). The organic layer was washed with saturated aqueous Na₂CO₃ solution (50 ml), dried (MgSO₄), filtered, and the solvent was removed under reduced pressure. The residue was purified by column chromatography on silica gel using 30% CH₂Cl₂/hexane as the eluent yielding the title compound as a colorless solid (194 mg, 95%).

¹H-NMR (500 MHz, CD₂Cl₂): δ 7.91 (d, *J* = 8.1 Hz, 2H), 7.79 (s, 2H), 7.41-7.38 (m, 2H), 7.36-7.32 (m, 4H), 7.24-7.22 (m, 6H), 5.04 (s, 2H), 2.58-2.34 (m, 8H), 1.10 (t, *J* = 7.6 Hz, 6H), 1.02 (t, *J* = 7.5 Hz, 6H);

¹³C-NMR (125 MHz, CD₂Cl₂): δ 150.7, 143.90, 143.89, 135.0, 133.9, 131.3, 129.6, 129.2, 128.9, 128.7, 127.2, 126.5, 124.6, 124.2, 113.4, 27.32, 27.30, 15.5, 15.4;

HRMS (ESI+) (*m/z*): [M+Na] calcd for C₄₀H₃₈O₂Na, 573.2764; found, 573.2768.

(S)-4-Chloro-2,6-bis(2,6-diethylphenyl)dinaphtho[2,1-d':1',2'-f][1,3,2]dioxaphosphepine 4-oxide (13ad)



To a solution of (S)-**13ac** (186 mg, 0.338 mmol) in pyridine (1 ml) under argon was added POCl₃ (95 μl, 155 mg, 1.014 mmol) at room temperature. The mixture was stirred at 60 °C for 1.5 h and then concentrated to dryness under vacuum. The residue was passed through a short silica gel column (5 g) using 20% EtOAc/hexane as the eluent yielding the title compound as a colorless solid (99%).

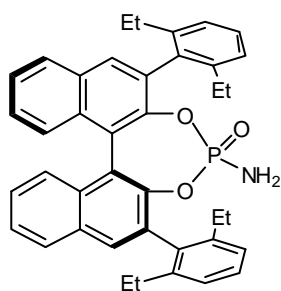
¹H-NMR (500 MHz, CD₂Cl₂): δ 8.01 (t, *J* = 7.1 Hz, 2H), 7.97 (s, 1H), 7.93 (s, 1H), 7.60-7.56 (m, 2H), 7.39-7.34 (m, 5H), 7.33 (t, *J* = 8.5 Hz, 1H), 7.27 (d, *J* = 7.7 Hz, 2H), 7.20 (d, *J* = 7.6 Hz, 1H), 7.18 (d, *J* = 7.5 Hz, 1H), 2.54-2.32 (m, 8H), 1.26 (t, *J* = 7.5 Hz, 3H), 1.18 (t, *J* = 7.5 Hz, 3H), 1.01 (t, *J* = 7.5 Hz, 3H, overlapped), 1.00 (t, *J* = 7.5 Hz, 3H, overlapped);

¹³C-NMR (125 MHz, CD₂Cl₂): δ 145.1, 144.9, 143.8, 143.5, 143.0, 142.9, 134.6, 134.4, 133.20, 133.15, 132.49, 132.45, 132.2, 131.52, 131.49, 128.9, 128.8, 127.5, 127.3, 127.2, 126.8, 126.3, 125.9, 125.6, 125.3, 122.6, 122.53, 122.47, 122.4, 27.9, 27.3, 27.12, 27.09, 16.2, 15.4, 15.0, 14.8 (including signals due to unassigned C-P-coupling, some signals are overlapped);

³¹P-NMR (202 MHz, CD₂Cl₂): δ 7.29 (s);

HRMS (ESI+) (*m/z*): [M+Na] calcd for C₄₀H₃₆O₃ClPNa, 653.1983; found, 653.1979.

(S)-4-Amino-2,6-bis(2,6-diethylphenyl)dinaphtho[2,1-*d'*:1',2'-*f'*][1,3,2]dioxaphosphepine 4-oxide (13ae)



A solution of (*S*)-**13ad** (95 mg, 0.15 mmol) in DCM (1 ml) under argon, was cooled to $-78\text{ }^{\circ}\text{C}$ and anhydrous ammonia gas was condensed into the reaction flask (ca. 7 ml). The cooling bath was removed and the mixture was allowed to warm to room temperature. The reaction mixture was then concentrated to dryness under vacuum. Residue was passed through short silica gel column (5 g) using CH₂Cl₂ as the eluent yielding the title compound as a colorless solid (75 mg, 82%).

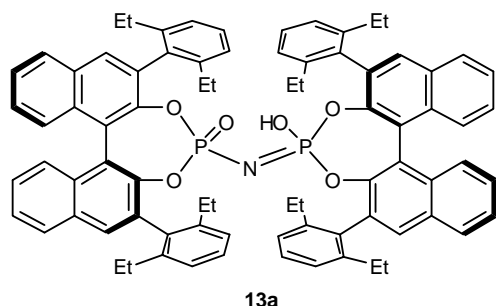
¹H-NMR (500 MHz, CD₂Cl₂): δ 7.99 (d, *J* = 8.3 Hz, 1H), 7.97 (d, *J* = 8.3 Hz, 1H), 7.92 (s, 1H), 7.86 (s, 1H), 7.56-7.51 (m, 2H), 7.38-7.32 (m, 6H), 7.25 (t, *J* = 7.3 Hz, 2H), 7.20 (d, *J* = 7.6 Hz, 1H), 7.14 (d, *J* = 7.6 Hz, 1H), 2.65 (d, *J* = 6.7 Hz, 2H), 2.58-2.29 (m, 8H), 1.26 (t, *J* = 7.5 Hz, 3H), 1.16 (t, *J* = 7.5 Hz, 3H), 1.01 (t, *J* = 7.6 Hz, 3H, overlapped), 1.00 (t, *J* = 7.6 Hz, 3H, overlapped);

¹³C-NMR (125 MHz, CD₂Cl₂): δ 146.0, 145.8, 144.0, 143.8, 142.9, 142.2, 135.6, 135.3, 132.7, 132.6, 132.51, 132.46, 132.4, 131.7, 131.5, 128.8, 128.71, 128.66, 128.5, 127.4, 127.3, 126.9, 126.8, 126.30, 126.26, 126.2, 125.8, 125.7, 125.1, 122.9, 122.8, 122.5, 122.4, 27.8, 27.3, 27.2, 27.1, 16.4, 15.3, 15.0, 14.8 (including signals due to unassigned C-P-coupling, some signals are overlapped);

³¹P-NMR (202 MHz, CD₂Cl₂): δ 12.07 (s);

HRMS (ESI+) (*m/z*): [M+Na] calcd for C₄₀H₃₈NO₃PNa, 634.2482; found, 634.2479.

***O,O*-syn-Imidodiphosphoric acid 13a**



Sodium hydride (60% dispersion of in mineral oil, 13.7 mg, 0.34 mmol) was added to a solution of (*S*)-**13ae** (70 mg, 0.114 mmol) and (*S*)-**13ad** (114 mg, 0.18 mmol) in THF (2 ml) under argon at room temperature. After 2.5 days at room temperature 10% aqueous HCl solution (5 ml) and DCM (5 ml) were added to the

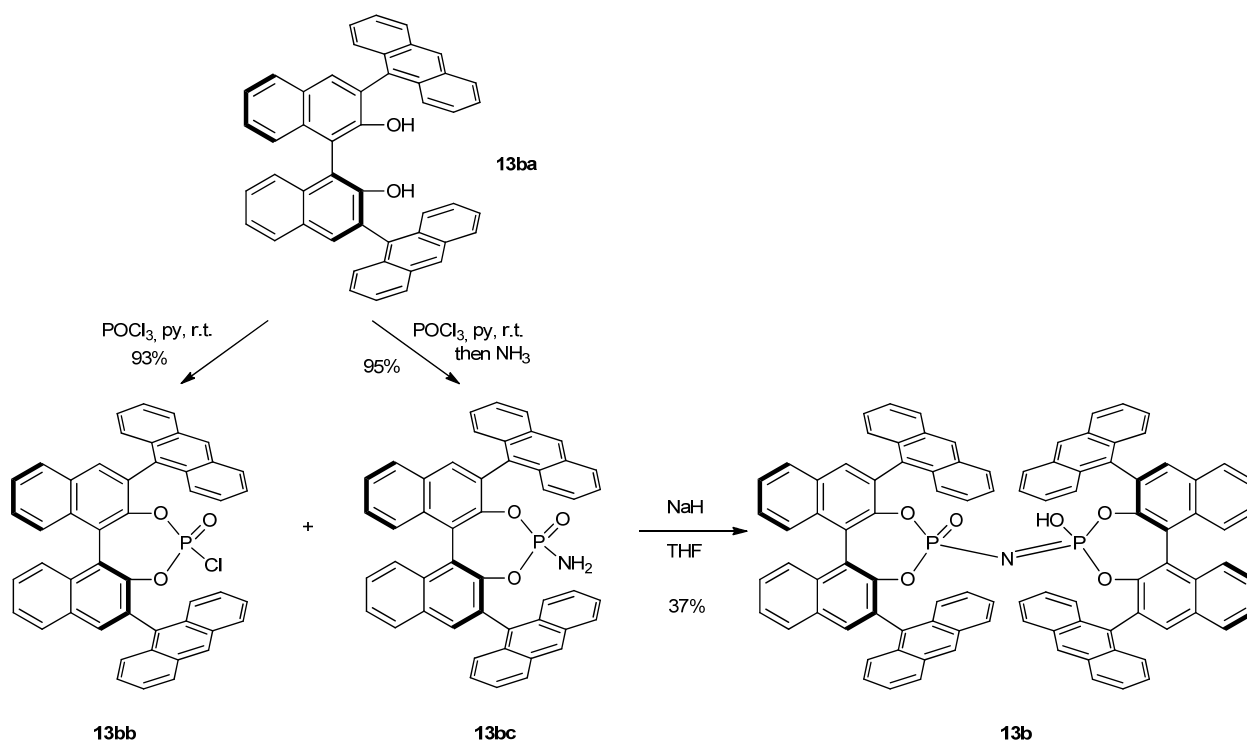
mixture, which was stirred for 4 h. The organic layer was separated and the solvent removed under reduced pressure. The residue was purified by column chromatography on aluminum oxide (activity I) using 0-12% EtOAc/DCM as the eluent giving a colorless solid. The solid was dissolved in CH₂Cl₂ (5 ml) and stirred with 3 N aqueous HCl (10 ml) for 4 h. The organic layer was separated, and concentrated under reduced pressure to give the title compound as a colorless solid (76 mg, 61%).

¹H-NMR (500 MHz, acetone-d₆): δ 8.05 (d, *J* = 8.2 Hz, 2H), 8.02 (d, *J* = 8.2 Hz, 2H), 7.89 (s, 2H), 7.69 (s, 2H), 7.55 (t, *J* = 7.5 Hz, 2H), 7.50 (t, *J* = 7.5 Hz, 2H), 7.45 (t, *J* = 7.6 Hz, 2H), 7.40 (d, *J* = 8.7 Hz, 2H), 7.28 (t, *J* = 7.7 Hz, 2H), 7.18 (t, *J* = 7.6 Hz, 2H), 7.11 (t, *J* = 7.6 Hz, 2H), 7.07 (d, *J* = 8.6, 2H), 7.04 (d, *J* = 7.6 Hz, 2H), 7.00 (d, *J* = 7.4 Hz, 2H), 6.93 (d, *J* = 7.4 Hz, 2H), 6.65 (d, *J* = 7.6 Hz, 2H), 2.33-2.07 (m, 12H), 1.96-1.89 (m, 2H), 1.37-1.31 (m, 2H), 1.05 (t, *J* = 7.7 Hz, 6H), 1.03 (t, *J* = 7.7 Hz, 6H), 0.79 (t, *J* = 7.5 Hz, 6H), 0.01 (t, *J* = 7.5 Hz, 6H);

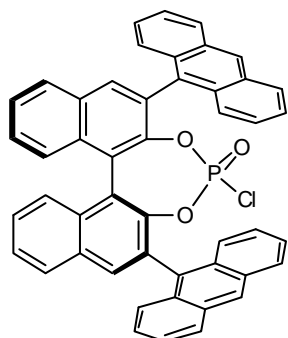
¹³C-NMR (125 MHz, acetone-d₆): δ 146.7, 146.4, 144.0, 143.6, 143.3, 142.7, 136.1, 136.0, 133.5, 133.1, 133.0, 132.8, 132.5, 132.0, 131.7, 129.2, 129.1, 128.6, 128.5, 127.5, 127.3, 127.1, 127.1, 126.8, 126.5, 126.4, 125.9, 125.5, 125.3, 123.2, 122.8, 28.0, 27.7, 27.4, 27.3, 15.8, 15.4, 15.3, 14.9;

³¹P-NMR (202 MHz, acetone-d₆): δ 5.73 (s);

HRMS (ESI⁻) (*m/z*): [M-H] calcd for C₈₀H₇₂NO₆P₂, 1204.4840; found, 1204.4846.

13b

(S)-2,6-Di(anthracen-9-yl)-4-chlorodinaphtho[2,1-d:1',2'-f][1,3,2]dioxaphosphepine 4-oxide (13bb)



To a solution of (*S*)-**13ba** (215.4 mg, 0.337 mmol) in pyridine (1 ml) under argon was added POCl_3 (94 μl , 155 mg, 1.011 mmol) at room temperature. The mixture was stirred for 20 h and then concentrated to dryness under vacuum. The residue was passed through a short silica gel column (5 g) using DCM as the eluent yielding the title compound as a colorless solid (226 mg, 93%).

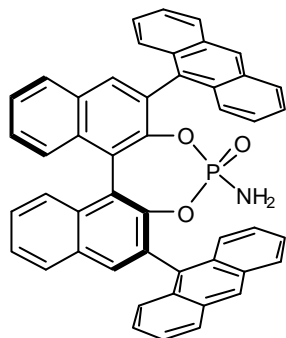
$^1\text{H-NMR}$ (500 MHz, CD_2Cl_2): δ 8.60 (s, 1H), 8.58 (s, 1H), 8.24 (s, 1H), 8.15 (s, 1H), 8.11-8.04 (m, 6H), 7.87 (dd, $J = 8.9$ Hz, 0.8 Hz, 1H), 7.76 (d, $J = 8.9$ Hz, 0.8 Hz, 1H), 7.74-7.67 (m, 5H), 7.64 (dd, $J = 8.8$, 0.7 Hz, 1H), 7.58-7.54 (m, 2H), 7.50-7.29 (m, 8H);

$^{13}\text{C-NMR}$ (125 MHz, CD_2Cl_2): δ 147.2, 147.1, 146.1, 146.0, 135.5, 135.2, 133.0, 132.5, 132.2, 132.0, 131.9, 131.42, 131.41, 131.3, 131.0, 130.70, 130.67, 130.6, 130.4, 129.90, 129.85, 129.1, 129.04, 129.00, 128.9, 128.6, 128.4, 128.3, 127.84, 127.77, 127.6, 127.3, 127.2, 126.7, 126.4, 126.2, 126.1, 126.0, 125.71, 125.70, 125.65, 125.43, 125.40, 123.0, 122.9 (including signals due to unassigned C-P-coupling, some signals are overlapped);

$^{31}\text{P-NMR}$ (202 MHz, CD_2Cl_2): δ 7.58 (s);

HRMS (ESI+) (m/z): $[M+Na]$ calcd for $C_{48}H_{28}O_3ClPNa$, 741.1357; found, 741.1359.

(S)-4-Amino-2,6-di(anthracen-9-yl)dinaphtho[2,1-d:1',2'-f][1,3,2]dioxaphosphepine 4-oxide (13bc)



To a solution of (S)-**13ba** (179.5 mg, 0.281 mmol) in pyridine (1 ml) under argon was added $POCl_3$ (78.6 μ l, 129.3 mg, 0.843 mmol) at room temperature. After 20 h the mixture was cooled to -78 °C and anhydrous ammonia gas was condensed into the reaction flask (ca. 7 ml). The cooling bath was removed and the mixture was allowed to warm to room temperature. The reaction mixture was then concentrated to dryness under vacuum. To the residue water (5 ml)

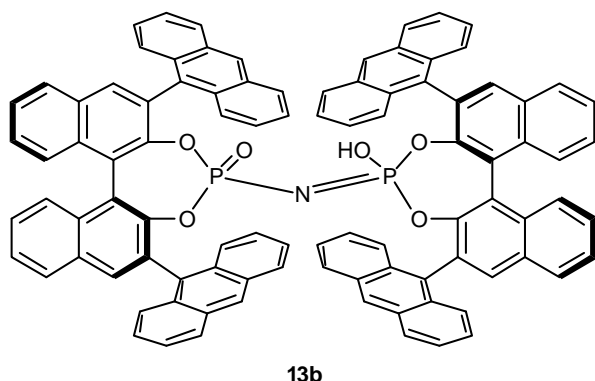
was added and the mixture was extracted with DCM (5 \cdot 5 ml). The organic extracts were washed with 10% HCl (10 ml) and brine (10 ml), dried ($MgSO_4$), filtered, and concentrated. The residue was purified by chromatography on a short silica gel column (5 g) using 0-2% EtOAc/ CH_2Cl_2 as the eluent yielding the title compound as a colorless solid (185 mg, 95%).

1H -NMR (500 MHz, CD_2Cl_2): δ 8.60 (s, 1H), 8.55 (s, 1H), 8.17 (s, 1H), 8.11-8.06 (m, 5H), 8.03 (d, J = 8.4 Hz, 2H), 7.81 (d, J = 8.9 Hz, 1H), 7.77-7.71 (m, 4H), 7.68-7.63 (m, 3H), 7.56-7.48 (m, 3H), 7.45-7.40 (m, 4H), 7.34-7.27 (m, 3H), 1.98 (d, J = 7.0 Hz, 2H);

^{13}C -NMR (125 MHz, CD_2Cl_2): δ 146.9, 146.8, 146.1, 146.0, 134.54, 134.50, 133.2, 133.0, 132.0, 131.9, 131.85, 131.83, 131.76, 131.6, 131.45, 131.38, 131.3, 131.19, 131.18, 130.9, 130.8, 130.6, 130.35, 130.32, 129.5, 129.0, 128.91, 128.87, 128.3, 128.25, 128.18, 127.9, 127.7, 127.6, 127.5, 127.4, 126.7, 126.63, 126.60, 126.5, 126.4, 126.1, 125.91, 125.85, 125.7, 125.5, 125.3, 123.2, 123.1, 122.94, 122.92 (including signals due to unassigned C-P-coupling, some signals are overlapped);

^{31}P -NMR (202 MHz, CD_2Cl_2): δ 11.84 (s);

HRMS (ESI+) (m/z): $[M+Na]$ calcd for $C_{48}H_{30}NO_3PNa$, 722.1856; found, 722.1855.

***O,O*-syn-Imidodiphosphoric acid 13b**

Sodium hydride (60% dispersion of in mineral oil, 24 mg, 0.60 mmol) was added to a solution of (*S*)-**13bc** (140 mg, 0.20 mmol) and (*S*)-**13bb** (173 mg, 0.24 mmol) in THF (2 ml) under argon at room temperature. After 4 days at room temperature, water (5 ml) was added and the mixture was extracted

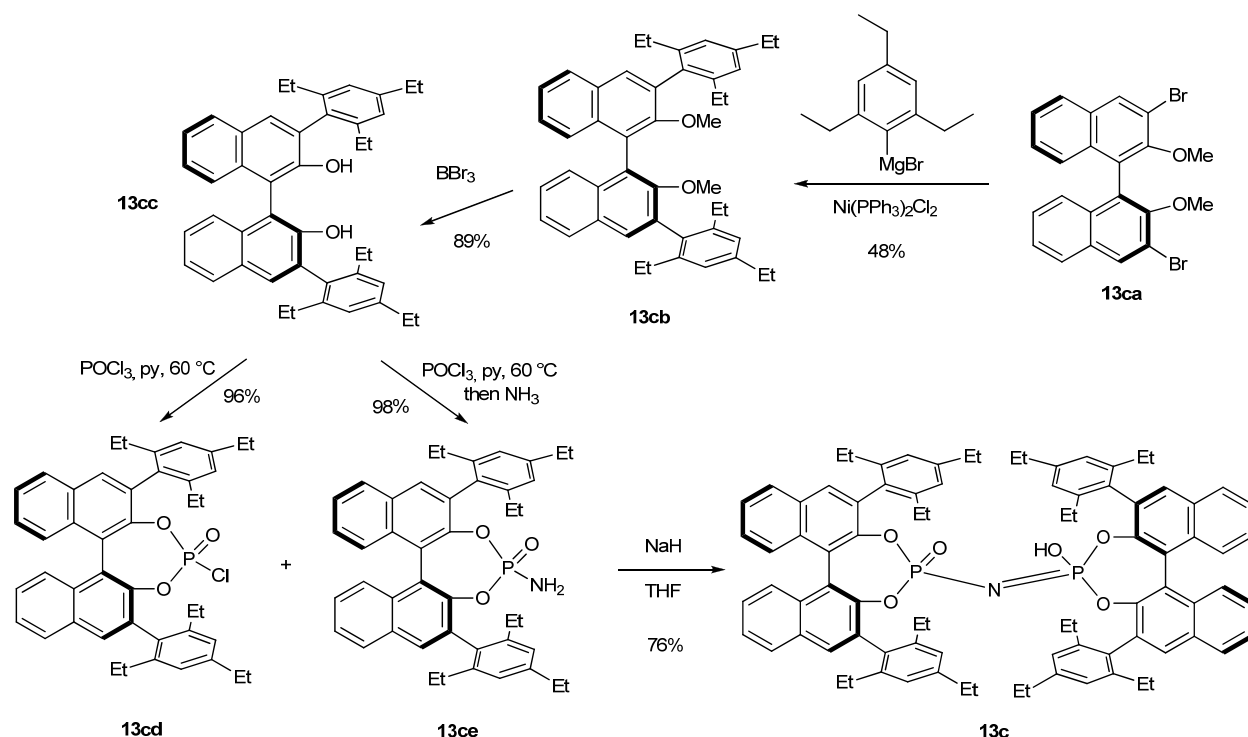
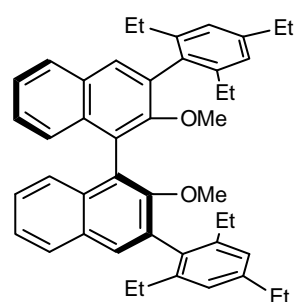
with CH₂Cl₂ (5 x 10 ml). The organic extracts were washed with brine, dried (MgSO₄), filtered, and the solvent was removed under reduced pressure. The residue was purified by column chromatography on silica gel using 0-4% EtOAc/DCM as the eluent giving a colorless solid. The solid was dissolved in CH₂Cl₂ (10 ml) and washed with 3 N aqueous HCl (10 ml). The organic layer was separated, and concentrated under reduced pressure to give the title compound as a yellowish solid (101 mg, 37%).

¹H-NMR (500 MHz, CD₂Cl₂): δ 8.21 (s, 2H), 8.06 (d, *J* = 8.4 Hz, 4H), 7.91 (s, 2H), 7.87 (d, *J* = 8.2 Hz, 2H), 7.83 (d, *J* = 8.6 Hz, 2H), 7.80 (s, 2H), 7.74-7.64 (m, 14H), 7.53 (t, *J* = 7.6 Hz, 2H), 7.48-7.39 (m, 8H), 7.36-7.33 (m, 2H), 7.31-7.27 (m, 6H), 7.11-7.10 (m, 4H), 6.91-6.87 (m, 2H), 5.87 (t, *J* = 7.4 Hz, 2H), 5.59-5.56 (m, 2H), 5.15 (broad s, 2.43H, acidic H + H₂O);

¹³C-NMR (125 MHz, CD₂Cl₂): δ 146.5, 146.4, 146.4, 146.1, 146.1, 146.0, 133.9, 133.1, 133.0, 132.8, 131.9, 131.4, 131.2, 131.1, 131.0, 131.0, 130.8, 130.7, 130.4, 130.3, 130.2, 130.2, 130.0, 129.0, 129.0, 128.8, 128.7, 128.5, 128.1, 127.5, 127.4, 127.3, 127.2, 127.1, 127.1, 126.8, 126.6, 126.2, 126.1, 125.5, 125.4, 125.2, 125.1, 124.4, 124.2, 124.0, 124.0, 122.5;

³¹P-NMR (202 MHz, CD₂Cl₂): δ 13.74 (s);

HRMS (ESI⁻) (*m/z*): [M-H] calcd for C₉₆H₅₆NO₆P₂, 1380.3588; found, 1380.3584.

13c**(S)-2,2'-Dimethoxy-3,3'-bis(2,4,6-triethylphenyl)-1,1'-binaphthalene (13cb)**

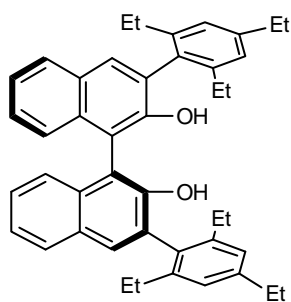
To magnesium turnings (583 mg, 24 mmol) activated with 1,2-dibromoethane in diethyl ether (4 ml), 2-bromo-1,3,5-triethylbenzene^{[160],[161]} (3.86 g, 16 mmol) and diethylether (20 ml) were added alternately during 30 min. After complete addition the mixture was refluxed (oil bath heating) for 21 h. After cooling to ambient temperature, the solution was added to a mixture of (S)-3,3'-dibromo-2,2'-dimethoxy-1,1'-binaphthalene (**13ca**, 1.89 g, 4.0 mmol) and $\text{Ni}(\text{PPh}_3)_2\text{Cl}_2$ (393 mg, 0.60 mmol) in anhydrous diethyl ether (40 mL). The reaction mixture was refluxed for 28 h, cooled to ambient temperature, carefully treated with saturated aqueous NH_4Cl solution (40 ml) and water (40 ml), and extracted with CH_2Cl_2 (100 ml, 50 ml). The combined organic layers were dried (MgSO_4), filtered, and the solvent removed under reduced pressure. The residue was purified by column chromatography on silica gel using 10-15% CH_2Cl_2 /hexane as the eluent yielding the title compound as a colorless solid (1.22 g, 48%).

$^1\text{H-NMR}$ (400 MHz, CD_2Cl_2): δ 7.89 (d, $J = 8.1$ Hz, 2H), 7.74 (s, 2H), 7.44-7.40 (m, 2H), 7.32-7.25 (m, 4H), 7.06 (s, 2H), 7.05 (m, 2H), 3.10 (s, 6H), 2.70 (q, $J = 7.6$ Hz, 4H), 2.51 (q, $J = 7.6$ Hz, 4H), 2.46 (q, $J = 7.6$ Hz, 4H), 1.30 (t, $J = 7.6$ Hz, 6H), 1.15 (t, $J = 7.6$ Hz, 6H), 1.08 (t, $J = 7.6$ Hz, 6H);

$^{13}\text{C-NMR}$ (100 MHz, CD_2Cl_2): δ 155.0, 144.0, 142.9, 142.8, 134.9, 134.4, 134.2, 131.4, 130.8, 128.3, 126.4, 125.9, 125.4 (2C), 125.3, 125.0, 60.1, 29.1, 27.4, 27.3, 15.8, 15.6, 15.4;

HRMS (ESI+) (m/z): $[\text{M}+\text{Na}]$ calcd for $\text{C}_{46}\text{H}_{50}\text{O}_2\text{Na}$, 657.3703; found, 657.3708.

(S)-3,3'-Bis(2,4,6-triethylphenyl)-[1,1'-binaphthalene]-2,2'-diol (13cc)



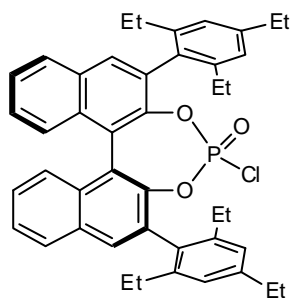
A 1 M solution of BBr_3 in CH_2Cl_2 (7.56 ml, 7.56 mmol) was added dropwise to the solution of (S)-**13cb** (1.20 g, 1.89 mmol) in CH_2Cl_2 (20 ml) at 0 °C under argon. After 40 h at room temperature, the solution was cooled to 0 °C, water (50 ml) was carefully added, and the mixture was extracted with CH_2Cl_2 (50 ml). The organic layer was washed with saturated aqueous Na_2CO_3 solution (50 ml), dried (MgSO_4), filtered, and the solvent was removed under reduced pressure. The residue was purified by column chromatography on silica gel using 20% CH_2Cl_2 /hexane as the eluent yielding the title compound as a colorless solid (1.02 g, 89%).

$^1\text{H-NMR}$ (400 MHz, CD_2Cl_2): δ 7.91 (d, J = 7.9 Hz, 2H), 7.78 (s, 2H), 7.41-7.37 (m, 2H), 7.35-7.31 (m, 2H), 7.24-7.22 (m, 2H), 7.09-7.07 (m, 4H), 5.06 (s, 2H), 2.70 (q, J = 7.6 Hz, 4H), 2.57-2.31 (m, 8H), 1.30 (t, J = 7.7 Hz, 6H), 1.10 (t, J = 7.6 Hz, 6H), 1.02 (t, J = 7.6 Hz, 6H);

$^{13}\text{C-NMR}$ (100 MHz, CD_2Cl_2): δ 150.9, 145.0, 143.9, 143.8, 133.9, 132.2, 131.5, 129.6, 129.4, 128.7, 127.1, 126.2, 124.6, 124.2, 113.5, 29.1, 27.37, 27.36, 15.7, 15.6, 15.5 (+1 aromatic C, overlapped);

HRMS (ESI+) (m/z): $[\text{M}+\text{Na}]$ calcd for $\text{C}_{44}\text{H}_{46}\text{O}_2\text{Na}$, 629.3390; found, 629.3387.

(S)-4-Chloro-2,6-bis(2,4,6-triethylphenyl)dinaphtho[2,1-d':1',2'-f][1,3,2]dioxaphosphepine 4-oxide (13cd)



To a solution of (S)-**13cc** (553 mg, 0.912 mmol) in pyridine (3 ml) under argon was added POCl_3 (255 μl , 420 mg, 2.74 mmol) at room temperature. The mixture was stirred at 60 °C for 1.5 h and then concentrated to dryness under vacuum. The residue was passed through a short silica gel column (10 g) using CH_2Cl_2 as the eluent yielding the title compound as a colorless solid (604 mg, 96%).

$^1\text{H-NMR}$ (400 MHz, CD_2Cl_2): δ 8.01-7.98 (m, 2H), 7.96 (s, 1H), 7.92 (s, 1H), 7.59-7.54 (m, 2H), 7.38-7.30 (m, 4H), 7.11-7.12 (m, 2H, two overlapped doublets with small J), 7.05 (d, J = 1.2 Hz,

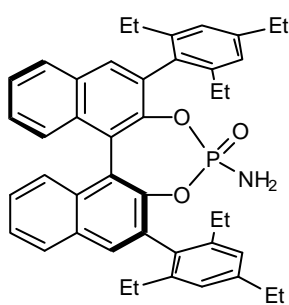
1H), 7.02 (d, $J = 1.2$ Hz, 1H), 2.74-2.69 (m, 4H), 2.55-2.29 (m, 8H), 1.32 (t, $J = 7.6$ Hz, 3H, overlapped), 1.31 (t, $J = 7.6$ Hz, 3H, overlapped), 1.26 (t, $J = 7.5$ Hz, 3H), 1.18 (t, $J = 7.6$ Hz, 3H), 1.01 (t, $J = 7.5$ Hz, 3H, overlapped), 0.99 (t, $J = 7.5$ Hz, 3H, overlapped);

$^{13}\text{C-NMR}$ (100 MHz, CD_2Cl_2): δ 145.3 (d, $J_{\text{C-P}} = 11.1$ Hz), 145.2 (d, $J_{\text{C-P}} = 9.1$ Hz), 144.9, 144.6, 143.6, 143.3, 142.9, 142.8, 133.4, 132.53, 132.49, 132.46, 132.44, 132.2, 132.0, 131.91, 131.90, 131.79, 131.77, 131.73, 128.8, 127.5, 127.3, 127.2, 126.8, 125.9, 125.5, 125.4, 125.0, 122.54 (d, $J_{\text{C-P}} = 2.5$ Hz), 122.48 (d, $J_{\text{C-P}} = 2.8$ Hz), 29.14, 19.12, 27.8, 27.3, 27.18, 27.15, 16.3, 15.57, 15.55, 15.49, 15.1, 14.9 (including signals due to unassigned C-P-coupling, some signals are overlapped);

$^{31}\text{P-NMR}$ (162 MHz, CD_2Cl_2): δ 8.26 (s);

HRMS (ESI+) (m/z): $[\text{M}+\text{Na}]$ calcd for $\text{C}_{44}\text{H}_{44}\text{O}_3\text{ClPNa}$, 709.2609; found, 709.2606.

(S)-4-Amino-2,6-bis(2,4,6-triethylphenyl)dinaphtho[2,1-*d*:1',2'-*f*][1,3,2]dioxaphosphepine 4-oxide (13ce)



To a solution of (S)-**13cc** (464 mg, 0.764 mmol) in pyridine (3 ml) under argon was added POCl_3 (214 μl , 351 mg, 2.29 mmol) at room temperature. After 1.5 h at 60 $^\circ\text{C}$, the mixture was cooled to -78 $^\circ\text{C}$ and anhydrous ammonia gas was condensed into the reaction flask (ca. 10 ml). The cooling bath was removed and the mixture was allowed to warm to room temperature. The reaction mixture was then

concentrated to dryness under vacuum. Residue was passed through short silica gel column (10 g) using CH_2Cl_2 as the eluent yielding the title compound as a colorless solid (500 mg, 98%).

$^1\text{H-NMR}$ (400 MHz, CD_2Cl_2): δ 7.99-7.94 (m, 2H), 7.91 (s, 1H), 7.84 (s, 1H), 7.55-7.50 (m, 2H), 7.37-7.31 (m, 4H), 7.10 (d, $J = 1.5$ Hz, 1H), 7.08 (d, $J = 1.4$ Hz, 1H), 7.05 (d, $J = 1.5$ Hz, 1H), 6.99 (d, $J = 1.4$ Hz, 1H), 2.74-2.63 (m, 6H), 2.58-2.28 (m, 8H), 1.31 (t, $J = 7.6$ Hz, 3H, overlapped), 1.28 (t, $J = 7.6$ Hz, 3H, overlapped), 1.25 (t, $J = 7.6$ Hz, 3H, overlapped), 1.17 (t, $J = 7.6$ Hz, 3H), 1.00 (t, $J = 7.5$ Hz, 3H, overlapped), 0.99 (t, $J = 7.5$ Hz, 3H, overlapped);

$^{13}\text{C-NMR}$ (100 MHz, CD_2Cl_2): δ 145.9 (d, $J_{\text{C-P}} = 10.7$ Hz), 145.2 (d, $J_{\text{C-P}} = 8.1$ Hz), 144.7, 144.2, 143.8, 143.6, 142.8, 142.1, 133.1, 132.88, 132.85, 132.68, 132.64, 132.61, 132.5, 132.41, 132.38, 131.7, 131.6, 128.7, 128.6, 127.4, 127.3, 126.8, 126.7, 126.2, 126.1, 125.8, 125.6, 125.3, 124.8, 122.8 (d, $J_{\text{C-P}} = 2.0$ Hz), 122.5 (d, $J_{\text{C-P}} = 2.0$ Hz), 29.1 (2C), 27.8, 27.3, 27.21, 27.17, 16.5,

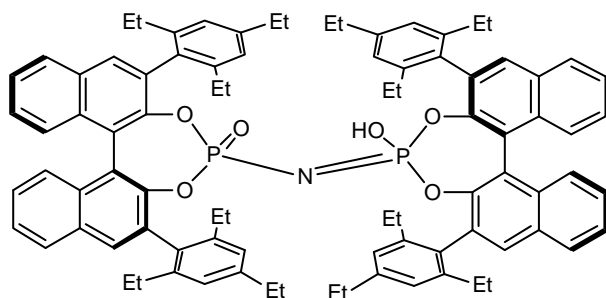
7. EXPERIMENTAL SECTION

15.53, 15.51, 15.4, 15.2, 14.9 (including signals due to unassigned C-P-coupling, some signals are overlapped);

$^{31}\text{P-NMR}$ (162 MHz, CD_2Cl_2): δ 13.20 (s);

HRMS (ESI+) (m/z): $[\text{M}+\text{Na}]$ calcd for $\text{C}_{44}\text{H}_{46}\text{NO}_3\text{PNa}$, 690.3108; found, 690.3114.

O,O-syn-Imidodiphosphoric acid **13c**



Sodium hydride (60% dispersion of in mineral oil, 84 mg, 2.1 mmol) was added to a solution of (*S*)-**13ce** (464 mg, 0.764 mmol) and (*S*)-**13cd** (577 mg, 0.84 mmol) in THF (5 ml) under argon at room temperature. After 14 h at room temperature, 10% aqueous HCl solution

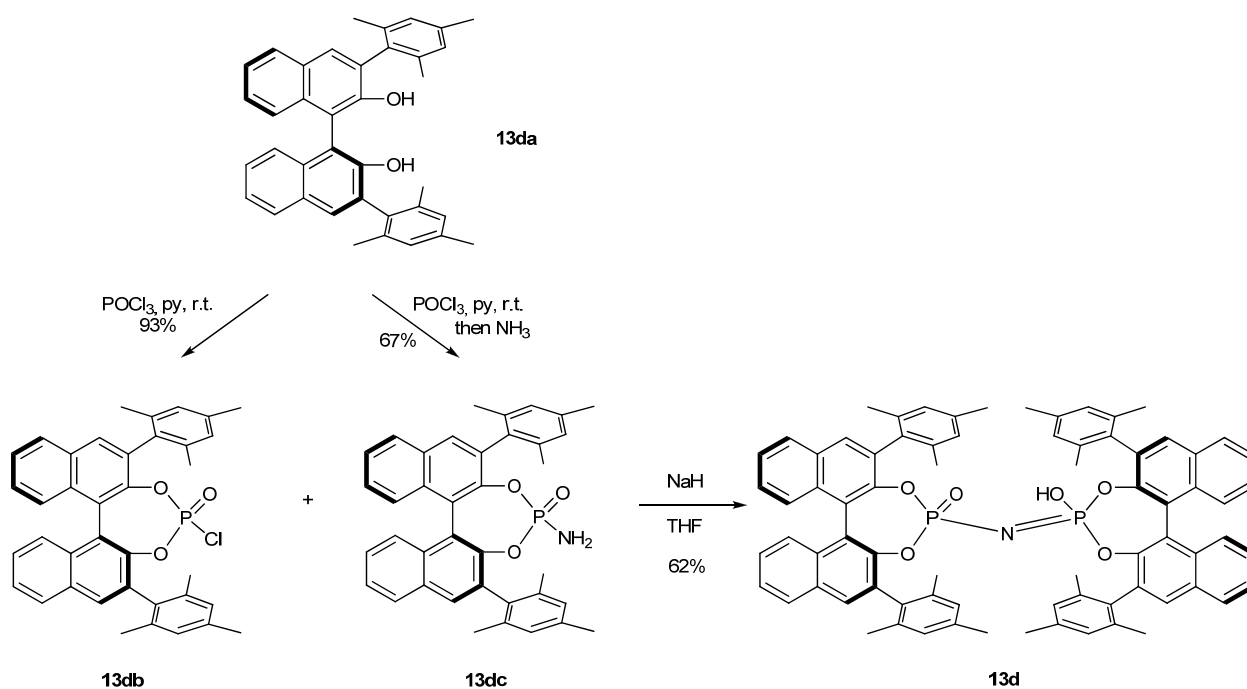
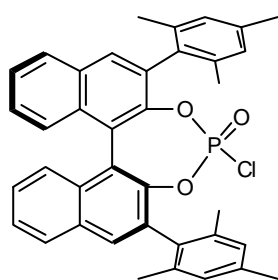
(10 ml) and DCM (10 ml) were added, and the mixture was stirred for 1 h. The organic layer was separated and the solvent was removed under reduced pressure. The residue was purified by column chromatography on aluminum oxide (activity I) using 20-100% CH_2Cl_2 /hexane followed by 2-8% EtOAc/DCM as the eluents giving a colorless solid. The solid was dissolved in CH_2Cl_2 (10 ml) and stirred with 3 N aqueous HCl (10 ml) for 4 h. The organic layer was separated, washed with 3 N aqueous HCl (10 ml) and concentrated under reduced pressure to give the title compound as a colorless solid (695 mg, 76%).

$^1\text{H-NMR}$ (500 MHz, CD_2Cl_2): δ 7.90 (d, $J = 8.2$ Hz, 1H), 7.87 (d, $J = 8.2$ Hz, 1H), 7.79 (s, 1H), 7.59 (s, 1H), 7.51 (t, $J = 7.5$ Hz, 1H), 7.46-7.38 (m, 3H), 7.23-7.20 (m, 1H), 7.05 (d, $J = 8.6$ Hz, 1H), 6.97 (s, 1H), 6.863 (s, 1H), 6.856 (s, 1H), 6.61 (broad s, 1.8H, acidic H + H_2O), 6.39 (s, 1H), 2.65-2.50 (m, 4H), 2.32-2.12 (m, 5H), 2.07-2.00 (m, 1H), 1.92-1.82 (m, 1H), 1.20 (t, $J = 7.6$ Hz, 3H, overlapped), 1.19 (t, $J = 7.6$ Hz, 3H, overlapped), 1.17-1.10 (m, 1H, overlapped), 1.08 (t, $J = 7.5$ Hz, 3H), 0.95 (t, $J = 7.5$ Hz, 3H), 0.82 (t, $J = 7.5$ Hz, 3H), 0.04 (t, $J = 7.5$ Hz, 3H);

$^{13}\text{C-NMR}$ (125 MHz, CD_2Cl_2): δ 146.4, 145.8, 144.2, 144.0, 143.8, 143.5, 143.4, 142.5, 133.1, 133.0, 132.94, 132.86, 132.82, 132.5, 132.4, 132.1, 131.6, 131.3, 128.6, 128.5, 127.6, 127.1, 126.5, 126.4, 125.9, 125.7, 125.6, 125.4, 124.72, 124.70, 122.7, 122.2, 29.0, 28.9, 27.28, 27.25, 26.99, 26.97, 15.85 (2C), 15.77, 15.3, 15.2, 14.9;

$^{31}\text{P-NMR}$ (202 MHz, CD_2Cl_2): δ 4.94 (s);

HRMS (ESI-) (m/z): $[\text{M}-\text{H}]$ calcd for $\text{C}_{88}\text{H}_{88}\text{NO}_6\text{P}_2$, 1316.6092; found, 1316.6096.

13d**(S)-4-Chloro-2,6-dimesityldinaphtho[2,1-d:1',2'-f][1,3,2]dioxaphosphepine 4-oxide (13db)**

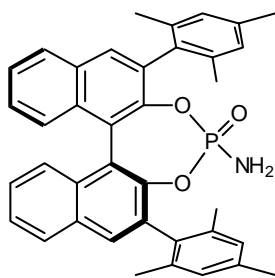
To a solution of **13da** (198 mg, 0.379 mmol) in pyridine (1.5 ml) under argon was added POCl_3 (106 μl , 174 mg, 1.137 mmol) at room temperature. The mixture was stirred for 20 h and then concentrated to dryness under vacuum. The residue was passed through a short silica gel column (5 g) using DCM as the eluent yielding the title compound as a colorless solid (219 mg, 93%).

$^1\text{H-NMR}$ (500 MHz, CD_2Cl_2): δ 8.01-7.99 (m, 2H), 7.93 (s, 1H), 7.89 (s, 1H), 7.58-7.55 (m, 2H), 7.36-7.34 (m, 4H), 7.03 (s, 2H), 6.98 (s, 1H), 6.95 (s, 1H), 2.36 (s, 6H), 2.22 (s, 3H), 2.18 (s, 3H), 2.07 (s, 3H), 2.02 (s, 3H);

$^{13}\text{C-NMR}$ (125 MHz, CD_2Cl_2): δ 145.5, 145.4, 145.1, 145.0, 138.2, 138.0, 137.60, 137.58, 137.0, 136.6, 133.3, 133.0, 132.95, 132.93, 132.90, 132.59, 132.57, 132.5, 132.3, 132.1, 132.0, 131.9, 129.0, 128.80, 128.76, 128.7, 128.5, 128.0, 127.4, 127.3, 127.2, 126.8, 122.72, 122.71, 122.53, 122.51, 21.5, 21.22, 21.21, 21.1, 20.4, 20.3 (including signals due to unassigned C-P-coupling, some signals are overlapped);

$^{31}\text{P-NMR}$ (202 MHz, CD_2Cl_2): δ 7.63 (s);

HRMS (ESI+) (m/z): $[\text{M}+\text{Na}]$ calcd for $\text{C}_{38}\text{H}_{32}\text{O}_3\text{ClPNa}$, 625.1670; found, 625.1671.

(S)-4-Amino-2,6-dimesityldinaphtho[2,1-d:1',2'-f][1,3,2]dioxaphosphepine 4-oxide (13dc)

To a solution of **13da** (165 mg, 0.316 mmol) in pyridine (1.5 ml) under argon was added POCl₃ (88 μl, 145 mg, 0.948 mmol) at room temperature. After 20 h the mixture was cooled to -78 °C and anhydrous ammonia gas was condensed into the reaction flask (ca. 7 ml). The cooling bath was removed and the mixture was allowed to warm to room temperature. The reaction mixture was then

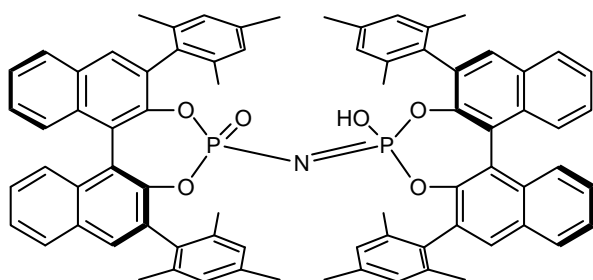
concentrated to dryness under vacuum. The residue was purified by chromatography on a short silica gel column (5 g) using CH₂Cl₂ as the eluent yielding the title compound as a colorless solid (127 mg, 67% + fractions containing a small amount of impurity).

¹H-NMR (500 MHz, CD₂Cl₂): δ 7.99-7.95 (m, 2H), 7.87 (s, 1H), 7.81 (s, 1H), 7.54-7.50 (m, 2H), 7.38-7.29 (m, 4H), 7.02 (s, 1H), 7.01 (s, 1H), 6.99 (s, 1H), 6.93 (s, 1H), 2.71 (d, *J* = 6.7 Hz, 2H), 2.35 (s, 3H), 2.31 (s, 3H), 2.20 (s, 3H), 2.19 (s, 3H), 2.06 (s, 3H), 2.00 (s, 3H);

¹³C-NMR (125 MHz, CD₂Cl₂): δ 145.1, 145.0, 138.05, 137.96, 137.8, 137.6, 137.0, 135.7, 134.0, 133.5, 133.4, 132.6, 132.43, 132.41, 132.14, 132.11, 131.8, 128.9, 128.7, 127.9, 127.32, 127.27, 126.9, 126.8, 126.23, 126.17, 122.9, 122.7, 21.4, 21.24, 21.22, 21.18, 20.5, 20.4 (including signals due to unassigned C-P-coupling, some signals are overlapped);

³¹P-NMR (202 MHz, CD₂Cl₂): δ 12.39 (s);

HRMS (ESI+) (*m/z*): [M+Na] calcd for C₃₈H₃₄NO₃PNa, 606.2169; found, 606.2165.

Imidodiphosphoric acid 13d

Sodium hydride (60% dispersion of in mineral oil, 25 mg, 0.63 mmol) was added to a solution of **13db** (153 mg, 0.253 mmol) and **13dc** (123 mg, 0.211 mmol) in THF (2 ml) under argon at room temperature. After 19 h at room temperature, 10% aqueous HCl

solution (10 ml) and DCM (10 ml) were added, and the mixture was stirred for 30 min. The organic layer was separated and the solvent was removed under reduced pressure. The residue was purified by column chromatography on aluminum oxide (activity III) using 0-12% EtOAc/DCM as the eluents giving a colorless solid. The solid was dissolved in CH₂Cl₂ (10 ml) and stirred with 3 N aqueous HCl (10 ml) for 1 h. The organic layer was separated, washed with 3 N

7. EXPERIMENTAL SECTION

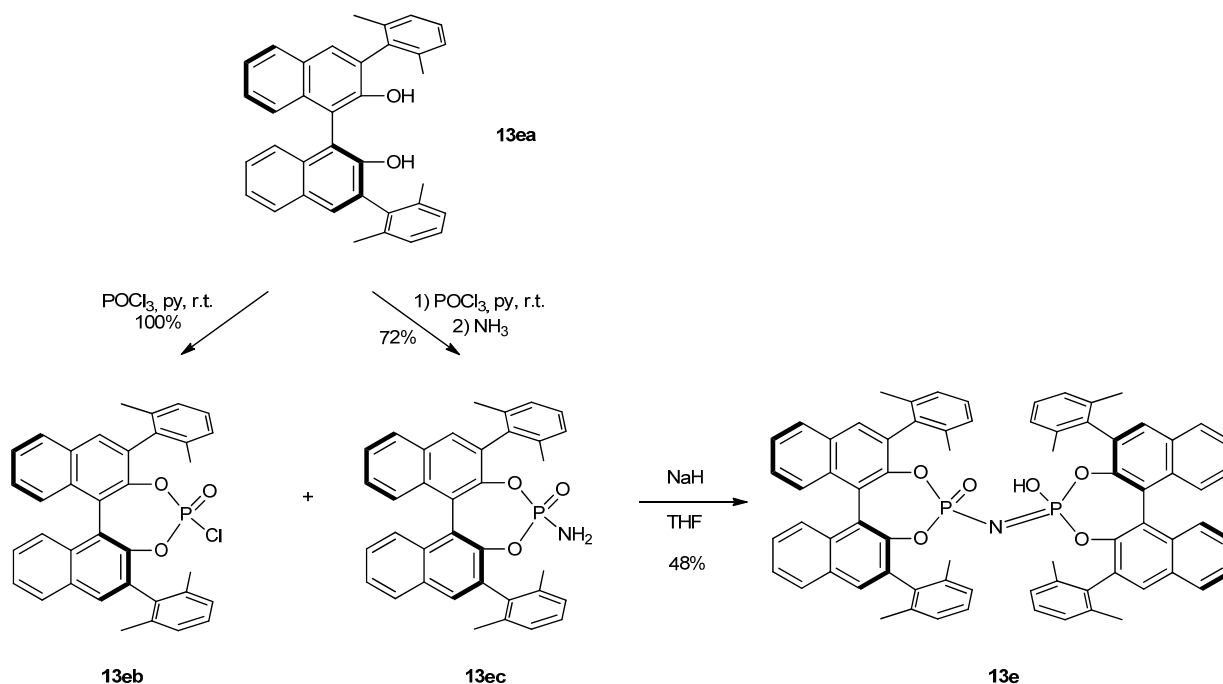
aqueous HCl (10 ml) and concentrated under reduced pressure to give the title compound as a colorless solid (150 mg, 62%).

¹H-NMR (500 MHz, CD₂Cl₂): δ 7.92-7.86 (m, 4H), 7.75 (s, 2H), 7.53-7.42 (m, 10H), 7.26-7.18 (m, 4H), 6.93 (s, 2H, overlapped with broad singlet), 6.87 (s, 2H, overlapped with broad singlet), 6.81 (bs, 3H, acidic H + H₂O, overlapped), 6.79 (s, 2H, overlapped with broad singlet), 6.29 (s, 2H), 2.30 (s, 6H), 2.18 (s, 6H), 2.05 (s, 6H), 1.90 (s, 6H), 1.79 (s, 6H), 0.84 (s, 6H);

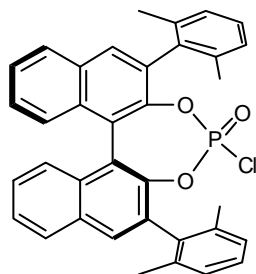
¹³C-NMR (125 MHz, CD₂Cl₂): δ 146.4, 146.0, 137.8, 137.4, 136.8, 136.7, 133.2, 132.9, 132.4, 131.8, 131.6, 128.5, 128.5, 128.3, 128.1, 128.0, 127.4, 127.1, 126.6, 126.5, 125.8, 122.7, 21.2, 21.2, 21.1, 20.2, 20.1, 19.4 (including signals due to unassigned C-P-coupling, some signals are overlapped);

³¹P-NMR (202 MHz, CD₂Cl₂): δ 3.91 (s);

HRMS (ESI⁻) (*m/z*): [M-H] calcd for C₇₆H₆₄NO₆P₂, 1148.4214; found, 1148.4204.

13e

(S)-4-Chloro-2,6-bis(2,6-dimethylphenyl)dinaphtho[2,1-d':1',2'-f][1,3,2]dioxaphosphepine 4-oxide (13eb)



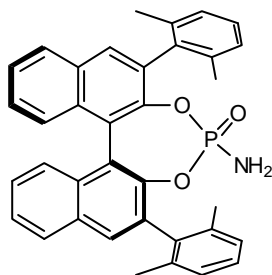
To a solution of **13ea** (820 mg, 1.66 mmol) in pyridine (5 ml) under argon was added POCl_3 (464 μl , 764 mg, 4.98 mmol) at room temperature. The mixture was stirred for 20 h and then concentrated to dryness under vacuum. The residue was passed through a short silica gel column (10 g) using DCM as the eluent yielding the title compound as a colorless solid (955 mg, 100%).

$^1\text{H-NMR}$ (500 MHz, CD_2Cl_2): δ 8.02 (d, $J = 8.2$ Hz, 1H, overlapped), 8.01 (d, $J = 8.2$ Hz, 1H, overlapped), 7.95 (s, 1H), 7.92 (s, 1H), 7.60-7.55 (m, 2H), 7.37-7.35 (m, 4H), 7.27-7.19 (m, 4H), 7.16-7.12 (m, 2H), 2.26 (s, 3H), 2.22 (s, 3H), 2.11 (s, 3H), 2.06 (s, 3H);

$^{13}\text{C-NMR}$ (125 MHz, CD_2Cl_2): δ 145.2, 145.1, 144.9, 144.8, 137.9, 137.2, 136.9, 135.8, 135.5, 133.1, 132.9, 132.8, 132.7, 132.5, 132.4, 132.10, 132.09, 131.85, 131.82, 128.81, 128.76, 128.5, 128.4, 128.3, 128.0, 127.7, 127.5, 127.29, 127.27, 127.2, 126.8, 122.78, 122.76, 122.6, 122.5, 21.6, 21.2, 20.5, 20.4 (including signals due to unassigned C-P-coupling, some signals are overlapped);

$^{31}\text{P-NMR}$ (202 MHz, CD_2Cl_2): δ 7.59 (s);

HRMS (ESI+) (m/z): $[\text{M}+\text{Na}]$ calcd for $\text{C}_{36}\text{H}_{28}\text{O}_3\text{ClPNa}$, 597.1357; found, 597.1351.

(S)-4-Amino-2,6-bis(2,6-dimethylphenyl)dinaphtho[2,1-d:1',2'-f][1,3,2]dioxaphosphepine 4-oxide (13ec)

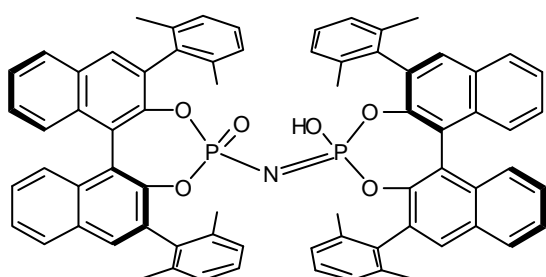
To a solution of **13eb** (460 mg, 0.8 mmol) in CH₂Cl₂ (3 ml) under argon at -78 °C anhydrous ammonia gas was condensed (ca. 5 ml). The cooling bath was removed and the mixture was allowed to warm to room temperature. The reaction mixture was passed through a short silica gel column (5 g) using DCM and 10% EtOAc/DCM as the eluents yielding the title compound as a colorless solid (320 mg, 72%).

¹H-NMR (500 MHz, CD₂Cl₂): δ 7.98 (t, *J* = 8.9 Hz, 2H), 7.89 (s, 1H), 7.84 (s, 1H), 7.55-7.51 (m, 2H), 7.39-7.31 (m, 4H), 7.27-7.15 (m, 5H), 7.10 (d, *J* = 7.07 Hz, 1H), 2.70 (d, *J* = 6.7 Hz, 2H), 2.23 (s, 6H), 2.11 (s, 3H), 2.04 (s, 3H);

¹³C-NMR (125 MHz, CD₂Cl₂): δ 145.9, 145.8, 144.94, 144.87, 138.2, 138.1, 137.2, 136.9, 136.4, 136.0, 133.37, 133.35, 132.63, 132.60, 132.5, 132.4, 132.2, 131.9, 131.8, 128.7, 128.3, 128.2, 128.1, 127.9, 127.8, 127.4, 127.3, 127.1, 127.0, 126.9, 126.3, 126.2, 122.99, 122.97, 122.74, 122.73, 21.6, 21.3, 20.6, 20.5 (including signals due to unassigned C-P-coupling, some signals are overlapped);

³¹P-NMR (202 MHz, CD₂Cl₂): δ 12.30 (s);

HRMS (ESI+) (*m/z*): [M+Na] calcd for C₃₆H₃₀NO₃PNa, 578.1856; found, 578.1861.

Imidodiphosphoric acid 13e

Sodium hydride (60% dispersion of in mineral oil, 25 mg, 0.63 mmol) was added to a solution of **13eb** (390 mg, 0.678 mmol) and **13ec** (314 mg, 0.565 mmol) in THF (4 ml) under argon at room temperature. After 22 h at room temperature, 10% aqueous HCl solution (10 ml) and DCM (10 ml) were added, and the mixture was stirred for 30 min. The organic layer was separated and the solvent was removed under reduced pressure. The residue was purified by column chromatography on aluminum oxide (activity III) using 50% DCM/hexane and 0-100% EtOAc/DCM as the eluents giving a colorless solid. The solid was dissolved in CH₂Cl₂ (10 ml) and stirred with 3 N aqueous HCl (10 ml) for 1 h. The organic layer was separated, washed with 3 N aqueous HCl (10 ml) and concentrated under reduced pressure to give the title compound as a colorless solid (299 mg, 48%).

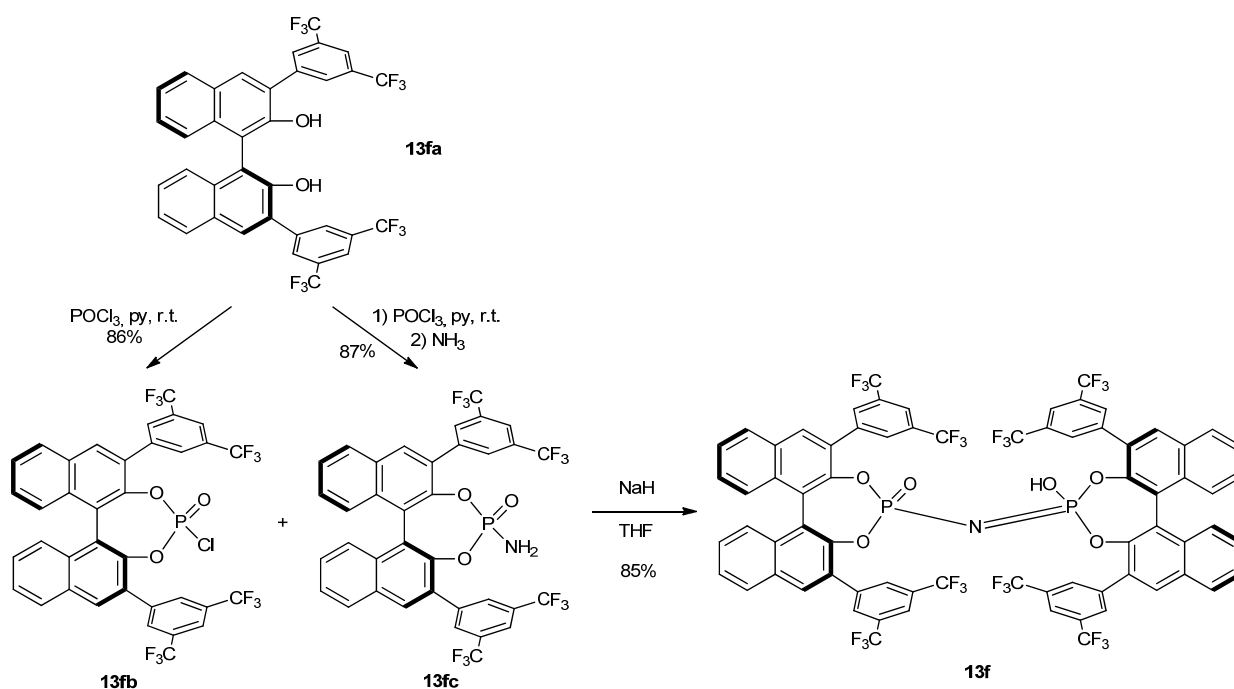
7. EXPERIMENTAL SECTION

¹H-NMR (500 MHz, CD₂Cl₂): δ 7.93 (d, *J* = 8.2 Hz, 2H), 7.88 (d, *J* = 8.1 Hz, 2H), 7.78 (s, 2H), 7.55-7.46 (m, 8H), 7.42 (t, *J* = 7.5 Hz, 2H), 7.25 (t, *J* = 7.6 Hz, 2H), 7.20 (d, *J* = 8.6 Hz, 2H), 7.14 (t, *J* = 7.5 Hz, 2H), 7.05 (d, *J* = 7.5 Hz, 2H), 7.01 (d, *J* = 7.4 Hz, 2H), 6.97-6.93 (m, 4H), 6.45 (d, *J* = 7.0 Hz, 2H), 4.71 (bs, 6.5H, acidic H + H₂O, overlapped), 2.04 (s, 6H), 1.91 (s, 6H), 1.82 (s, 6H), 0.86 (s, 6H);

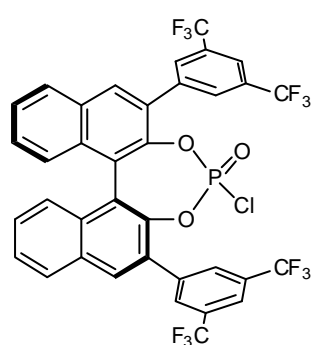
¹³C-NMR (125 MHz, CD₂Cl₂): δ 146.1, 145.7, 138.5, 138.0, 137.0, 136.9, 136.8, 136.5, 133.4, 133.2, 132.8, 132.5, 132.1, 131.92, 131.87, 131.4, 128.7, 128.4, 127.81, 127.76, 127.4, 127.3, 127.2, 127.1, 126.9, 126.8, 126.6, 125.9, 122.8, 122.7, 21.24, 21.20, 20.3, 19.6 (including signals due to unassigned C-P-coupling, some signals are overlapped);

³¹P-NMR (202 MHz, CD₂Cl₂): δ 3.61 (s);

HRMS (ESI⁻) (*m/z*): [M-H] calcd for C₇₂H₅₆NO₆P₂, 1092.3588; found, 1092.3588.

13f

(S)-2,6-Bis(3,5-bis(trifluoromethyl)phenyl)-4-chlorodinaphtho[2,1-d:1',2'-f][1,3,2]dioxaphosphine 4-oxide (13fb)



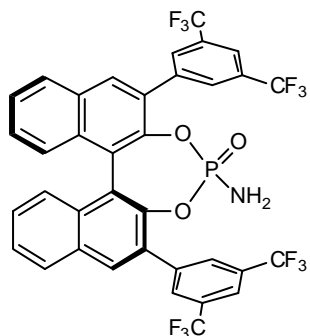
To a solution of **13fa** (736 mg, 1.04 mmol) in pyridine (5 ml) under argon was added POCl_3 (293 μl , 482 mg, 3.12 mmol) at room temperature. The mixture was stirred for 18 h and then concentrated to dryness under vacuum. The residue was passed through a short silica gel column (10 g) using EtOAc as the eluent yielding the title compound as a colorless solid (706 mg, 86%).

$^1\text{H-NMR}$ (500 MHz, CD_2Cl_2): δ 8.27 (s, 2H), 8.23 (s, 1H), 8.20 (s, 1H), 8.19 (s, 2H), 8.12-8.10 (m, 2H), 8.01 (d, $J = 9.5$ Hz, 2H), 7.68-7.64 (m, 2H), 7.49-7.40 (m, 4H);

$^{13}\text{C-NMR}$ (125 MHz, CD_2Cl_2): δ 143.7, 143.6, 143.6, 143.5, 138.9, 138.7, 133.1, 133.0, 132.8, 132.8, 132.7, 132.6, 132.4, 132.3, 132.1, 131.8, 131.6, 131.0, 131.0, 130.6, 130.6, 130.5, 130.5, 129.3, 129.3, 128.5, 127.7, 127.6, 127.4, 127.3, 127.1, 127.0, 124.9, 124.8, 123.4, 123.4, 123.2, 123.2, 122.7, 122.6, 122.5, 122.5, 122.4, 122.4, 122.4, 122.3, 120.6, 120.5 (including signals due to unassigned C-F and C-P-coupling, some signals are overlapped);

$^{31}\text{P-NMR}$ (202 MHz, CD_2Cl_2): δ 8.31 (s);

HRMS (ESI+) (m/z): $[\text{M}+\text{Na}]$ calcd for $\text{C}_{36}\text{H}_{16}\text{O}_3\text{ClF}_{12}\text{PNa}$, 813.0226; found, 813.0233.

(S)-4-Amino-2,6-bis(3,5-bis(trifluoromethyl)phenyl)dinaphtho[2,1-d:1',2'-f][1,3,2]dioxaphosphine 4-oxide (13fc)

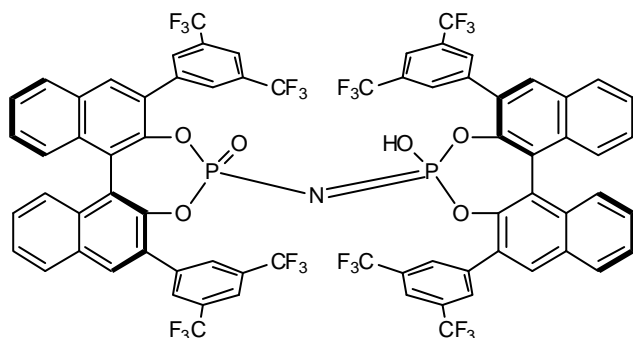
To a solution of **13fa** (611 mg, 0.86 mmol) in pyridine (4 ml) under argon was added POCl_3 (243 μl , 400 mg, 2.58 mmol) at room temperature. After 18 h the mixture was cooled to $-78\text{ }^\circ\text{C}$ and anhydrous ammonia gas was condensed into the reaction flask (ca. 7 ml). The cooling bath was removed and the mixture was allowed to warm to room temperature. The reaction mixture was then concentrated to dryness under vacuum. The residue was purified by chromatography on silica gel using 0-40% EtOAc/ CH_2Cl_2 as the eluents yielding the title compound as a colorless solid (575, 87%).

$^1\text{H-NMR}$ (500 MHz, CD_2Cl_2): δ 8.37 (s, 2H), 8.23 (s, 2H), 8.20 (s, 1H), 8.14 (s, 1H), 8.09-8.07 (m, 2H), 7.97 (s, 2H), 7.62-7.58 (m, 2H), 7.43-7.38 (m, 4H), 2.91 (d, $J = 8.0$ Hz, 2H);

$^{13}\text{C-NMR}$ (125 MHz, CD_2Cl_2): δ 144.3, 144.2, 143.7, 143.7, 139.5, 132.9, 132.8, 132.5, 132.3, 132.2, 132.1, 131.9, 131.9, 131.8, 131.7, 131.5, 131.5, 131.5, 131.3, 131.2, 131.2, 130.9, 130.9, 130.4, 130.4, 129.2, 129.1, 128.1, 128.0, 127.2, 127.1, 127.1, 125.0, 124.9, 123.7, 123.7, 123.1, 123.1, 122.8, 122.7, 122.2, 122.2, 122.1, 122.0, 122.0, 121.9, 120.7, 120.5 (including signals due to unassigned C-F and C-P-coupling, some signals are overlapped);

$^{31}\text{P-NMR}$ (202 MHz, CD_2Cl_2): δ 12.22 (s);

HRMS (ESI+) (m/z): $[\text{M}+\text{H}]$ calcd for $\text{C}_{36}\text{H}_{19}\text{NO}_3\text{F}_{12}\text{P}$, 772.0906; found, 772.0908.

Imidodiphosphoric acid 13f

Sodium hydride (60% dispersion of in mineral oil, 22 mg, 0.54 mmol) was added to a solution of **13fb** (171 mg, 0.216 mmol) and **13fc** (139 mg, 0.18 mmol) in THF (2 ml) under argon at room temperature. After 2.5 days at room temperature water (10 ml) was added and the mixture was extracted with CH_2Cl_2 , washed with brine, dried (MgSO_4), filtered and concentrated. The residue was purified by column chromatography on silica gel using 0-3% EtOAc/DCM as the eluents giving a colorless solid. The solid was dissolved in CH_2Cl_2 (10 ml) and washed with 3 N aqueous HCl (10 ml). The organic layer was separated and

7. EXPERIMENTAL SECTION

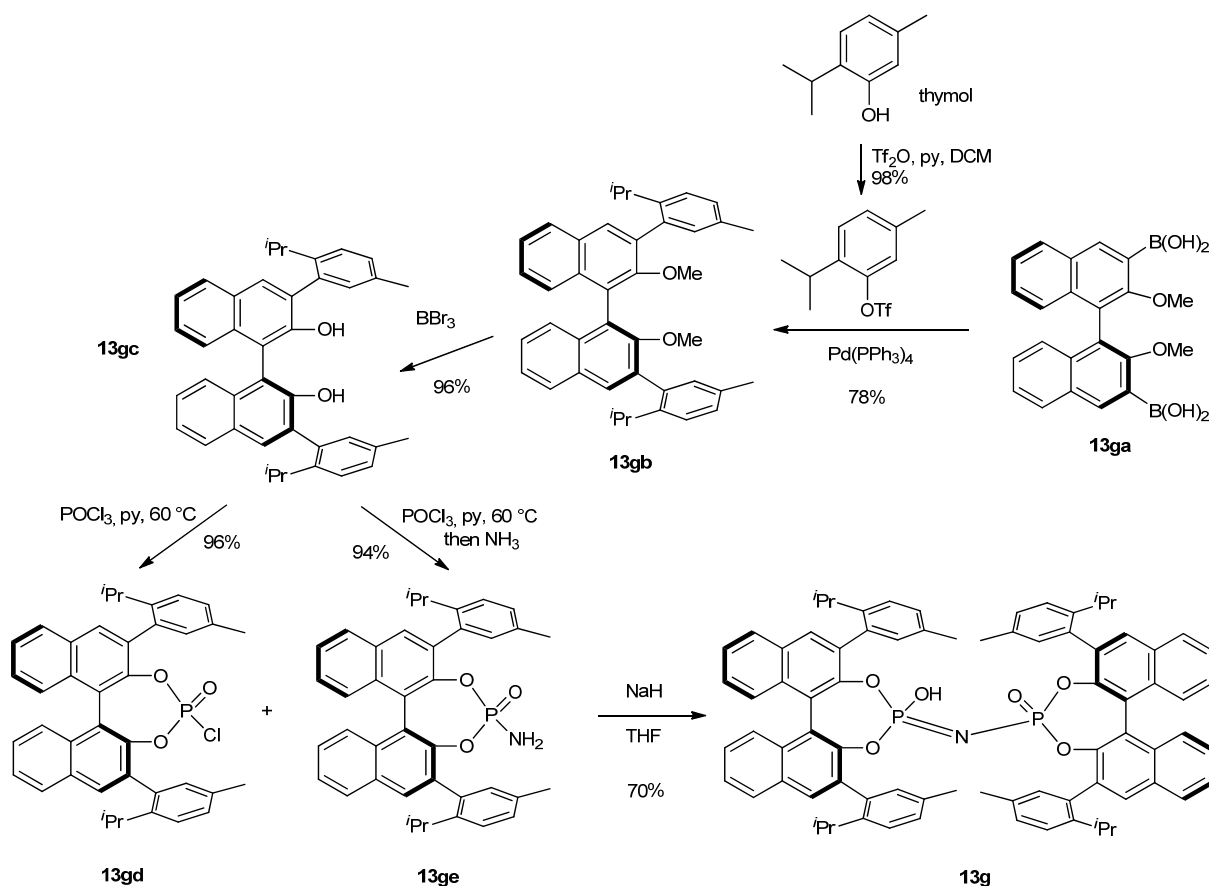
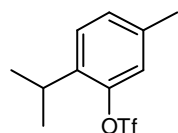
concentrated under reduced pressure to give the title compound as a colorless solid (234 mg, 85%).

¹H-NMR (500 MHz, CD₂Cl₂): δ 8.12 (s, 2H), 8.07 (d, *J* = 8.7 Hz, 2H, overlapped), 8.06 (s, 4H, overlapped), 7.92 (s, 2H), 7.86-7.81 (m, 4H), 7.78 (bs, 3.5H, acidic H + H₂O), 7.68-7.61 (m, 4H), 7.57 (t, *J* = 7.5 Hz, 2H), 7.51 (s, 2H), 7.37-7.34 (m, 6H), 7.25 (d, *J* = 8.5 Hz, 2H), 6.84 (s, 2H);

¹³C-NMR (125 MHz, CD₂Cl₂): δ 144.79, 144.76, 144.7, 144.0, 143.95, 143.91, 139.3, 138.9, 132.8, 132.3, 132.2, 131.9, 131.7, 131.6, 131.5, 131.37, 131.35, 131.26, 131.1, 131.0, 130.8, 130.74, 130.66, 130.6, 130.53, 130.51, 129.9, 129.6, 129.2, 128.4, 127.9, 127.0, 126.9, 126.8, 125.0, 124.6, 124.0, 122.8, 122.6, 122.4, 121.7 (m), 120.9 (m), 120.6, 120.3 (including signals due to unassigned C-F and C-P-coupling, some signals are overlapped);

³¹P-NMR (202 MHz, CD₂Cl₂): δ 3.03 (s);

HRMS (ESI⁻) (*m/z*): [M-H] calcd for C₇₂H₃₂NO₆F₂₄P₂, 1524.1327; found, 1524.1333.

13g**2-Isopropyl-5-methylphenyl trifluoromethanesulfonate**

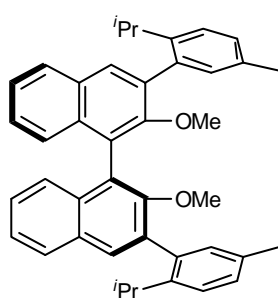
Tf_2O (4.0 ml, 6.77 g, 24 mmol) was added dropwise to the solution of thymol (2-isopropyl-5-methylphenol, 3.0 g, 20 mmol) and pyridine (4.85 ml, 4.75 g, 60 mmol) in dry CH_2Cl_2 (20 ml) at 0°C under argon. The mixture was stirred at

room temperature for 14 h. Then water (40 ml) was added and the mixture was extracted with CH_2Cl_2 . Combined organic extracts were washed with aq. 1 N HCl, water, and brine, dried (MgSO_4), filtered, and the solvent was removed under reduced pressure yielding the title compound as a colorless liquid (5.51 g, 98%).

$^1\text{H-NMR}$ (500 MHz, CDCl_3): δ 7.27 (d, $J = 8.0$ Hz, 1H), 7.14 (d, $J = 8.0$ Hz, 1H), 7.03 (s, 1H), 3.28-3.20 (m, 1H), 2.34 (s, 3H), 1.24 (d, $J = 6.8$ Hz, 6H);

$^{13}\text{C-NMR}$ (125 MHz, CDCl_3): δ 146.9, 137.9, 137.7, 129.4, 127.4, 121.5, 118.6 (q, $J(\text{C-F}) = 320$ Hz) 26.8, 23.1, 20.8;

HRMS (EI(Fe)) (m/z): $[\text{M}+\text{Na}]$ calcd for $\text{C}_{11}\text{H}_{13}\text{O}_3\text{F}_3\text{S}$, 282.0538; found, 282.0535.

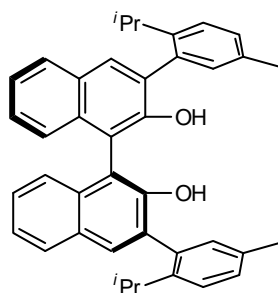
(S)-3,3'-Bis(2-isopropyl-5-methylphenyl)-2,2'-dimethoxy-1,1'-binaphthalene (13gb)

A suspension of **13ga** (2.41 g, 6.0 mmol), 2-isopropyl-5-methylphenyl trifluoromethanesulfonate (6.78 g, 24 mmol) and Ba(OH)₂·8H₂O (7.5 g, 24 mmol) in dioxane/water 3:1 (60 ml) was degassed by bubbling argon gas for 15 min. Pd(PPh₃)₄ (348 mg, 0.3 mmol) was added and the mixture was stirred for 1.5 h at room temperature, and further 1 h at 100 °C. After being cooled at room temperature water (500 ml) was added and the mixture extracted with CH₂Cl₂ (2 · 250 ml). Combined organic extracts were washed with water (500 ml), dried (MgSO₄), filtered, and the solvent removed under reduced pressure. The residue was purified by column chromatography on silica gel using 10-50% CH₂Cl₂/hexane as the eluents yielding the title compound as a colorless solid (2.7 g, 78%).

¹H-NMR (500 MHz, CDCl₃): δ 7.88-7.86 (m, 2H), 7.82-7.81 (m, 2H), 7.42-7.37 (m, 2H), 7.33-7.19 (m, 10H), 3.25 (s, 1.6H), 3.16 (s, 0.9H), 3.11-2.94 (multiplet including two singlets, 5.6H), 2.39-2.35 (four singlets, 6H), 1.22-1.14 (m, 7.2H), 1.06 (d, *J* = 6.9 Hz, 3.3H), 0.99 (d, *J* = 6.9 Hz, 1.6H) (spectra complicated due to presence of rotamers);

¹³C-NMR (125 MHz, CDCl₃): δ 154.8, 154.5, 154.3, 154.1, 144.7, 144.7, 144.6, 144.4, 137.6, 137.5, 137.4, 135.9, 135.8, 135.6, 135.3, 134.6, 134.5, 134.4, 133.7, 133.7, 133.6, 133.6, 131.0, 130.8, 130.8, 130.7, 130.6, 130.5, 130.4, 130.4, 128.8, 128.7, 128.7, 128.6, 127.9, 127.9, 127.8, 126.1, 126.0, 125.9, 125.8, 125.8, 125.6, 125.2, 125.2, 125.1, 125.0, 125.0, 124.9, 124.9, 124.8, 124.7, 124.7, 60.5, 60.4, 60.4, 60.3, 30.1, 30.0, 29.9, 29.8, 25.2, 25.2, 25.1, 25.0, 23.3, 23.2, 23.1, 23.0, 21.0, 21.0, 20.9 (including signals due to presence of rotamers);

HRMS (ESI+) (*m/z*): [M+Na] calcd for C₄₂H₄₂O₂Na, 601.3077; found, 601.3080.

(S)-3,3'-Bis(2-isopropyl-5-methylphenyl)-[1,1'-binaphthalene]-2,2'-diol (13gc)

A 1 M solution of BBr₃ in CH₂Cl₂ (18.7 ml, 18.7 mmol) was added dropwise to the solution of (S)-**13gb** (2.7 g, 4.66 mmol) in CH₂Cl₂ (20 ml) at 0 °C under argon. After 60 h at room temperature, the solution was cooled to 0 °C, water (200 ml) was carefully added, and the mixture was extracted with CH₂Cl₂. The organic layer was washed with saturated aqueous Na₂CO₃ solution (100 ml), dried (MgSO₄), filtered, and the

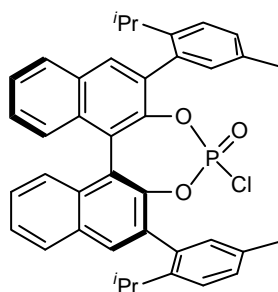
solvent was removed under reduced pressure. The residue was purified by column chromatography on silica gel using 40% CH₂Cl₂/hexane as the eluent yielding the title compound as a colorless solid (2.46 g, 96%).

¹H-NMR (500 MHz, CD₂Cl₂): δ 7.93-7.90 (m, 2H), 7.85 (two singlets, 2H), 7.42-7.15 (m, 12H), 5.18 (0.4H), 5.15 (three singlets, 1.5H), 3.01-2.92 (m, 1.1H), 2.91-2.82 (m, 0.9H), 2.39 (s, 1.4H), 2.38 (s, 2.5H), 2.36 (s, 2.0H), 1.21-1.19 (two doublets, 3.4H), 1.17-1.13 (m, 6.1H), 1.09 (d, *J* = 6.9 Hz, 1.4H), 1.07 (d, *J* = 6.9 Hz, 1.3H) (spectra complicated due to presence of rotamers);

¹³C-NMR (125 MHz, CD₂Cl₂): δ 150.9, 150.9, 150.8, 150.8, 145.4, 145.4, 145.4, 135.9, 135.9, 135.8, 135.8, 135.7, 133.8, 133.7, 133.6, 133.5, 131.5, 131.4, 131.4, 131.4, 131.3, 131.3, 131.3, 131.3, 129.9, 129.9, 129.7, 129.6, 129.6, 128.8, 128.7, 127.3, 127.2, 126.0, 125.9, 125.8, 124.9, 124.7, 124.4, 124.4, 124.4, 113.1, 113.0, 112.9, 30.6, 30.6, 30.6, 30.5, 24.9, 24.9, 24.8, 24.8, 23.6, 23.6, 23.5, 23.5, 21.1, 21.0 (including signals due to presence of rotamers);

HRMS (ESI+) (*m/z*): [M+Na] calcd for C₄₀H₃₈O₂Na, 573.2764; found, 573.2766.

(S)-4-Chloro-2,6-bis(2-isopropyl-5-methylphenyl)dinaphtho[2,1-d:1',2'-f][1,3,2]dioxaphosphepine 4-oxide (13gd)



To a solution of (*S*)-**13gc** (292 mg, 0.53 mmol) in pyridine (2 ml) under argon was added POCl₃ (148 μl, 244 mg, 1.59 mmol) at room temperature. The mixture was stirred at 60 °C for 1.5 h and then concentrated to dryness under vacuum. The residue was passed through a short silica gel column (5 g) using CH₂Cl₂ as the eluent yielding the title compound as a colorless solid (322 mg, 96%).

¹H-NMR (500 MHz, CD₂Cl₂): δ 8.04-7.95 (m, 4H), 7.60-7.56 (m, 2H), 7.46-7.35 (m, 4.4H), 7.33-7.30 (m, 1.6H), 7.28-7.23 (m, 2.7H), 7.18-7.10 (m, 1.2H), 3.17-3.11 (m, 0.2H), 3.07-2.99 (m, 0.2H), 2.84-2.75 (m, 1.6H), 2.39-2.36 (m, 4.7H), 2.32-2.31 (m, 1.2H), 1.47-1.45 (m, 0.5H), 1.34 (d, *J* = 6.8 Hz, 0.8H), 1.22-1.14 (m, 6H), 1.05-1.03 (m, 2.3H), 0.98 (d, *J* = 6.8 Hz, 2.5H) (spectra complicated due to presence of rotamers);

¹³C-NMR (125 MHz, CD₂Cl₂): δ 145.2, 145.1, 144.9, 144.9, 144.8, 144.8, 144.7, 135.3, 135.0, 135.0, 134.7, 134.4, 134.3, 134.2, 134.1, 134.1, 133.2, 133.1, 133.0, 132.5, 132.5, 132.4, 132.3, 132.3, 132.2, 132.2, 131.8, 131.6, 131.5, 130.0, 130.0, 129.9, 129.9, 129.7, 128.9, 128.8, 127.6, 127.5, 127.4, 127.3, 127.3, 127.2, 127.0, 126.9, 126.6, 125.5, 125.4, 125.3, 122.2, 122.1, 30.8,

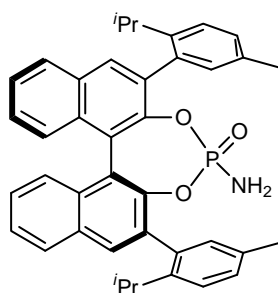
7. EXPERIMENTAL SECTION

30.7, 30.2, 29.9, 26.9, 25.9, 25.3, 25.1, 23.9, 23.6, 23.4, 23.0, 22.9, 21.0, 21.0 (including signals due to presence of rotamers and unassigned C-P-coupling);

³¹P-NMR (202 MHz, CD₂Cl₂): δ 7.78 (major), 7.60, 7.52, 7.47 (including signals due to presence of rotamers);

HRMS (ESI+) (*m/z*): [M+Na] calcd for C₄₀H₃₆O₃ClPNa, 653.1983; found, 653.1978.

(*S*)-4-Amino-2,6-bis(2-isopropyl-5-methylphenyl)dinaphtho[2,1-*d*:1',2'-*f*][1,3,2]dioxaphosphine 4-oxide (**13ge**)



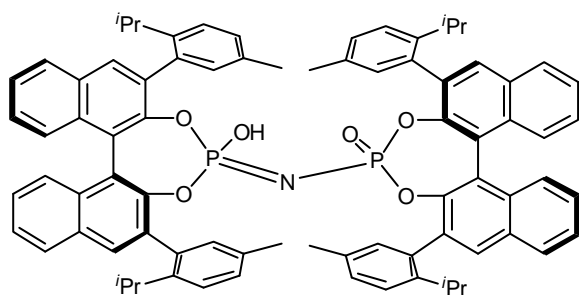
To a solution of (*S*)-**13gc** (242 mg, 0.44 mmol) in pyridine (2 ml) under argon was added POCl₃ (123 μl, 202 mg, 1.32 mmol) at room temperature. After 1.5 h at 60 °C, the mixture was cooled to -78 °C and anhydrous ammonia gas was condensed into the reaction flask (ca. 10 ml). The cooling bath was removed and the mixture was allowed to warm to room temperature. The reaction mixture was then concentrated to dryness under vacuum. Residue was passed through short silica gel column (10 g) using 5% EtOAc/CH₂Cl₂ as the eluent yielding the title compound as a colorless solid (252 mg, 94%).

¹H-NMR (500 MHz, CD₂Cl₂): δ 8.05-7.85 (m, 4H), 7.58-7.52 (m, 2H), 7.46 (d, *J* = 8.6 Hz, 1.6H), 7.42-7.21 (m, 6.9H), 7.12-7.03 (m, 1.1H), 6.84 (d, *J* = 7.8 Hz, 0.2H), 3.14-3.03 (m, 0.4H), 2.90-2.76 (m, 1.6H), 2.72-2.61 (m, 2H), 2.38-2.27 (m, 5.2H), 2.04 (s, 0.7H), 1.46-1.44 (m, 0.4H), 1.34-1.31 (m, 0.9), 1.22-1.19 (m, 2.6H), 1.17-1.09 (m, 3.4H), 1.06-1.03 (m, 2.2H), 0.99-0.96 (m, 2.6H) (spectra complicated due to presence of rotamers);

¹³C-NMR (125 MHz, CD₂Cl₂): δ 145.5, 145.4, 145.3, 144.9, 144.9, 144.6, 136.0, 135.9, 135.9, 135.4, 135.3, 135.1, 134.8, 134.7, 134.7, 134.7, 134.7, 134.6, 132.6, 132.4, 132.3, 132.1, 131.9, 131.6, 131.5, 129.9, 129.9, 129.6, 129.5, 129.0, 128.8, 128.7, 127.4, 127.4, 126.9, 126.9, 126.8, 126.4, 126.4, 126.3, 125.8, 125.7, 125.1, 125.1, 122.6, 122.6, 122.3, 122.3, 30.8, 30.7, 30.6, 30.2, 30.0, 26.6, 25.7, 25.3, 24.9, 24.1, 23.7, 23.5, 23.0, 23.0, 21.2, 21.1, 21.0, 20.9 (including signals due to presence of rotamers and unassigned C-P-coupling);

³¹P-NMR (202 MHz, CD₂Cl₂): δ 13.2, 12.2, 12.1 (major), 11.8 (including signals due to presence of rotamers);

HRMS (ESI+) (*m/z*): [M+Na] calcd for C₄₀H₃₈NO₃PNa, 634.2482; found, 634.2478.

Imidodiphosphoric acid **13g**

Sodium hydride (60% dispersion of in mineral oil, 47 mg, 1.18 mmol) was added to a solution of (S)-**13ge** (241 mg, 0.394 mmol) and (S)-**13gd** (298 mg, 0.473 mmol) in THF (3 ml) under argon at room temperature. After 18 h at room temperature, 10% aqueous HCl solution (10 ml)

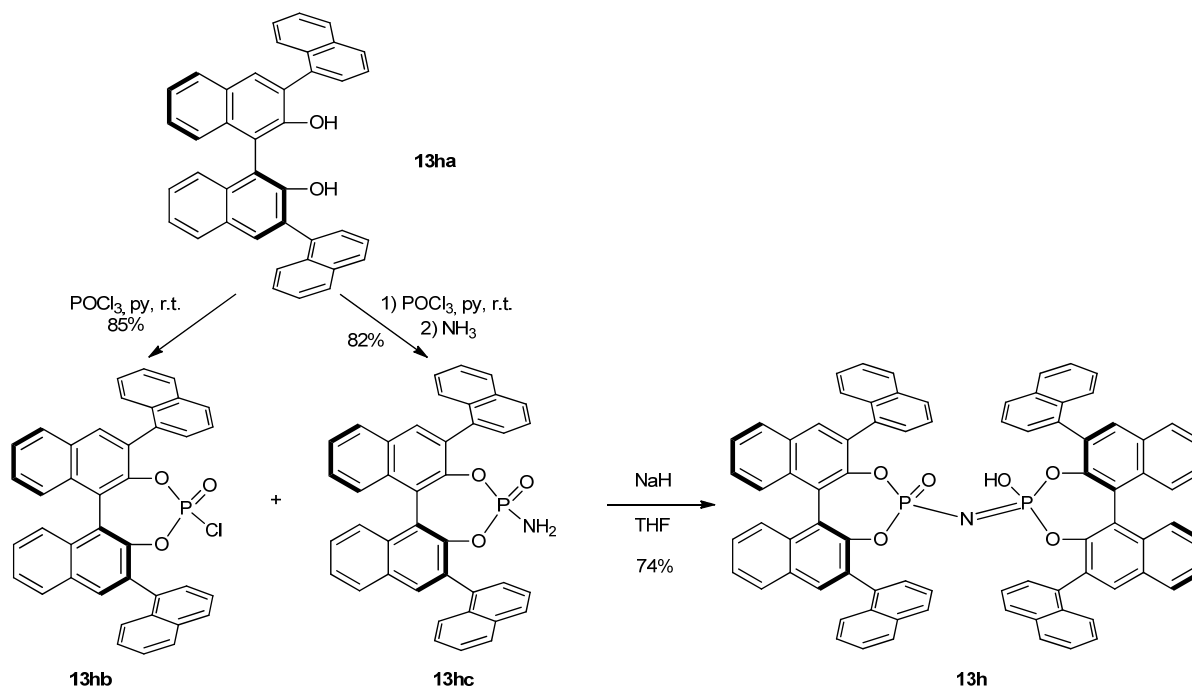
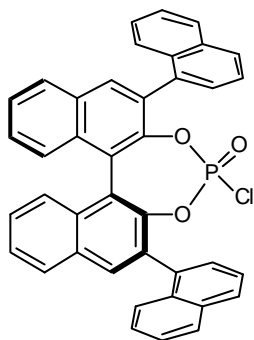
and DCM (10 ml) were added, and the mixture was stirred for 1 h. The organic layer was separated and the solvent was removed under reduced pressure. The residue was purified by column chromatography on aluminum oxide (activity III, 20 g) using 0-16% EtOAc/DCM as the eluents giving a colorless solid. The solid was dissolved in CH₂Cl₂ (10 ml) and stirred with 3 N aqueous HCl (10 ml) for 1 h. The organic layer was separated and concentrated under reduced pressure to give the title compound as a colorless solid (334 mg, 70%).

¹H-NMR (500 MHz, DMSO-d₆): δ 8.27 (d, *J* = 8.2 Hz, 2H), 8.00 (d, *J* = 8.2 Hz, 2H), 7.84 (s, 2H), 7.63-7.60 (m, 4H), 7.45 (t, *J* = 7.5 Hz, 2H), 7.35-7.28 (m, 4H), 7.17 (d, *J* = 7.9 Hz, 2H), 7.11-7.08 (m, 4H), 7.05 (s, 2H), 7.02 (d, *J* = 8.0 Hz, 2H), 6.94 (d, *J* = 8.0 Hz, 2H), 6.51 (s, 2H), 5.85 (d, *J* = 8.0 Hz, 2H), 2.41-2.35 (m, 4H), 2.34 (s, 6H), 2.14 (s, 6H), 0.91 (d, *J* = 6.9 Hz, 6H), 0.85 (d, *J* = 6.8 Hz, 6H), 0.42 (d, *J* = 6.8 Hz, 6H), -0.15 (d, *J* = 6.8 Hz, 6H) (actual spectra is complicated by the presence of additional signals due to small amounts of other rotamers, which are not included here);

¹³C-NMR (125 MHz, DMSO-d₆): δ 143.0, 142.5, 135.5, 135.2, 134.1, 133.4, 133.0, 132.0, 132.0, 131.7, 131.6, 131.0, 130.9, 130.6, 130.3, 128.9, 128.6, 128.3, 126.7, 126.2, 125.8, 125.7, 125.3, 124.9, 123.4, 123.0, 121.8, 120.3, 29.3, 28.8, 25.3, 25.0, 24.3, 23.9, 23.6, 23.2, 23.0, 20.9, 20.8, 20.2;

³¹P-NMR (202 MHz, DMSO-d₆): δ -13.9 (s), (additional signals at 2.33, -0.5, -0.9, -2.2 due to small amounts of other rotamers);

HRMS (ESI⁻) (*m/z*): [M-H] calcd for C₈₀H₇₂NO₆P₂, 1204.4840; found, 1204.4829.

13h**(S)-4-Chloro-2-(naphthalen-1-yl)-6-(naphthalen-4-yl)dinaphtho[2,1-d:1',2'-f][1,3,2]dioxaphosphine 4-oxide (13hb)**

To a solution of **13ha** (516 mg, 0.958 mmol) in pyridine (3.3 ml) under argon was added POCl_3 (267 μl , 441 mg, 2.87 mmol) at room temperature. The mixture was stirred for 16 h and then concentrated to dryness under vacuum. The residue was passed through a short silica gel column (10 g) using DCM as the eluent yielding the title compound as a colorless solid (514 mg, 85%).

$^1\text{H-NMR}$ (500 MHz, CD_2Cl_2): δ 8.22-8.19 (m, 1H), 8.15-8.14 (m, 1H), 8.10-8.03 (m, 2H), 8.00-7.93 (m, 4.4H), 7.87 (d, $J = 8.5$ Hz, 0.1H), 7.83 (d, $J = 8.4$ Hz, 0.2H), 7.75 (dd, $J = 7.1, 1.0$ Hz, 0.3H), 7.70 (dt, $J = 7.0, 1.0$ Hz, 0.6H), 7.67-7.53 (m, 8.5H), 7.52-7.45 (m, 4.1H), 7.43-7.37 (m, 1.9H) (spectra complicated due to presence of rotamers);

$^{13}\text{C-NMR}$ (125 MHz, CD_2Cl_2): δ 145.3, 145.2, 145.1, 145.1, 145.1, 145.0, 145.0, 135.0, 135.0, 134.6, 134.4, 134.4, 134.3, 133.7, 133.7, 133.6, 133.6, 133.3, 132.9, 132.8, 132.8, 132.8, 132.7, 132.6, 132.6, 132.5, 132.2, 131.9, 131.7, 131.5, 131.5, 129.6, 129.6, 129.5, 129.4, 129.3, 129.3, 129.1, 129.1, 129.0, 129.0, 128.9, 128.8, 128.8, 128.7, 128.5, 128.5, 128.4, 127.7, 127.7, 127.7, 127.6, 127.5, 127.5, 127.4, 127.2, 127.2, 126.9, 126.8, 126.7, 126.6, 126.5, 126.5, 126.4, 126.2, 126.0, 125.9, 125.8, 125.7, 125.4, 125.2, 125.2, 123.5, 123.5, 123.4, 123.4, 122.7, 122.7, 122.7,

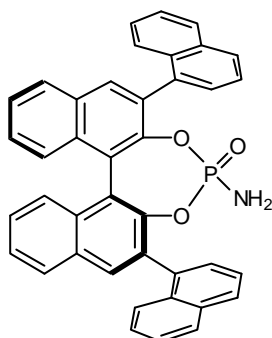
7. EXPERIMENTAL SECTION

122.6, 122.5, 122.5 (including signals due to presence of rotamers and unassigned C-P-coupling);

³¹P-NMR (202 MHz, CD₂Cl₂): δ 7.76, 7.68 (major), 7.54, 7.45 (spectra complicated due to presence of rotamers);

HRMS (ESI+) (*m/z*): [M+Na] calcd for C₄₀H₂₄O₃ClPNa, 641.1044; found, 641.1046.

(S)-4-Amino-2-(naphthalen-1-yl)-6-(naphthalen-4-yl)dinaphtho[2,1-d:1',2'-f][1,3,2]dioxaphosphine 4-oxide (13hc)



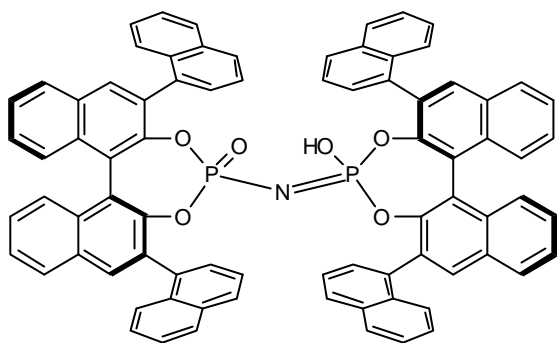
To a solution of **13ha** (430 mg, 0.798 mmol) in pyridine (2.8 ml) under argon was added POCl₃ (223 μl, 368 mg, 2.39 mmol) at room temperature. After 18 h at room temperature, the mixture was cooled to -78 °C and anhydrous ammonia gas was condensed into the reaction flask (ca. 5 ml). The cooling bath was removed and the mixture was allowed to warm to room temperature. The reaction mixture was then concentrated to dryness under vacuum. Residue was passed through short silica gel column (10 g) using 0-2% EtOAc/CH₂Cl₂ as the eluent yielding the title compound as a colorless solid (395 mg, 82%).

¹H-NMR (500 MHz, CD₂Cl₂): δ 8.16-8.13 (m, 1H), 8.09-8.00 (m, 2.9H), 7.99-7.81 (m, 4.6H), 7.77-7.32 (m, 15.8H), 2.53 (d, *J* = 6.8 Hz, 0.3H), 2.50 (m, *J* 6.8 Hz, 1H), 2.24 (d, *J* = 7.1 Hz, 0.1H), 2.17 (d, *J* = 7.2 Hz, 0.5H) (spectra complicated due to presence of rotamers);

¹³C-NMR (125 MHz, CD₂Cl₂): δ 145.9, 145.8, 145.7, 145.7, 145.1, 145.1, 136.1, 135.3, 134.7, 134.5, 134.1, 134.0, 133.8, 133.7, 133.6, 133.6, 133.6, 133.4, 133.4, 133.4, 133.3, 133.3, 133.2, 133.2, 133.2, 133.0, 133.0, 132.9, 132.8, 132.7, 132.6, 132.6, 132.5, 132.2, 132.0, 131.9, 131.9, 131.4, 129.5, 129.3, 129.2, 129.0, 128.9, 128.9, 128.8, 128.7, 128.7, 128.7, 128.6, 128.3, 128.3, 128.2, 128.2, 127.5, 127.5, 127.4, 127.4, 127.4, 127.3, 127.3, 127.2, 127.1, 126.9, 126.8, 126.7, 126.6, 126.6, 126.6, 126.5, 126.5, 126.4, 126.4, 126.3, 126.1, 126.1, 126.0, 125.8, 125.7, 125.6, 125.3, 125.1, 125.1, 123.7, 123.7, 123.3, 123.3, 122.8, 122.8, 122.6, 122.6, 122.6, 122.6, (including signals due to presence of rotamers and unassigned C-P-coupling);

³¹P-NMR (202 MHz, CD₂Cl₂): δ 12.12, 11.94 (major), 11.77, 11.73 (spectra complicated due to presence of rotamers);

HRMS (ESI+) (*m/z*): [M+Na] calcd for C₄₀H₂₆NO₃PNa, 622.1543; found, 622.1543.

Imidodiphosphoric acid **13h**

Sodium hydride (60% dispersion of in mineral oil, 63 mg, 1.58 mmol) was added to a solution of **13hb** (392 mg, 0.633 mmol) and **13hc** (316 mg, 0.528 mmol) in THF (4 ml) under argon at room temperature. After 18 h at room temperature, 10% aqueous HCl solution (15 ml) and DCM (15 ml) were added, and the mixture was stirred for 1

h. The organic layer was separated and aqueous one extracted with DCM (4 · 10 ml). Combined organic extracts were washed with brine and the solvent was removed under reduced pressure. The residue was purified by column chromatography on silica using 50% DCM/hexane, followed by DCM and 2-100% EtOAc/hexane as the eluents. The solid was dissolved in CH₂Cl₂ (25 ml) and stirred with 3 N aqueous HCl (25 ml) for 2 h. The organic layer was separated, washed with 3 N aqueous HCl (25 ml) and concentrated under reduced pressure. The residue was purified again by column chromatography under the same conditions and acidified as described to give the title compound as a colorless solid (460 mg, 74%).

¹H-NMR (500 MHz, DMSO-d₆): δ 8.13-7.12 (m, 46H), 6.75 (bs, 0.5H), 6.67 (t, *J* = 7.5 Hz, 1H), 6.55 (t, *J* = 7.1 Hz, 0.5H), 5.96-5.85 (m, 1.8H) (spectra complicated due to presence of rotamers);

¹³C-NMR (125 MHz, DMSO-d₆): δ 146.9, 146.9, 146.8, 146.7, 146.1, 134.7, 134.6, 134.2, 133.9, 133.9, 133.6, 133.3, 133.2, 133.0, 132.9, 132.5, 132.5, 132.3, 132.3, 132.3, 132.2, 132.1, 132.0, 131.9, 131.9, 131.8, 131.8, 131.7, 131.6, 131.3, 131.2, 131.2, 131.0, 130.9, 130.8, 130.6, 130.5, 130.1, 130.0, 128.8, 128.7, 128.6, 128.5, 128.4, 128.2, 128.1, 127.7, 127.6, 127.5, 127.3, 127.2, 126.8, 126.5, 126.3, 126.1, 125.8, 125.7, 125.6, 125.5, 125.4, 125.4, 125.2, 125.1, 124.9, 124.9, 124.8, 122.9, 122.3, 122.2, 122.1, 122.0 (including signals due to presence of rotamers and unassigned C-P-coupling);

³¹P-NMR (202 MHz, DMSO-d₆): δ 0.69, -0.20, -0.48 (bs, major), -0.74(s, major) (spectra complicated due to presence of rotamers);

HRMS (ESI⁻) (*m/z*): [M-H] calcd for C₈₀H₄₈NO₆P₂, 1180.2962; found, 1180.2971.

7.5.2. X-Ray data for compounds 13a-c

X-Ray structure of 13c

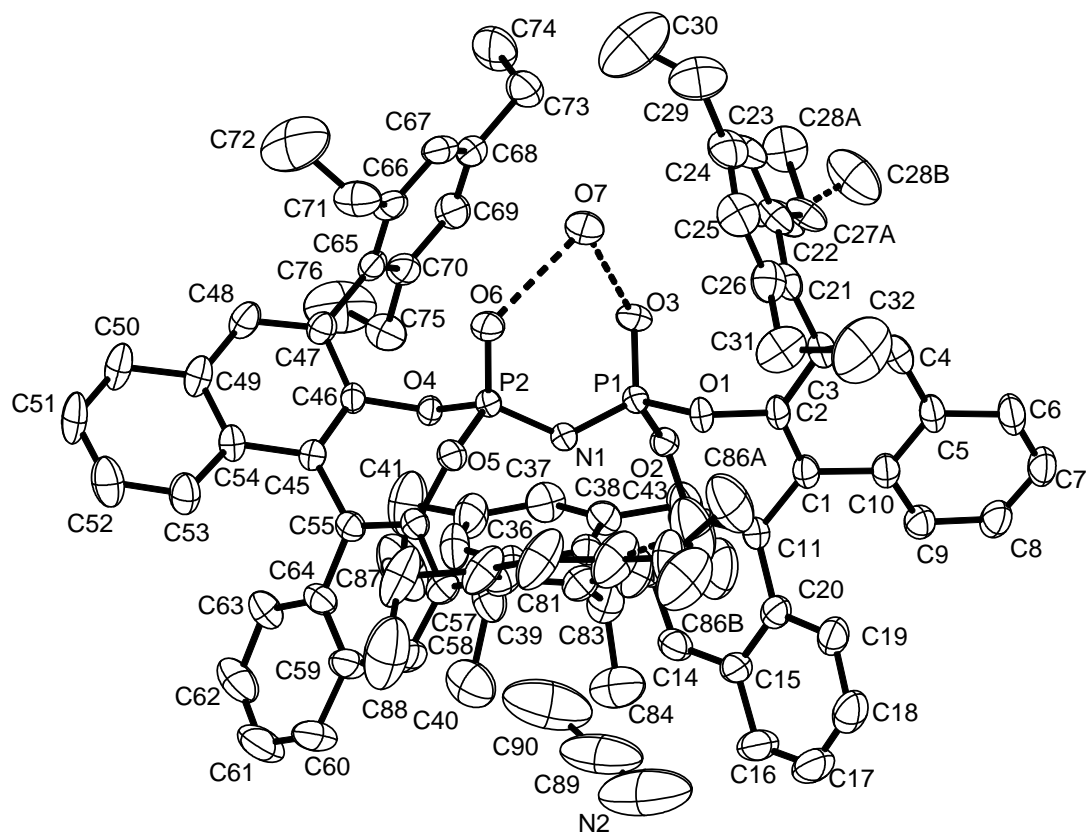


Figure 7.2. Single crystal X-ray structure determination of 13c. The crystals were grown from concentrated solution in hot and wet CH_3CN by slowly cooling the solution to room temperature. The molecular structure of $\mathbf{13c}\cdot[\text{H}_2\text{O}]\cdot[\text{CH}_3\text{CN}]$, showing the $\text{O}-\text{H}\cdots\text{O}$ hydrogen bonding interactions between the imidodiphosphate $\mathbf{13c}$ and the solute water molecule O7. Probability ellipsoids are shown at the 50% level. H atoms omitted for clarity. Two of the ethyl groups in the 2,4,6-triethylphenyl groups are disordered over two positions (C27, C28 [A:B = 0.5:0.5] and C85, C86 [A:B = 0.62:0.38]). Bond distances in the water-imidodiphosphate region (O7/O3-P1-N1-P2-O6) indicate disorder of the H atoms attached to O3, O6 and O7, which could not be located in a difference Fourier synthesis: O3 \cdots O7 2.479(4) Å, O6 \cdots O7 2.483(4) Å. Intensity data were collected on an Enraf-Nonius CAD4 diffractometer, equipped with a graphite monochromator, using Mo-K α radiation generated on a Bruker-Nonius FR591 rotating anode. Data were absorption corrected and scaled using the program

7. EXPERIMENTAL SECTION

SADABS (Bruker AXS, 2008). The structure was solved and refined using the programs SHELXS and SHELXL, both programs from G. M. Sheldrick.^[153] X-ray crystallographic data have been deposited in the Cambridge Crystallographic Data Centre database (<http://www.ccdc.cam.ac.uk/>) under accession code CCDC 864762.

Crystal data and structure refinement for 13c.

Identification code	7553
Empirical formula	C ₉₀ H ₉₁ N ₂ O ₇ P ₂
Color	colorless
Formula weight	1374.59 g · mol ⁻¹
Temperature	200 K
Wavelength	0.71073 Å
Crystal system	Orthorhombic
Space group	P2₁2₁2₁, (no. 19)
Unit cell dimensions	a = 15.4764(13) Å α = 90°. b = 16.426(2) Å β = 90°. c = 30.614(2) Å γ = 90°.
Volume	7782.6(14) Å ³
Z	4
Density (calculated)	1.173 Mg · m ⁻³
Absorption coefficient	0.112 mm ⁻¹
F(000)	2924 e
Crystal size	0.351 x 0.219 x 0.182 mm ³
θ range for data collection	2.63 to 31.32°.
Index ranges	-14 ≤ h ≤ 22, -24 ≤ k ≤ 24, -44 ≤ l ≤ 44
Reflections collected	107767
Independent reflections	25375 [R _{int} = 0.0628]
Reflections with I > 2σ(I)	16444
Completeness to θ = 31.32°	99.7 %
Absorption correction	Gaussian
Max. and min. transmission	0.98 and 0.97

7. EXPERIMENTAL SECTION

Refinement method	Full-matrix least-squares on F^2	
Data / restraints / parameters	25375 / 0 / 960	
Goodness-of-fit on F^2	1.107	
Final R indices [$I > 2\sigma(I)$]	$R_1 = 0.0718$	$wR^2 = 0.1431$
R indices (all data)	$R_1 = 0.1271$	$wR^2 = 0.1650$
Absolute structure parameter	0.10(8)	
Largest diff. peak and hole	0.592 and -0.352 e · Å ⁻³	

Atomic coordinates and equivalent isotropic displacement parameters (Å²) for 13c. U_{eq} is defined as one third of the trace of the orthogonalized U_{ij} tensor.

	x	y	z	U_{eq}
P(1)	0.2300(1)	0.3809(1)	0.3952(1)	0.025(1)
P(2)	0.1359(1)	0.4895(1)	0.3398(1)	0.025(1)
N(1)	0.2147(1)	0.4590(1)	0.3671(1)	0.028(1)
N(2)	0.5246(5)	0.6920(5)	0.5417(2)	0.170(4)
O(1)	0.3027(1)	0.3315(1)	0.3693(1)	0.029(1)
O(2)	0.2740(1)	0.4000(1)	0.4413(1)	0.027(1)
O(3)	0.1555(1)	0.3271(1)	0.4067(1)	0.035(1)
O(4)	0.0861(1)	0.5508(1)	0.3714(1)	0.025(1)
O(5)	0.1645(1)	0.5462(1)	0.2998(1)	0.029(1)
O(6)	0.0767(1)	0.4297(1)	0.3190(1)	0.036(1)
O(7)	0.0601(2)	0.2874(1)	0.3453(1)	0.058(1)
C(1)	0.4170(2)	0.2999(2)	0.4184(1)	0.029(1)
C(2)	0.3533(2)	0.2731(2)	0.3905(1)	0.028(1)
C(3)	0.3379(2)	0.1903(2)	0.3801(1)	0.033(1)
C(4)	0.3960(2)	0.1353(2)	0.3966(1)	0.040(1)
C(5)	0.4633(2)	0.1573(2)	0.4257(1)	0.035(1)
C(6)	0.5203(2)	0.0980(2)	0.4434(1)	0.045(1)
C(7)	0.5782(2)	0.1190(2)	0.4750(1)	0.047(1)
C(8)	0.5821(2)	0.1981(2)	0.4902(1)	0.043(1)
C(9)	0.5310(2)	0.2576(2)	0.4723(1)	0.036(1)
C(10)	0.4718(2)	0.2396(2)	0.4385(1)	0.032(1)
C(11)	0.4270(2)	0.3874(2)	0.4292(1)	0.029(1)
C(12)	0.3572(2)	0.4336(2)	0.4433(1)	0.026(1)
C(13)	0.3660(2)	0.5099(2)	0.4641(1)	0.030(1)
C(14)	0.4467(2)	0.5425(2)	0.4664(1)	0.039(1)
C(15)	0.5196(2)	0.5045(2)	0.4473(1)	0.038(1)
C(16)	0.6027(2)	0.5421(2)	0.4470(1)	0.054(1)

7. EXPERIMENTAL SECTION

C(17)	0.6698(2)	0.5063(3)	0.4263(1)	0.064(1)
C(18)	0.6596(2)	0.4321(3)	0.4053(1)	0.058(1)
C(19)	0.5818(2)	0.3921(2)	0.4058(1)	0.045(1)
C(20)	0.5097(2)	0.4272(2)	0.4275(1)	0.034(1)
C(21)	0.2612(2)	0.1629(2)	0.3550(1)	0.036(1)
C(22)	0.1894(2)	0.1321(2)	0.3777(1)	0.040(1)
C(23)	0.1188(2)	0.1036(2)	0.3541(1)	0.047(1)
C(24)	0.1173(2)	0.1049(2)	0.3082(1)	0.049(1)
C(25)	0.1878(2)	0.1376(2)	0.2873(1)	0.051(1)
C(26)	0.2607(2)	0.1665(2)	0.3097(1)	0.043(1)
C(27A)	0.1965(10)	0.1176(7)	0.4245(5)	0.043(3)
C(28A)	0.1168(5)	0.0943(5)	0.4475(2)	0.056(2)
C(27B)	0.1801(11)	0.1405(7)	0.4294(5)	0.041(3)
C(28B)	0.1933(8)	0.0591(6)	0.4513(3)	0.083(3)
C(29)	0.0417(3)	0.0721(3)	0.2831(1)	0.075(1)
C(30)	-0.0404(4)	0.1031(5)	0.2947(2)	0.120(3)
C(31)	0.3368(2)	0.1978(3)	0.2838(1)	0.061(1)
C(32)	0.4031(4)	0.1302(4)	0.2742(2)	0.113(2)
C(33)	0.2909(2)	0.5517(2)	0.4856(1)	0.032(1)
C(34)	0.2504(2)	0.6180(2)	0.4660(1)	0.038(1)
C(35)	0.1844(2)	0.6582(2)	0.4880(1)	0.049(1)
C(36)	0.1575(2)	0.6336(2)	0.5292(1)	0.052(1)
C(37)	0.1980(2)	0.5682(2)	0.5480(1)	0.047(1)
C(38)	0.2639(2)	0.5261(2)	0.5273(1)	0.039(1)
C(39)	0.2773(3)	0.6505(2)	0.4218(1)	0.048(1)
C(40)	0.3335(3)	0.7262(3)	0.4245(1)	0.071(1)
C(41)	0.0897(3)	0.6827(3)	0.5536(2)	0.083(2)
C(42)	0.1296(4)	0.7412(3)	0.5861(2)	0.102(2)
C(43)	0.3074(2)	0.4567(2)	0.5510(1)	0.051(1)
C(44)	0.3772(3)	0.4846(3)	0.5820(2)	0.094(2)
C(45)	0.0456(2)	0.6677(2)	0.3312(1)	0.027(1)
C(46)	0.0214(2)	0.5999(2)	0.3541(1)	0.026(1)
C(47)	-0.0656(2)	0.5778(2)	0.3632(1)	0.031(1)
C(48)	-0.1281(2)	0.6314(2)	0.3506(1)	0.038(1)
C(49)	-0.1091(2)	0.7032(2)	0.3268(1)	0.037(1)
C(50)	-0.1754(2)	0.7579(2)	0.3143(1)	0.049(1)
C(51)	-0.1580(2)	0.8240(2)	0.2890(1)	0.058(1)
C(52)	-0.0730(3)	0.8389(2)	0.2750(1)	0.058(1)
C(53)	-0.0069(2)	0.7880(2)	0.2873(1)	0.043(1)
C(54)	-0.0220(2)	0.7204(2)	0.3153(1)	0.032(1)
C(55)	0.1389(2)	0.6852(2)	0.3219(1)	0.028(1)
C(56)	0.1927(2)	0.6265(2)	0.3043(1)	0.027(1)
C(57)	0.2749(2)	0.6447(2)	0.2859(1)	0.034(1)
C(58)	0.3038(2)	0.7233(2)	0.2894(1)	0.044(1)
C(59)	0.2568(2)	0.7831(2)	0.3120(1)	0.042(1)
C(60)	0.2902(3)	0.8633(2)	0.3183(1)	0.060(1)
C(61)	0.2471(3)	0.9187(2)	0.3426(2)	0.069(1)
C(62)	0.1691(3)	0.8975(2)	0.3622(1)	0.063(1)

7. EXPERIMENTAL SECTION

C(63)	0.1329(2)	0.8227(2)	0.3562(1)	0.045(1)
C(64)	0.1750(2)	0.7638(2)	0.3299(1)	0.035(1)
C(65)	-0.0857(2)	0.4973(2)	0.3839(1)	0.031(1)
C(66)	-0.1143(2)	0.4330(2)	0.3576(1)	0.035(1)
C(67)	-0.1291(2)	0.3577(2)	0.3769(1)	0.038(1)
C(68)	-0.1176(2)	0.3446(2)	0.4211(1)	0.037(1)
C(69)	-0.0896(2)	0.4091(2)	0.4464(1)	0.039(1)
C(70)	-0.0728(2)	0.4862(2)	0.4287(1)	0.036(1)
C(71)	-0.1297(2)	0.4420(2)	0.3087(1)	0.052(1)
C(72)	-0.2205(4)	0.4503(5)	0.2952(2)	0.115(2)
C(73)	-0.1355(2)	0.2621(2)	0.4416(1)	0.049(1)
C(74)	-0.2042(3)	0.2668(3)	0.4765(2)	0.076(1)
C(75)	-0.0425(2)	0.5532(2)	0.4586(1)	0.046(1)
C(76)	-0.1097(4)	0.5810(4)	0.4900(2)	0.109(2)
C(77)	0.3233(2)	0.5821(2)	0.2599(1)	0.040(1)
C(78)	0.3799(2)	0.5279(2)	0.2803(1)	0.044(1)
C(79)	0.4218(2)	0.4700(3)	0.2555(1)	0.064(1)
C(80)	0.4096(3)	0.4642(3)	0.2101(2)	0.080(2)
C(81)	0.3565(3)	0.5207(3)	0.1909(1)	0.080(2)
C(82)	0.3141(2)	0.5807(3)	0.2143(1)	0.059(1)
C(83)	0.4007(2)	0.5335(2)	0.3285(1)	0.048(1)
C(84)	0.4794(3)	0.5862(3)	0.3364(1)	0.072(1)
C(85A)	0.4600(7)	0.4108(6)	0.1791(4)	0.067(3)
C(86A)	0.4559(8)	0.3266(7)	0.1954(4)	0.094(4)
C(85B)	0.4518(16)	0.3759(14)	0.1921(7)	0.100(7)
C(86B)	0.4983(9)	0.4067(10)	0.1525(5)	0.098(6)
C(87)	0.2632(3)	0.6459(3)	0.1884(1)	0.075(1)
C(88)	0.3246(4)	0.7056(4)	0.1658(2)	0.115(2)
C(89)	0.4543(7)	0.7032(5)	0.5522(2)	0.119(3)
C(90)	0.3663(6)	0.7152(5)	0.5641(2)	0.151(3)

Bond lengths [Å] and angles [°] for 13c.

C(1)-C(2)	1.376(4)	C(1)-C(10)	1.442(4)
C(1)-C(11)	1.483(4)	C(2)-O(1)	1.399(3)
C(2)-C(3)	1.416(4)	C(3)-C(4)	1.372(4)
C(3)-C(21)	1.485(4)	C(4)-C(5)	1.418(4)
C(5)-C(10)	1.414(4)	C(5)-C(6)	1.422(4)
C(6)-C(7)	1.362(5)	C(7)-C(8)	1.383(5)
C(8)-C(9)	1.371(4)	C(9)-C(10)	1.413(4)
C(11)-C(12)	1.388(4)	C(11)-C(20)	1.439(4)
C(12)-O(2)	1.402(3)	C(12)-C(13)	1.411(4)
C(13)-C(14)	1.362(4)	C(13)-C(33)	1.502(4)
C(14)-C(15)	1.416(5)	C(15)-C(20)	1.414(4)
C(15)-C(16)	1.427(4)	C(16)-C(17)	1.351(6)
C(17)-C(18)	1.388(6)	C(18)-C(19)	1.371(5)

7. EXPERIMENTAL SECTION

C(19)-C(20)	1.421(4)	C(21)-C(26)	1.386(4)
C(21)-C(22)	1.406(4)	C(22)-C(23)	1.392(5)
C(22)-C(27A)	1.455(17)	C(22)-C(27B)	1.594(14)
C(23)-C(24)	1.404(5)	C(24)-C(25)	1.374(5)
C(24)-C(29)	1.501(5)	C(25)-C(26)	1.403(5)
C(26)-C(31)	1.511(5)	C(27A)-C(28A)	1.470(17)
C(27B)-C(28B)	1.511(15)	C(29)-C(30)	1.414(7)
C(31)-C(32)	1.540(7)	C(33)-C(34)	1.393(4)
C(33)-C(38)	1.408(4)	C(34)-C(35)	1.390(4)
C(34)-C(39)	1.513(5)	C(35)-C(36)	1.388(5)
C(36)-C(37)	1.371(5)	C(36)-C(41)	1.520(5)
C(37)-C(38)	1.386(4)	C(38)-C(43)	1.509(4)
C(39)-C(40)	1.521(5)	C(41)-C(42)	1.516(7)
C(43)-C(44)	1.510(6)	C(45)-C(46)	1.368(4)
C(45)-C(54)	1.444(4)	C(45)-C(55)	1.499(4)
C(46)-O(4)	1.391(3)	C(46)-C(47)	1.421(4)
C(47)-C(48)	1.365(4)	C(47)-C(65)	1.500(4)
C(48)-C(49)	1.416(4)	C(49)-C(50)	1.417(4)
C(49)-C(54)	1.422(4)	C(50)-C(51)	1.359(5)
C(51)-C(52)	1.404(6)	C(52)-C(53)	1.375(5)
C(53)-C(54)	1.420(4)	C(55)-C(56)	1.383(4)
C(55)-C(64)	1.429(4)	C(56)-O(5)	1.396(3)
C(56)-C(57)	1.422(4)	C(57)-C(58)	1.370(4)
C(57)-C(77)	1.500(4)	C(58)-C(59)	1.404(5)
C(59)-C(64)	1.416(4)	C(59)-C(60)	1.428(5)
C(60)-C(61)	1.353(6)	C(61)-C(62)	1.391(6)
C(62)-C(63)	1.363(5)	C(63)-C(64)	1.418(4)
C(65)-C(70)	1.397(4)	C(65)-C(66)	1.400(4)
C(66)-C(67)	1.390(4)	C(66)-C(71)	1.522(4)
C(67)-C(68)	1.383(4)	C(68)-C(69)	1.381(4)
C(68)-C(73)	1.519(4)	C(69)-C(70)	1.401(4)
C(70)-C(75)	1.504(4)	C(71)-C(72)	1.471(6)
C(73)-C(74)	1.508(6)	C(75)-C(76)	1.489(6)
C(77)-C(78)	1.398(5)	C(77)-C(82)	1.403(5)
C(78)-C(79)	1.379(5)	C(78)-C(83)	1.513(5)
C(79)-C(80)	1.404(6)	C(80)-C(81)	1.372(7)
C(80)-C(85A)	1.511(10)	C(80)-C(85B)	1.68(2)
C(81)-C(82)	1.384(5)	C(82)-C(87)	1.548(6)
C(83)-C(84)	1.514(5)	C(85A)-C(86A)	1.472(14)
C(85B)-C(86B)	1.50(2)	C(87)-C(88)	1.531(7)
C(89)-N(2)	1.148(11)	C(89)-C(90)	1.424(11)
N(1)-P(2)	1.560(2)	N(1)-P(1)	1.562(2)
O(1)-P(1)	1.5977(19)	O(2)-P(1)	1.5984(19)
O(3)-P(1)	1.4959(19)	O(4)-P(2)	1.5938(18)
O(5)-P(2)	1.6015(19)	O(6)-P(2)	1.487(2)
C(2)-C(1)-C(10)	117.8(3)	C(2)-C(1)-C(11)	121.6(2)
C(10)-C(1)-C(11)	120.6(3)	C(1)-C(2)-O(1)	118.0(2)

7. EXPERIMENTAL SECTION

C(1)-C(2)-C(3)	124.6(2)	O(1)-C(2)-C(3)	117.3(2)
C(4)-C(3)-C(2)	116.1(3)	C(4)-C(3)-C(21)	120.9(3)
C(2)-C(3)-C(21)	122.9(2)	C(3)-C(4)-C(5)	123.0(3)
C(10)-C(5)-C(4)	119.1(2)	C(10)-C(5)-C(6)	119.5(3)
C(4)-C(5)-C(6)	121.4(3)	C(7)-C(6)-C(5)	120.4(3)
C(6)-C(7)-C(8)	120.4(3)	C(9)-C(8)-C(7)	120.7(3)
C(8)-C(9)-C(10)	121.2(3)	C(9)-C(10)-C(5)	117.5(3)
C(9)-C(10)-C(1)	123.4(3)	C(5)-C(10)-C(1)	118.9(3)
C(12)-C(11)-C(20)	117.1(3)	C(12)-C(11)-C(1)	121.2(2)
C(20)-C(11)-C(1)	121.7(2)	C(11)-C(12)-O(2)	119.0(2)
C(11)-C(12)-C(13)	123.4(2)	O(2)-C(12)-C(13)	117.2(2)
C(14)-C(13)-C(12)	117.5(3)	C(14)-C(13)-C(33)	120.5(3)
C(12)-C(13)-C(33)	122.0(2)	C(13)-C(14)-C(15)	122.4(3)
C(20)-C(15)-C(14)	119.1(3)	C(20)-C(15)-C(16)	118.9(3)
C(14)-C(15)-C(16)	122.0(3)	C(17)-C(16)-C(15)	120.5(4)
C(16)-C(17)-C(18)	120.7(3)	C(19)-C(18)-C(17)	121.1(4)
C(18)-C(19)-C(20)	120.0(4)	C(15)-C(20)-C(19)	118.7(3)
C(15)-C(20)-C(11)	119.2(3)	C(19)-C(20)-C(11)	122.1(3)
C(26)-C(21)-C(22)	120.4(3)	C(26)-C(21)-C(3)	120.7(3)
C(22)-C(21)-C(3)	118.9(3)	C(23)-C(22)-C(21)	118.9(3)
C(23)-C(22)-C(27A)	121.1(7)	C(21)-C(22)-C(27A)	119.1(7)
C(23)-C(22)-C(27B)	118.4(7)	C(21)-C(22)-C(27B)	122.2(7)
C(27A)-C(22)-C(27B)	17.3(7)	C(22)-C(23)-C(24)	121.9(3)
C(25)-C(24)-C(23)	117.3(3)	C(25)-C(24)-C(29)	121.3(3)
C(23)-C(24)-C(29)	121.4(4)	C(24)-C(25)-C(26)	122.8(3)
C(21)-C(26)-C(25)	118.7(3)	C(21)-C(26)-C(31)	122.3(3)
C(25)-C(26)-C(31)	119.0(3)	C(22)-C(27A)-C(28A)	116.7(12)
C(28B)-C(27B)-C(22)	110.6(7)	C(30)-C(29)-C(24)	116.3(4)
C(26)-C(31)-C(32)	112.0(4)	C(34)-C(33)-C(38)	119.5(3)
C(34)-C(33)-C(13)	121.1(3)	C(38)-C(33)-C(13)	119.3(3)
C(35)-C(34)-C(33)	119.5(3)	C(35)-C(34)-C(39)	118.0(3)
C(33)-C(34)-C(39)	122.5(3)	C(36)-C(35)-C(34)	121.6(3)
C(37)-C(36)-C(35)	118.2(3)	C(37)-C(36)-C(41)	121.6(4)
C(35)-C(36)-C(41)	120.0(4)	C(36)-C(37)-C(38)	122.4(3)
C(37)-C(38)-C(33)	118.9(3)	C(37)-C(38)-C(43)	119.0(3)
C(33)-C(38)-C(43)	122.0(3)	C(34)-C(39)-C(40)	113.3(3)
C(42)-C(41)-C(36)	112.2(4)	C(38)-C(43)-C(44)	113.1(3)
C(46)-C(45)-C(54)	117.6(2)	C(46)-C(45)-C(55)	121.1(2)
C(54)-C(45)-C(55)	121.3(2)	C(45)-C(46)-O(4)	118.0(2)
C(45)-C(46)-C(47)	124.6(2)	O(4)-C(46)-C(47)	117.3(2)
C(48)-C(47)-C(46)	116.8(3)	C(48)-C(47)-C(65)	122.8(2)
C(46)-C(47)-C(65)	120.3(2)	C(47)-C(48)-C(49)	122.3(3)
C(48)-C(49)-C(50)	121.2(3)	C(48)-C(49)-C(54)	119.4(2)
C(50)-C(49)-C(54)	119.4(3)	C(51)-C(50)-C(49)	121.2(3)
C(50)-C(51)-C(52)	119.9(3)	C(53)-C(52)-C(51)	120.5(3)
C(52)-C(53)-C(54)	121.2(3)	C(53)-C(54)-C(49)	117.6(3)
C(53)-C(54)-C(45)	123.5(3)	C(49)-C(54)-C(45)	118.9(2)
C(56)-C(55)-C(64)	117.4(3)	C(56)-C(55)-C(45)	121.4(2)

7. EXPERIMENTAL SECTION

C(64)-C(55)-C(45)	121.1(2)	C(55)-C(56)-O(5)	120.5(2)
C(55)-C(56)-C(57)	123.1(3)	O(5)-C(56)-C(57)	116.1(2)
C(58)-C(57)-C(56)	117.3(3)	C(58)-C(57)-C(77)	121.6(3)
C(56)-C(57)-C(77)	120.8(3)	C(57)-C(58)-C(59)	121.9(3)
C(58)-C(59)-C(64)	119.8(3)	C(58)-C(59)-C(60)	121.7(3)
C(64)-C(59)-C(60)	118.6(3)	C(61)-C(60)-C(59)	121.1(4)
C(60)-C(61)-C(62)	119.8(3)	C(63)-C(62)-C(61)	121.6(4)
C(62)-C(63)-C(64)	120.2(3)	C(59)-C(64)-C(63)	118.6(3)
C(59)-C(64)-C(55)	119.1(3)	C(63)-C(64)-C(55)	122.3(3)
C(70)-C(65)-C(66)	120.8(3)	C(70)-C(65)-C(47)	120.1(3)
C(66)-C(65)-C(47)	119.0(2)	C(67)-C(66)-C(65)	118.6(3)
C(67)-C(66)-C(71)	118.6(3)	C(65)-C(66)-C(71)	122.9(3)
C(68)-C(67)-C(66)	122.2(3)	C(69)-C(68)-C(67)	118.0(3)
C(69)-C(68)-C(73)	120.7(3)	C(67)-C(68)-C(73)	121.3(3)
C(68)-C(69)-C(70)	122.4(3)	C(65)-C(70)-C(69)	118.0(3)
C(65)-C(70)-C(75)	123.0(3)	C(69)-C(70)-C(75)	119.0(3)
C(72)-C(71)-C(66)	115.8(3)	C(74)-C(73)-C(68)	112.0(3)
C(76)-C(75)-C(70)	113.6(3)	C(78)-C(77)-C(82)	119.8(3)
C(78)-C(77)-C(57)	120.9(3)	C(82)-C(77)-C(57)	119.2(3)
C(79)-C(78)-C(77)	119.2(3)	C(79)-C(78)-C(83)	118.7(3)
C(77)-C(78)-C(83)	122.0(3)	C(78)-C(79)-C(80)	121.9(4)
C(81)-C(80)-C(79)	117.3(4)	C(81)-C(80)-C(85A)	115.7(5)
C(79)-C(80)-C(85A)	126.3(5)	C(81)-C(80)-C(85B)	132.4(9)
C(79)-C(80)-C(85B)	109.3(9)	C(85A)-C(80)-C(85B)	24.9(7)
C(80)-C(81)-C(82)	122.9(4)	C(81)-C(82)-C(77)	118.6(4)
C(81)-C(82)-C(87)	117.9(4)	C(77)-C(82)-C(87)	123.4(3)
C(78)-C(83)-C(84)	111.3(3)	C(86A)-C(85A)-C(80)	108.1(9)
C(86B)-C(85B)-C(80)	99.3(15)	C(88)-C(87)-C(82)	111.1(3)
N(2)-C(89)-C(90)	178.2(8)	P(2)-N(1)-P(1)	132.57(15)
C(2)-O(1)-P(1)	120.75(16)	C(12)-O(2)-P(1)	120.55(16)
C(46)-O(4)-P(2)	118.91(16)	C(56)-O(5)-P(2)	124.19(16)
O(3)-P(1)-N(1)	119.91(12)	O(3)-P(1)-O(1)	111.12(11)
N(1)-P(1)-O(1)	104.52(11)	O(3)-P(1)-O(2)	103.62(11)
N(1)-P(1)-O(2)	112.92(11)	O(1)-P(1)-O(2)	103.76(10)
O(6)-P(2)-N(1)	119.90(12)	O(6)-P(2)-O(4)	112.33(11)
N(1)-P(2)-O(4)	104.85(11)	O(6)-P(2)-O(5)	103.13(11)
N(1)-P(2)-O(5)	112.31(11)	O(4)-P(2)-O(5)	103.26(10)

X-Ray structure of 13b

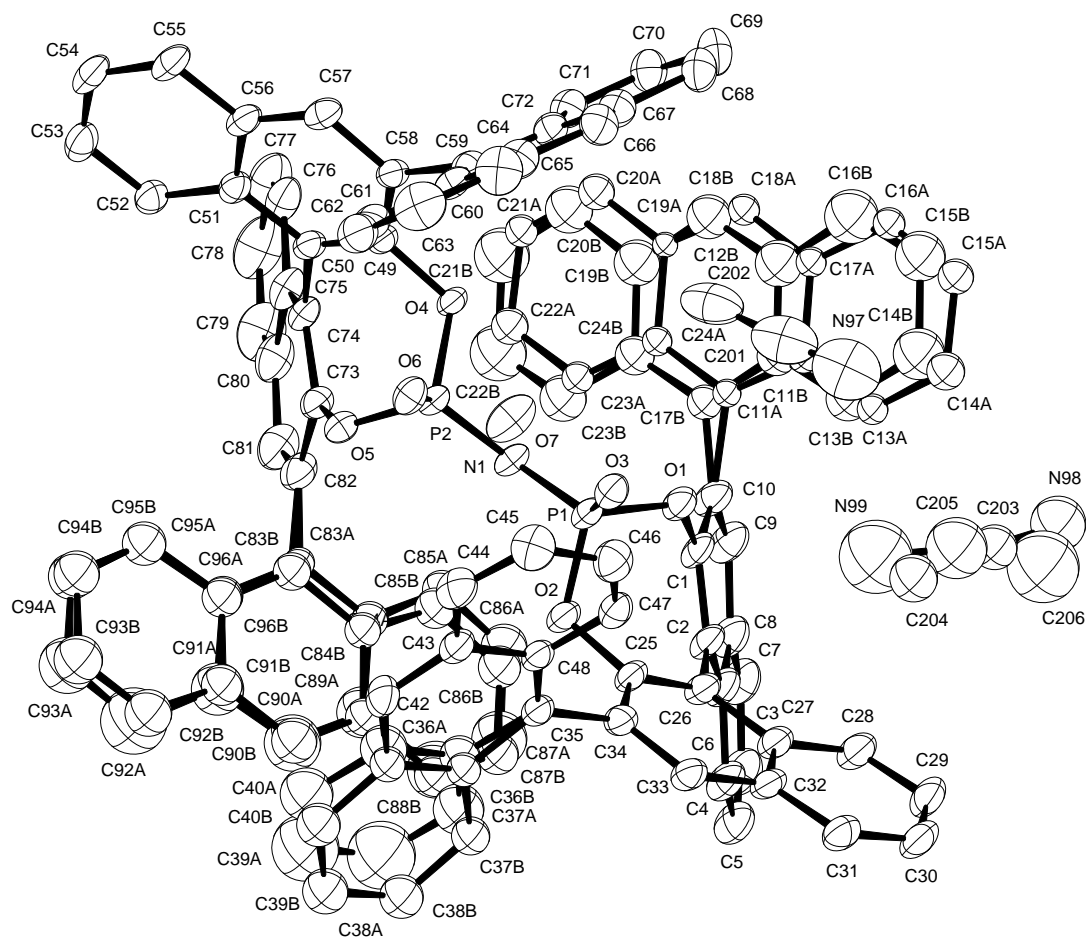


Figure 7.3. Single crystal X-ray structure determination of 13b. The crystals were grown from concentrated solution in hot and wet CH_3CN by slowly cooling the solution to room temperature. X-ray crystallographic data have been deposited in the Cambridge Crystallographic Data Centre database (<http://www.ccdc.cam.ac.uk/>) under accession code CCDC 898368.

Crystal data and structure refinement for 13b.

Identification code	7630
Empirical formula	$\text{C}_{100}\text{H}_{62.50}\text{N}_3\text{O}_7\text{P}_2$
Color	colorless
Formula weight	$1479.97\text{ g}\cdot\text{mol}^{-1}$
Temperature	100 K
Wavelength	0.71073 \AA

7. EXPERIMENTAL SECTION

Crystal system	Orthorhombic	
Space group	P2₁2₁2₁, (no. 19)	
Unit cell dimensions	a = 14.576(3) Å	α = 90°.
	b = 22.186(4) Å	β = 90°.
	c = 22.822(4) Å	γ = 90°.
Volume	7380(2) Å ³	
Z	4	
Density (calculated)	1.332 Mg · m ⁻³	
Absorption coefficient	0.124 mm ⁻¹	
F(000)	3078 e	
Crystal size	0.40 x 0.17 x 0.08 mm ³	
θ range for data collection	1.66 to 28.35°.	
Index ranges	-19 ≤ h ≤ 19, -29 ≤ k ≤ 29, -30 ≤ l ≤ 30	
Reflections collected	177678	
Independent reflections	18400 [R _{int} = 0.0731]	
Reflections with I > 2σ(I)	15160	
Completeness to θ = 27.50°	100.0 %	
Absorption correction	Gaussian	
Max. and min. transmission	1.00 and 0.80	
Refinement method	Full-matrix least-squares on F ²	
Data / restraints / parameters	18400 / 3 / 961	
Goodness-of-fit on F ²	1.072	
Final R indices [I > 2σ(I)]	R ₁ = 0.0648	wR ² = 0.1654
R indices (all data)	R ₁ = 0.0874	wR ² = 0.1870
Absolute structure parameter	-0.04(9)	
Largest diff. peak and hole	0.873 and -0.473 e · Å ⁻³	

7. EXPERIMENTAL SECTION

Atomic coordinates and equivalent isotropic displacement parameters (\AA^2) for 13b.

U_{eq} is defined as one third of the trace of the orthogonalized U_{ij} tensor.

	x	y	z	U_{eq}
P(1)	0.6598(1)	0.2662(1)	0.7131(1)	0.025(1)
P(2)	0.7059(1)	0.1443(1)	0.7431(1)	0.022(1)
O(1)	0.7278(2)	0.3161(1)	0.6868(1)	0.030(1)
O(2)	0.6114(1)	0.3013(1)	0.7660(1)	0.028(1)
O(3)	0.5953(2)	0.2529(1)	0.6645(1)	0.029(1)
O(4)	0.7934(1)	0.1166(1)	0.7103(1)	0.023(1)
O(5)	0.7129(2)	0.1180(1)	0.8077(1)	0.026(1)
O(6)	0.6202(2)	0.1145(1)	0.7207(1)	0.029(1)
O(7)	0.5201(2)	0.1532(1)	0.6455(1)	0.046(1)
N(1)	0.7168(2)	0.2140(1)	0.7421(1)	0.024(1)
N(97)	0.6718(4)	0.3093(3)	0.5054(2)	0.085(2)
N(98)	0.7220(8)	0.4982(5)	0.5056(5)	0.072(3)
N(99)	0.6336(13)	0.4158(8)	0.5831(8)	0.128(6)
C(1)	0.7734(2)	0.3582(1)	0.7212(2)	0.030(1)
C(2)	0.7241(2)	0.4021(1)	0.7501(2)	0.031(1)
C(3)	0.7736(2)	0.4429(1)	0.7869(2)	0.033(1)
C(4)	0.7295(2)	0.4863(1)	0.8222(2)	0.037(1)
C(5)	0.7786(3)	0.5221(2)	0.8601(2)	0.041(1)
C(6)	0.8752(3)	0.5169(2)	0.8635(2)	0.044(1)
C(7)	0.9203(3)	0.4766(2)	0.8295(2)	0.040(1)
C(8)	0.8712(2)	0.4385(2)	0.7905(2)	0.037(1)
C(9)	0.9168(2)	0.3959(2)	0.7549(2)	0.039(1)
C(10)	0.8704(2)	0.3561(1)	0.7202(2)	0.036(1)
C(11A)	0.9180(4)	0.3153(3)	0.6709(3)	0.019(2)
C(11B)	0.9298(4)	0.3204(2)	0.6293(2)	0.036(2)
C(12A)	0.9202(4)	0.3320(3)	0.6134(3)	0.021(1)
C(12B)	0.9824(4)	0.2818(3)	0.5950(2)	0.052(2)
C(13A)	0.8740(5)	0.3817(3)	0.5904(3)	0.022(2)
C(13B)	0.8851(7)	0.3672(5)	0.6010(4)	0.046(3)
C(14A)	0.8785(6)	0.3955(4)	0.5336(4)	0.034(2)
C(14B)	0.8912(9)	0.3766(6)	0.5420(6)	0.063(3)
C(15A)	0.9335(5)	0.3601(3)	0.4952(3)	0.030(1)
C(15B)	0.9501(8)	0.3362(6)	0.5076(5)	0.059(2)
C(16A)	0.9815(5)	0.3105(3)	0.5164(3)	0.024(1)
C(16B)	0.9912(9)	0.2916(6)	0.5349(6)	0.069(3)
C(17A)	0.9760(4)	0.2946(3)	0.5755(3)	0.022(1)
C(17B)	0.9236(3)	0.3111(2)	0.6894(2)	0.029(2)
C(18A)	1.0221(4)	0.2449(3)	0.5966(3)	0.023(1)
C(18B)	1.0289(4)	0.2340(3)	0.6208(3)	0.046(2)
C(19A)	1.0173(3)	0.2268(2)	0.6545(3)	0.015(1)
C(19B)	1.0227(4)	0.2247(2)	0.6809(3)	0.050(2)
C(20A)	1.0594(5)	0.1753(3)	0.6745(4)	0.030(1)
C(20B)	1.0682(7)	0.1740(5)	0.7017(6)	0.053(2)

7. EXPERIMENTAL SECTION

C(21A)	1.0576(4)	0.1618(3)	0.7338(4)	0.025(1)
C(21B)	1.0656(9)	0.1675(6)	0.7607(6)	0.072(3)
C(22A)	1.0052(5)	0.1973(3)	0.7744(3)	0.032(1)
C(22B)	1.0207(9)	0.2094(6)	0.8012(6)	0.075(3)
C(23A)	0.9605(4)	0.2473(3)	0.7529(3)	0.024(1)
C(23B)	0.9705(7)	0.2535(4)	0.7757(5)	0.051(2)
C(24A)	0.9625(4)	0.2642(3)	0.6929(3)	0.021(1)
C(24B)	0.9701(4)	0.2632(2)	0.7152(2)	0.036(2)
C(25)	0.5685(2)	0.3557(1)	0.7500(1)	0.027(1)
C(26)	0.6234(2)	0.4056(1)	0.7416(2)	0.029(1)
C(27)	0.5797(2)	0.4591(1)	0.7195(2)	0.031(1)
C(28)	0.6295(2)	0.5105(1)	0.7021(2)	0.037(1)
C(29)	0.5872(3)	0.5593(2)	0.6768(2)	0.040(1)
C(30)	0.4914(3)	0.5595(2)	0.6695(2)	0.041(1)
C(31)	0.4405(2)	0.5108(2)	0.6859(2)	0.036(1)
C(32)	0.4836(2)	0.4594(1)	0.7106(2)	0.030(1)
C(33)	0.4311(2)	0.4082(1)	0.7256(2)	0.030(1)
C(34)	0.4721(2)	0.3559(1)	0.7443(1)	0.027(1)
C(35)	0.4149(2)	0.3017(1)	0.7592(2)	0.026(1)
C(36A)	0.3459(6)	0.2383(3)	0.8323(3)	0.052(3)
C(36B)	0.3819(4)	0.2932(2)	0.8178(2)	0.028(2)
C(37A)	0.4373(6)	0.3228(4)	0.8635(4)	0.061(3)
C(37B)	0.4034(3)	0.3361(2)	0.8600(2)	0.035(1)
C(38A)	0.4188(8)	0.3087(5)	0.9217(3)	0.110(6)
C(38B)	0.3688(3)	0.3304(2)	0.9165(2)	0.045(1)
C(39A)	0.3639(9)	0.2594(5)	0.9351(3)	0.107(6)
C(39B)	0.3126(3)	0.2819(2)	0.9307(2)	0.049(2)
C(40A)	0.3275(7)	0.2242(4)	0.8904(4)	0.066(3)
C(40B)	0.2912(3)	0.2391(2)	0.8884(2)	0.045(1)
C(41A)	0.4008(6)	0.2876(3)	0.8188(3)	0.038(2)
C(41B)	0.3258(4)	0.2447(2)	0.8320(2)	0.030(2)
C(42)	0.3046(2)	0.2019(2)	0.7879(2)	0.037(1)
C(43)	0.3258(2)	0.2131(1)	0.7298(2)	0.031(1)
C(44)	0.2916(3)	0.1755(2)	0.6844(2)	0.039(1)
C(45)	0.3028(3)	0.1906(2)	0.6268(2)	0.043(1)
C(46)	0.3507(3)	0.2433(2)	0.6121(2)	0.040(1)
C(47)	0.3904(2)	0.2787(1)	0.6539(2)	0.030(1)
C(48)	0.3789(2)	0.2653(1)	0.7143(1)	0.026(1)
C(49)	0.8035(2)	0.0536(1)	0.7136(1)	0.023(1)
C(50)	0.8346(2)	0.0295(1)	0.7653(1)	0.024(1)
C(51)	0.8369(2)	-0.0351(1)	0.7708(1)	0.026(1)
C(52)	0.8536(2)	-0.0646(1)	0.8245(2)	0.031(1)
C(53)	0.8518(2)	-0.1265(2)	0.8276(2)	0.035(1)
C(54)	0.8352(2)	-0.1615(1)	0.7781(2)	0.036(1)
C(55)	0.8191(2)	-0.1345(1)	0.7253(2)	0.033(1)
C(56)	0.8182(2)	-0.0704(1)	0.7210(2)	0.027(1)
C(57)	0.7933(2)	-0.0428(1)	0.6682(2)	0.029(1)
C(58)	0.7828(2)	0.0191(1)	0.6634(1)	0.025(1)

7. EXPERIMENTAL SECTION

C(59)	0.7461(2)	0.0425(1)	0.6071(1)	0.027(1)
C(60)	0.6559(2)	0.0268(1)	0.5913(2)	0.030(1)
C(61)	0.5934(2)	-0.0014(2)	0.6309(2)	0.035(1)
C(62)	0.5080(2)	-0.0182(2)	0.6125(2)	0.040(1)
C(63)	0.4794(3)	-0.0100(2)	0.5550(2)	0.051(1)
C(64)	0.5349(3)	0.0178(2)	0.5158(2)	0.047(1)
C(65)	0.6250(3)	0.0381(2)	0.5329(2)	0.035(1)
C(66)	0.6817(3)	0.0671(2)	0.4940(2)	0.036(1)
C(67)	0.7710(2)	0.0840(2)	0.5089(2)	0.034(1)
C(68)	0.8305(3)	0.1124(2)	0.4679(2)	0.039(1)
C(69)	0.9186(3)	0.1268(2)	0.4828(2)	0.042(1)
C(70)	0.9520(3)	0.1134(2)	0.5391(2)	0.035(1)
C(71)	0.8973(2)	0.0866(2)	0.5805(2)	0.032(1)
C(72)	0.8042(2)	0.0714(1)	0.5667(1)	0.029(1)
C(73)	0.7963(2)	0.1100(1)	0.8370(1)	0.026(1)
C(74)	0.8583(2)	0.0684(1)	0.8158(1)	0.027(1)
C(75)	0.9467(2)	0.0645(2)	0.8434(2)	0.034(1)
C(76)	1.0185(2)	0.0289(2)	0.8212(2)	0.039(1)
C(77)	1.1026(3)	0.0284(2)	0.8477(2)	0.052(1)
C(78)	1.1192(3)	0.0628(2)	0.8983(3)	0.065(1)
C(79)	1.0525(3)	0.0964(2)	0.9203(2)	0.058(1)
C(80)	0.9624(3)	0.0988(2)	0.8948(2)	0.042(1)
C(81)	0.8926(3)	0.1347(2)	0.9177(2)	0.045(1)
C(82)	0.8088(3)	0.1409(2)	0.8901(2)	0.036(1)
C(83A)	0.7434(5)	0.1774(3)	0.9174(3)	0.022(2)
C(83B)	0.7162(7)	0.1736(4)	0.9159(4)	0.034(2)
C(84A)	0.7480(6)	0.2410(3)	0.9160(3)	0.031(2)
C(84B)	0.7161(6)	0.2374(3)	0.9139(3)	0.030(2)
C(85A)	0.8210(7)	0.2719(4)	0.8901(4)	0.035(2)
C(85B)	0.7913(7)	0.2731(4)	0.8929(4)	0.039(2)
C(86A)	0.8284(8)	0.3325(4)	0.8942(4)	0.050(2)
C(86B)	0.7918(7)	0.3341(4)	0.8943(4)	0.043(2)
C(87A)	0.7587(9)	0.3659(6)	0.9228(5)	0.072(3)
C(87B)	0.7133(6)	0.3645(4)	0.9154(4)	0.041(2)
C(88A)	0.6867(10)	0.3396(6)	0.9456(6)	0.077(3)
C(88B)	0.6386(6)	0.3334(4)	0.9312(4)	0.041(2)
C(89A)	0.6794(8)	0.2740(5)	0.9471(5)	0.062(2)
C(89B)	0.6385(5)	0.2695(3)	0.9334(3)	0.034(1)
C(90A)	0.6039(10)	0.2440(6)	0.9715(6)	0.076(3)
C(90B)	0.5678(7)	0.2365(4)	0.9558(4)	0.049(2)
C(91A)	0.6045(9)	0.1810(5)	0.9787(5)	0.065(3)
C(91B)	0.5713(6)	0.1744(4)	0.9618(4)	0.040(2)
C(92A)	0.5371(13)	0.1469(8)	1.0138(8)	0.105(5)
C(92B)	0.5031(7)	0.1426(4)	0.9892(4)	0.052(2)
C(93A)	0.5342(10)	0.0862(6)	1.0145(6)	0.075(3)
C(93B)	0.5059(8)	0.0826(5)	0.9951(5)	0.056(2)
C(94A)	0.6043(8)	0.0539(5)	0.9879(5)	0.050(3)
C(94B)	0.5824(8)	0.0506(5)	0.9754(5)	0.049(3)

7. EXPERIMENTAL SECTION

C(95A)	0.6705(7)	0.0823(4)	0.9556(4)	0.032(2)
C(95B)	0.6491(8)	0.0782(5)	0.9493(5)	0.045(3)
C(96A)	0.6742(7)	0.1472(4)	0.9489(4)	0.037(2)
C(96B)	0.6490(7)	0.1425(4)	0.9409(4)	0.037(2)
C(201)	0.7085(4)	0.2723(3)	0.5334(3)	0.066(1)
C(202)	0.7538(3)	0.2287(2)	0.5661(2)	0.062(1)
C(203)	0.6773(7)	0.4732(5)	0.5343(4)	0.048(2)
C(204)	0.6172(7)	0.4412(5)	0.5702(5)	0.054(2)
C(205)	0.6610(12)	0.4531(7)	0.5479(7)	0.089(4)
C(206)	0.6873(15)	0.5077(9)	0.5248(9)	0.123(7)

Bond lengths [Å] and angles [°] for 13b.

P(1)-O(3)	1.485(2)	P(1)-N(1)	1.570(2)
P(1)-O(2)	1.600(2)	P(1)-O(1)	1.604(2)
P(2)-O(6)	1.503(2)	P(2)-N(1)	1.555(2)
P(2)-O(5)	1.589(2)	P(2)-O(4)	1.601(2)
O(1)-C(1)	1.389(4)	O(2)-C(25)	1.409(3)
O(4)-C(49)	1.407(3)	O(5)-C(73)	1.398(4)
N(97)-C(201)	1.170(8)	N(98)-C(203)	1.076(13)
N(99)-C(205)	1.221(16)	C(1)-C(2)	1.379(4)
C(1)-C(10)	1.415(4)	C(2)-C(3)	1.430(5)
C(2)-C(26)	1.484(4)	C(3)-C(4)	1.409(5)
C(3)-C(8)	1.429(5)	C(4)-C(5)	1.376(5)
C(5)-C(6)	1.415(6)	C(6)-C(7)	1.355(6)
C(7)-C(8)	1.420(5)	C(8)-C(9)	1.414(5)
C(9)-C(10)	1.364(5)	C(10)-C(17B)	1.447(5)
C(10)-C(11A)	1.602(7)	C(12A)-C(11A)	1.364(10)
C(12A)-C(13A)	1.394(10)	C(12A)-C(17A)	1.448(8)
C(13B)-C(14B)	1.365(16)	C(13B)-C(11B)	1.386(12)
C(13A)-C(14A)	1.333(12)	C(14B)-C(15B)	1.468(17)
C(14A)-C(15A)	1.424(11)	C(15B)-C(16B)	1.314(17)
C(15A)-C(16A)	1.391(10)	C(16B)-C(12B)	1.393(15)
C(16A)-C(17A)	1.397(10)	C(17A)-C(18A)	1.378(8)
C(18A)-C(19A)	1.383(8)	C(19A)-C(20A)	1.375(9)
C(19A)-C(24A)	1.446(8)	C(20A)-C(21A)	1.386(10)
C(20B)-C(21B)	1.355(17)	C(20B)-C(19B)	1.388(11)
C(21A)-C(22A)	1.436(10)	C(21B)-C(22B)	1.466(18)
C(22A)-C(23A)	1.379(9)	C(22B)-C(23B)	1.353(16)
C(23A)-C(24A)	1.419(9)	C(23B)-C(24B)	1.399(12)
C(24A)-C(11A)	1.400(9)	C(24B)-C(19B)	1.3900
C(24B)-C(17B)	1.3900	C(19B)-C(18B)	1.3900
C(18B)-C(12B)	1.3900	C(12B)-C(11B)	1.3900
C(11B)-C(17B)	1.3900	C(25)-C(26)	1.379(4)
C(25)-C(34)	1.410(4)	C(26)-C(27)	1.439(4)
C(27)-C(28)	1.408(5)	C(27)-C(32)	1.415(4)

7. EXPERIMENTAL SECTION

C(28)-C(29)	1.374(5)	C(29)-C(30)	1.406(5)
C(30)-C(31)	1.364(5)	C(31)-C(32)	1.419(4)
C(32)-C(33)	1.413(4)	C(33)-C(34)	1.373(4)
C(34)-C(35)	1.501(4)	C(35)-C(48)	1.405(4)
C(35)-C(41A)	1.412(6)	C(35)-C(36B)	1.434(4)
C(36A)-C(41A)	1.3900	C(36A)-C(40A)	1.3900
C(36A)-C(42)	1.429(7)	C(41A)-C(37A)	1.3900
C(37A)-C(38A)	1.3900	C(38A)-C(39A)	1.3900
C(39A)-C(40A)	1.3900	C(37B)-C(38B)	1.3900
C(37B)-C(36B)	1.3900	C(38B)-C(39B)	1.3900
C(39B)-C(40B)	1.3900	C(40B)-C(41B)	1.3900
C(41B)-C(36B)	1.3900	C(41B)-C(42)	1.417(5)
C(42)-C(43)	1.383(5)	C(43)-C(44)	1.422(5)
C(43)-C(48)	1.436(4)	C(44)-C(45)	1.366(6)
C(45)-C(46)	1.404(5)	C(46)-C(47)	1.363(5)
C(47)-C(48)	1.422(5)	C(49)-C(50)	1.373(4)
C(49)-C(58)	1.412(4)	C(50)-C(51)	1.440(4)
C(50)-C(74)	1.480(4)	C(51)-C(56)	1.406(5)
C(51)-C(52)	1.412(4)	C(52)-C(53)	1.374(4)
C(53)-C(54)	1.393(5)	C(54)-C(55)	1.366(5)
C(55)-C(56)	1.426(4)	C(56)-C(57)	1.400(5)
C(57)-C(58)	1.384(4)	C(58)-C(59)	1.486(4)
C(59)-C(72)	1.407(4)	C(59)-C(60)	1.408(5)
C(60)-C(61)	1.427(5)	C(60)-C(65)	1.427(5)
C(61)-C(62)	1.366(5)	C(62)-C(63)	1.388(6)
C(63)-C(64)	1.355(6)	C(64)-C(65)	1.442(5)
C(65)-C(66)	1.373(5)	C(66)-C(67)	1.397(5)
C(67)-C(68)	1.422(5)	C(67)-C(72)	1.431(5)
C(68)-C(69)	1.367(6)	C(69)-C(70)	1.408(5)
C(70)-C(71)	1.372(5)	C(71)-C(72)	1.433(5)
C(73)-C(74)	1.379(4)	C(73)-C(82)	1.404(4)
C(74)-C(75)	1.435(4)	C(75)-C(76)	1.407(5)
C(75)-C(80)	1.417(5)	C(76)-C(77)	1.366(5)
C(77)-C(78)	1.406(8)	C(78)-C(79)	1.324(8)
C(79)-C(80)	1.438(6)	C(80)-C(81)	1.394(6)
C(81)-C(82)	1.381(5)	C(82)-C(83A)	1.398(8)
C(82)-C(83B)	1.642(10)	C(83A)-C(96A)	1.409(12)
C(83A)-C(84A)	1.413(10)	C(83B)-C(96B)	1.327(13)
C(83B)-C(84B)	1.417(11)	C(84A)-C(85A)	1.397(12)
C(84A)-C(89A)	1.429(13)	C(84B)-C(89B)	1.408(11)
C(84B)-C(85B)	1.434(12)	C(85A)-C(86A)	1.352(13)
C(85B)-C(86B)	1.355(12)	C(86A)-C(87A)	1.416(17)
C(86B)-C(87B)	1.413(13)	C(87A)-C(88A)	1.308(18)
C(87B)-C(88B)	1.337(12)	C(88A)-C(89A)	1.458(17)
C(88B)-C(89B)	1.419(11)	C(89A)-C(90A)	1.401(17)
C(89B)-C(90B)	1.363(12)	C(90A)-C(91A)	1.408(18)
C(90B)-C(91B)	1.387(13)	C(91A)-C(96A)	1.432(14)
C(91A)-C(92A)	1.48(2)	C(91B)-C(92B)	1.369(13)

7. EXPERIMENTAL SECTION

C(91B)-C(96B)	1.419(12)	C(92A)-C(93A)	1.35(2)
C(92B)-C(93B)	1.339(14)	C(93A)-C(94A)	1.387(17)
C(93B)-C(94B)	1.396(15)	C(94A)-C(95A)	1.369(15)
C(94B)-C(95B)	1.296(16)	C(95A)-C(96A)	1.449(13)
C(95B)-C(96B)	1.439(14)	C(201)-C(202)	1.389(9)
C(203)-C(204)	1.394(15)	C(205)-C(206)	1.375(16)
O(3)-P(1)-N(1)	120.22(13)	O(3)-P(1)-O(2)	112.41(13)
N(1)-P(1)-O(2)	105.95(13)	O(3)-P(1)-O(1)	104.41(13)
N(1)-P(1)-O(1)	109.86(13)	O(2)-P(1)-O(1)	102.64(12)
O(6)-P(2)-N(1)	121.11(13)	O(6)-P(2)-O(5)	102.03(13)
N(1)-P(2)-O(5)	111.89(13)	O(6)-P(2)-O(4)	109.50(12)
N(1)-P(2)-O(4)	107.04(13)	O(5)-P(2)-O(4)	104.01(11)
C(1)-O(1)-P(1)	123.3(2)	C(25)-O(2)-P(1)	114.7(2)
C(49)-O(4)-P(2)	116.01(18)	C(73)-O(5)-P(2)	123.1(2)
P(2)-N(1)-P(1)	133.28(17)	C(2)-C(1)-O(1)	119.7(3)
C(2)-C(1)-C(10)	123.4(3)	O(1)-C(1)-C(10)	116.6(3)
C(1)-C(2)-C(3)	117.8(3)	C(1)-C(2)-C(26)	119.3(3)
C(3)-C(2)-C(26)	122.9(3)	C(4)-C(3)-C(8)	117.9(3)
C(4)-C(3)-C(2)	122.6(3)	C(8)-C(3)-C(2)	119.5(3)
C(5)-C(4)-C(3)	121.2(3)	C(4)-C(5)-C(6)	120.3(4)
C(7)-C(6)-C(5)	120.4(4)	C(6)-C(7)-C(8)	120.5(3)
C(9)-C(8)-C(7)	121.4(3)	C(9)-C(8)-C(3)	118.8(3)
C(7)-C(8)-C(3)	119.8(3)	C(10)-C(9)-C(8)	122.2(3)
C(9)-C(10)-C(1)	117.7(3)	C(9)-C(10)-C(17B)	117.6(3)
C(1)-C(10)-C(17B)	124.4(4)	C(9)-C(10)-C(11A)	123.9(3)
C(1)-C(10)-C(11A)	117.5(4)	C(17B)-C(10)-C(11A)	15.5(3)
C(11A)-C(12A)-C(13A)	124.4(6)	C(11A)-C(12A)-C(17A)	115.6(6)
C(13A)-C(12A)-C(17A)	120.0(6)	C(14B)-C(13B)-C(11B)	122.9(10)
C(14A)-C(13A)-C(12A)	121.5(7)	C(13B)-C(14B)-C(15B)	118.2(12)
C(13A)-C(14A)-C(15A)	120.0(8)	C(16B)-C(15B)-C(14B)	118.2(11)
C(16A)-C(15A)-C(14A)	120.3(7)	C(15B)-C(16B)-C(12B)	122.8(11)
C(15A)-C(16A)-C(17A)	120.5(6)	C(18A)-C(17A)-C(16A)	120.7(6)
C(18A)-C(17A)-C(12A)	121.6(6)	C(16A)-C(17A)-C(12A)	117.7(6)
C(17A)-C(18A)-C(19A)	122.7(5)	C(20A)-C(19A)-C(18A)	122.4(6)
C(20A)-C(19A)-C(24A)	121.4(6)	C(18A)-C(19A)-C(24A)	116.2(5)
C(19A)-C(20A)-C(21A)	119.7(7)	C(21B)-C(20B)-C(19B)	114.4(10)
C(20A)-C(21A)-C(22A)	121.4(6)	C(20B)-C(21B)-C(22B)	124.9(12)
C(23A)-C(22A)-C(21A)	117.6(7)	C(23B)-C(22B)-C(21B)	115.3(12)
C(22A)-C(23A)-C(24A)	123.1(6)	C(22B)-C(23B)-C(24B)	122.7(10)
C(11A)-C(24A)-C(23A)	123.3(6)	C(11A)-C(24A)-C(19A)	120.2(6)
C(23A)-C(24A)-C(19A)	116.4(5)	C(19B)-C(24B)-C(17B)	120.0
C(19B)-C(24B)-C(23B)	117.3(5)	C(17B)-C(24B)-C(23B)	122.6(6)
C(20B)-C(19B)-C(18B)	115.2(7)	C(20B)-C(19B)-C(24B)	124.7(7)
C(18B)-C(19B)-C(24B)	120.0	C(19B)-C(18B)-C(12B)	120.0
C(18B)-C(12B)-C(11B)	120.0	C(18B)-C(12B)-C(16B)	119.4(7)
C(11B)-C(12B)-C(16B)	120.6(7)	C(13B)-C(11B)-C(17B)	122.7(6)
C(13B)-C(11B)-C(12B)	117.3(6)	C(17B)-C(11B)-C(12B)	120.0

7. EXPERIMENTAL SECTION

C(11B)-C(17B)-C(24B)	120.0	C(11B)-C(17B)-C(10)	114.3(4)
C(24B)-C(17B)-C(10)	125.6(4)	C(26)-C(25)-O(2)	117.8(3)
C(26)-C(25)-C(34)	124.3(3)	O(2)-C(25)-C(34)	117.9(3)
C(25)-C(26)-C(27)	117.0(3)	C(25)-C(26)-C(2)	121.0(3)
C(27)-C(26)-C(2)	121.8(3)	C(28)-C(27)-C(32)	117.8(3)
C(28)-C(27)-C(26)	122.6(3)	C(32)-C(27)-C(26)	119.4(3)
C(29)-C(28)-C(27)	121.7(3)	C(28)-C(29)-C(30)	119.9(3)
C(31)-C(30)-C(29)	120.4(3)	C(30)-C(31)-C(32)	120.3(3)
C(33)-C(32)-C(27)	119.9(3)	C(33)-C(32)-C(31)	120.2(3)
C(27)-C(32)-C(31)	119.9(3)	C(34)-C(33)-C(32)	121.3(3)
C(33)-C(34)-C(25)	117.6(3)	C(33)-C(34)-C(35)	120.3(3)
C(25)-C(34)-C(35)	122.0(3)	C(48)-C(35)-C(41A)	121.4(4)
C(48)-C(35)-C(36B)	118.6(3)	C(41A)-C(35)-C(36B)	12.2(4)
C(48)-C(35)-C(34)	120.2(3)	C(41A)-C(35)-C(34)	118.4(4)
C(36B)-C(35)-C(34)	120.1(3)	C(41A)-C(36A)-C(40A)	120.0
C(41A)-C(36A)-C(42)	122.1(5)	C(40A)-C(36A)-C(42)	117.9(5)
C(36A)-C(41A)-C(37A)	120.0	C(36A)-C(41A)-C(35)	118.1(5)
C(37A)-C(41A)-C(35)	121.9(5)	C(38A)-C(37A)-C(41A)	120.0
C(37A)-C(38A)-C(39A)	120.0	C(40A)-C(39A)-C(38A)	120.0
C(39A)-C(40A)-C(36A)	120.0	C(38B)-C(37B)-C(36B)	120.0
C(37B)-C(38B)-C(39B)	120.0	C(40B)-C(39B)-C(38B)	120.0
C(39B)-C(40B)-C(41B)	120.0	C(36B)-C(41B)-C(40B)	120.0
C(36B)-C(41B)-C(42)	118.8(3)	C(40B)-C(41B)-C(42)	121.2(3)
C(41B)-C(36B)-C(37B)	120.0	C(41B)-C(36B)-C(35)	121.1(3)
C(37B)-C(36B)-C(35)	118.9(3)	C(43)-C(42)-C(41B)	120.7(3)
C(43)-C(42)-C(36A)	118.9(4)	C(41B)-C(42)-C(36A)	13.1(4)
C(42)-C(43)-C(44)	121.0(3)	C(42)-C(43)-C(48)	120.1(3)
C(44)-C(43)-C(48)	118.9(3)	C(45)-C(44)-C(43)	121.0(3)
C(44)-C(45)-C(46)	119.6(3)	C(47)-C(46)-C(45)	121.6(4)
C(46)-C(47)-C(48)	120.5(3)	C(35)-C(48)-C(47)	122.8(3)
C(35)-C(48)-C(43)	119.0(3)	C(47)-C(48)-C(43)	118.1(3)
C(50)-C(49)-O(4)	117.9(3)	C(50)-C(49)-C(58)	123.8(3)
O(4)-C(49)-C(58)	118.3(3)	C(49)-C(50)-C(51)	118.0(3)
C(49)-C(50)-C(74)	121.3(3)	C(51)-C(50)-C(74)	120.5(3)
C(56)-C(51)-C(52)	118.5(3)	C(56)-C(51)-C(50)	118.8(3)
C(52)-C(51)-C(50)	122.7(3)	C(53)-C(52)-C(51)	120.3(3)
C(52)-C(53)-C(54)	121.3(3)	C(55)-C(54)-C(53)	120.0(3)
C(54)-C(55)-C(56)	119.9(3)	C(57)-C(56)-C(51)	120.1(3)
C(57)-C(56)-C(55)	119.9(3)	C(51)-C(56)-C(55)	119.9(3)
C(58)-C(57)-C(56)	122.1(3)	C(57)-C(58)-C(49)	116.8(3)
C(57)-C(58)-C(59)	117.1(3)	C(49)-C(58)-C(59)	126.0(3)
C(72)-C(59)-C(60)	120.5(3)	C(72)-C(59)-C(58)	120.6(3)
C(60)-C(59)-C(58)	118.1(3)	C(59)-C(60)-C(61)	122.8(3)
C(59)-C(60)-C(65)	119.4(3)	C(61)-C(60)-C(65)	117.8(3)
C(62)-C(61)-C(60)	120.4(4)	C(61)-C(62)-C(63)	121.9(4)
C(64)-C(63)-C(62)	120.2(4)	C(63)-C(64)-C(65)	120.5(4)
C(66)-C(65)-C(60)	119.7(3)	C(66)-C(65)-C(64)	121.3(3)
C(60)-C(65)-C(64)	119.0(3)	C(65)-C(66)-C(67)	122.0(3)

7. EXPERIMENTAL SECTION

C(66)-C(67)-C(68)	121.8(3)	C(66)-C(67)-C(72)	119.1(3)
C(68)-C(67)-C(72)	119.1(3)	C(69)-C(68)-C(67)	120.9(3)
C(68)-C(69)-C(70)	120.2(3)	C(71)-C(70)-C(69)	121.2(3)
C(70)-C(71)-C(72)	120.1(3)	C(59)-C(72)-C(67)	119.3(3)
C(59)-C(72)-C(71)	122.2(3)	C(67)-C(72)-C(71)	118.5(3)
C(74)-C(73)-O(5)	119.2(3)	C(74)-C(73)-C(82)	122.9(3)
O(5)-C(73)-C(82)	117.6(3)	C(73)-C(74)-C(75)	118.3(3)
C(73)-C(74)-C(50)	120.6(3)	C(75)-C(74)-C(50)	121.1(3)
C(76)-C(75)-C(80)	118.6(3)	C(76)-C(75)-C(74)	122.9(3)
C(80)-C(75)-C(74)	118.4(3)	C(77)-C(76)-C(75)	120.9(4)
C(76)-C(77)-C(78)	120.9(4)	C(79)-C(78)-C(77)	119.4(4)
C(78)-C(79)-C(80)	122.5(5)	C(81)-C(80)-C(75)	119.9(3)
C(81)-C(80)-C(79)	122.4(4)	C(75)-C(80)-C(79)	117.6(4)
C(82)-C(81)-C(80)	122.1(3)	C(81)-C(82)-C(83A)	117.2(4)
C(81)-C(82)-C(73)	117.4(3)	C(83A)-C(82)-C(73)	125.4(4)
C(81)-C(82)-C(83B)	127.4(4)	C(83A)-C(82)-C(83B)	12.4(4)
C(73)-C(82)-C(83B)	114.7(4)	C(82)-C(83A)-C(96A)	116.2(6)
C(82)-C(83A)-C(84A)	122.5(7)	C(96A)-C(83A)-C(84A)	121.3(7)
C(96B)-C(83B)-C(84B)	122.2(8)	C(96B)-C(83B)-C(82)	122.1(7)
C(84B)-C(83B)-C(82)	115.5(7)	C(85A)-C(84A)-C(83A)	122.4(7)
C(85A)-C(84A)-C(89A)	119.5(8)	C(83A)-C(84A)-C(89A)	117.9(8)
C(89B)-C(84B)-C(83B)	119.7(8)	C(89B)-C(84B)-C(85B)	116.2(7)
C(83B)-C(84B)-C(85B)	124.2(8)	C(86A)-C(85A)-C(84A)	121.2(9)
C(86B)-C(85B)-C(84B)	123.2(9)	C(85A)-C(86A)-C(87A)	119.6(11)
C(85B)-C(86B)-C(87B)	118.7(9)	C(88A)-C(87A)-C(86A)	121.7(12)
C(88B)-C(87B)-C(86B)	120.3(8)	C(87A)-C(88A)-C(89A)	120.9(12)
C(87B)-C(88B)-C(89B)	121.7(8)	C(90A)-C(89A)-C(84A)	120.2(10)
C(90A)-C(89A)-C(88A)	122.8(11)	C(84A)-C(89A)-C(88A)	116.6(10)
C(90B)-C(89B)-C(84B)	117.1(7)	C(90B)-C(89B)-C(88B)	123.4(8)
C(84B)-C(89B)-C(88B)	119.5(7)	C(89A)-C(90A)-C(91A)	120.9(12)
C(89B)-C(90B)-C(91B)	122.8(9)	C(90A)-C(91A)-C(96A)	117.9(11)
C(90A)-C(91A)-C(92A)	124.6(12)	C(96A)-C(91A)-C(92A)	117.5(12)
C(92B)-C(91B)-C(90B)	122.0(8)	C(92B)-C(91B)-C(96B)	118.5(8)
C(90B)-C(91B)-C(96B)	119.5(8)	C(93A)-C(92A)-C(91A)	122.7(16)
C(93B)-C(92B)-C(91B)	122.4(9)	C(92A)-C(93A)-C(94A)	119.2(14)
C(92B)-C(93B)-C(94B)	119.8(10)	C(95A)-C(94A)-C(93A)	121.2(11)
C(95B)-C(94B)-C(93B)	120.5(11)	C(94A)-C(95A)-C(96A)	122.7(9)
C(94B)-C(95B)-C(96B)	121.9(10)	C(83A)-C(96A)-C(91A)	120.1(8)
C(83A)-C(96A)-C(95A)	123.5(8)	C(91A)-C(96A)-C(95A)	116.3(9)
C(83B)-C(96B)-C(91B)	118.3(8)	C(83B)-C(96B)-C(95B)	124.9(9)
C(91B)-C(96B)-C(95B)	116.8(8)	N(97)-C(201)-C(202)	178.9(6)
N(98)-C(203)-C(204)	178.2(12)	N(99)-C(205)-C(206)	160.1(19)
C(12A)-C(11A)-C(24A)	123.7(6)	C(12A)-C(11A)-C(10)	122.2(5)
C(24A)-C(11A)-C(10)	114.0(6)		

X-Ray structure of 13a

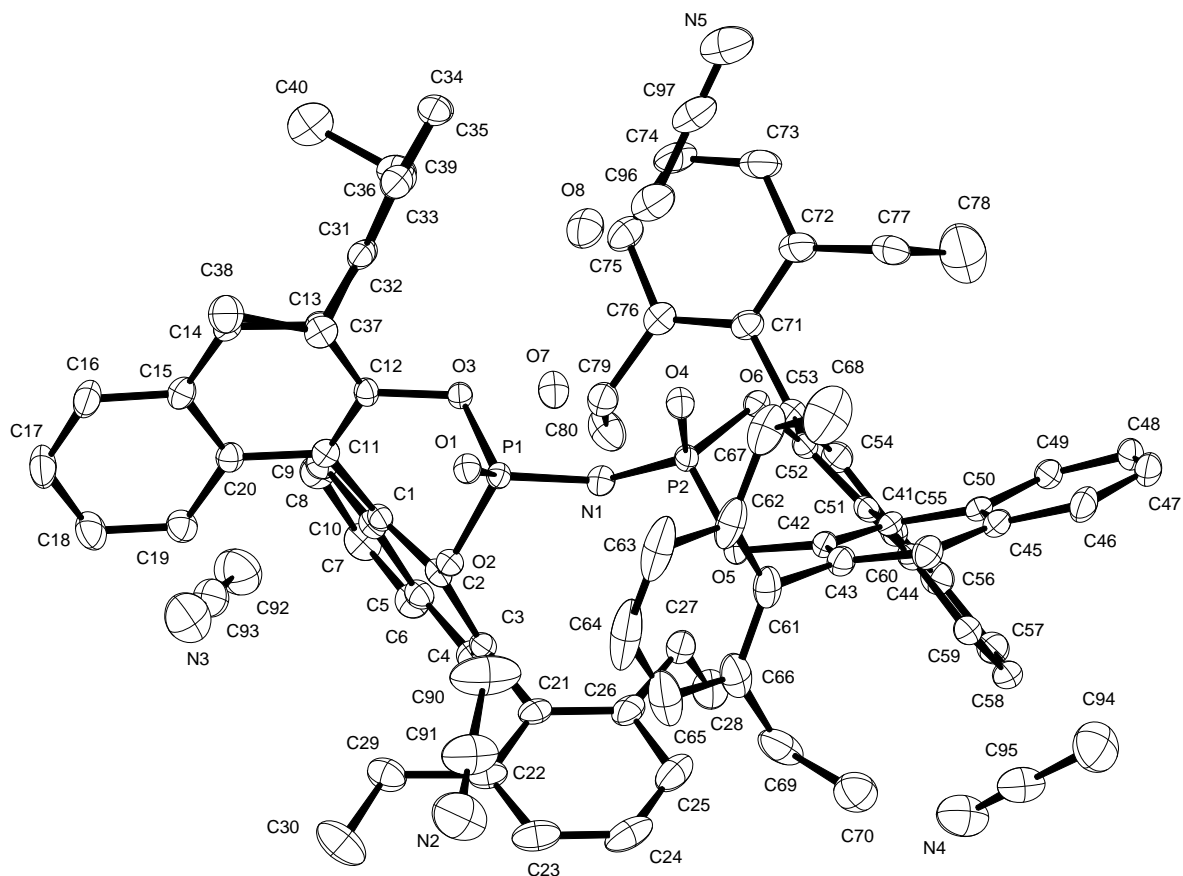


Figure 7.4. Single crystal X-ray structure determination of 13a. The crystals were grown from concentrated solution in hot and wet CH_3CN by slowly cooling the solution to room temperature. X-ray crystallographic data have been deposited in the Cambridge Crystallographic Data Centre database (<http://www.ccdc.cam.ac.uk/>) under accession code CCDC 898367.

Crystal data and structure refinement for 13a.

Identification code	7361
Empirical formula	$\text{C}_{80}\text{H}_{73}\text{N}_5\text{O}_6\text{P}_2 \cdot 4(\text{C}_2\text{H}_3\text{N}), 2(\text{H}_2\text{O})$
Color	colorless
Formula weight	$1406.58 \text{ g} \cdot \text{mol}^{-1}$
Temperature	100 K
Wavelength	1.54184 \AA

7. EXPERIMENTAL SECTION

Crystal system	Orthorhombic	
Space group	P2₁ 2₁ 2₁, (no. 19)	
Unit cell dimensions	a = 14.0382(5) Å	α = 90°.
	b = 21.6713(8) Å	β = 90°.
	c = 25.5217(9) Å	γ = 90°.
Volume	7764.4(5) Å ³	
Z	4	
Density (calculated)	1.203 Mg · m ⁻³	
Absorption coefficient	0.980 mm ⁻¹	
F(000)	2984 e	
Crystal size	0.35 x 0.30 x 0.12 mm ³	
θ range for data collection	2.67 to 67.18°.	
Index ranges	-15 ≤ h ≤ 16, -25 ≤ k ≤ 25, -30 ≤ l ≤ 30	
Reflections collected	178444	
Independent reflections	13797 [R _{int} = 0.0489]	
Reflections with I > 2σ(I)	13421	
Completeness to θ = 67.18°	99.4 %	
Absorption correction	Gaussian	
Max. and min. transmission	0.90 and 0.72	
Refinement method	Full-matrix least-squares on F ²	
Data / restraints / parameters	13797 / 6 / 952	
Goodness-of-fit on F ²	1.041	
Final R indices [I > 2σ(I)]	R ₁ = 0.0310	wR ² = 0.0836
R indices (all data)	R ₁ = 0.0319	wR ² = 0.0842
Absolute structure parameter	0.013(10)	
Largest diff. peak and hole	0.740 and -0.418 e · Å ⁻³	

7. EXPERIMENTAL SECTION

Atomic coordinates and equivalent isotropic displacement parameters (\AA^2) for 13a.

U_{eq} is defined as one third of the trace of the orthogonalized U_{ij} tensor.

	x	y	z	U_{eq}
P(1)	0.6292(1)	0.4845(1)	0.5572(1)	0.015(1)
P(2)	0.5607(1)	0.4745(1)	0.4518(1)	0.016(1)
O(1)	0.6834(1)	0.4260(1)	0.5595(1)	0.019(1)
O(2)	0.5643(1)	0.4847(1)	0.6091(1)	0.016(1)
O(3)	0.6979(1)	0.5432(1)	0.5652(1)	0.017(1)
O(4)	0.6403(1)	0.4362(1)	0.4306(1)	0.021(1)
O(5)	0.4613(1)	0.4387(1)	0.4465(1)	0.017(1)
O(6)	0.5520(1)	0.5293(1)	0.4098(1)	0.018(1)
O(7)	0.7506(1)	0.3725(1)	0.4798(1)	0.025(1)
O(8)	0.8943(1)	0.3823(1)	0.4164(1)	0.034(1)
N(1)	0.5652(1)	0.5005(1)	0.5087(1)	0.018(1)
N(2)	0.4365(2)	0.2354(1)	0.6299(1)	0.061(1)
N(3)	0.7465(2)	0.2824(1)	0.7213(1)	0.051(1)
N(4)	0.1063(2)	0.3914(1)	0.3988(1)	0.048(1)
N(5)	0.8952(1)	0.5958(1)	0.3308(1)	0.051(1)
C(1)	0.5921(1)	0.5809(1)	0.6515(1)	0.017(1)
C(2)	0.5293(1)	0.5400(1)	0.6294(1)	0.017(1)
C(3)	0.4290(1)	0.5486(1)	0.6299(1)	0.018(1)
C(4)	0.3954(1)	0.6032(1)	0.6501(1)	0.020(1)
C(5)	0.4571(1)	0.6500(1)	0.6684(1)	0.020(1)
C(6)	0.4222(1)	0.7079(1)	0.6860(1)	0.025(1)
C(7)	0.4822(1)	0.7529(1)	0.7031(1)	0.027(1)
C(8)	0.5817(1)	0.7422(1)	0.7034(1)	0.027(1)
C(9)	0.6179(1)	0.6870(1)	0.6872(1)	0.023(1)
C(10)	0.5571(1)	0.6390(1)	0.6695(1)	0.018(1)
C(11)	0.6938(1)	0.5634(1)	0.6570(1)	0.017(1)
C(12)	0.7456(1)	0.5461(1)	0.6136(1)	0.017(1)
C(13)	0.8440(1)	0.5325(1)	0.6153(1)	0.018(1)
C(14)	0.8873(1)	0.5332(1)	0.6636(1)	0.021(1)
C(15)	0.8361(1)	0.5440(1)	0.7101(1)	0.021(1)
C(16)	0.8802(1)	0.5369(1)	0.7598(1)	0.028(1)
C(17)	0.8290(2)	0.5440(1)	0.8048(1)	0.034(1)
C(18)	0.7314(1)	0.5601(1)	0.8023(1)	0.030(1)
C(19)	0.6874(1)	0.5680(1)	0.7551(1)	0.024(1)
C(20)	0.7383(1)	0.5601(1)	0.7075(1)	0.019(1)
C(21)	0.3636(1)	0.4983(1)	0.6123(1)	0.020(1)
C(22)	0.3504(1)	0.4470(1)	0.6457(1)	0.025(1)
C(23)	0.2897(1)	0.4002(1)	0.6292(1)	0.034(1)
C(24)	0.2442(1)	0.4038(1)	0.5812(1)	0.038(1)
C(25)	0.2573(1)	0.4537(1)	0.5491(1)	0.034(1)
C(26)	0.3169(1)	0.5025(1)	0.5641(1)	0.025(1)
C(27)	0.3257(1)	0.5577(1)	0.5289(1)	0.029(1)
C(28)	0.2435(2)	0.6031(1)	0.5355(1)	0.034(1)

7. EXPERIMENTAL SECTION

C(29)	0.4009(2)	0.4448(1)	0.6980(1)	0.030(1)
C(30)	0.3849(2)	0.3870(1)	0.7307(1)	0.045(1)
C(31)	0.9029(1)	0.5196(1)	0.5675(1)	0.019(1)
C(32)	0.9348(1)	0.4596(1)	0.5572(1)	0.020(1)
C(33)	0.9968(1)	0.4507(1)	0.5150(1)	0.025(1)
C(34)	1.0249(1)	0.4993(1)	0.4834(1)	0.029(1)
C(35)	0.9923(1)	0.5582(1)	0.4940(1)	0.027(1)
C(36)	0.9323(1)	0.5696(1)	0.5360(1)	0.023(1)
C(37)	0.9059(1)	0.4045(1)	0.5903(1)	0.023(1)
C(38)	0.9810(1)	0.3851(1)	0.6305(1)	0.032(1)
C(39)	0.9070(1)	0.6354(1)	0.5495(1)	0.029(1)
C(40)	0.9820(2)	0.6636(1)	0.5860(1)	0.039(1)
C(41)	0.3970(1)	0.4692(1)	0.3641(1)	0.017(1)
C(42)	0.4332(1)	0.4228(1)	0.3952(1)	0.017(1)
C(43)	0.4418(1)	0.3607(1)	0.3789(1)	0.020(1)
C(44)	0.4157(1)	0.3472(1)	0.3284(1)	0.024(1)
C(45)	0.3864(1)	0.3933(1)	0.2927(1)	0.022(1)
C(46)	0.3705(1)	0.3797(1)	0.2389(1)	0.027(1)
C(47)	0.3497(1)	0.4255(1)	0.2040(1)	0.029(1)
C(48)	0.3406(1)	0.4869(1)	0.2212(1)	0.027(1)
C(49)	0.3526(1)	0.5014(1)	0.2730(1)	0.023(1)
C(50)	0.3762(1)	0.4552(1)	0.3104(1)	0.020(1)
C(51)	0.3885(1)	0.5332(1)	0.3848(1)	0.017(1)
C(52)	0.4675(1)	0.5626(1)	0.4041(1)	0.017(1)
C(53)	0.4715(1)	0.6271(1)	0.4138(1)	0.020(1)
C(54)	0.3876(1)	0.6590(1)	0.4105(1)	0.022(1)
C(55)	0.3004(1)	0.6300(1)	0.3972(1)	0.021(1)
C(56)	0.2131(1)	0.6632(1)	0.3955(1)	0.025(1)
C(57)	0.1302(1)	0.6346(1)	0.3818(1)	0.026(1)
C(58)	0.1302(1)	0.5712(1)	0.3694(1)	0.024(1)
C(59)	0.2130(1)	0.5381(1)	0.3699(1)	0.022(1)
C(60)	0.3005(1)	0.5666(1)	0.3833(1)	0.019(1)
C(61)	0.4780(1)	0.3118(1)	0.4153(1)	0.027(1)
C(62)	0.5724(2)	0.2908(1)	0.4109(1)	0.036(1)
C(63)	0.6053(2)	0.2477(1)	0.4476(1)	0.052(1)
C(64)	0.5462(3)	0.2245(1)	0.4857(1)	0.064(1)
C(65)	0.4524(2)	0.2431(1)	0.4880(1)	0.056(1)
C(66)	0.4166(2)	0.2875(1)	0.4535(1)	0.036(1)
C(67)	0.6389(2)	0.3112(1)	0.3681(1)	0.040(1)
C(68)	0.6485(2)	0.2661(1)	0.3228(1)	0.060(1)
C(69)	0.3126(2)	0.3045(1)	0.4553(1)	0.041(1)
C(70)	0.2533(2)	0.2613(1)	0.4209(1)	0.041(1)
C(71)	0.5658(1)	0.6597(1)	0.4176(1)	0.022(1)
C(72)	0.6134(1)	0.6715(1)	0.3701(1)	0.033(1)
C(73)	0.6987(2)	0.7049(1)	0.3714(1)	0.037(1)
C(74)	0.7356(2)	0.7258(1)	0.4182(1)	0.035(1)
C(75)	0.6896(1)	0.7127(1)	0.4645(1)	0.029(1)
C(76)	0.6044(1)	0.6794(1)	0.4654(1)	0.022(1)

7. EXPERIMENTAL SECTION

C(77)	0.5780(2)	0.6482(1)	0.3175(1)	0.049(1)
C(78)	0.5159(3)	0.6915(2)	0.2898(1)	0.070(1)
C(79)	0.5566(1)	0.6674(1)	0.5171(1)	0.025(1)
C(80)	0.4943(2)	0.7209(1)	0.5351(1)	0.036(1)
C(90)	0.5132(2)	0.3356(1)	0.5942(1)	0.064(1)
C(91)	0.4704(2)	0.2796(1)	0.6148(1)	0.051(1)
C(92)	0.7058(2)	0.3977(1)	0.7048(1)	0.052(1)
C(93)	0.7278(2)	0.3327(1)	0.7135(1)	0.036(1)
C(94)	0.1284(2)	0.3595(1)	0.3019(1)	0.054(1)
C(95)	0.1166(2)	0.3774(1)	0.3559(1)	0.037(1)
C(96)	0.7922(2)	0.5582(1)	0.4090(1)	0.042(1)
C(97)	0.8500(1)	0.5795(1)	0.3652(1)	0.039(1)

Table 3. Bond lengths [Å] and angles [°] for 13a.

P(1)-O(1)	1.4799(12)	P(1)-O(2)	1.6080(11)
P(1)-O(3)	1.6090(12)	P(1)-N(1)	1.5704(14)
P(2)-O(4)	1.4927(12)	P(2)-O(5)	1.6017(11)
P(2)-O(6)	1.6039(11)	P(2)-N(1)	1.5591(13)
O(2)-C(2)	1.3950(19)	O(3)-C(12)	1.4072(19)
O(5)-C(42)	1.4112(18)	O(6)-C(52)	1.397(2)
N(2)-C(91)	1.137(3)	N(3)-C(93)	1.139(3)
N(4)-C(95)	1.143(3)	N(5)-C(97)	1.140(3)
C(1)-C(2)	1.371(2)	C(1)-C(10)	1.429(2)
C(1)-C(11)	1.485(2)	C(2)-C(3)	1.421(2)
C(3)-C(4)	1.373(2)	C(3)-C(21)	1.493(2)
C(4)-C(5)	1.412(2)	C(5)-C(6)	1.420(2)
C(5)-C(10)	1.424(2)	C(6)-C(7)	1.361(3)
C(7)-C(8)	1.416(3)	C(8)-C(9)	1.365(3)
C(9)-C(10)	1.419(2)	C(11)-C(12)	1.376(2)
C(11)-C(20)	1.435(2)	C(12)-C(13)	1.413(2)
C(13)-C(14)	1.374(2)	C(13)-C(31)	1.499(2)
C(14)-C(15)	1.408(2)	C(15)-C(16)	1.419(2)
C(15)-C(20)	1.418(2)	C(16)-C(17)	1.363(3)
C(17)-C(18)	1.414(3)	C(18)-C(19)	1.365(3)
C(19)-C(20)	1.420(2)	C(21)-C(22)	1.412(2)
C(21)-C(26)	1.398(2)	C(22)-C(23)	1.390(3)
C(22)-C(29)	1.512(3)	C(23)-C(24)	1.384(3)
C(24)-C(25)	1.368(3)	C(25)-C(26)	1.402(3)
C(26)-C(27)	1.502(3)	C(27)-C(28)	1.525(3)
C(29)-C(30)	1.522(3)	C(31)-C(32)	1.401(2)
C(31)-C(36)	1.410(2)	C(32)-C(33)	1.397(2)
C(32)-C(37)	1.518(2)	C(33)-C(34)	1.384(3)
C(34)-C(35)	1.383(3)	C(35)-C(36)	1.386(3)
C(36)-C(39)	1.511(2)	C(37)-C(38)	1.531(3)
C(39)-C(40)	1.532(3)	C(41)-C(42)	1.378(2)

7. EXPERIMENTAL SECTION

C(41)-C(50)	1.436(2)	C(41)-C(51)	1.488(2)
C(42)-C(43)	1.414(2)	C(43)-C(44)	1.371(2)
C(43)-C(61)	1.498(2)	C(44)-C(45)	1.414(3)
C(45)-C(46)	1.421(2)	C(45)-C(50)	1.423(2)
C(46)-C(47)	1.365(3)	C(47)-C(48)	1.407(3)
C(48)-C(49)	1.368(2)	C(49)-C(50)	1.422(2)
C(51)-C(52)	1.371(2)	C(51)-C(60)	1.432(2)
C(52)-C(53)	1.419(2)	C(53)-C(54)	1.369(2)
C(53)-C(71)	1.504(2)	C(54)-C(55)	1.418(2)
C(55)-C(56)	1.421(2)	C(55)-C(60)	1.420(2)
C(56)-C(57)	1.365(3)	C(57)-C(58)	1.410(3)
C(58)-C(59)	1.366(3)	C(59)-C(60)	1.417(2)
C(61)-C(62)	1.407(3)	C(61)-C(66)	1.403(3)
C(62)-C(63)	1.401(3)	C(62)-C(67)	1.503(3)
C(63)-C(64)	1.372(5)	C(64)-C(65)	1.378(5)
C(65)-C(66)	1.397(3)	C(66)-C(69)	1.507(3)
C(67)-C(68)	1.521(3)	C(69)-C(70)	1.530(3)
C(71)-C(72)	1.407(3)	C(71)-C(76)	1.401(2)
C(72)-C(73)	1.400(3)	C(72)-C(77)	1.518(3)
C(73)-C(74)	1.378(3)	C(74)-C(75)	1.378(3)
C(75)-C(76)	1.397(3)	C(76)-C(79)	1.504(3)
C(77)-C(78)	1.463(4)	C(79)-C(80)	1.524(3)
C(90)-C(91)	1.452(3)	C(92)-C(93)	1.459(3)
C(94)-C(95)	1.442(3)	C(96)-C(97)	1.456(3)
O(1)-P(1)-O(2)	105.08(6)	O(1)-P(1)-O(3)	111.41(6)
O(1)-P(1)-N(1)	121.02(7)	O(2)-P(1)-O(3)	103.53(6)
N(1)-P(1)-O(2)	108.95(7)	N(1)-P(1)-O(3)	105.54(7)
O(4)-P(2)-O(5)	110.70(6)	O(4)-P(2)-O(6)	103.14(6)
O(4)-P(2)-N(1)	120.47(7)	O(5)-P(2)-O(6)	103.71(6)
N(1)-P(2)-O(5)	106.78(7)	N(1)-P(2)-O(6)	110.84(7)
C(2)-O(2)-P(1)	120.53(10)	C(12)-O(3)-P(1)	115.52(10)
C(42)-O(5)-P(2)	116.08(10)	C(52)-O(6)-P(2)	121.16(10)
P(2)-N(1)-P(1)	132.68(9)	C(2)-C(1)-C(10)	118.79(15)
C(2)-C(1)-C(11)	119.56(14)	C(10)-C(1)-C(11)	121.64(14)
O(2)-C(2)-C(3)	117.76(14)	C(1)-C(2)-O(2)	118.78(14)
C(1)-C(2)-C(3)	123.26(15)	C(2)-C(3)-C(21)	120.64(14)
C(4)-C(3)-C(2)	117.16(15)	C(4)-C(3)-C(21)	122.07(15)
C(3)-C(4)-C(5)	122.16(16)	C(4)-C(5)-C(6)	121.85(16)
C(4)-C(5)-C(10)	119.40(15)	C(6)-C(5)-C(10)	118.75(16)
C(7)-C(6)-C(5)	121.46(17)	C(6)-C(7)-C(8)	119.67(16)
C(9)-C(8)-C(7)	120.58(17)	C(8)-C(9)-C(10)	121.02(17)
C(5)-C(10)-C(1)	118.65(15)	C(9)-C(10)-C(1)	122.82(16)
C(9)-C(10)-C(5)	118.51(15)	C(12)-C(11)-C(1)	120.10(14)
C(12)-C(11)-C(20)	118.63(15)	C(20)-C(11)-C(1)	121.12(14)
O(3)-C(12)-C(13)	118.80(14)	C(11)-C(12)-O(3)	117.89(14)
C(11)-C(12)-C(13)	123.29(15)	C(12)-C(13)-C(31)	123.61(14)
C(14)-C(13)-C(12)	117.19(15)	C(14)-C(13)-C(31)	119.17(14)

7. EXPERIMENTAL SECTION

C(13)-C(14)-C(15)	122.17(15)	C(14)-C(15)-C(16)	120.89(16)
C(14)-C(15)-C(20)	119.75(15)	C(20)-C(15)-C(16)	119.32(16)
C(17)-C(16)-C(15)	120.71(17)	C(16)-C(17)-C(18)	120.10(17)
C(19)-C(18)-C(17)	120.52(17)	C(18)-C(19)-C(20)	120.80(16)
C(15)-C(20)-C(11)	118.40(15)	C(15)-C(20)-C(19)	118.52(15)
C(19)-C(20)-C(11)	122.94(15)	C(22)-C(21)-C(3)	118.36(15)
C(26)-C(21)-C(3)	120.34(15)	C(26)-C(21)-C(22)	121.29(16)
C(21)-C(22)-C(29)	119.66(15)	C(23)-C(22)-C(21)	118.28(18)
C(23)-C(22)-C(29)	122.06(17)	C(24)-C(23)-C(22)	120.62(19)
C(25)-C(24)-C(23)	120.79(18)	C(24)-C(25)-C(26)	120.94(19)
C(21)-C(26)-C(25)	118.07(18)	C(21)-C(26)-C(27)	122.71(16)
C(25)-C(26)-C(27)	119.19(17)	C(26)-C(27)-C(28)	112.69(16)
C(22)-C(29)-C(30)	116.23(18)	C(32)-C(31)-C(13)	120.20(14)
C(32)-C(31)-C(36)	120.73(15)	C(36)-C(31)-C(13)	118.83(15)
C(31)-C(32)-C(37)	122.66(15)	C(33)-C(32)-C(31)	118.23(15)
C(33)-C(32)-C(37)	119.11(15)	C(34)-C(33)-C(32)	121.40(17)
C(35)-C(34)-C(33)	119.68(16)	C(34)-C(35)-C(36)	121.01(17)
C(31)-C(36)-C(39)	121.72(16)	C(35)-C(36)-C(31)	118.94(16)
C(35)-C(36)-C(39)	119.13(16)	C(32)-C(37)-C(38)	113.88(15)
C(36)-C(39)-C(40)	110.75(15)	C(42)-C(41)-C(50)	118.04(15)
C(42)-C(41)-C(51)	120.41(14)	C(50)-C(41)-C(51)	121.32(14)
O(5)-C(42)-C(43)	118.80(14)	C(41)-C(42)-O(5)	117.28(14)
C(41)-C(42)-C(43)	123.91(14)	C(42)-C(43)-C(61)	121.29(14)
C(44)-C(43)-C(42)	117.18(15)	C(44)-C(43)-C(61)	121.52(15)
C(43)-C(44)-C(45)	122.14(16)	C(44)-C(45)-C(46)	121.38(16)
C(44)-C(45)-C(50)	119.50(15)	C(46)-C(45)-C(50)	119.07(16)
C(47)-C(46)-C(45)	120.86(17)	C(46)-C(47)-C(48)	120.19(16)
C(49)-C(48)-C(47)	120.49(17)	C(48)-C(49)-C(50)	121.01(17)
C(45)-C(50)-C(41)	118.80(15)	C(49)-C(50)-C(41)	122.72(16)
C(49)-C(50)-C(45)	118.32(15)	C(52)-C(51)-C(41)	119.71(14)
C(52)-C(51)-C(60)	118.23(15)	C(60)-C(51)-C(41)	122.00(15)
O(6)-C(52)-C(53)	117.15(14)	C(51)-C(52)-O(6)	119.00(14)
C(51)-C(52)-C(53)	123.55(15)	C(52)-C(53)-C(71)	120.63(15)
C(54)-C(53)-C(52)	116.91(15)	C(54)-C(53)-C(71)	121.52(15)
C(53)-C(54)-C(55)	122.27(15)	C(54)-C(55)-C(56)	121.86(16)
C(54)-C(55)-C(60)	119.19(15)	C(60)-C(55)-C(56)	118.90(16)
C(57)-C(56)-C(55)	120.92(17)	C(56)-C(57)-C(58)	119.99(16)
C(59)-C(58)-C(57)	120.64(17)	C(58)-C(59)-C(60)	120.78(16)
C(55)-C(60)-C(51)	118.89(15)	C(59)-C(60)-C(51)	122.35(15)
C(59)-C(60)-C(55)	118.73(15)	C(62)-C(61)-C(43)	119.93(18)
C(66)-C(61)-C(43)	119.21(18)	C(66)-C(61)-C(62)	120.86(18)
C(61)-C(62)-C(67)	123.21(18)	C(63)-C(62)-C(61)	118.2(2)
C(63)-C(62)-C(67)	118.6(2)	C(64)-C(63)-C(62)	121.2(3)
C(63)-C(64)-C(65)	120.1(2)	C(64)-C(65)-C(66)	121.2(3)
C(61)-C(66)-C(69)	121.61(18)	C(65)-C(66)-C(61)	118.4(2)
C(65)-C(66)-C(69)	119.9(2)	C(62)-C(67)-C(68)	114.7(2)
C(66)-C(69)-C(70)	111.05(18)	C(72)-C(71)-C(53)	116.63(15)
C(76)-C(71)-C(53)	122.65(15)	C(76)-C(71)-C(72)	120.70(16)

7. EXPERIMENTAL SECTION

C(71)-C(72)-C(77)	123.04(17)	C(73)-C(72)-C(71)	118.69(18)
C(73)-C(72)-C(77)	118.26(18)	C(74)-C(73)-C(72)	120.77(19)
C(73)-C(74)-C(75)	120.04(17)	C(74)-C(75)-C(76)	121.35(18)
C(71)-C(76)-C(79)	122.61(15)	C(75)-C(76)-C(71)	118.41(17)
C(75)-C(76)-C(79)	118.97(16)	C(78)-C(77)-C(72)	114.2(2)
C(76)-C(79)-C(80)	112.93(15)	N(2)-C(91)-C(90)	178.6(3)
N(3)-C(93)-C(92)	178.3(3)	N(4)-C(95)-C(94)	179.3(3)
N(5)-C(97)-C(96)	179.6(3)		

8. BIBLIOGRAPHY

- [1] F. A. Carey, *Organic Chemistry*, 6th ed., McGraw-Hill, **2006**.
- [2] J. E. Aho, P. M. Pihko, T. K. Rissa, *Chem. Rev.* **2005**, *105*, 4406.
- [3] F. Perron, K. F. Albizati, *Chem. Rev.* **1989**, *89*, 1617.
- [4] W. Francke, W. Kitching, *Curr. Org. Chem.* **2001**, *5*, 233.
- [5] W. Felix, G. Rimbach, H. Wengenroth, *Arzneim.-Forsch.* **1969**, *19*, 1860.
- [6] C. P. Mavragani, H. M. Moutsopoulos, *Clinic Rev. Allerg. Immunol.* **2007**, *32*, 287.
- [7] D. Seebach, A. R. Sting, M. Hoffmann, *Angew. Chem. Int. Ed.* **1996**, *35*, 2708.
- [8] H.-G. Schmalz, E. Heßler, J. W. Bats, G. Dürner, *Tetrahedron Lett.* **1994**, *35*, 4543.
- [9] N. Rehnberg, A. Sundin, G. Magnusson, *J. Org. Chem.* **1990**, *55*, 5477.
- [10] E. M. Carreira, L. Kvaerno, *Classics in Stereoselective Synthesis*, Wiley-VCH, **2009**.
- [11] H. Matsutani, S. Ichikawa, J. Yaruva, T. Kasumoto, T. Hiyama, *J. Am. Chem. Soc.* **1997**, *119*, 4541.
- [12] S. G. Davies, L. M. A. R. B. Correia, *Chem. Commun.* **1996**, 1803.
- [13] M. D. Spantulescu, M. A. Boudreau, J. C. Vederas, *Org. Lett.* **2009**, *11*, 645.
- [14] M. Uchiyama, M. Oka, S. Harai, A. Ohta, *Tetrahedron Lett.* **2001**, *42*, 1931.
- [15] S. D. Rychnovsky, B. M. Bax, *Tetrahedron Lett.* **2000**, *41*, 3593.
- [16] M. Uchiyama, S. Satoh, A. Ohta, *Tetrahedron Lett.* **2001**, *42*, 1559.
- [17] P. Cohen, C. F. B. Holmes, Y. Tsukitani, *Trends Biochem. Sci.* **1990**, *15*, 98.
- [18] S. B. Singh, D. L. Zink, B. Heimbach, O. Genilloud, A. Teran, K. C. Silverman, R. B. Lingham, P. Felock, D. J. Hazuda, *Org. Lett.* **2002**, *4*, 1123.
- [19] A. Agtarap, J. W. Chamberlin, M. Pinkerton, L. K. Steinrauf, *J. Am. Chem. Soc.* **1967**, *89*, 5737.
- [20] T. Ueno, H. Takahashi, M. Oda, M. Mizunuma, A. Yokoyama, Y. Goto, Y. Mizushina, K. Sakaguchi, H. Hayashi, *Biochemistry* **2000**, *39*, 5995.
- [21] F. M. Uckun, C. Mao, A. O. Vassilev, H. Huang, S.-T. Jan, *Bioorg. Med. Chem. Lett.* **2000**, *10*, 541.
- [22] O. Barun, K. Kumar, S. Sommer, A. Langerak, T. U. Mayer, O. Müller, H. Waldmann, *Eur. J. Org. Chem.* **2005**, 4773.
- [23] G. Zinzalla, L.-G. Milroy, S. V. Ley, *Org. Biomol. Chem.* **2006**, *4*, 1977.
- [24] M. Brasholz, S. Sörgel, C. Azap, H.-U. Reißig, *Eur. J. Org. Chem.* **2007**, 3801.

8. BIBLIOGRAPHY

- [25] R. Baker, R. Herbert, P. E. Howse, O. T. Jones, W. Francke, W. Reith, *J. Chem. Soc., Chem. Commun.* **1980**, 52.
- [26] G. Haniotakis, W. Francke, K. Mori, H. Redlich, V. Schurig, *J. Chem. Ecol.* **1986**, *12*, 1559.
- [27] H. Redlich, W. Francke, *Angew. Chem. Int. Ed. Engl.* **1984**, *23*, 519.
- [28] K. Mori, H. Watanabe, K. Yanagi, M. Minobe, *Tetrahedron* **1985**, *41*, 3663.
- [29] S. Takahashi, A. Toyoda, Y. Sekiyama, H. Takagi, T. Nogawa, M. Uramoto, R. Suzuki, H. Koshino, T. Kumano, S. Panthee, T. Dairi, J. Ishikawa, H. Ikeda, Y. Sakaki, H. Osada, *Nat. Chem. Biol.* **2011**, *7*, 461.
- [30] H. Audrain, J. Thorhauge, R. G. Hazell, K. A. Jørgensen, *J. Org. Chem.* **2000**, *65*, 4487.
- [31] S. B. Moilanen, J. S. Potuzak, D. S. Tan, *J. Am. Chem. Soc.* **2006**, *128*, 1792.
- [32] J. S. Potuzak, S. B. Moilanen, D. S. Tan, *J. Am. Chem. Soc.* **2005**, *127*, 13796.
- [33] L. R. Takaoka, A. J. Buckmelter, T. E. LaCruz, S. D. Rychnovsky, *J. Am. Chem. Soc.* **2005**, *127*, 528.
- [34] PhD thesis: M. Fritzsche, Universität Hamburg (Hamburg), **2006**.
- [35] T. Akiyama, *Chem. Rev.* **2007**, *107*, 5744.
- [36] M. Terada, *Synthesis* **2010**, 1929.
- [37] S. E. Reisman, A. G. Doyle, E. N. Jacobsen, *J. Am. Chem. Soc.* **2008**, *130*, 7198.
- [38] M. Terada, H. Tanaka, K. Sorimachi, *J. Am. Chem. Soc.* **2009**, *131*, 3430.
- [39] Q.-W. Zhang, C.-A. Fan, H.-J. Zhang, Y.-Q. Tu, Y.-M. Zhao, P. Gu, Z.-M. Chen, *Angew. Chem. Int. Ed.* **2009**, *48*, 8572.
- [40] B. List, R. A. Lerner, C. F. Barbas, *J. Am. Chem. Soc.* **2000**, *122*, 2395.
- [41] K. A. Ahrendt, C. J. Borths, D. W. C. MacMillan, *J. Am. Chem. Soc.* **2000**, *122*, 4243.
- [42] Thematic issue on Organocatalysis, Ed. B. List, *Chem. Rev.* **2007**, *107*, 5413.
- [43] A. Berkessel, H. Groeger, *Asymmetric Organocatalysis: from Biomimetic Concepts to Applications in Asymmetric Synthesis*, Wiley-VCH, Weinheim, **2005**.
- [44] B. List, *Angew. Chem. Int. Ed.* **2010**, *49*, 1730.
- [45] G. Bredig, P. S. Fiske, *Biochem. Z.* **1912**, *46*, 7.
- [46] V. Prelog, M. Wilhelm, *Helv. Chim. Acta* **1954**, *37*, 1634.
- [47] H. Pracejus, *Liebigs Ann. Chem.* **1960**, *634*, 9.
- [48] Z. G. Hajos, D. R. Parrish, *German Patent DE 2102623*, **1971**.
- [49] Z. G. Hajos, D. R. Parrish, *J. Org. Chem.* **1974**, *39*, 1615.

- [50] U. Eder, G. Sauer, R. Wiechert, *German Patent DE 2014757*, **1971**.
- [51] U. Eder, G. Sauer, R. Wiechert, *Angew. Chem. Int. Ed. Engl.* **1971**, *10*, 496.
- [52] J. Seayad, B. List, *Org. Biomol. Chem.* **2005**, *3*, 719.
- [53] P. Muller, *Pure Appl. Chem.* **1994**, *66*, 1077.
- [54] M. S. Sigman, E. N. Jacobsen, *J. Am. Chem. Soc.* **1998**, *120*, 4901.
- [55] Y. Huang, A. K. Unni, A. N. Thadani, V. H. Rawal, *Nature* **2003**, *424*, 146.
- [56] A. G. Doyle, E. N. Jacobsen, *Chem. Rev.* **2007**, *107*, 5713.
- [57] J. Alemán, A. Parra, H. Jiang, K. A. Jørgensen, *Chem. Eur. J.* **2011**, *17*, 6890.
- [58] T. Akiyama, J. Itoh, K. Yokota, K. Fuchibe, *Angew. Chem. Int. Ed.* **2004**, *43*, 1566.
- [59] D. Uraguchi, M. Terada, *J. Am. Chem. Soc.* **2004**, *126*, 5356.
- [60] M. Hatano, K. Moriyama, T. Maki, K. Ishihara, *Angew. Chem. Int. Ed.* **2010**, *49*, 3823.
- [61] M. Klusmann, L. Ratjen, S. Hoffmann, V. Wakchaure, R. Goddard, B. List, *Synlett* **2010**, 2189.
- [62] T. Hashimoto, K. Maruoka, *J. Am. Chem. Soc.* **2007**, *129*, 10054.
- [63] D. Kampen, A. Ladépêche, G. Claßen, B. List, *Adv. Synth. Catal.* **2008**, *350*, 962.
- [64] M. Hatano, T. Maki, K. Moriyama, M. Arinobe, K. Ishihara, *J. Am. Chem. Soc.* **2008**, *130*, 16858.
- [65] P. García-García, F. Lay, P. García-García, C. Rabalakos, B. List, *Angew. Chem. Int. Ed.* **2009**, *48*, 4363.
- [66] L.-Y. Chen, H. He, W.-H. Chan, A. W. M. Lee, *J. Org. Chem.* **2011**, *76*, 7141.
- [67] H. Xu, S. J. Zuend, M. G. Woll, Y. Tao, E. N. Jacobsen, *Science* **2010**, *327*, 986.
- [68] E. M. Beck, A. M. Hyde, E. N. Jacobsen, *Org. Lett.* **2011**, *13*, 4260.
- [69] B. M. Nugent, R. A. Yoder, J. N. Johnston, *J. Am. Chem. Soc.* **2004**, *126*, 3418.
- [70] D. Uraguchi, D. Nakashima, T. Ooi, *J. Am. Chem. Soc.* **2009**, *131*, 7242.
- [71] S. Hoffmann, A. M. Seayad, B. List, *Angew. Chem. Int. Ed.* **2005**, *44*, 7424.
- [72] G. Adair, S. Mukherjee, B. List, *Aldrichimica Acta* **2008**, *41*, 31.
- [73] S. Mayer, B. List, *Angew. Chem. Int. Ed.* **2006**, *45*, 4193.
- [74] G. L. Hamilton, E. J. Kang, M. Mba, F. D. Toste, *Science* **2007**, *317*, 496.
- [75] S. Mukherjee, B. List, *J. Am. Chem. Soc.* **2007**, *129*, 11336.
- [76] X.-H. Chen, X.-Y. Xu, H. Liu, L.-F. Cun, L.-Z. Gong, *J. Am. Chem. Soc.* **2006**, *128*, 14802.
- [77] T. Akiyama, Y. Saitoh, H. Morita, K. Fuchibe, *Adv. Synth. Catal.* **2005**, *347*, 1523.

8. BIBLIOGRAPHY

- [78] G. B. Rowland, H. Zhang, E. B. Rowland, S. Chennamadhavuni, Y. Wang, J. C. Antilla, *J. Am. Chem. Soc.* **2005**, *127*, 15696.
- [79] Q.-S. Guo, D.-M. Du, J. Xu, *Angew. Chem. Int. Ed.* **2008**, *47*, 759.
- [80] K. Mori, K. Ehara, K. Kurihara, T. Akiyama, *J. Am. Chem. Soc.* **2011**, *133*, 6166.
- [81] X.-H. Chen, W.-Q. Zhang, L.-Z. Gong, *J. Am. Chem. Soc.* **2008**, *130*, 5652.
- [82] N. Momiyama, T. Konno, Y. Furiya, T. Iwamoto, M. Terada, *J. Am. Chem. Soc.* **2011**, *133*, 19294.
- [83] F. Xu, D. Huang, C. Han, W. Shen, X. Lin, Y. Wang, *J. Org. Chem.* **2010**, *75*, 8677.
- [84] I. Čorić, S. Müller, B. List, *J. Am. Chem. Soc.* **2010**, *132*, 17370.
- [85] M. Terada, K. Sorimachi, D. Uraguchi, *Synlett* **2006**, *2006*, 133.
- [86] G. Pousse, A. Devineau, V. Dalla, L. Humphreys, M.-C. Lasne, J. Rouden, J. Blanchet, *Tetrahedron* **2009**, *65*, 10617.
- [87] N. D. Shapiro, V. Rauniyar, G. L. Hamilton, J. Wu, F. D. Toste, *Nature* **2011**, *470*, 245.
- [88] D. Nakashima, H. Yamamoto, *J. Am. Chem. Soc.* **2006**, *128*, 9626.
- [89] C. H. Cheon, H. Yamamoto, *Chem. Commun.* **2011**, *47*, 3043.
- [90] M. Rueping, B. J. Nachtsheim, W. Ieawsuwan, I. Atodiresei, *Angew. Chem. Int. Ed.* **2011**, *50*, 6706.
- [91] C. H. Cheon, H. Yamamoto, *J. Am. Chem. Soc.* **2008**, *130*, 9246.
- [92] S. Vellalath, I. Čorić, B. List, *Angew. Chem. Int. Ed.* **2010**, *49*, 9749.
- [93] R. Chênevert, M. Desjardins, R. Gagnon, *Chem. Lett.* **1990**, *19*, 33.
- [94] J. Milton, S. Brand, M. F. Jones, C. M. Rayner, *Tetrahedron Lett.* **1995**, *36*, 6961.
- [95] S. J. Fletcher, C. M. Rayner, *Tetrahedron Lett.* **1999**, *40*, 7139.
- [96] G. S. Weatherhead, J. H. Houser, J. G. Ford, J. Y. Jamieson, R. R. Schrock, A. H. Hoveyda, *Tetrahedron Lett.* **2000**, *41*, 9553.
- [97] A. H. Hoveyda, R. R. Schrock, *Chem. Eur. J.* **2001**, *7*, 945.
- [98] H. Frauenrath, T. Philipps, *Angew. Chem. Int. Ed.* **1986**, *25*, 274.
- [99] H. Frauenrath, S. Reim, A. Wiesner, *Tetrahedron: Asymmetry* **1998**, *9*, 1103.
- [100] H. Nagano, T. Katsuki, *Chem. Lett.* **2002**, *31*, 782.
- [101] S. Handa, L. M. Slaughter, *Angew. Chem. Int. Ed.* **2012**, *51*, 2912.
- [102] Y. Liang, E. B. Rowland, G. B. Rowland, J. A. Perman, J. C. Antilla, *Chem. Commun.* **2007**, 4477.
- [103] G. Li, F. R. Fronczek, J. C. Antilla, *J. Am. Chem. Soc.* **2008**, *130*, 12216.

8. BIBLIOGRAPHY

- [104] X. Cheng, S. Vellalath, R. Goddard, B. List, *J. Am. Chem. Soc.* **2008**, *130*, 15786.
- [105] M. Rueping, A. P. Antonchick, E. Sugiono, K. Grenader, *Angew. Chem. Int. Ed.* **2009**, *48*, 908.
- [106] G. K. Ingle, M. G. Mormino, L. Wojtas, J. C. Antilla, *Org. Lett.* **2011**, *13*, 4822.
- [107] I. Čorić, S. Vellalath, B. List, *J. Am. Chem. Soc.* **2010**, *132*, 8536.
- [108] S. Müller, *Dissertation*, Köln University **2012**.
- [109] J.-H. Xie, Q.-L. Zhou, *Acc. Chem. Res.* **2008**, *41*, 581.
- [110] Y. K. Chung, G. C. Fu, *Angew. Chem. Int. Ed.* **2009**, *48*, 2225.
- [111] M. Jiang, S.-F. Zhu, Y. Yang, L.-Z. Gong, X.-G. Zhou, Q.-L. Zhou, *Tetrahedron: Asymmetry* **2006**, *17*, 384.
- [112] V. B. Birman, A. L. Rheingold, K.-C. Lam, *Tetrahedron: Asymmetry* **1999**, *10*, 125.
- [113] E. Vedejs, X. Chen, *J. Am. Chem. Soc.* **1997**, *119*, 2584.
- [114] J. R. Dehli, V. Gotor, *Chem. Soc. Rev.* **2002**, *31*, 365.
- [115] E. Vedejs, M. Jure, *Angew. Chem. Int. Ed.* **2005**, *44*, 3974.
- [116] R. Kourist, P. Domínguez de María, U. T. Bornscheuer, *ChemBioChem* **2008**, *9*, 491.
- [117] B. List, D. Shabat, G. Zhong, J. M. Turner, A. Li, T. Bui, J. Anderson, R. A. Lerner, C. F. Barbas, III *J. Am. Chem. Soc.* **1999**, *121*, 7283.
- [118] D. J. Schipper, S. Rousseaux, K. Fagnou, *Angew. Chem. Int. Ed.* **2009**, *48*, 8343.
- [119] B. Karatas, S. Rendler, R. Fröhlich, M. Oestreich, *Org. Biomol. Chem.* **2008**, *6*, 1435.
- [120] E. R. Jarvo, C. A. Evans, G. T. Copeland, S. J. Miller, *J. Org. Chem.* **2001**, *66*, 5522.
- [121] M. C. Angione, S. J. Miller, *Tetrahedron* **2006**, *62*, 5254.
- [122] Y. Zhao, A. W. Mitra, A. H. Hoveyda, M. L. Snapper, *Angew. Chem. Int. Ed.* **2007**, *46*, 8471.
- [123] S.-y. Tosaki, K. Hara, V. Gnanadesikan, H. Morimoto, S. Harada, M. Sugita, N. Yamagiwa, S. Matsunaga, M. Shibasaki, *J. Am. Chem. Soc.* **2006**, *128*, 11776.
- [124] K. Hara, S.-y. Tosaki, V. Gnanadesikan, H. Morimoto, S. Harada, M. Sugita, N. Yamagiwa, S. Matsunaga, M. Shibasaki, *Tetrahedron* **2009**, *65*, 5030.
- [125] R. Shintani, K. Takatsu, T. Hayashi, *Org. Lett.* **2008**, *10*, 1191.
- [126] Reduction: D. J. Aldous, A. S. Batsanov, D. S. Yufit, A. J. Dalençon, W. M. Dutton, P. G. Steel, *Org. Biomol. Chem.* **2006**, *4*, 2912.
- [127] Transacetalization: D. Tobia, B. Rickborn, *J. Org. Chem.* **1986**, *51*, 3849.

- [128] Transacetalization: G. Stork, J. J. La Clair, P. Spargo, R. P. Nargund, N. Totah, *J. Am. Chem. Soc.* **1996**, *118*, 5304.
- [129] Elimination to dihydrofuranes: R. D. Miller, D. R. McKean, *Tetrahedron Lett.* **1982**, *23*, 323.
- [130] Substitution: D. S. Brown, M. Bruno, R. J. Davenport, S. V. Ley, *Tetrahedron* **1989**, *45*, 4293.
- [131] Friedel-Crafts reaction: T. Esumi, D. Hojyo, H. Zhai, Y. Fukuyama, *Tetrahedron Lett.* **2006**, *47*, 3979.
- [132] Acetal-ene reaction: A. Ladépêche, E. Tam, J.-E. Ancel, L. Ghosez, *Synthesis* **2004**, 1375.
- [133] Oxidation to γ -lactones: E. Ehlinger, P. Magnus, *J. Am. Chem. Soc.* **1980**, *102*, 5004.
- [134] Oxidation to γ -lactones: R. Pedrosa, S. Sayalero, M. Vicente, *Tetrahedron* **2006**, *62*, 10400.
- [135] D. A. Mulholland, K. McFarland, M. Randrianarivelosia, *Biochem. Syst. Ecol.* **2006**, *34*, 365.
- [136] J. J. Beck, S.-C. Chou, *J. Nat. Prod.* **2007**, *70*, 891.
- [137] M. J. Xiong, Z. H. Li, *Curr. Org. Chem.* **2007**, *11*, 833.
- [138] I. Čorić, B. List, *Nature* **2012**, *483*, 315.
- [139] R. I. Storer, D. E. Carrera, Y. Ni, D. W. C. MacMillan, *J. Am. Chem. Soc.* **2006**, *128*, 84.
- [140] S. Müller, M. J. Webber, B. List, *J. Am. Chem. Soc.* **2011**.
- [141] R. K. Boeckman Jr., K. J. Bruza, *Tetrahedron* **1981**, *37*, 3997.
- [142] R. Amouroux, *Heterocycles* **1984**, *22*, 1489.
- [143] K. Haraguchi, K. Konno, K. Yamada, Y. Kitagawa, K. T. Nakamura, Hiromichi Tanaka, *Tetrahedron* **2010**, *66*, 4587.
- [144] I. Kadota, H. Takamura, K. Sato, Y. Yamamoto, *J. Org. Chem.* **2002**, *67*, 3494.
- [145] R. E. Marker, R. B. Wagner, P. R. Ulshafer, E. L. Wittbecker, D. P. J. Goldsmith, C. H. Ruof, *J. Am. Chem. Soc.* **1947**, *69*, 2167.
- [146] M. E. Wall, C. R. Eddy, S. Serota, *J. Am. Chem. Soc.* **1954**, *76*, 2849.
- [147] Q.-W. Zhang, C.-A. Fan, H.-J. Zhang, Y.-Q. Tu, Y.-M. Zhao, P. Gu, Z.-M. Chen, *Angew. Chem. Int. Ed.* **2009**, *48*, 8572.
- [148] A. Natarajan, L. S. Kaanumalle, S. Jockusch, C. L. D. Gibb, B. C. Gibb, N. J. Turro, V. Ramamurthy, *J. Am. Chem. Soc.* **2007**, *129*, 4132.

8. BIBLIOGRAPHY

- [149] Y. Nishioka, T. Yamaguchi, M. Yoshizawa, M. Fujita, *J. Am. Chem. Soc.* **2007**, *129*, 7000.
- [150] S. R. Shenoy, F. R. P. Crisóstomo, T. Iwasawa, J. Rebek Jr., *J. Am. Chem. Soc.* **2008**, *130*, 5658.
- [151] C. J. Hastings, M. D. Pluth, R. G. Bergman, K. N. Raymond, *J. Am. Chem. Soc.* **2010**, *132*, 6938.
- [152] A. Greiner, *Tetrahedron Lett.* **1989**, *30*, 3547.
- [153] G. M. Sheldrick, *Acta Cryst.* **2008**, *A64*, 112.
- [154] H. D. Flack, *Acta Cryst.* **1983**, *A39*, 876.
- [155] R. W. W. Hooft, L. H. Straver, A. L. Spek, *J. Appl. Cryst.* **2008**, *41*, 96.
- [156] H. C. Brown, S. V. Kulkarni, U. S. Racherla, *J. Org. Chem.* **1994**, *59*, 365.
- [157] X.-X. Xu, H.-Q. Dong, *J. Org. Chem.* **1995**, *60*, 3039.
- [158] D. H. T. Phan, B. Kim, V. M. Dong, *J. Am. Chem. Soc.* **2009**, *131*, 15608.
- [159] J.-E. Nyström, T. D. McCanna, P. Helquist, R. Amouroux, *Synthesis* **1988**, *1988*, 56.
- [160] J. Clayden, J. H. Pink, N. Westlund, C. S. Frampton, *J. Chem. Soc., Perkin Trans. 1* **2002**, 901.
- [161] R. C. Fuson, J. Corse, *J. Am. Chem. Soc.* **1938**, *60*, 2063.

9. APPENDIX

9.1. Erklärung

“Ich versichere, dass ich die von mir vorgelegte Dissertation selbständig angefertigt, die benutzten Quellen und Hilfsmittel vollständig angegeben und die Stellen der Arbeit – einschließlich Tabellen, Karten und Abbildungen –, die anderen Werken im Wortlaut oder dem Sinn nach entnommen sind, in jedem Einzelfall als Entlehnung kenntlich gemacht habe; dass diese Dissertation noch keiner anderen Fakultät oder Universität zur Prüfung vorgelegen hat; dass sie – abgesehen von unten angegebenen Teilpublikationen – noch nicht veröffentlicht worden ist sowie, dass ich eine solche Veröffentlichung vor Abschluss des Promotionsverfahrens nicht vornehmen werde. Die Bestimmungen der Promotionsordnung sind mir bekannt. Die von mir vorgelegte Dissertation ist von Herrn Professor Dr. Benjamin List betreut worden.“

Mülheim an der Ruhr, Juni 2012

Bisher sind folgende Teilpublikationen veröffentlicht worden:

“Asymmetric Spiroacetalization Catalysed by Confined Brønsted Acids”, I. Čorić, B. List, *Nature* **2012**, *483*, 315.

“Kinetic Resolution of Homoaldols via Catalytic Asymmetric Transacetalization”, I. Čorić,[‡] S. Müller,[‡] B. List, *J. Am. Chem. Soc.* **2010**, *132*, 17370. ([‡]equal contribution)

“N-Phosphinyl Phosphoramidate—A Chiral Brønsted Acid Motif for the Direct Asymmetric N,O-Acetalization of Aldehydes”, S. Vellalath, I. Čorić, B. List, *Angew. Chem. Int. Ed.* **2010**, *49*, 9749.

“Catalytic Asymmetric Transacetalization”, I. Čorić, S. Vellalath, B. List, *J. Am. Chem. Soc.* **2010**, *132*, 8536. Erratum: *J. Am. Chem. Soc.* **2010**, *132*, 12155.

9.2. Lebenslauf

Ilija Čorić

Geboren am 4. April 1983
in Zagreb, Kroatien
Staatsangehörigkeit kroatisch

Akademischer Werdegang

Promotion

09.2008 – 06.2012 Dissertation im Arbeitskreis von Prof. Dr. Benjamin List
Max-Planck-Institut für Kohlenforschung, Mülheim an der Ruhr
mit dem Titel „Asymmetric Brønsted Acid Catalysis: Acetals
& Confined Catalysts“

Hochschulstudium

10.2005 – 10.2006 Diplomarbeit im Arbeitskreis von Prof. Dr. Vitomir Šunjić
Naturwissenschaftlich-Mathematische Fakultät,
Universität Zagreb, Kroatien
mit dem Titel „Synthesis of Resveratrol-Biotin Conjugate“

10.2002 – 10.2006 Naturwissenschaftlich-Mathematische Fakultät,
Universität Zagreb, Kroatien
Abschluß: Diplom-Chemiker

Schulbildung

10.2002 – 10.2006 Gymnasium für Naturwissenschaften und Mathematik,
Zagreb, Kroatien
Abschluß: Abitur